Green Organocatalysis: An (eco)-toxicity and biodegradation study of organocatalysts

By Thomas Hayes B.A. (Hons)

Under the supervision of Dr. Nicholas Gathergood

School of Chemical Sciences

Dublin City University

For the award of Ph.D in Organic Chemistry

December 2011

Dedicated to Mam and Dad

Declaration

I hereby certify that this material, which I now submit for assessment on the programme of study leading to the award of Ph.D is entirely my own work, that I have exercised reasonable care to ensure that the work is original, and does not to the best of my knowledge breach any law of copyright, and has not been taken from the work of others save and to the extent that such work has been cited and acknowledged within the text of my work.

Signed: _____ (Candidate)

Thomas Hayes

ID No.: __57116954___

Date: _____

Abstract

A series of novel (a)chiral substituted BINOLs and achiral biquinoline compounds were synthesised and characterised. Different substituents were incorporated within the structure of these molecules to enhance biodegradation. These substituents were selected according to Boethling's 'rules of thumb' for designing biodegradable chemicals.

Final novel compounds were screened for antimicrobial activity and tested for biodegradation. As well a number of known organocatalysts were also studied for antimicrobial activity, tested for biodegradation and cytotoxicity, apoptosis and cell viability studies were performed against three blood cell lines. Both enantiomers of amino acids (L and D) and BINOLs (*S* and *R*) were screened for anti-microbial activity to determine the affect of stereochemistry. Antimicrobial studies were performed using the minimum inhibitory concentration assay. Highest concentration was dependant on chemical solubility, however, for most compounds tested the highest concentration was 2 mM. Test organisms used for this study included fungi, Gram positive and Gram negative bacteria. Growth inhibition of microbes was noted for some compounds within tested concentration range. (*R*)-3,3'-Dibromo-H_8-BINOL was found to be a hit antimicrobial agent for Gram positive bacteria with an MIC value in the low micromolar range.

Cytotoxicity, apoptosis and cell viability studies of organocatalysts were carried out against the blood cell lines human erythroid progenitors, HL-60 and K-562 using the promega protocols, respectively. A Maruoka phase-transfer catalyst was found to reduce cell viability and promote apoptosis for all three cell lines studied.

Biodegradation studies of organocatalysts were performed using the CO_2 headspace test (ISO 14593). BINOL and derivatives showed poor biodegradation under the parameters of the CO_2 headspace test (ISO 14593). L-Prolinamide passed the CO_2 headspace test (ISO 14593) and can be classified as a readily biodegradable catalyst. For the inhibitory control biodegradation assay, a Maruoka phase-transfer catalyst was found to have an inhibitory effect on the activity of the inoculum. All other organocatalysts studied, showed low inhibition for the inhibitory control biodegradation assay.

Chiral substituted BINOLs were synthesised and evaluated as asymmetric catalysts for the Morita-Baylis-Hillman reaction. For this study, test substrates hydrocinnamaldehyde and 2-cyclohexen-1-one were reacted together in the presence of triethylphosphine in THF and BINOL derived catalysts (2 mol%) in THF at room temperature. However, preliminary results show catalysts performed poorly when compared to known optimal catalyst.

Acknowledgements

I would like to thank Dr. Nick Gathergood for giving me the opportunity to carry out this work in his research group and for his support and guidance during my Ph.D.

I would like to thank Dr. Brid Quilty for allowing me to do microbiological work in her lab.

I would also like to thank Dr Marcel Špulák for performing antimicrobial studies, Dr Teresa Garcia for biodegradation studies and Dr Petr Bartunek for cytotoxicity, apoptosis and cell viability studies.

I'd also like to thank the EPA for funding this research.

As well a special thanks to all my colleagues in the Gathergood research group.

And finally a huge thank you to my parents Beatrice and Tom for their support throughout my research.

Table of Contents

Abbreviations

A

acac: Acetyl acetone

AIDs: Acquired immunodeficiency syndrome

ATCC: American Type Culture Collection

ATR: Attenuated total reflectance

B

BCL_6: B-cell lymphoma 6 protein

BINOL: 1,1'-Bi-2-naphthol

Biph: Biphenyl

BOC: *tert*-butoxycarbonyl

BQM: BINOL quinine methides

C

º C: Degree Celsius

CFT: (−)-2-β-carbomethoxy-3β-(4-fluorophenyl)tropane

C/L: Carbon per litre

CLSI: Clinical Laboratory Standard Institute

CNS: Central nervous system

CO_2: Carbon dioxide

conc: Concentrated

D

DAT: Dopamine re-uptake transporter protein

DCE: Dichloroethane

DCM: Dichloromethane

DME: Dimethoxyethane

DMEM: Dulbecco's modified eagle medium

DMF: Dimethylformamide

DMSO: Dimethyl sulfoxide

DNA: Deoxyribonucleic acid

D2PM: Diphenylpyrrolidinemethanol

1,3-dppp: 1,3-*Bis*(diphenylphosphino)propane

dr: Diastereomer ratio

D-Tyr-tRNA: D-Tyrosine-tRNA

E

EA: Ethyl acetate

EC_{50}: Half maximal effective concentration

ee: Enantiomeric excess

EI: Electron impact

ESBL: Extended-spectrum beta-lactamase

et al.: and others

F

Fig: Figure

G

g: Gram

g/mol^{-1}: Grams per mole

GC: Gas chromatography

H

h: Hour

H8-BINOL: 5,5',6,6',7,7', 8,8'-Octahydro-1,1'-bi-2-naphthol

$HClO_4$: Perchloric acid

Hex: Hexane

HPLC: High performance liquid chromatography

HIV: Human immunodeficiency virus

Hz: Hertz

I

IC: Inhibitory concentration

IL: Ionic liquid

IR: Infra-red

ISO: International Organization for Standardization

J

J: Coupling constant

M

MBH: Morita-Baylis-Hillman

mg: Milligram

MH: Mueller Hinton broth

MHz: Megahertz

MIC: Minimum inhibitory concentration

mmol: Millimole

Mpt: Melting point

MRSA: Methicillin Resistant Staphylococcus aureus

MS:Mass spectrometry

m/z: Mass to charge ratio

N

Naph: Naphthyl

NGF: Nerve growth factor

nm: Nanomolar

NMP: *N*-Methyl-2-pyrrolidone

NMR: Nuclear Magnetic Resonance

NTf_2: *Bis*(trifluoromethyl)sulfonyl amide

O

$OctOSO_3$: Octyl sulfate

OECD: Organisation for Economic Co-operation and Development

P

PAHs: Polycyclic aromatic hydrocarbons

PTC: Phase-transfer catalyst

p53: p53 tumor suppressor protein

PF_6: Hexafluorophosphate

Ph: Phenyl

PTSA: *para*-Toluenesulfonic acid

ppm: parts per million

PIntB: 2-(di-*tert*-butylphosphino)-1-phenylindole

R

rpm: Revolutions per minute

RPMI: Roswell park memorial institute medium

RT: Room temperature

S

SDS: Sodium dodecyl sulfate

Sir: Silent information regulator

T

TADDOL: α,α,α,α-Tetraaryl-1,3-dioxolane-4,5-dimethanols

THF: Tetrahydrofuran

ThIC: Theoretical maximum inorganic carbon

TIC: Total inorganic carbon

TLC: Thin layer chromatography

TMEDA: Tetramethylethylenediamine

TMS: Tetramethylsilane

TOC: Total organic carbon

Tol: Toluene

TRIP: 3,3'-*Bis*(2,4,6-triisopropylphenyl)-1,1'-binaphthyl-2,2'-diyl hydrogen phosphate

V

VAPOL: 2,2'-Diphenyl-(4-biphenanthrol)

Chapter 1: Literature Review

1.1 Introduction to organocatalysis

1.1.1 Asymmetric organocatalysis

The synthesis of enantiomerically pure compounds is of fundamental importance for chemical and pharmaceutical industries today.[1,2] One strategy that can be used for the generation of enantiopure compounds is asymmetric synthesis. This approach can involve the employment of asymmetric catalysts, which act as chiral promoters for the conversion of achiral substrates into chiral products.[3] There are three branches of asymmetric catalysts reported in the literature, transition metal catalysis,[4] biocatalysis[5] and organocatalysis.[6-13] Organocatalysis has re-emerged as an alternative asymmetric methodology and involves the use of small chiral organic molecules called organocatalysts in sub-stoichiometric amounts to catalyze a reaction enantioselectively.[6] After seminal reports made by List and Barbas[14] and MacMillan,[15] in 2000, organocatalysis as a synthetic methodology gained momentum. Since their initial reports the number of publications on organocatalysis has steadily risen.[6-13]

1.1.2 Classes of organocatalysts

Organocatalysts, a word coined by MacMillan is used to define organic molecules as catalysts for synthesis.[12] These catalysts avoid the application of toxic metals (many compounds/complexes of which have undesirable toxicities) and is one of the main reasons this field as a whole has gained such prominence. Many classes of organocatalysts have been reported (Figure 1.1) and the field is ever expanding.[6-13]

One of the first reports, for the use of an organocatalyst was made in the 1970s by the industrial groups of Eder, Sauer and Wiechert [16] and Hajos and Parrish.[17] They reported the use of (*S*)-proline, a natural amino acid, for an intramolecular Aldol reaction of a triketone (**1**) (Scheme 1.1).

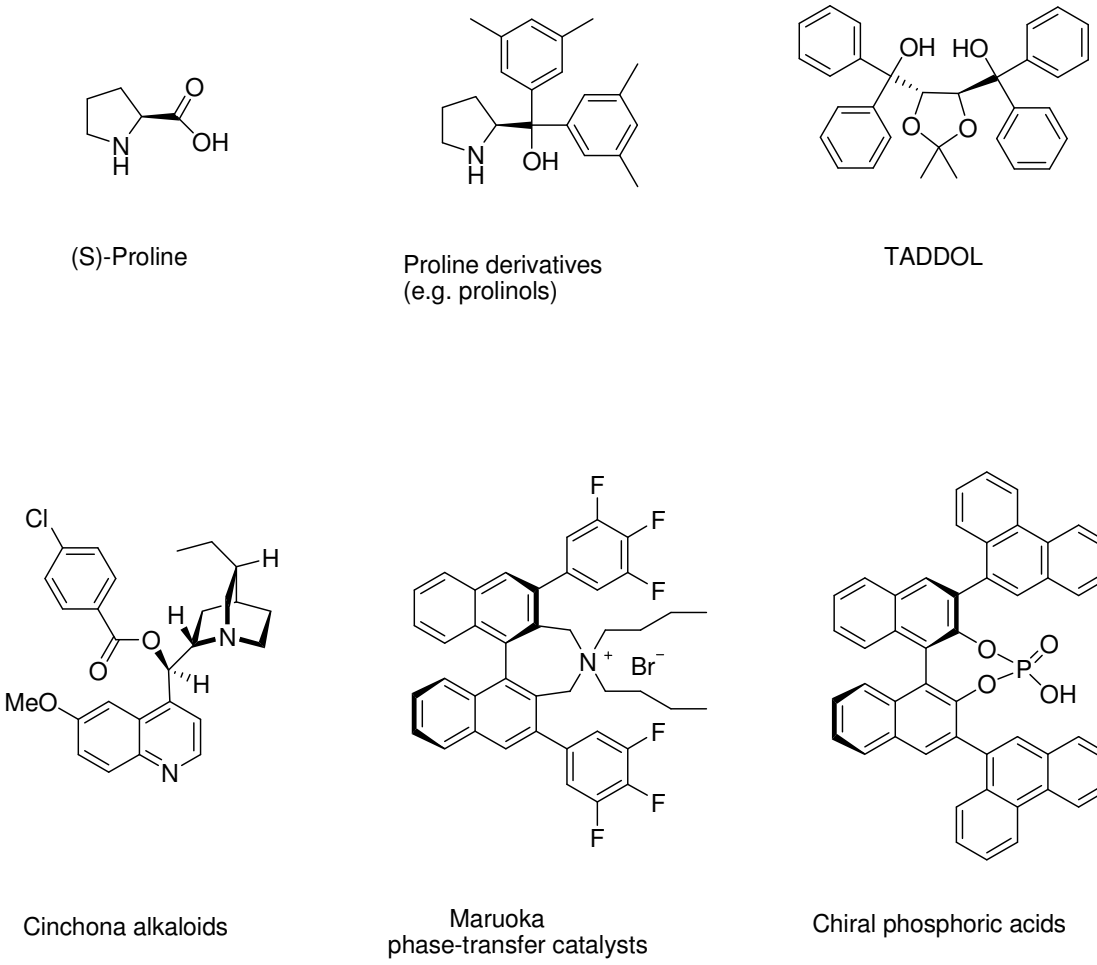

Fig. 1.1 A selection of the main classes of organocatalysts

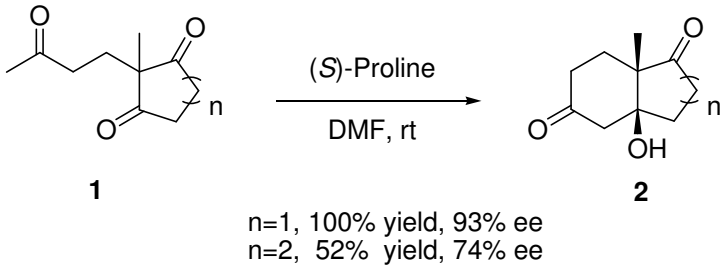

Scheme 1.1: The Hajos-Parrish-Eder-Sauer-Wiechert reaction[16,17]

Since the revival of organocatalysis in 2000,[14, 15] many reports have been made for the application of (*S*)-proline in the Aldol,[18] Mannich,[19] Michael[20] and Baylis-Hillman reactions.[21] However, (*S*)-proline has proven to be inefficient for some reactions such as the Michael reaction (low ee obtained in some cases) and has also been found to require a higher catalyst loading compared to transition metal catalysts.[20] These initial drawbacks have lead to numerous modifications being made to the structure of (*S*)-proline. The purpose of modifying (*S*)-proline and other chiral catalysts, can be for widening of reaction and substrate range, to improve solvent compatibility, to lower catalyst loading and for the attachment to solid support which allows for easier recyclability.[22-24] Modified proline derivatives have demonstrated wide usage for a number of reactions.[6-13] As well, acyclic amino acids have emerged as a class of organocatalysts, however, the reaction range has proven to be quite limited to date.[25,26] For instance, (*S*)-tryptophan[27] and (*S*)-alanine[28] have been demonstrated as asymmetric catalysts for the Aldol reaction. Cinchona alkaloids are another class of asymmetric catalysts and numerous modifications have been applied to their scaffold.[29] The BINOL backbone which is the focus of this project, has found applications as a chiral unit for the design and development of organocatalysts such as chiral phosphoric acids[30-32] and Maruoka phase-transfer catalysts.[33]

1.1.3 Advantages of organocatalysts

There are several advantages for using an organocatalyst compared to transition metal catalysts or biocatalysts.[6]

- Both enantioseries are more readily available
- Robust
- Inexpensive
- Inert towards moisture and oxygen
- Absolute solvents generally not required
- Metal-free

These advantages are the fundamental reason organocatalysis as a synthetic methodology has received so much attention. However, organocatalysts do have their drawbacks such as high catalyst loading which still need to be addressed before their wide adoption by industry.[6]

1.2 Organocatalysis in synthetic reactions

1.2.1 Aldol reaction

The Aldol reaction is a useful carbon-carbon bonding forming reaction, also providing high "atom-economy".[34,35] It is a typical example of electrophilic substitution at the alpha carbon in enols or enolate anions. The fundamental transformation usually catalyzed by base or equivalent acid is a dimerization of an aldehyde or ketone to form a β-hydroxyl aldehyde or ketone by α-carbanionic addition of one reactant molecule to the carbonyl group of a second reactant molecule.[36]

In 2000, with the inspiration of the action of class I aldolases, List *et al*. were first to demonstrate the ability of (*S*)-proline (**5**) to mediate intermolecular asymmetric Aldol reactions between unmodified acetone (**3**) and a variety of aldehydes with moderate to good enantioselectivities (Scheme 1.2).[14] In this reaction, the ketones acted as source of nucleophile and aldehydes as electrophiles. Modest enantiomeric excess (60-77% ee) were obtained for the synthesis of aromatic Aldols (**6a**, **6b** and **6c**). Unbranched aldehydes (e.g. pentanal) did not yield any significant amount of the desired cross-Aldol product. However, the reaction of acetone (**3**) with isobutyraldehyde gave the Aldol product (**6d**) in 97% yield and 96% ee.

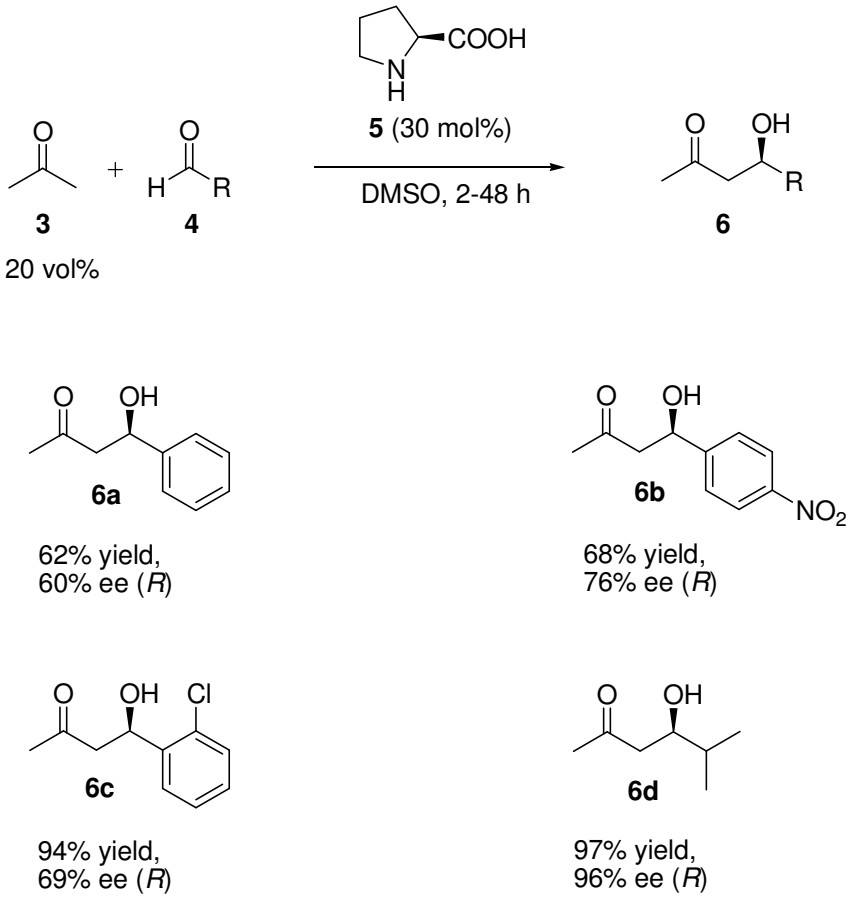

Scheme 1.2: Intermolecular Aldol reaction between acetone (**3**) and aldehydes catalyzed by (*S*)-proline (**5**) [14]

Carter and coworkers have designed and synthesised a novel (*S*)-proline-sulfonamide derivative (**8**) which is capable of catalyzing the Aldol reaction in non-polar solvents.[37] Catalysis of the Aldol reaction with (*S*)-proline (**5**) must be performed in polar solvents such as DMF and DMSO. Carter was able to expand the solvent scope for catalysis of the Aldol reaction with a proline derivative, by designing a more hydrophobic (*S*)-proline sulfonamide catalyst (**8**) (Scheme 1.3). The placement of a dodecyl hydrocarbon on the *para* position of the phenyl substituent generates a lipophilic (*S*)-proline sulfonamide catalyst (**8**) which can readily dissolve in non-polar solvents. For instance, 300 mg of (*S*)-proline sulfonamide (**8**) is soluble in 1 mL of DCM while 300 mg of (*S*)-proline (**5**) is not readily soluble in the same volume of DCM.[38] From an industrial perspective, non-polar solvents are easier to remove and recycle compared to polar solvents.[37]

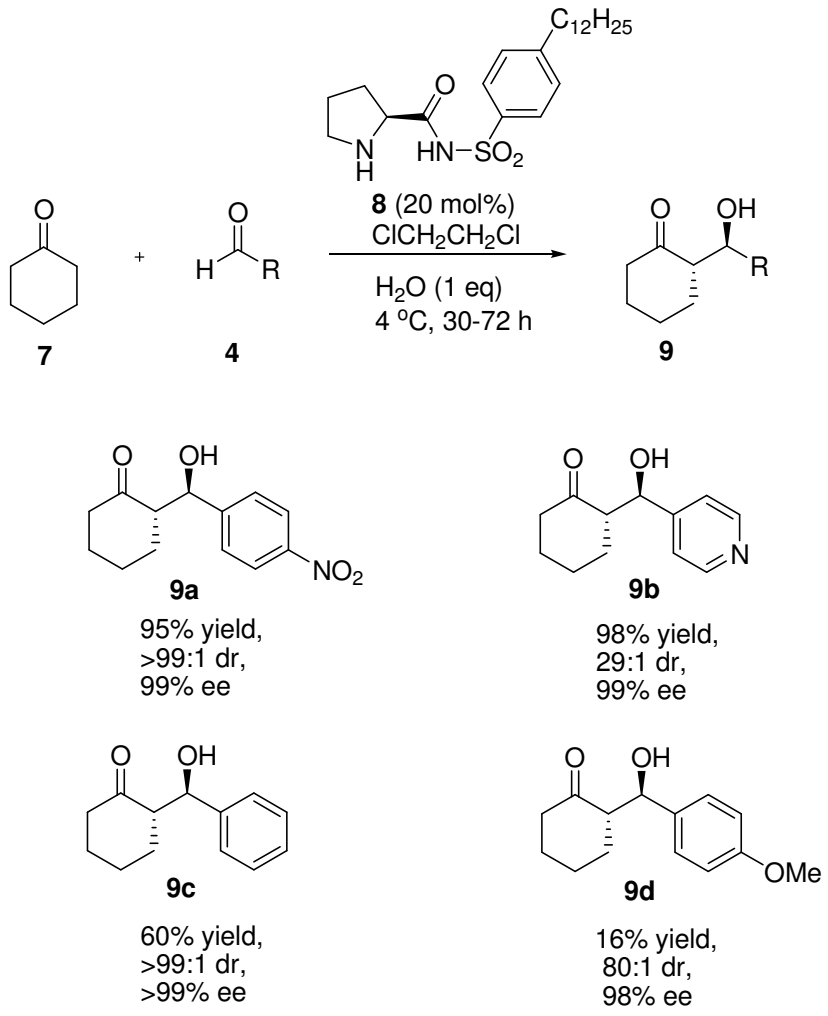

Scheme 1.3: Intermolecular Aldol reaction catalyzed by (*S*)-proline sulfonamide (**8**) [37]

For their study, cyclohexanone (**7**) was reacted with various aldehydes using the (*S*)-proline sulfonamide catalyst (**8**). Optimum conditions for their Aldol reaction were 20 mol% of **8**, DCE as solvent, 1 equivalent of water was found to enhance reaction rate and diastereoselectivity and the reactions were performed at 4 °C. Electron deficient aldehydes performed better than electron rich aldehydes in terms of product yield for the Aldol reaction (Scheme 1.3). The *para*-nitrobenzaldehyde substrate gave a yield of 95% with an ee of 99% and dr of >99:1 while *para*-methoxybenzaldehyde furnished a low yield of 16% with an ee of 98% and dr of 80:1.

1.2.2 Michael reaction

The Michael reaction is a key C-C bond forming reaction that involves various Michael donor and acceptor molecules. Recent interest in the direct asymmetric organocatalyzed Michael reaction is due to the diverse array of products that can be obtained, such as γ-nitrocarbonyl compounds, functionalised pyrrolidines and 1,4-Michael adducts.[11] There are many modes of activation for the catalyzed Michael reaction, including catalysis *via* iminium ion-based activation of the Michael acceptor and enamine-based activation of Michael donor molecules. The potential usage of organocatalysts for the Michael reaction has been investigated using a wide range of Michael donors and acceptors.

A (*S*)-diphenylprolinol silyl ether catalyst (**12**) has been reported to be effective for addition of nitroalkanes to α,β-unsaturated aldehydes *via* chiral iminium ion catalysis (Scheme 1.4).[39] Addition to α,β-unsaturated aldehydes is more challenging because of the competitive 1, 2-addition reaction.[39] The (*S*)-diphenylprolinol silyl ether (**12**) generates Michael products using methanol as solvent in moderate yields and enantioselectivities greater than 90%. Aromatic α,β-unsaturated aldehydes generated products with higher yields compared to aliphatic analogs. Similar enantioselectivities were obtained using aliphatic and aromatic α,β-unsaturated aldehydes. However, longer reaction times were required for aliphatic α,β-unsaturated aldehydes (42-120 h) compared to aromatic α,β-unsaturated aldehydes (16-48 h).

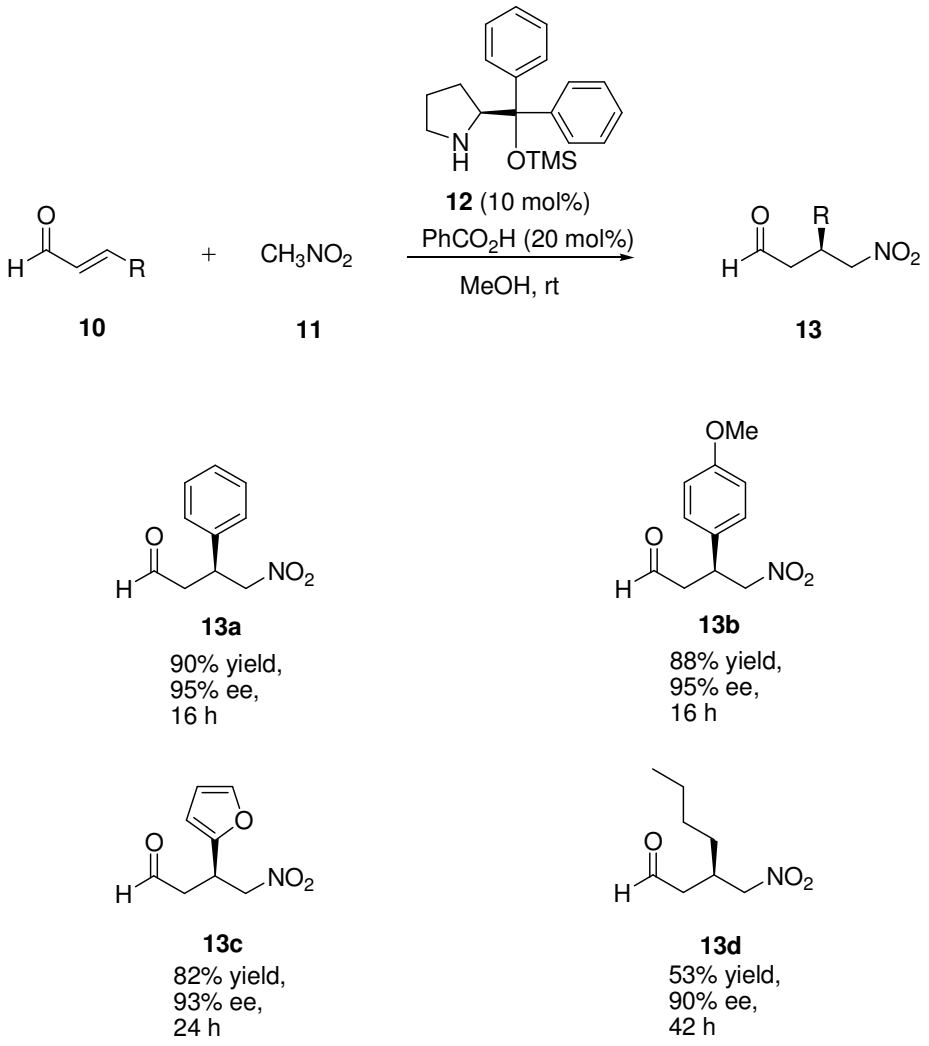

Scheme 1.4: Intermolecular Micheal reaction of α,β-unsaturated aldehydes with nitromethane (**11**) *via* iminium ion catalysis [39]

Jacobsen and coworkers have reported an enantioselective direct conjugate addition of acetone (**3**) to nitroalkenes using a chiral primary amine-thiourea catalyst (**15**) (Scheme 1.5).[40] Jacobsen catalyst (**15**) is a bifunctional catalyst, the primary amine activates the acetone (**3**) substrate to generate a nucleophilic enamine and the electrophilic nitroalkene substrates are further activated by the thiourea functional group. Thiourea catalyst (**15**) was applied at a loading of 10 mol% for the Michael reaction between acetone (**3**) and nitroalkenes (Scheme 1.5), furnishing the nitroalkane products in good yields (>70%) and with high ee (>94%).

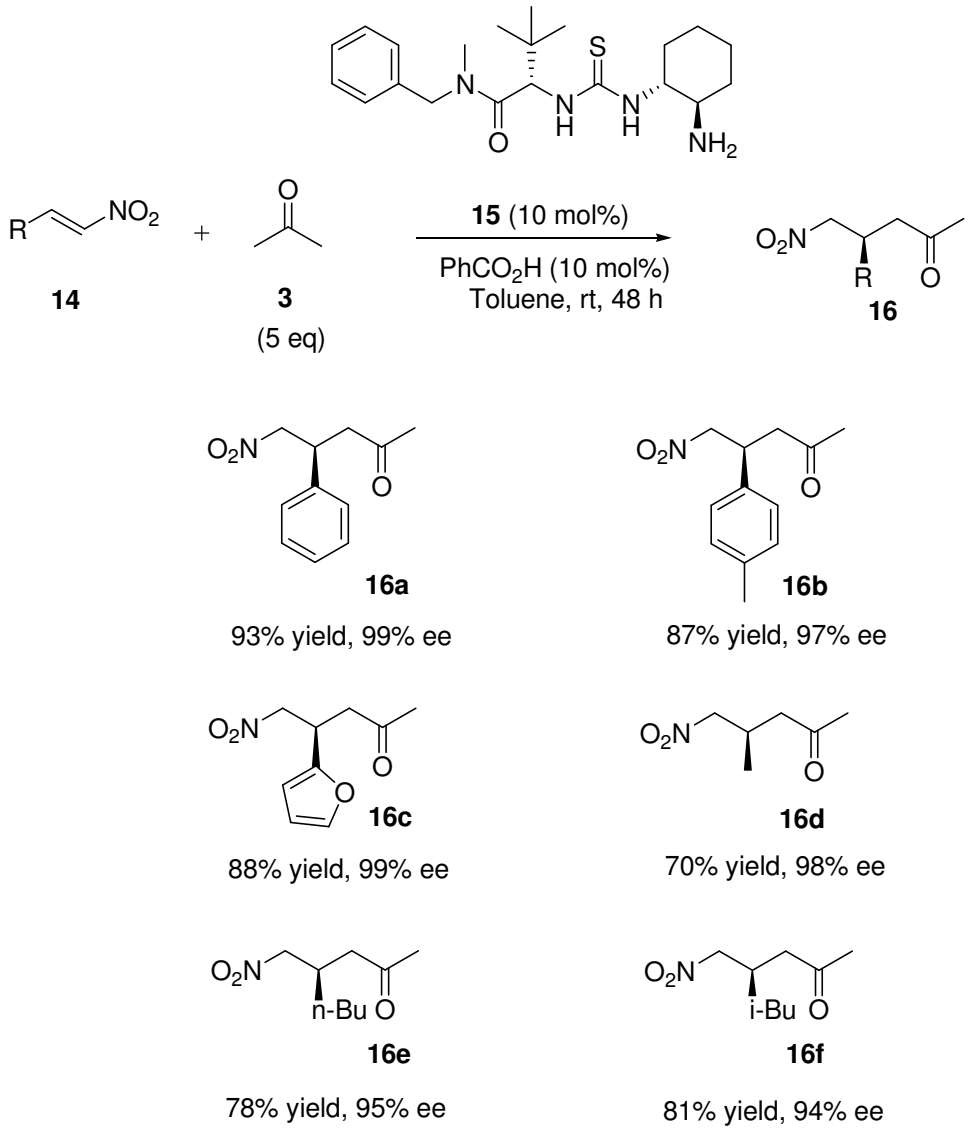

Scheme 1.5: Enantioselective Michael addition of acetone (**3**) to nitroalkenes catalyzed by Jacobsen thiourea (**15**) [40]

Aromatic, heteroaromatic and aliphatic nitroalkenes were good substrates for this reaction. The addition of 10 mol% benzoic acid was required to avoid the formation of the bisalkylation product, therefore ensuring that higher yields of the monoalkylated product were obtained. Without the addition of benzoic acid, a bisalkylated byproduct for **16a** was obtained in 40 % yield. The acid suppressed this byproduct without erosion of enantioselectivity. Non-polar solvents (DCM, toluene) were found to be optimum for this reaction with toluene giving the best results.

1.2.3 Diels-Alder reaction

The Diels-Alder reaction occurs between a conjugated diene and an alkene, usually called the dienophile to form six-membered rings.[41] Organocatalysts have been reported for the asymmetric Diels-Alder reaction.

MacMillan and coworkers developed a chiral amine capable of activating α,β-unsaturated ketones as dienophiles for the asymmetric Diels-Alder reaction.[42] The chiral imidazolidinone (**19**) was applied for the reaction of cyclopentadiene (**18**) with various acyclic enones (Scheme 1.6). Good yields (>78%) and ee (>90%) were obtained for most Diels-Alder products. Modification of the dienophile at R^1 (Me, *n*-Pr, *i*-Pr) had little impact on yields and ee being obtained for the Diels-Alder products. However, substituents present at R^2 had an influence on the yield and ee being obtained for the Diels-Alder adduct. A methyl group at R^2 resulted in a lower ee (61%) for the Diels-Alder product when compared to the ee for ethyl group (90%). An *iso*-propyl substituent at R^2 yielded the Diels-Alder adduct as racemate with a low yield of 24%. This transformation was performed in water which is a green safe medium.

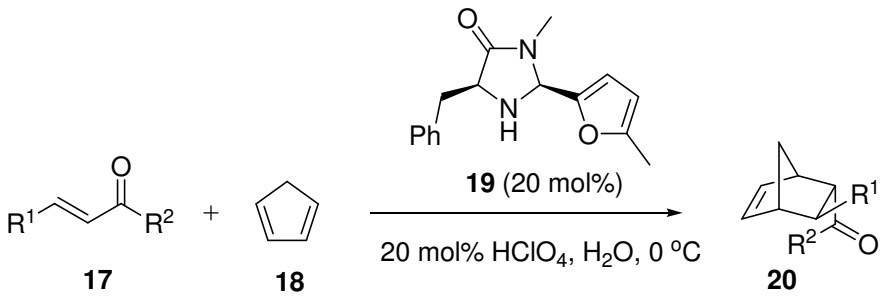

entry	R^1	R^2	% yield	*endo*:*exo*	% ee
20a	Me	Me	85	14:1	61
20b	Me	Et	89	25:1	90
20c	Me	*n*-Bu	83	22:1	92
20d	Me	*i*-Pr	24	8:1	0
20e	*n*-Pr	Et	84	15:1	92
20f	*i*-Pr	Et	78	6:1	90

Scheme 1.6: Organocatalyzed Diels-Alder reaction between cyclopentadiene (**18**) and acyclic enones (**20a-f**) [42]

The chiral amine (**19**) was further evaluated for the cycloaddition between ethyl vinyl ketone (**21**) and a range of dienes (Scheme 1.7). Good yields (>79%) and ee (>85%) were obtained for the alkyl-, alkoxy-, amino-, and aryl-substituted cyclohexenyl ketone products. This reaction was performed in the polar protic solvent ethanol.

MacMillans imidazolidinone catalyst (**19**) has proven to be versatile for the catalysis of various dienes and dienophiles in the asymmetric Diels-Alder reaction.

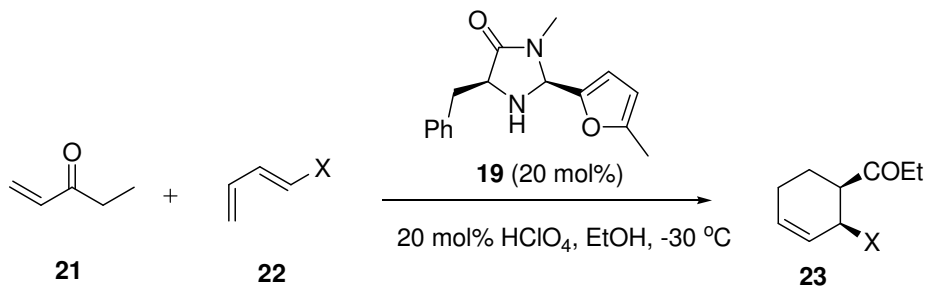

entry	diene	product	*endo*:*exo*	% yield	% ee
23a	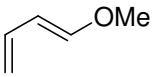	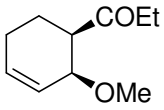	>200:1	88	96
23b	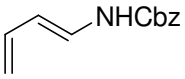	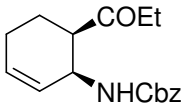	>100:1	91	98
23c	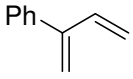	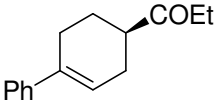	>200:1	92	90
23d	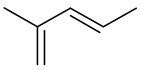	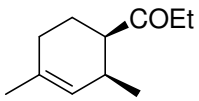	>200:1	90	90
23e	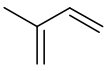	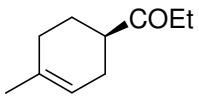	>200:1	79	85

Scheme 1.7: Organocatalyzed Diels-Alder reaction between ethyl vinyl ketone (**21**) and dienes (**23a-e**) [42]

1.2.4 BINOL derivatives as organocatalysts

1.2.4.1 BINOL overview

1,1'-Bi-2-naphthol or commonly referred to as BINOL is an axial chiral biaryl molecule which can be obtained in two enantiomers (Figure 1.2).

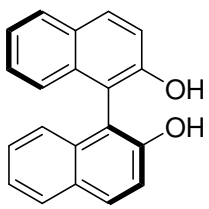

(*S*)-(−)-BINOL

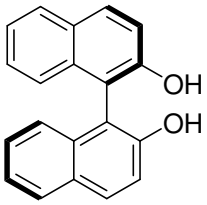

(*R*)-(+)-BINOL

Fig. 1.2 Enantiomers of BINOL

BINOL was first synthesized in racemic form by Von Richter in 1873.[43] Since then, the synthesis and application of BINOL in asymmetric synthesis has been widely reported.[44] Also modified versions of BINOL have been prepared to broaden their catalytic scope.[45] Most of these modifications occur at the 3,3' or 6,6' positions on the BINOL scaffold (Figure 1.3).

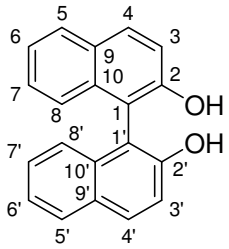

Fig. 1.3 Numbering of BINOL scaffold

There are some examples of polysubstituted BINOLs (where more than one position is modified).[46-53] BINOL and its derivatives have been applied as ligands for transition metal catalysts[44, 45] and more recently as a scaffold for organocatalysts.[30-33]

1.2.4.2 Scaffold for organocatalysts

In 2004, a new class of organocatalysts named the chiral phosphoric Brønsted acid catalysts were independently reported by the research groups of Akiyama and Terada.[54,55] Both groups reported on the phosphorylation of modified BINOL derivatives to yield a chiral phosphoric acid which functions as a Brønsted acid catalyst. Since then, the Brønsted acid activation of imine and carbonyl substrates using chiral phosphoric acids has received great attention especially for reactions like the Mannich, aza-Diels-Alder and aza-Baylis-Hillman.[30-32] In general, reactions involving prochiral basic substrates (imines) that can be activated by general acid catalysis may potentially be activated by chiral phosphoric acids in an enantioselective manner.

Terada and co-workers in their first report described an enantioselective direct Mannich reaction involving various *N*-Boc-protected arylimine derivatives and acetyl acetone catalyzed by phosphoric acid derivatives, a new family of chiral Brønsted acid catalysts.[54] Initially, a selection of catalysts (Scheme 1.8) were evaluated against *N*-Boc-protected arylimine **24** and acetyl acetone (acac) to furnish β-aminoketone **25** in high yields. The enantiomer excess (ee) of products varied depending on catalysts. Absence of bulky substituents at the 3,3'-position of the phosphoric acid catalyst proved detrimental for ee. For instance, using **26b** as catalyst, the product was obtained with an ee of 12% while in the case of **27** an ee of 56% is achieved. The presence of 3,3'-bisaryl substituents for catalysts **28** and **29** increased the ee of product further (90% and 95% respectively).

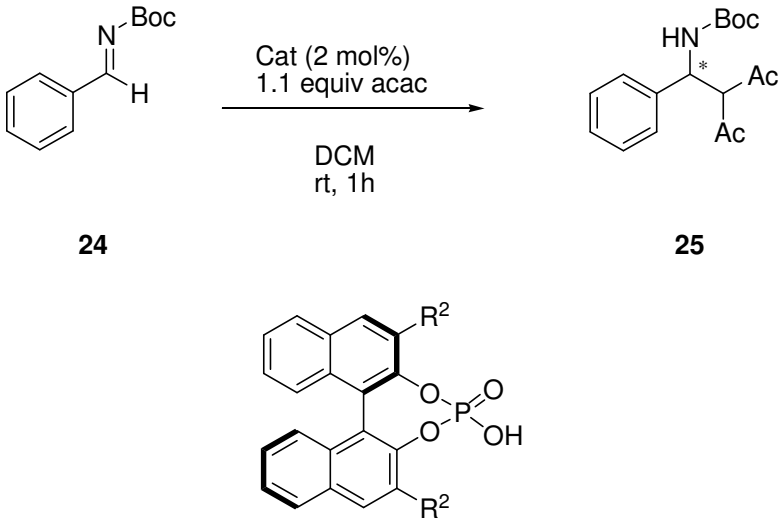

Catalyst	R^2	Yield (%) **25**	ee (%)
26b	H	92	12
27	Ph	95	56
28	4-Biph	88	90
29	4-(β-Naph)-C_6H_4	99	95

Scheme 1.8: Optimization of chiral phosphoric acid catalysts for Mannich reaction.[54]

The highest enantiomeric excess (95%) was obtained with catalyst **29** and was further evaluated against test substrates containing methoxy, methyl and bromo substituents at the *para* position of the phenyl ring to yield the products as in Scheme 1.9. Products (**25a-25d**) were generated with good yields (93-99%) and high ee (90-98%).

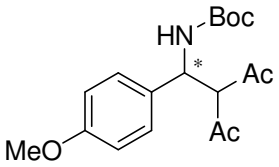

25a

93% yield
90% ee

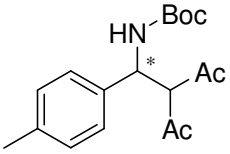

25b

98% yield
94% ee

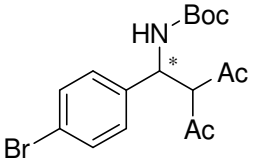

25c

96% yield
98% ee

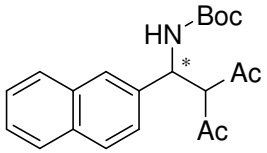

25d

99% yield
92% ee

Scheme 1.9: Chiral products obtained using catalyst **29**.[54]

Akiyama *et al.* reported the enantioselective Mannich-type reaction of silyl enolates with aldimines catalyzed by a chiral Brønsted phosphoric acid.[55] For their initial experiment, they screened aldimine **30** (1 equivalent) and ketene silyl acetal **31** (3 equivalents) with 30 mol% of the chiral phosphoric acid catalysts (Scheme 1.10).

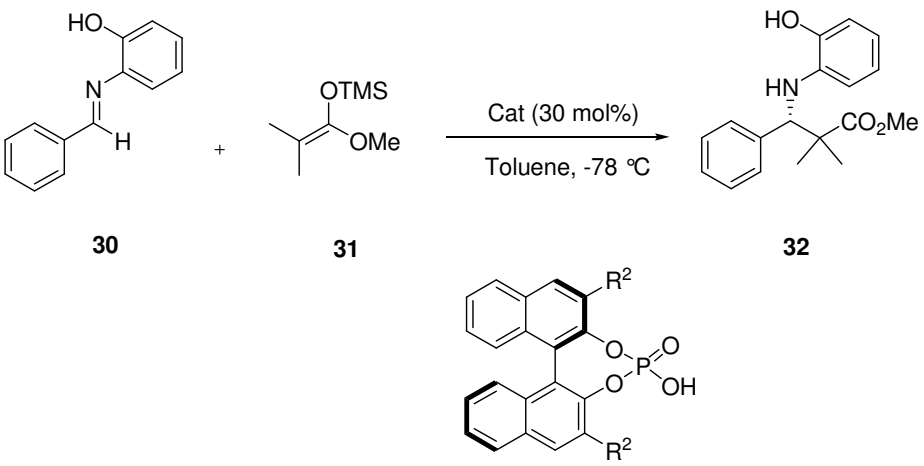

Catalyst	R^2	Time (h)	Yield (%)	ee (%)
26b	H	22	57	0
27	Ph	20	100	27
33	2,4,6-$Me_3C_6H_2$	27	100	60
34	4-$MeOC_6H_4$	46	99	52
35	4-$NO_2C_6H_4$	4	96	87

Scheme 1.10: Optimization of chiral phosphoric acid catalysts [55]

Catalyst **26b** gave a moderate yield albeit with no enantioselectivity. The presence of aromatic groups at the 3,3'-position induced good enantioselectivity. A nitro group at the *para* position of the aromatic ring exerted a significant increase in ee (87%) with high yields (96%) being obtained and the reaction time lowered to 4h. They found that aromatic solvents (e.g. toluene) produced high enantioselectivities, whereas protic solvents (e.g. ethanol) produced racemates. In further optimization reactions the catalyst loading was lowered to 10 mol% with high enantioselectivity being retained.

The reaction scope was further extended with different aldimines and ketene silyl acetals using **35** as catalyst (10 mol%). Products were furnished with good yields, high *syn* selectivity and with excellent enantioselectivity being obtained (Scheme 1.11).

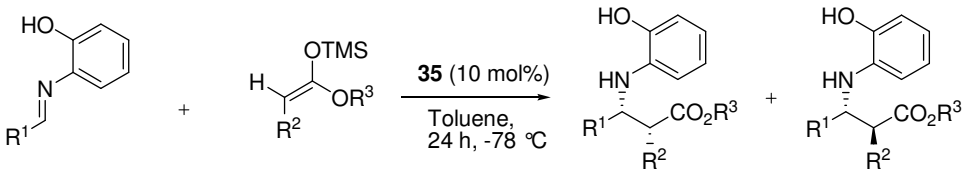

1.5 eq

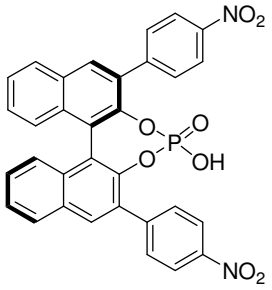

R^1	R^2	R^3	Yield (%)	*syn/anti*	ee (%)-*syn*
Ph	Me	Et	100	87:13	96
p-$MeOC_6H_4$	Me	Et	100	92:8	88
p-ClC_6H_4	Me	Et	100	86:14	83
Ph	$PhCH_2$	Et	100	93:7	91
Ph	Ph_3SiO	Me	79	100:0	91

Scheme 1.11: Enantioselective Mannich-type reaction [55]

1.2.5 Alkylation reactions via chiral phase-transfer catalysis

Chiral phase-transfer catalysis is a synthetic methodology that offers many advantages as it involves mild reaction conditions, simple reaction procedures and the possibility to conduct on large-scale.[56,57] The preparation of optically active α-amino acid derivatives by chiral phase-transfer catalysis with a prochiral protected glycine derivative called *N*-(diphenylmethylene)-glycine *tert*-butyl ester (**36**) (Scheme 1.12) has been achieved by various research groups using chiral organocatalysts.[58]

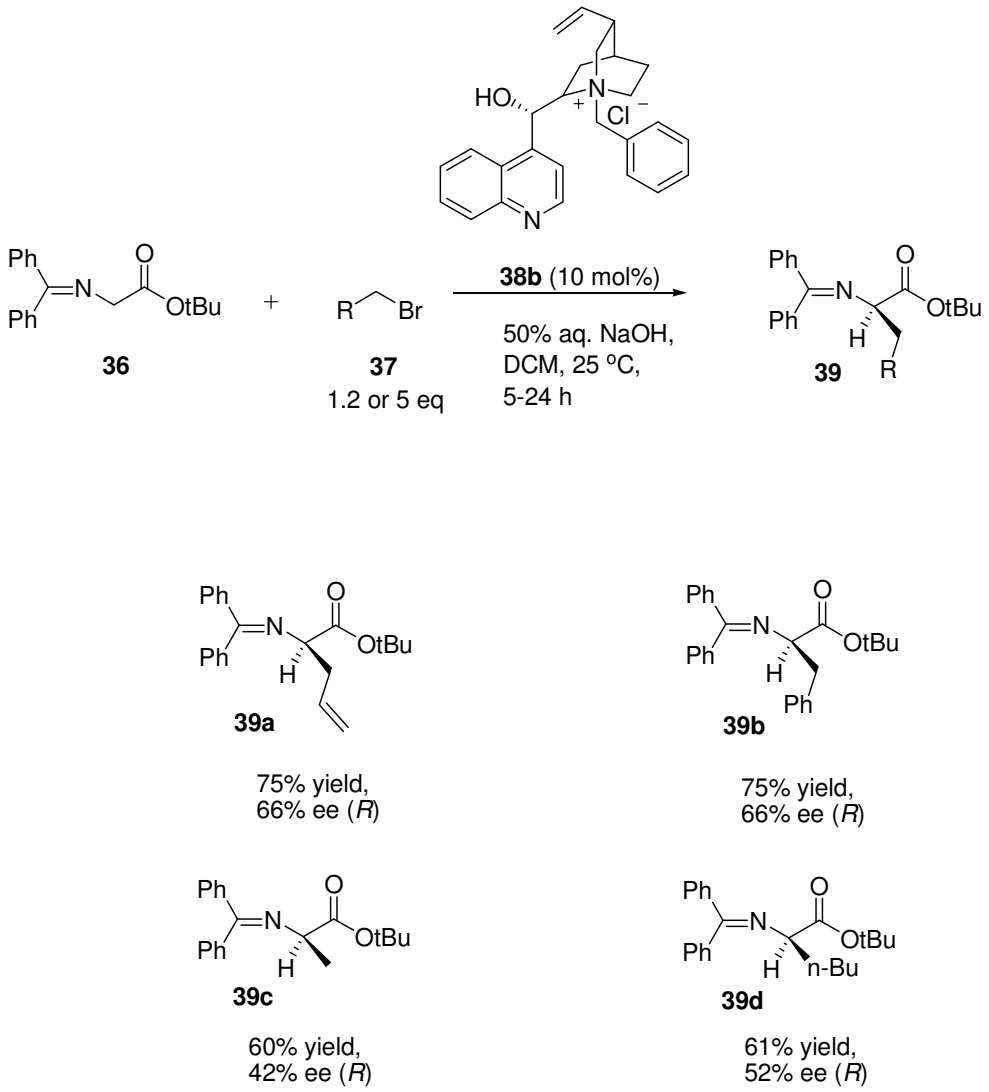

Scheme 1.12: Asymmetric alkylation of **36** with alkyl halides using the phase-transfer catalyst *N*-benzylcinchoninium chloride (**38b**) [59]

The alkylation of the glycine Schiff base ester (**36**) by the *N*-benzylcinchoninium chloride phase-transfer catalyst (**38b**) has been demonstrated by the O'Donnell research group.[59] This transformation leads to the enantioselective synthesis of amino acid precursors, which can furnish enantiopure amino acids subsequent to recrystallisation and acid hydrolysis. O'Donnell cinchonine derived phase-transfer catalyst (**38b**) gave moderate yields (>42%) and ee (>60%) for the alkylated Schiff base ester products (Scheme 1.12). However, they found it possible to obtain enantiopure α-amino acid derivatives by

recrystallisation of the enriched alkylated Schiff base ester products.

Phase-transfer catalysts developed by the Maruoka group have resulted in lower catalyst loadings being employed for the asymmetric alkylation of glycine Schiff base ester (**36**). Maruoka and coworkers have designed and developed a series of chiral phase-transfer catalysts based on the binaphthyl backbone.[60] Quaternary ammonium salt (**40**) (Scheme 1.13) is one example of a phase-transfer catalyst synthesised by the Maruoka research group.

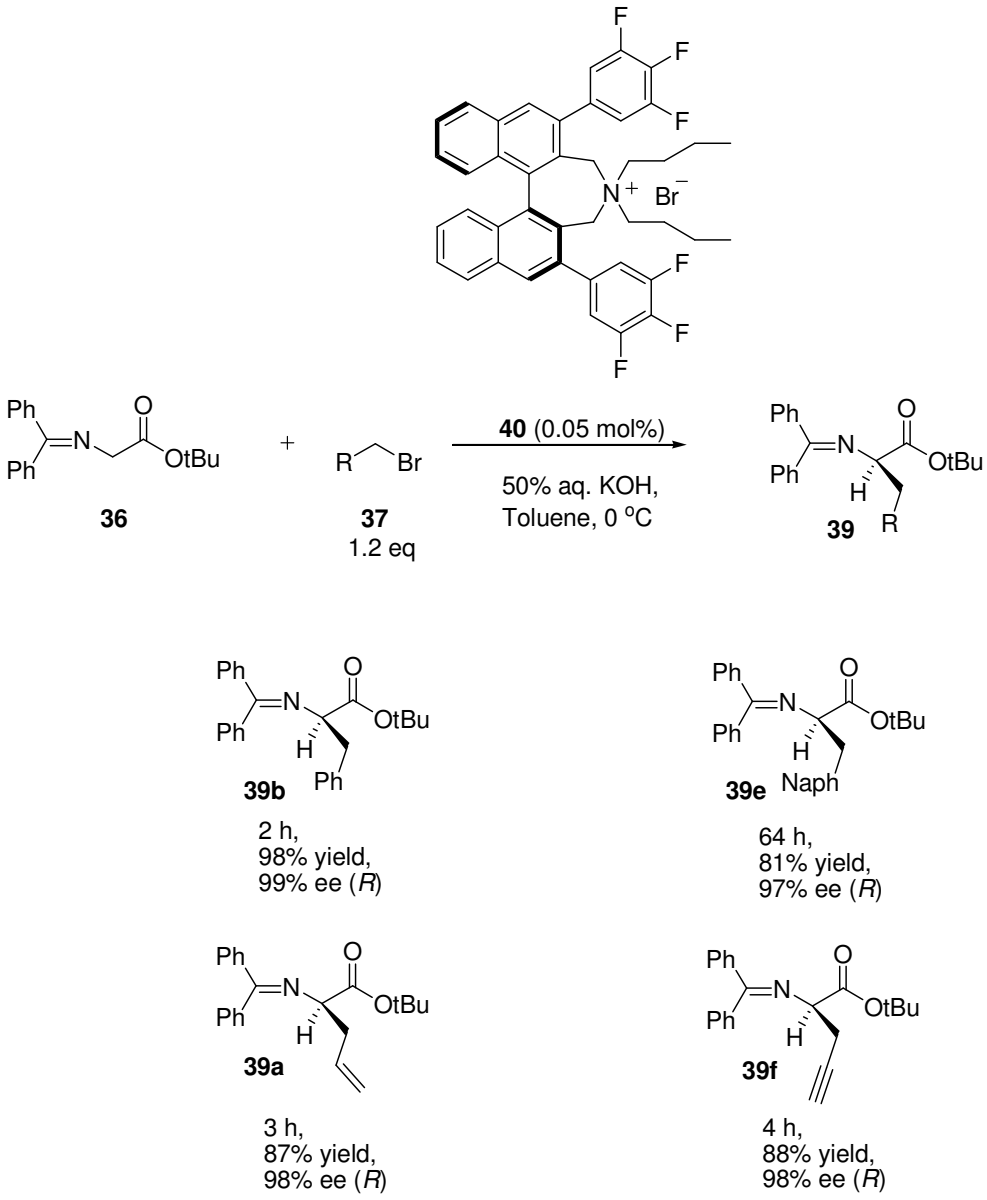

Scheme 1.13: Enantioselective alkylation of **36** using Maruoka catalyst (**40**) [61]

Maruoka catalyst (**40**) was applied for the enantioselective phase-transfer alkylation of prochiral protected glycine derivative (**36**) and was found to be highly effective at a catalyst loading of 0.05 mol%.[61] A range of alkylating agents were evaluated for the alkylation of **36**. High yields (>81%) and good enantioselectivities (>97%) were obtained for the alkylated products (Scheme 1.13).

Organocatalysts have shown great versatility as catalysts for asymmetric synthesis. They have been employed as catalysts for many carbon-carbon, carbon-oxygen and carbon-nitrogen bond forming reactions.[6-13] Their reaction scope continues to expand, evident from the papers being published to date.[6-13] Their inherent advantages over many (but not all) metal based catalysts continue to drive research within the organocatalysis field.

1.3 Environmental Concerns

1.3.1 Toxicity and biodegradation aspects

Considering the number of structures which have been reported as organocatalysts,[6-13] very little information has been reported about their potential environmental impact. In early reports, it was mentioned that organocatalysts were at an advantage to transition metal catalysts on the basis they were non-toxic and environmental benign.[16,25] This statement was made because organocatalysts do not contain a metal and the early examples came from natural molecules such as (*S*)-proline whose environmental impact would be considered negligible. However, as the structures of organocatalysts become more complex than there parent natural molecules due to structural modification for a more efficient catalyst, the environmental profile of the natural or synthetic molecule can not be assumed. For instance, a proline derivative will have a different environmental

impact and toxicological profile than (*S*)-proline. Currently, the design of new organocatalysts is from the perspective of expanding reaction and substrate scope, widening solvent compatibility, achieving recyclability and lowering the catalyst load, giving no consideration to the hazard posed by this new catalyst.[22-24] Considering the importance of green chemistry for a more sustainable chemical industry,[62] the design process for newer organocatalysts should take the 12 Principles of Green Chemistry into account when possible.[63] The relevant principles that organocatalyst design should adhere to are underlined as follows,

1. Prevention: It is better to prevent waste than to treat or clean up waste after it has been created.

2. Atom Economy: Synthetic methods should be designed to maximize the incorporation of all materials used in the process into the final product.

3. Less Hazardous Chemical Syntheses: Wherever practicable, synthetic methods should be designed to use and generate substances that possess little or no toxicity to human health and the environment.

4. Designing Safer Chemicals: Chemical products should be designed to effect their desired function while minimizing their toxicity.

5. Safer Solvents and Auxiliaries: The use of auxiliary substances (e.g., solvents, separation agents, etc.) should be made unnecessary wherever possible and innocuous when used.

6. Design for Energy Efficiency: Energy requirements of chemical processes should be recognized for their environmental and economic impacts and should be minimized. If possible, synthetic methods should be conducted at ambient temperature and pressure.

7. Use of Renewable Feedstocks: A raw material or feedstock should be renewable rather than depleting whenever technically and economically practicable.

8. Reduce Derivatives: Unnecessary derivatization (use of blocking groups, protection/deprotection, temporary modification of physical/chemical processes) should be minimized or avoided if possible, because such steps require additional reagents and can generate waste.

9. Catalysis: Catalytic reagents (as selective as possible) are superior to stoichiometric reagents.

10. Design for Degradation: Chemical products should be designed so that at the end of their function they break down into innocuous degradation products and do not persist in the environment.

11. Real-time analysis for Pollution Prevention: Analytical methodologies need to be further developed to allow for real-time, in-process monitoring and control prior to the formation of hazardous substances.

12. Inherently Safer Chemistry for Accident Prevention: Substances and the form of a substance used in a chemical process should be chosen to minimize the potential for chemical accidents, including releases, explosions, and fires.

Clearly, being a catalyst these molecules satisfy principle 9. However, reports which satisfy principles 3, 4 and 10 are lacking for organocatalysts. Evidently, there is a need for these principles to be applied if organocatalysts are to be classified as truly green reagents and therefore satisfy principle 1. By making these compounds non-toxic and biodegradable a clear advantage will be gained among some of its competitors (transition metal catalysts) and the apparent drawbacks such as high catalyst loading might prove less prohibitive for their transition into industry.

The focus of this project is to design a novel class of green organocatalysts by reducing toxicity and improving biodegradability.

1.3.2 Environmental impact of organocatalysts

At the outset of the project we set out to establish the toxicity, ecotoxicity and biodegradation data currently known in the literature for organocatalysts. A comprehensive literature search was performed on the proline-derived organocatalysts and BINOL organocatalysts and we found a lack of environmental impact data for these compounds. Representative catalysts presented and evaluated in chapter 2 showed no data regarding environmental impact. However, a number of reports were identified regarding the biological activity of some catalysts such as diphenylprolinol, BINOL and BINOL derivatives. These papers are presented in sections 1.3.2.1 and 1.3.2.2.

1.3.2.1 Biological activity of diphenylprolinol (41)

Diphenylprolinol (D2PM) (**41**) has been used as a novel recreational drug and is sold as a legal high in street headshops.[64] It is a phenethylamine analogue that acts as a stimulant with a mechanism of action that may involve inhibition of the dopamine reuptake transporter protein (DAT).[65, 66] D2PM (**41**) has a structure similar to pipradrol which is known to possess a stimulant effect on the central nervous system (CNS) (Figure 1.4).[67]

D2PM (**41**) Pipradrol (**42**)

Fig. 1.4 Structures of D2PM (**41**) and Pipradrol (**42**)

A patent application reported that both enantiomers of diphenylprolinol (**41a** and **41b**) have been shown to have activity at the cocaine binding site on the dopamine transporter protein and the patent also suggests that D2PM (**41a** and **41b**) may be useful in treating cocaine addition.[68] In their study, four prolinol derivatives and a cocaine analogue (−)-2-β-carbomethoxy-3β-(4-fluorophenyl)tropane (CFT) were screened for *in vitro* selectivity and binding potency to the cocaine binding site on the DAT protein (Table 1.1).

$Ki_{binding}$ expresses the compounds ability to bind to the cocaine binding site on the DAT protein and Ki_{uptake} expresses their ability to block dopamine re-uptake into neurons by the dopamine transporter. A lower $Ki_{binding}$ reflects the greater ability of the compound to antagonise cocaine's binding to DAT. A higher Ki_{uptake} reflects the compounds inability to inhibit the functioning of DAT.

In Vitro **activity of CFT and prolinol derivatives**			
Compound	Affinity to the cocaine binding site ($Ki_{binding}$)	Effect on dopamine uptake (Ki_{uptake})	Uptake to binding ratio ($Ki_{uptake}/Ki_{binding}$)
Cocaine analogue CFT	0.12 μM	0.20 μM	1.67
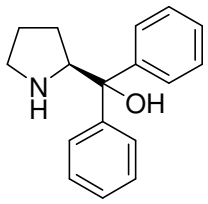 (−)-(*S*)-**41a**	0.40	1.65	4.12
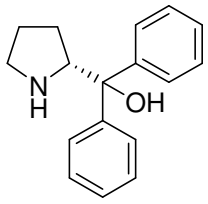 (+)-(*R*)-**41b**	0.04	0.17	4.25
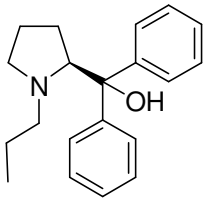 (−)-(*S*)-**43**	3.30	10.3	3.12
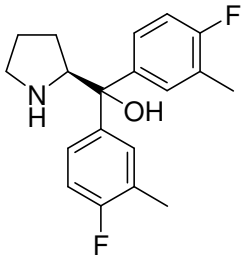 (−)-(*S*)-**44**	0.26	0.44	1.69

Table 1.1: *In Vitro* activity of compounds for DAT [68]

Partial agonists and antagonists of the cocaine binding site on the DAT protein may show efficacy in treating cocaine addiction. Specifically, a cocaine antagonist must bind to the cocaine binding site and not inhibit dopamine re-uptake in order to have potential in the

treatment of cocaine addiction. Prolinol derivatives bind to the cocaine binding site with comparable $Ki_{binding}$ to the cocaine analogue CFT, however, the Ki_{uptake} is higher, a uptake to binding ratio of at least 2 or greater suggests these compounds could antagonize cocaine's binding to the DAT while having a minimal effect on transport function.

Later reports on D2PM (**41**) suggest that it does exhibit biological activity for the CNS as D2PM (**41**) has found use as a legal high. A recent report has associated the recreational use of D2PM (**41**) with cardiovascular toxicity.[64] In their report they mention a case where an individual presents himself to the emergency department in a hospital, with high blood pressure and chest pain after ingesting a legal high called 'head candy' which contained the substance D2PM (**41**). Following toxicological analysis of the patient serum they detected the presence of D2PM (**41**) and glaucine at concentrations of 0.17 mg/L and 0.10 mg/L, respectively. Since no reports of cardiovascular toxicity have been made regarding the usage of glaucine, they reasoned that D2PM (**41**) was the cause of the cardiovascular toxic effect.

Recreational usage of D2PM (**41b**) has been reported on a recreational drug website.[69] A user of the drug reports ingesting 25 mg of (*R*)-diphenylprolinol (**41b**), followed by 20 mg six hours later. The user describes a feeling of euphoria after 2 hours with symptoms similar to amphetamines such as jaw clenching, babbling speech and dilated pupils but does not mention any heart problems.

Yoshida and coworkers have shown D2PM (**41a** and **41b**) to produce inhibitory effects on nerve growth factor (NGF)-induced neurite outgrowth.[70] Both enantiomers of D2PM (**41a** and **41b**) induced a dose-dependent cell death in PC12 cells. The IC_{50} values of (*R*)-diphenylprolinol (**41b**) and (*S*)-diphenylprolinol (**41a**) were 1.00 mM and 0.77 mM, respectively, after 24 hours. From their results they suggest that diphenylprolinol may act as a neurotoxin and cause impaired neuronal development.

1.3.2.2 Biological activity of BINOL and BINOL derivatives

A literature search was done to establish current toxicity, ecotoxicity and biodegradation data reported for BINOL. No literature search was performed for metal complexes containing BINOL as a ligand. A few reports have been published regarding the biological activity of BINOL and BINOL derivatives. However, no reports were found for BINOL in relation to environmental impact in terms of ecotoxicity and biodegradation.

A patent application filed in 2007 reported BINOL and BINOL derivatives as inhibitors for the Sir2 enzyme.[71] Sir2 (Silent information regulator 2, Sirtuin) is a NAD+ dependant deacetylase enzyme which has been found to inhibit p53 and activate BCL6 proteins. The tumor suppressor protein p53 responds to DNA damage and when p53 becomes activated it induces the expression of pro-apoptotic genes which promote programmed cell death for cells that would otherwise go on to produce tumors.[71] The activity of p53 depends on acetylation and such acetylation is reversed by Sir2 (inactivated *via* deacetylation on lysine 382). As well, a deacetylated BCL6 results in the inhibition of p53. Therefore, it is important to prevent the deacetylase activity of Sir2 in order to maintain BCL6 and p53 in an acetylated state (Figure 1.5). A functioning p53 allows for apoptosis of damaged cells to occur, therefore preventing tumorigenesis. An effective Sir2 inhibitor maintains the activity of p53 therefore allowing for the apoptosis of damaged cells. The Sir2 enzyme is believed to be implicated in biological conditions and disorders such as cancer (Specifically B-cell lymphomas), HIV/AIDS, silenced genes, metabolism, apoptosis, aging, malaria and infectious disease (e.g. *Trypanosoma brucei* (African sleeping sickness), Leishmaniasis (e.g. *Leishmania infantum*), *Mycobacterium tuberculosis* and Anthrax.[71]

Sir2 reaction products in the absence of a Sir2 inhibitor (I)

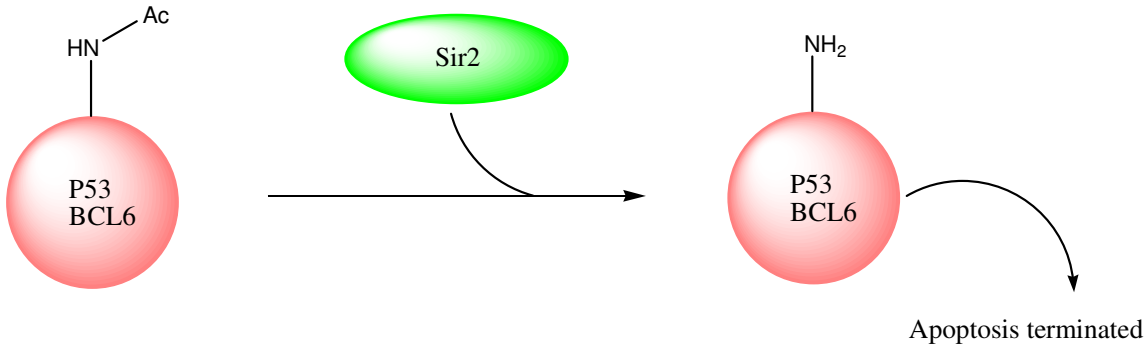

Affect of an inhibitor (I) on Sir2 activity and apoptosis

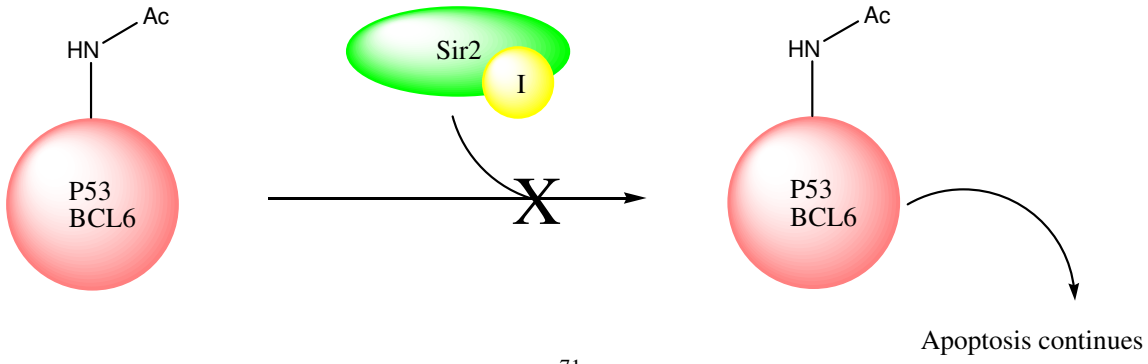

Fig. 1.5 Sir2 activity with/without inhibitor [71]

The patent reported in 2007 describes the development of potent Sir2 inhibitors at the nanomolar concentration.[71] A number of compounds (Figure 1.6) were screened at different concentrations for Sir2 activity.

Initially, a series of naphthyl containing compounds (**45a** and **46a-46e**) were screened at 286 μM for Sir2 inhibition activity (Figure 1.7). Sir2 activity was measured using a HST2-based assay.[71] BINOL (**45a**) was superior at inhibiting Sir2 compared to other naphthyl compounds (Figure 1.7).

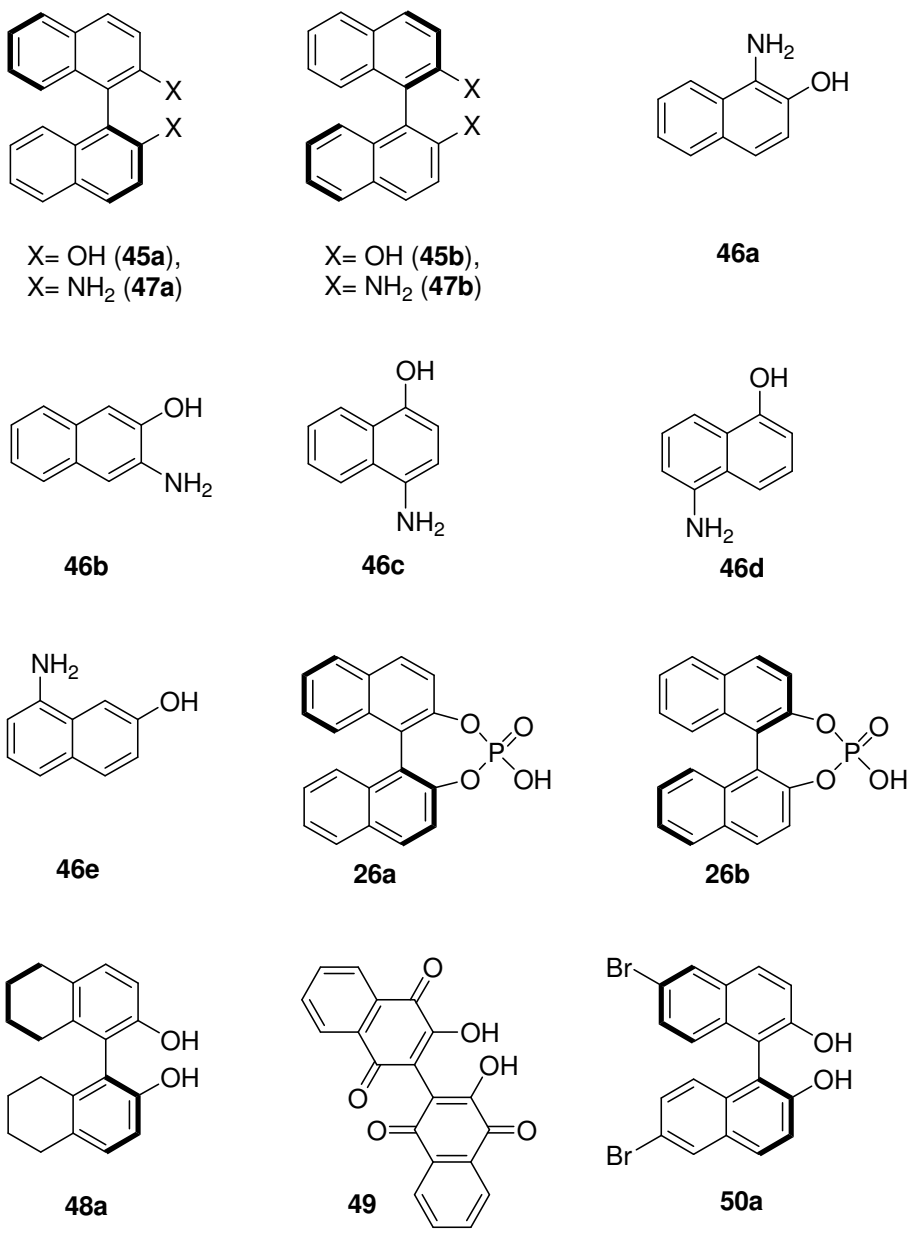

Fig. 1.6 Compounds evaluated as Sir2 inhibitors.[71]

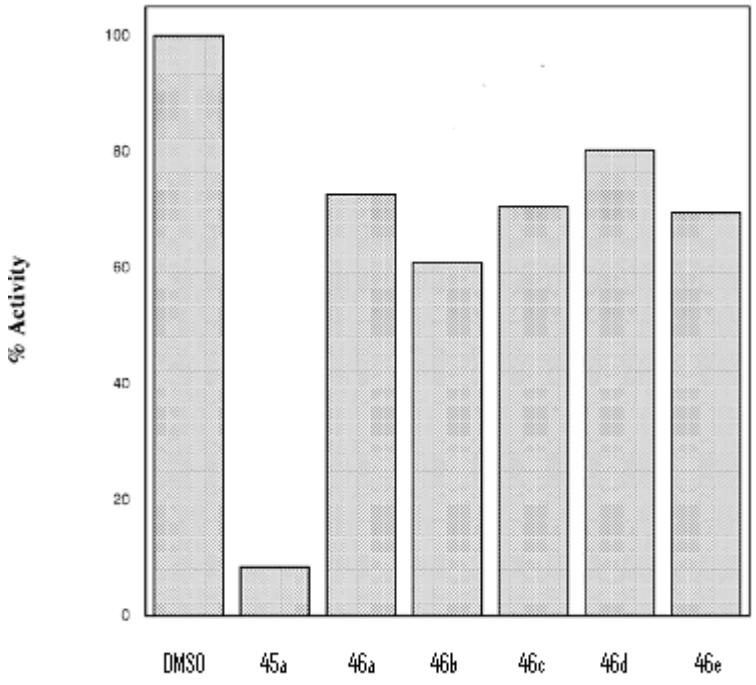

Fig. 1.7 Naphthyl derivatives screened for Sir2 inhibitory activity at 286 μM [71]

Further studies with modified BINOL derivatives (**26a**, **26b**, **45a**, **45b**, **47a**, **47b**, **48a** and **49**) at 143 μM helped to identify important determinants for Sir2 binding. For instance, the aromatic nature and the conformation of the binaphthyl ring system plus substituents at the 2,2'-position had an impact on Sir2 inhibition. The (*S*)-enantiomers of BINOL (**45a**) and the chiral phosphoric acid derivative (**26a**) were more active than the (*R*)-enantiomers (**26b** and **45b**). A primary amine substituent at the 2,2'-position was significantly less active when compared to BINOL. The presence of saturated rings on the BINOL scaffold resulted in lower inhibition for the Sir2 enzyme when compared to BINOL (Figure 1.8).

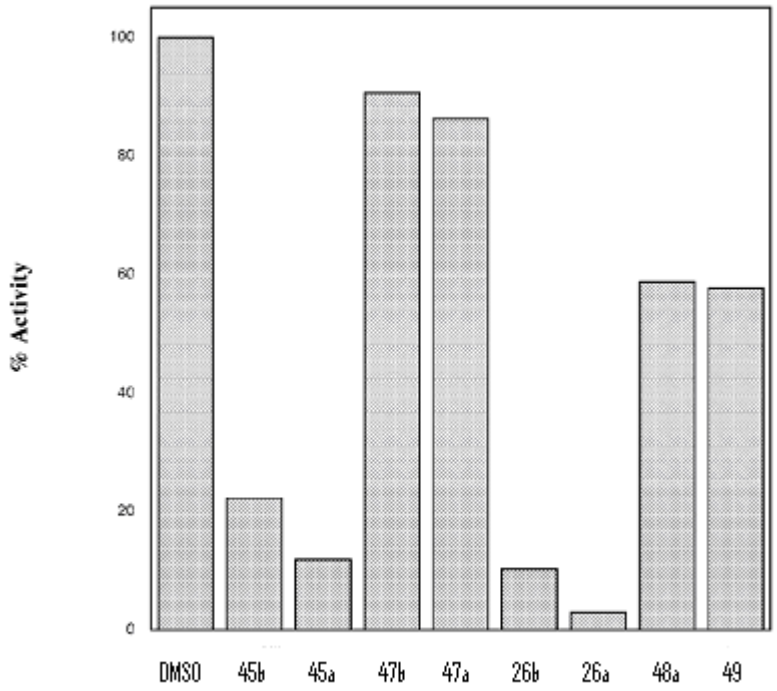

Fig. 1.8 BINOL and BINOL derivatives screened for Sir2 inhibitory activity at 143 μM [71]

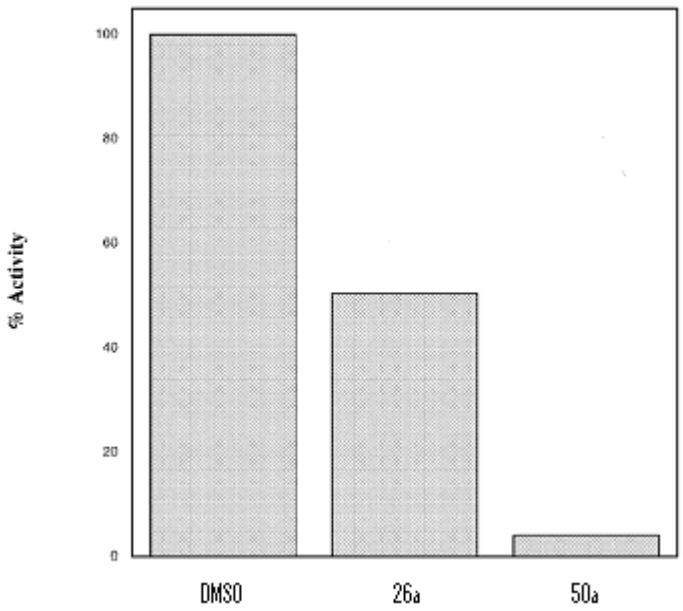

Fig. 1.9 (*S*)-Chiral phosphoric acid (**26a**) and (*S*)-6,6'-dibromoBINOL (**50a**) screened for Sir2 inhibitory activity at 50 μM. [71]

Subsequent to those findings they proceeded with the (*S*)-enantiomers of BINOL derivatives for further studies. The BINOL derivative containing electronegative bromine groups at the 6-position (**50a**) was screened at 50 μM and found to be a potent Sir2 inhibitor (Figure 1.9).

The electron deficient (*S*)-6,6'-dibromoBINOL derivative (**50a**) gave the best inhibition for the Sir2 enzyme.
The authors evaluated (*S*)-6,6'-dibromoBINOL (**50a**) at 500 nM against Ramos cells (an *in vitro* cell line derived from an American Burkitt lymphoma). Ramos cells are a cell model of non-Hodgkins lymphoma (NHL). They found that the acetylation state of BCL6 and p53 for Ramos cells treated with (*S*)-6,6'-dibromoBINOL (**50a**) had increased.[71] They suggest that (*S*)-6,6'-dibromoBINOL (**50a**) could promote apoptosis for Ramos cells.

The structural features required for effective inhibition of the Sir2 enzyme with BINOL derivatives are an *S*-enantiomer, electron deficient unsaturated aromatic rings and the presence of hydroxyl substituents at the 2-position. (*S*)-6,6'-DibromoBINOL (**50a**) was found to be the best inhibitor of the Sir2 enzyme among the BINOL derivatives studied.

Freccero and coworkers have synthesised and evaluated a series of specifically designed BINOL derivatives as photoprecursors for the generation of reactive BINOL quinone methides (BQMs) (Figure 1.10).[72] BQMs are reactive intermediates capable of alkylating DNA which in turn inhibits both DNA replication and gene expression by preventing the melting of the two strands of DNA. Irradiation of BINOL derivatives (**51a-51g**) at 360 nm can lead to the photogeneration of the BQMs. All water soluble BQM precursors (**51a-51g**) were studied for their ability to alkylate and cross link plasmid DNA and oligonucleotides by gel electrophoresis. Sequences analysis by gel electrophoresis, HPLC and MS determined that alkylation occurred for the purines, mainly for guanine. Further studies showed that the BQM was able to alkylate the N7 position of guanines.

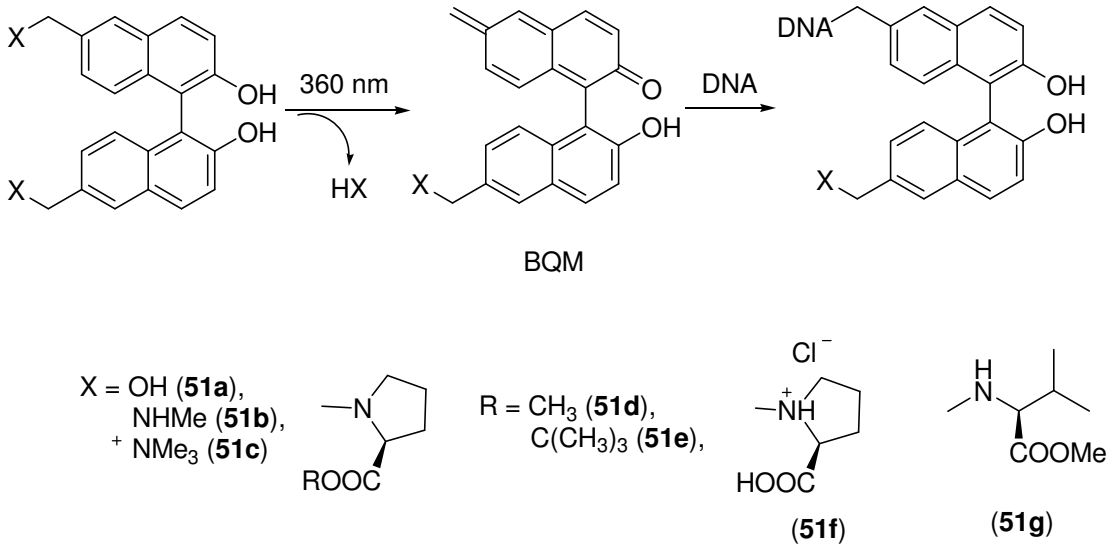

Fig. 1.10 Phototriggerable BINOL derivatives (**51a-51g**) used for generating BQMs for the alkylation of DNA [72]

Photoprecursors (**51a-51g**) were tested for cytotoxic and photocytotoxic effects on two human cancer epithelial cell lines: A549 (human lung adenocarcinoma) and HT-29 (human colorectal adenocarcinoma). Results from their study were defined in terms of EC_{50} values for the effective drug concentration able to kill 50 % of the cell population after photoirradiation and CC_{50} values for the cytotoxic concentration that killed 50% of cell population without photoirradiation. **51e** and **51g** were found to be the most active on both cell lines with EC_{50} values in the high nanomolar range. Compound **51e** gave an EC_{50} value of 0.9 μM for the A549 cell line and 0.5 μM for the HT-29 cell line while **51g** was reported with EC_{50} of 1.2 μM for A549 and 0.2 μM for HT-29. However, these compounds (**51e** and **51g**) exhibited cytotoxicity prior to UV irradiation at low doses. **51e** showed a CC_{50} value of 4.5 μM for A549 and 5 μM for HT-29 while **51g** gave a CC_{50} value of 6.5 μM for A549 and 1.4 μM for HT-29. Compounds **51c** and **51d** were less active for photocytotoxicity with reported EC_{50} values in the low micromolar range (1.5 - 9 μM), however, **51c** was less cytotoxic (CC_{50} value of 200 μM for both A549 and HT-29) than **51d** (CC_{50} value of 20 μM for A549 and 27 μM for HT-29). Remaining

derivatives **51a**, **51b** and **51f** were less active for both photocytotoxicity and cytotoxicity for studied cell lines. Their study determined that the water soluble BINOL derivative (**51c**) was the most promising photocross-linking agent exhibiting purine selectivity and promising phototoxicity versus cytotoxicity.

In an earlier report by Freccero, BINOL derivatives with substituents at the 3-position were reported as phototriggerable DNA alkylating agents. Similar substituents to those shown in Figure 1.10 were placed at the 3-position of BINOL. These compounds were capable of generating quinone methides upon irradiation at 360 nm and were studied for DNA alkylation.[73, 74]

1.3.3 'Rules of thumb': Guidelines for improving biodegradability

The design of biodegradable chemicals is important and confers with the principles of green chemistry. Biodegradable chemicals will not bioaccumulate in the environment therefore reducing the potential toxic effects from the parent molecule and its metabolites.

A chemical substance that proves to be non-biodegradable in the environment could be modified to allow for its degradation, this approach has been achieved for surfactants[75] and ionic liquids.[76,77] Factors that were applied to improve biodegradation of surfactants and ionic liquids were based on the presence of certain structural motifs.

Boethling *et al*. have reviewed and reported a list of structural features that have been observed to improve the biodegradability of chemicals.[78] Structural motifs that have been found to have a positive effect on biodegradability are:

- Benzene rings
- Unsubstituted linear alkyl branches (generally ≥4 carbons)
- Functional groups that are potential sites for enzymes (esters and amides)
- Oxygenated molecules containing hydroxyl, aldehyde, ketone, ethoxylate and carboxylic acid groups

Structural motifs that can have a negative effect on biodegradability are:

- Substituted alkyl branches (especially quaternary carbon)
- Halogen groups (especially fluorine and chlorine)
- Polycyclic residues with more than three fused rings
- Tertiary amine, nitro, nitroso, azo and arylamino groups
- Heterocyclic residues such as imidazole
- Aliphatic ether bonds (except in ethoxylates)

It must be emphasised that the presence of substituents that improve biodegradation will not guarantee biodegradability, as well, the presence of substituents that have a negative effect on biodegradability do not prohibit biodegradation in every case. By designing new compounds with structural motifs that improve biodegradation, it may be possible to minimize or eliminate their impact on the environment.

1.3.4 CO_2 headspace test (ISO 14593)

The CO_2 headspace test (ISO 14593) evaluates the ultimate biodegradation of organic chemicals.[79] Biodegradation of an organic chemical involves metabolism of the parent compound either to a metabolite (referred to as primary biodegradation) or complete mineralisation to innocuous products such as CO_2, water and biomass (referred to as ultimate biodegradation). Using the CO_2 headspace test (ISO 14593) it is possible to assess water insoluble (hydrophobic) and water soluble organic chemicals. This assay is based on the Sturm test [80] and was formed by the amalgamation of independent studies by Struijis and Stoltenkamp [81] and by Birch and Fletcher [82] to give the current CO_2 headspace test (ISO 14593) which was ring tested in 1995.[83] A similar procedure has been adopted as an OECD guideline (method 310) for assessing ready biodegradability of organic chemicals.[84]

The CO_2 headspace test (ISO 14593) is based on the principal that CO_2 is evolved as the organic substance is being mineralised by a microbial community and if the percentage CO_2 evolved is >60% ThIC (theoretical maximum inorganic carbon production) after 28

days, the organic chemical is deemed to be readily biodegradable. A readily biodegradable chemical should pose little impact on the environment due to it being rapidly removed in aquatic environments.

The procedure for the CO_2 headspace test (ISO 14593) involves the addition of the test substance as the sole source of carbon (20 mg C/L) and energy to a mineral salts medium containing a mixed microbial community. The assay is incubated for a period of 28 days in sealed bottles with a headspace of air to facilitate aerobic biodegradation.
Measurements of evolved CO_2 are taken at standard intervals (usually 7 days) over a 28 day period (4 measurements). In order for a chemical to be deemed readily biodegradable it must evolve >60% CO_2 after 28 days. The percentage biodegradation is expressed as a percentage of the theoretical maximum inorganic carbon (ThIC) that would be evolved, if 100% mineralisation of the test substance to CO_2 occurred.

The percentage biodegradation is calculated from the following equation:

$$\% \text{ biodegradation} = (TIC_t - TIC_b)/TOC \times 100$$

Where:

- TIC_t = mg TIC (total inorganic carbon) in bottle at time t
- TIC_b = mean amount (mg) of TIC in blank bottles at time t
- TOC (total organic carbon) = mg TOC initially added to bottle (TOC = ThIC)

The data obtained for % biodegradation is represented by a biodegradation curve as seen in Figure 1.11.

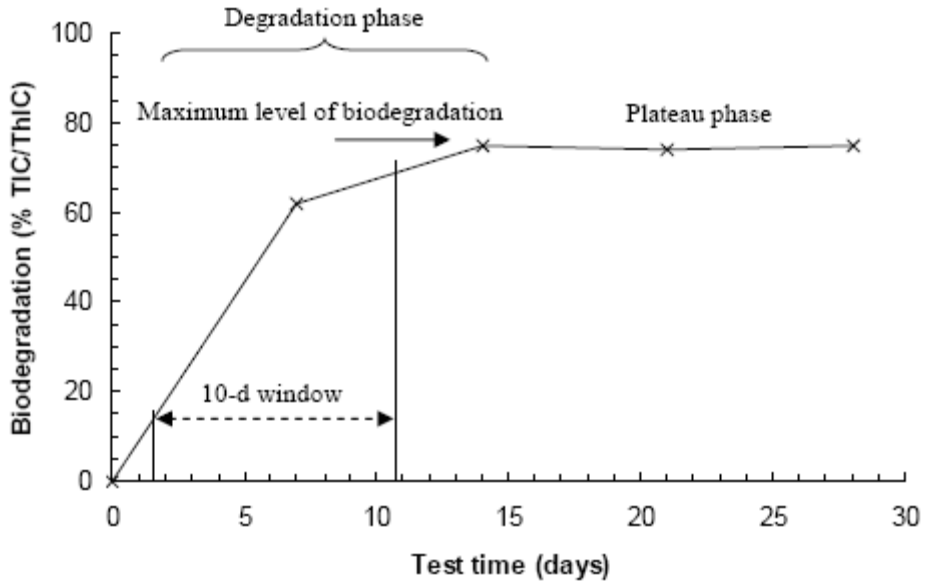

Fig. 1.11 An example of the biodegradation curve using the OECD CO_2 headspace test (method 310). [84]

Time of incubation (days) is represented along the X-axis and % biodegradation along the Y-axis. The 10-day window is the ten days immediately following the attainment of 10% biodegradation.[84] Plateau phase is the phase in which the maximal degradation has been reached and the biodegradation curve has levelled out. A readily biodegradable chemical should give a biodegradation curve similar to Figure 1.11.

In conjunction with the test substance experiments, control experiments are also run. A reference substance (readily biodegradable) such as sodium *n*-dodecyl sulphate (SDS) is tested as a control experiment, this substance will give a pass value (>60% CO_2) within the 28 day timescale and ensures that the inoculum is active. A blank control experiment is also performed, which contains no test substance.

When the organic test substance fails the CO_2 headspace test, this could imply that the sample is inhibitory to the inoculum or is poorly biodegradable. In order to determine if the test substance is inhibitory to the inoculum, an inhibitory control experiment is run whereby the test substance and reference substance (SDS) are added together to the inoculum. An inhibitory effect is apparent when CO_2 evolution has decreased for SDS

biodegradation. The extent to which this occurs, determines whether or not the test substance is inhibiting the activity of the inoculum. However, if the test substance is not inhibiting the inoculum sufficiently (>25% inhibition) and fails the CO_2 headspace test, it implys that the organic chemical is not readily biodegradable.
Surfactants [85] and ionic liquids [77] are examples of chemicals that have been evaluated using the CO_2 headspace test (ISO 14593).

1.3.5 Pyridinium ionic liquids: Designed biodegradable chemicals

Ionic liquids (ILs) are a class of organic chemicals whose environmental impact in terms of toxicity and biodegradation has been investigated.[86] Early examples of ILs were found to be non-biodegradable.[77] However, by applying the principles ('rules of thumb') that were employed for designing biodegradable surfactants, it was possible to design and synthesize biodegradable ionic liquids.

Biodegradable pyridinium ionic liquids have been designed and synthesised by the Scammells research group.[87] Scammells and coworkers were able to manipulate the pyridinium core with substituents that enhance biodegradation. Modification of the pyridinium core occurred at the nitrogen-position (*N*-position) and at the C3-position. They synthesised pyridinium ILs with *n*-butyl, methyl and ethoxycarbonylmethyl substituents at the *N*-position of pyridine while methyl, *n*-butylester and *n*-butylamide substituents were placed at the 3-position of pyridine (Figures 1.12 and 1.15). Pyridinium ILs with different anions such as $OctOSO_3^-$, NTf_2^- and PF_6^- were also prepared. Pyridinium ILs synthesised by Scammells were evaluated for ready biodegradability using the CO_2 headspace test (ISO 14593).[79] Under the guidelines of the CO_2 headspace test (ISO 14593), compounds which reach a biodegradation level higher than 60% CO_2 evolution after 28 days are deemed readily biodegradable.

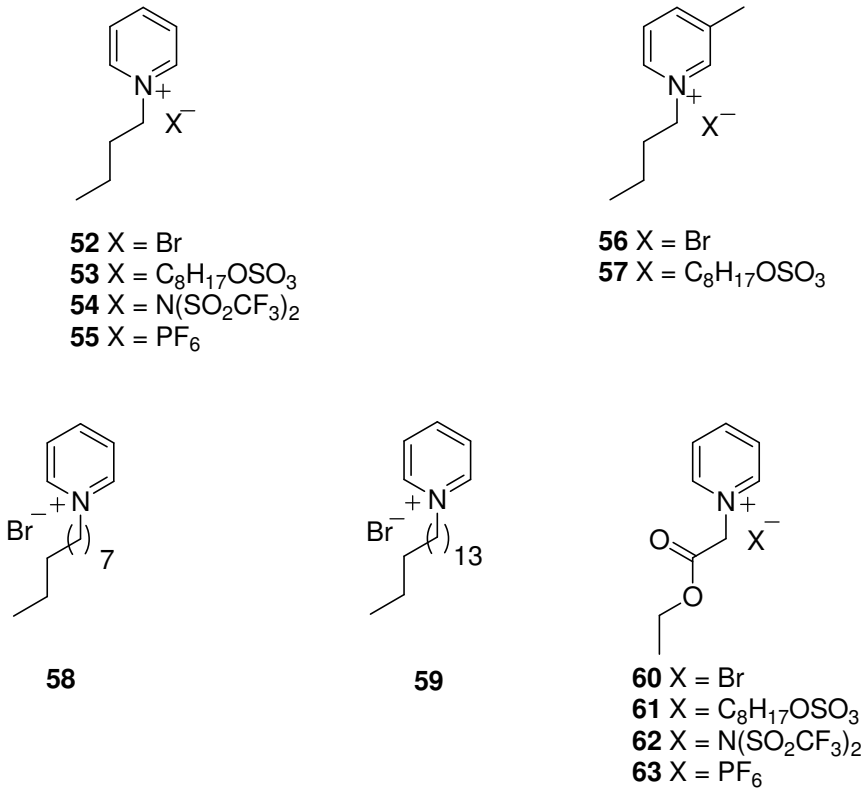

Fig. 1.12 Pyridinium ionic liquids with 1-alkyl and 1-alkylester side chains.[87]

The 1-butylpyridinium salts containing Br^-, NTf_2^- and PF_6^- showed low biodegradability (1-3%) over a 28 day period (Figure 1.13). Introduction of a methyl substituent at the 3-position had little impact on biodegradation (Figure 1.13). However, the presence of the $OctOSO_3^-$ anion for the 1-butylpyridinium salts gave increased levels of biodegradation (37-40%) This result can be attributed to the known biodegradable $OctOSO_3^-$ anion and not to degradation of the pyridinium core. 1-Alkylpyridinium bromides with long alkyl chains C_{10} and C_{16} (**58** and **59**) exhibited poor biodegradability at 9% and 0%, respectively. The introduction of an ester group in the *N*-alkyl substituent leads to ready biodegradable pyridinium ILs (Figure 1.14). Both **60** and **61** showed biodegradability at 87% and 89%, respectively. These compounds (**60** and **61**) also attained ready biodegradability after 7 days (71% and 74%, respectively). ILs **62** and **63** showed ready biodegradability at 64% and 86%, respectively.

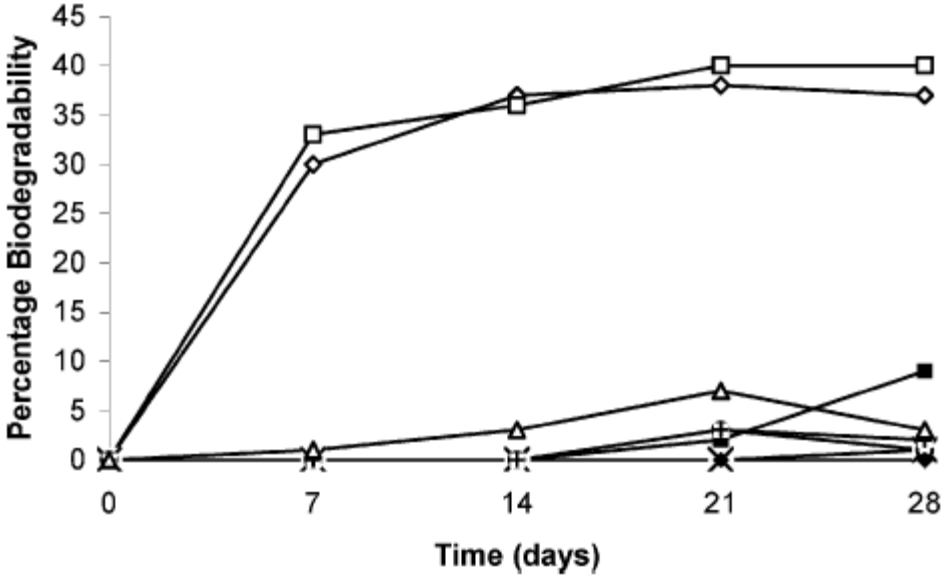

Fig. 1.13 Biodegradation curves for **52** (○), **53** (□), **54** (+), **55** (Δ), **56** (x), **57** (◊), **58** (■) and **59** (♦).[87]

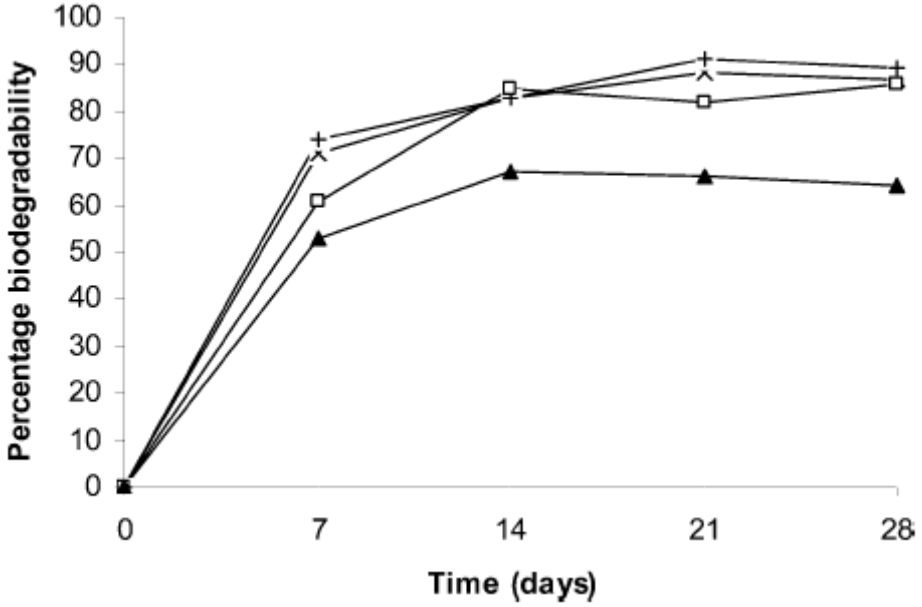

Fig. 1.14 Biodegradation curves for **60** (x), **61** (+), **62** (▲) and **63** (□).[87]

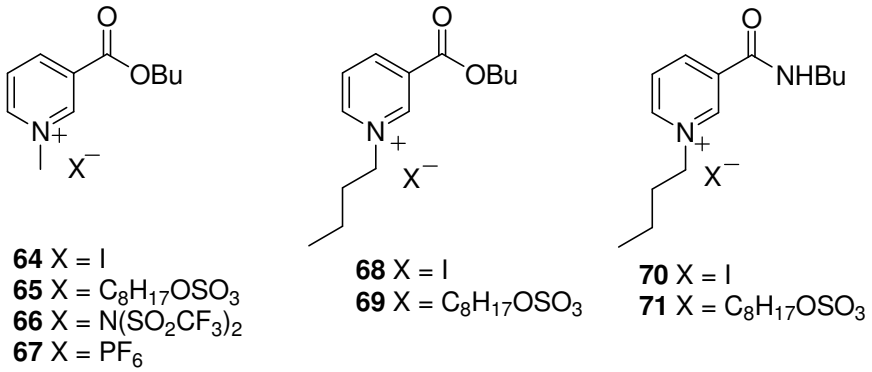

64 X = I
65 X = $C_8H_{17}OSO_3$
66 X = $N(SO_2CF_3)_2$
67 X = PF_6

68 X = I
69 X = $C_8H_{17}OSO_3$

70 X = I
71 X = $C_8H_{17}OSO_3$

Fig. 1.15 Pyridinium ionic liquids derived from nicotinic acid.[87]

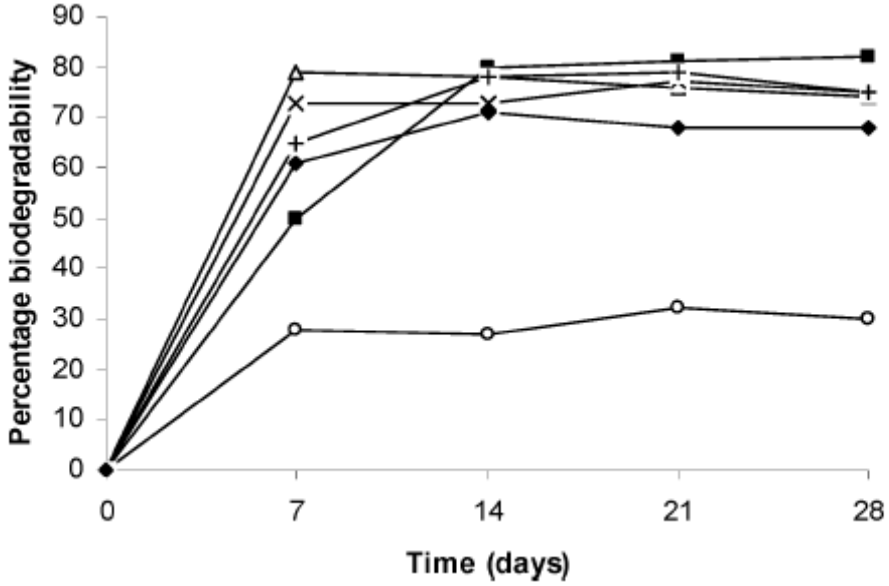

Fig. 1.16 Biodegradation curves for **64** (Δ), **65** (x), **66** (♦), **67** (+), **69** (■) and **71** (○).[87]

A series of pyridinium ILs were made from nicotinic acid which had ester and amide moiety's present at the 3-position of the pyridine ring and alkyl substituents (*n*-butyl and methyl) present at the *N*-position (Figure 1.15). Pyridinium ILs containing ester groups showed high levels of biodegradability. ILs **64**, **66** and **67** gave biodegradation values of 72%, 68% and 75% respectively. (Figure 1.16) The $OctOSO_3^-$ anion containing pyridinium ILs (**65** and **69**) showed biodegradation at 75% and 84% respectively. Pyridinium IL (**71**) containing the amide moiety showed poor biodegradation with a value of 30% being recorded after 28 days.

From Scammells investigations with pyridinium ILs, it is clear that it is possible to enhance poorly biodegradable organic chemicals towards biodegradation by structural modifications that are in line with the 'rules of thumb'.

1.3.6 Similarity of BINOL to Polycyclic Aromatic Hydrocarbons

The main reason for focusing on the BINOL scaffold as part of our study was due to their similarity with polycyclic aromatic hydrocarbons (PAHs) which are known pollutants and contaminants.[88] Polycyclic aromatic hydrocarbons (PAHs) are a class of organic molecules that consist of two or more fused benzene rings in linear, angular or clustered arrangements such as anthracene (**74**) and benzo[a]pyrene (**77**) (Figure 1.17).[89]

PAHs are lipophilic, hydrophobic and have low water solubility. For instance phenanthrene (**73**) has a water solubility of 1.30 mg/L and benzo[a]pyrene (**77**) 0.003 mg/L.[90] PAHs are natural constituents of fossil fuels and can be formed by the incomplete combustion of organic material such as wood and vegetation. Their poor biodegradability, potential carcinogenic, mutagenic and tertagenic properties means they are of high concern for human health and the environment.[91]

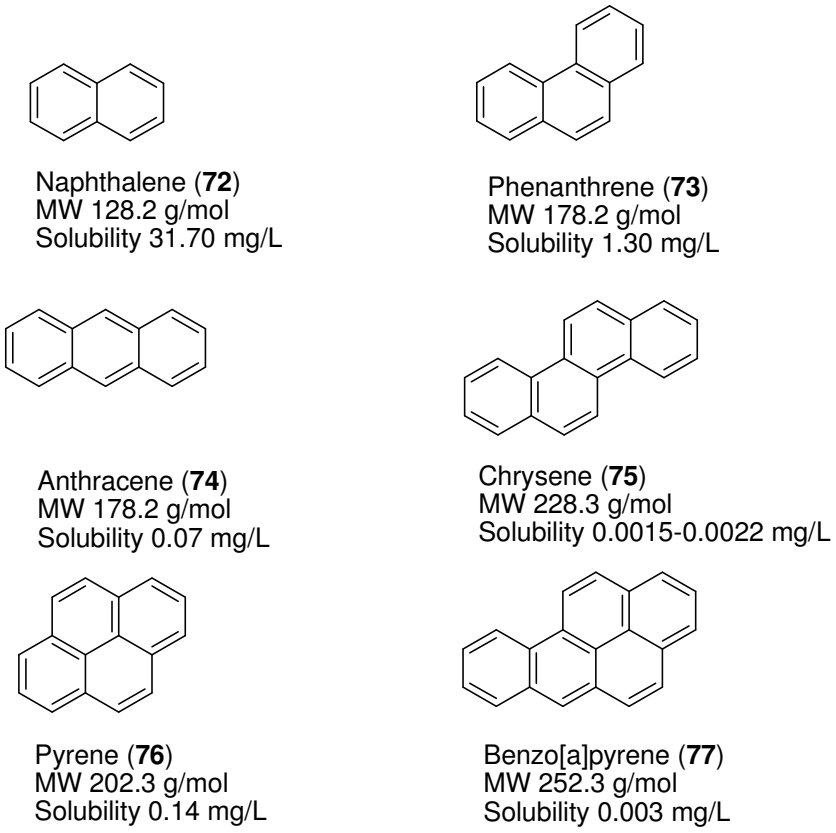

Fig. 1.17 Selection of polycyclic aromatic hydrocarbons (PAHs)

Benzo[a]pyrene (**77**) is a known carcinogen and has been classified as a high priority pollutant by the EPA.[92, 93] The fate of PAHs in the environment can include photo-oxidation, bioaccumulation, adsorption and microbial degradation.[90, 94] Low water solubility and adsorption to the soil are the two major factors that limit PAH bioavailability for biodegradation. BINOL and its derivatives share many features to PAHs such as number of rings, hydrophobicity, poor water solubility and high molecular weight. These similar features will undoubtly impact upon the biodegradability for BINOL. The focus of our work is to determine the biodegradability of BINOL and improve the biodegradability for the biaryl scaffold of BINOL.

1.3.7 Designing non-toxic biodegradable polysubstituted BINOLs

An aim of this project is to design and synthesise BINOL derivatives with substituents which may improve their biodegradation. Currently known BINOL and BINOL derivatives would be expected to have a poor biodegradation profile as many of these compounds have features such as fused rings, quaternary carbons, presence of carbon-halogen bonds, high molecular weight and poor water solubility which would severely limit there biodegradability. For our study, we proposed to apply the 'rules of thumb' to the BINOL scaffold (see section 1.3.3).[78] Structural features that have a positive effect for biodegradation like carboxylic acid and hydroxyl groups were selected for incorporation at position 6,6' of the BINOL scaffold. Combined with a lack of information in the literature for polysubstituted BINOLs (3,3', 6,6' Substituted) a novel set of polysubstituted BINOLs were proposed. These compounds were synthesized in 1-3 steps from a known key intermediate. It is anticipated these compounds would have improved biodegradation properties in the environment.

1.3.8 Historical development of organocatalysts: chiral phase-transfer catalysts and chiral phosphoric acids as a case study

1.3.8.1 Chiral phase-transfer catalysts

The achiral phase-transfer catalyst (**78**) was evaluated by Junggren and coworkers in 1972 for the alkylation of benzylcyanide with various alkyl halides (Scheme 1.14).[95] Monoalkylated products were obtained in good yields (72-90%) within a reaction time of 10-30 minutes by phase-transfer catalysis. Interestingly, the tetrabutylammonium cation has been found to have antimicrobial activity[96], is toxic in aquatic organisms[97], acts as a non-depolarizing muscle relaxant[98] and a potassium channel antagonist.[99]

In 1975, Fiaud reported *N*-benzyl-*N*-methyl ephedrinium bromide (**79**) as a chiral phase-transfer catalyst (PTC) for the alkylation of β-keto esters with claimed ee's of only 15%.[100]

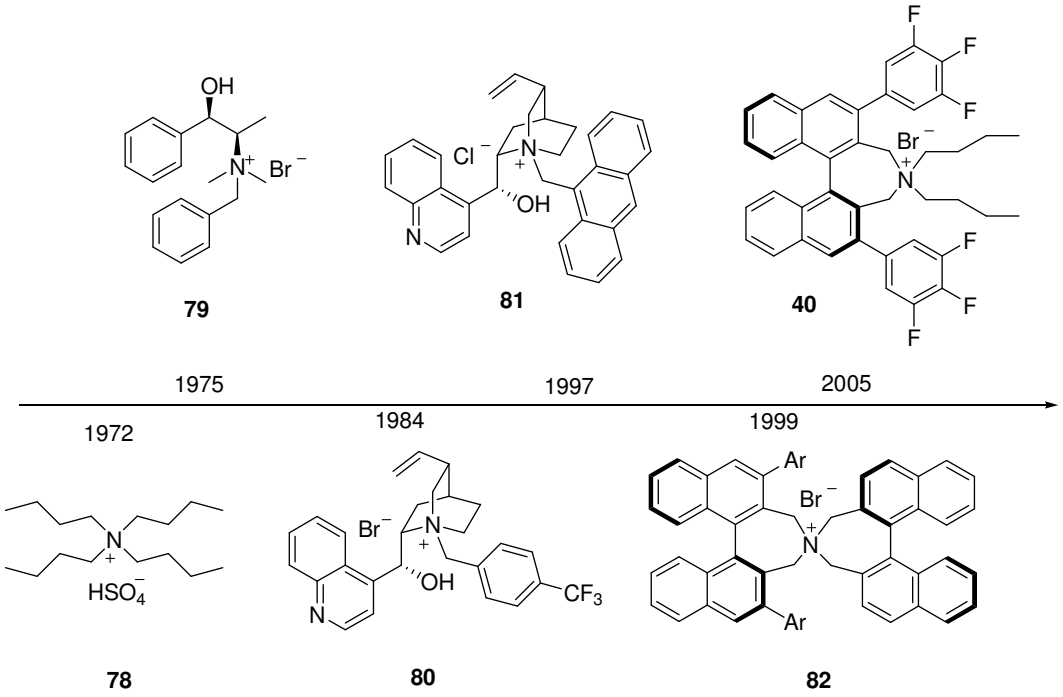

Fig. 1.18 Timeline for phase-transfer catalyst development, from achiral (**78**) to Maruoka catalyst (**40**)

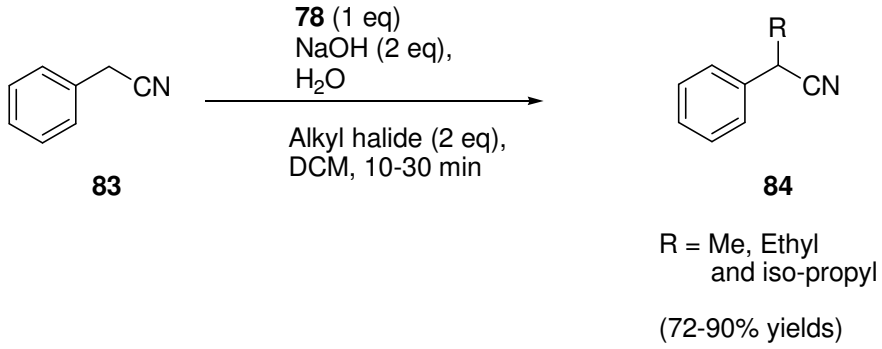

Scheme 1.14: Alkylation of benzyl cyanide using achiral PTC (**78**).[95]

The first efficient chiral phase-transfer catalyst, *N*-(*p*-(trifluoromethyl)-benzyl)cinchonium bromide (**80**), was documented by the Merck group in 1984 for the asymmetric methylation of 6,7-dichloro-5-methoxy-2-phenyl-1-indanone to furnish the

(*S*)-α-methylated indanone in 95% yield and 92% ee.[101] In 1997, a cinchona alkaloid-derived quaternary ammonium phase-transfer catalyst bearing a *N*-anthracenylmethyl function was developed by Lygo and Corey independently.[102,103] Lygo's catalyst (**81**) was evaluated for the asymmetric alkylation of *N*-(diphenylmethylene)-glycine *tert*-butyl ester (**36**) and the corresponding alkylated products were formed with higher enantioselectivity when compared to results obtained with PTC (**80**).[102] Maruoka designed and synthesised phase-transfer catalysts based on the binaphthyl backbone (**40** and **82**) and applied these catalysts for the asymmetric alkylation of *N*-(diphenylmethylene)-glycine *tert*-butyl ester (**36**).[60, 61] For instance, PTC (**40**) was employed at a catalyst loading of 0.05 mol% for the alkylation of **36** with various alkyl halides and the alkylated products were obtained in good yields (81-98%) and high ee (97-98%) (Scheme 1.15).

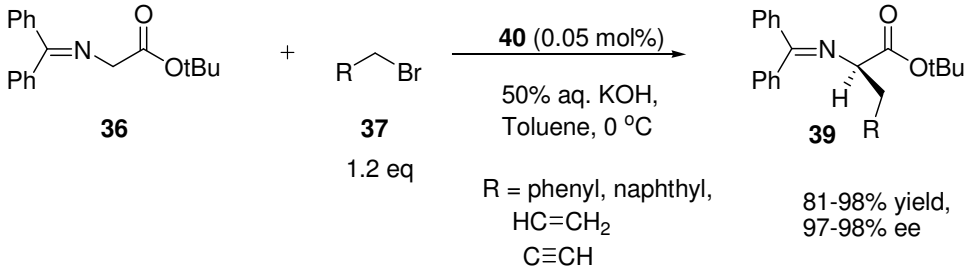

Scheme 1.15: Alkylation of **36** with various alkyl halides using PTC (**40**) [61]

The advantage of the Maruoka catalysts are the low loadings (0.02 - 1 mol%) that can be employed for the alkylation reactions compared to the higher catalyst loadings (generally 10 mol%) used for the cinchona alkaloid-derived phase-transfer catalysts. As can be seen from the timeline (Figure 1.18), the structures of the phase-transfer catalysts from achiral PTC (**78**) to the chiral Maruoka catalyst (**40**) have become more complex. Early examples of chiral phase-transfer catalysts were derived from the chiral pool and were made in one synthetic step. However, more recent examples are not based from the chiral pool and require many steps to be synthesised. The design and development of phase-transfer catalysts has all been based on synthetic performance to date with little consideration for the environmental impact of the catalyst.

1.3.8.2 Chiral phosphoric acid

Chiral phosphoric acids as a class of organocatalysts emerged in 2004 following the independent seminal reports of Terada and Akiyama.[54,55] Terada applied the chiral phosphoric acids (**26b** and **27**) for the Mannich reaction and obtained good yields (92-95%) for products, however, ee was lower when the unsubstituted phosphoric acid catalyst (**26b**) was used. By placing bulky substituents *ortho* to the phosphoric acid moiety such as a phenyl group (**27**) the ee increased for products.[54] Further modification of chiral phosphoric acid with bulkier groups leads to higher ee.

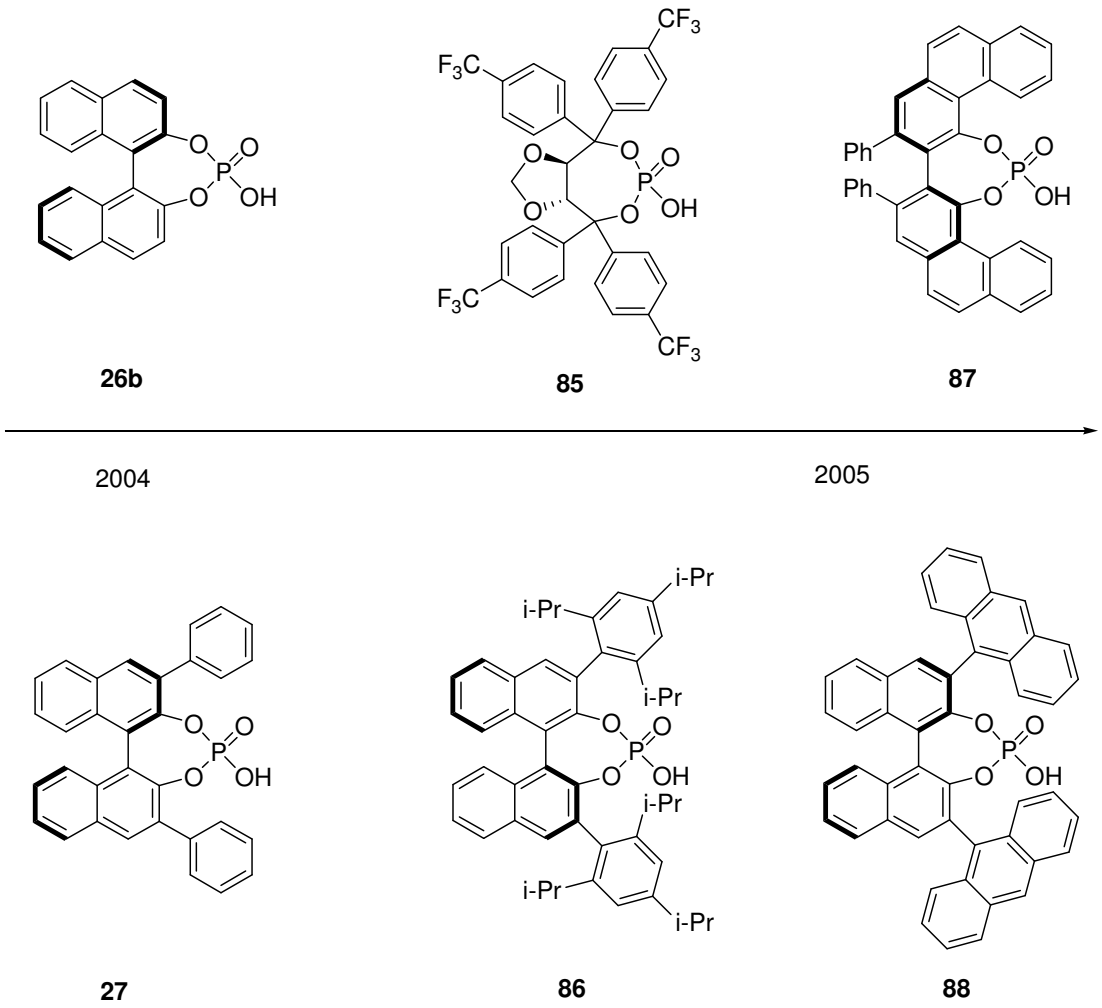

Fig. 1.19 Timeline for development of chiral phosphoric acids

In 2005 a large number of diverse scaffolds were utilised for developing more efficient chiral phosphoric acids in terms of ee. Akiyama reported a chiral phosphoric acid (**85**) derived from TADDOL and applied it for the Mannich reaction with good yields and ee being obtained for the respective products.[104]

TRIP catalyst (**86**) was synthesised by List for the asymmetric transfer hydrogenation of imines, the presence of *iso*-propyl substituents at the *ortho* and *para* positions on the phenyl group were important for obtaining high ee.[105] The chiral VAPOL scaffold was used by Antilla in designing the chiral phosphoric acid (**87**) for a Brønsted acid catalyzed imine amidation with good yields and ee being reported for products.[106]

Terada found the placement of anthracene as a bulky group *ortho* to the phosphoric acid moiety (**88**) beneficial for attaining high ee in the alkylation of α-Diazoester substrates.[107]

As can be seen from the chiral phosphoric acid timeline (Figure 1.19) complexity for the chiral scaffolds has increased. Structural features such as CF_3, substituted rings and polycyclic aromatic hydrocarbons (anthracene and phenanthrene) are not in line with the 'rules of thumb' and may lead to undesirable toxicity and biodegradation.

1.4 Conclusion

Enantioselective organocatalysis, as an asymmetric catalytic methodology has had a major impact on organic synthesis over the past 12 years and has bridged the fields of stereochemistry and pharmaceutically active molecules. Organocatalysts have been found to catalyze a wide variety of carbon-carbon, carbon-nitrogen and carbon-oxygen bond forming reactions. New classes of organocatalysts are still being reported. In early publications one of the prominent advantages of organocatalysts over metal-catalyzed processes was their low toxicity and absence of heavy metal ions contaminating final products or accumulating in the environment. However, there has not been a detailed study of structure-toxicity relationships of organocatalysts. For naturally occurring (*S*)-proline, a low toxicity and environmental impact would be expected, however, the

development of closely related proline derivatives raises question over the toxicity of novel catalysts. The potential toxicity of organocatalysts to humans and other organisms is significant, while ecotoxicity has the potential to limit biodegradation. Reports of diphenylprolinol as a recreational drug and the cytotoxicity data reported for some BINOL derivatives shows the potential hazards for organocatalysts. There is need to investigate the structure-toxicity relationship of organocatalysts. Also the biodegradability of organocatalysts needs to be assessed using biodegradation assays such as the CO_2 headspace test (ISO 14593). Non-biodegradable catalysts could possibly be re-designed according to the 'rules of thumb' for the development of biodegradable alternatives. Toxicity and biodegradation data for organocatalysts will assist in the design of sustainable, efficient catalysts for synthesis and the pharmaceutical industry.

1.5 References

(1) J. M. Hawkins and T. J. N. Watson, *Angew. Chem. Int. Ed.,* 2004, **43**,3224-3228.

(2) J. Halpern and B. M. Trost, *Proc. Natl. Acad. Sci.,* 2004, **101**, 5347-5347.

(3) M. Christmann and S. Bräse, *Asymmetric Synthesis-The Essentials*, WILEY-VCH Verlag GmbH & Co. KGaA, Weinheim, 2008.

(4) T. Ikariya, K. Murata and R. Noyori, *Org. Biomol. Chem.,* 2006, **4**, 393-406.

(5) D. J. Pollard and J. M. Woodley, *Trends Biotechnol.,* 2007, **25**, 66-73.

(6) A. Berkessel and H. Gröger, *Asymmetric Organocatalysis*, WILEY-VCH Verlag GmbH & Co. KGaA, Weinheim, 2005.

(7) P. I. Dalko and L. Moisan, *Angew. Chem. Int. Ed.,* 2001, **40**, 3726-3748.

(8) P. I. Dalko and L. Moisan, *Angew. Chem. Int. Ed.,* 2004, **43**, 5138-5175.

(9) A. G. Doyle and E. N. Jacobsen, *Chem. Rev.,* 2007, **107**, 5713-5743.

(10) M. J. Gaunt, C. C. C. Johansson, A. McNally and N. T. Vo, *Drug Discov. Today,* 2007, **12**, 8-27.

(11) H. Pellissier, *Tetrahedron,* 2007, **63**, 9267-9331.

(12) D. W. C. MacMillan, *Nature,* 2008, **455**, 304-308.

(13) S. Bertelsen and K. A. Jørgensen, *Chem. Soc. Rev.,* 2009, **38**, 2178-2189.

(14) B. List, R. A. Lerner and C. F. Barbas, *J. Am. Chem. Soc.,* 2000, **122**, 2395-2396.

(15) K. A. Ahrendt, C. J. Borths and D. W. C. MacMillan, *J. Am. Chem. Soc.,* 2000, **122**, 4243-4244.

(16) U. Eder, G. Sauer and R. Wiechert, *Angew. Chem. In. Ed.,* 1971, **10**, 496-497.

(17) Z. G. Hajos and D. R. Parrish, *J. Org. Chem.,* 1974, **39**, 1612-1615.

(18) B. M. Trost and C. S. Brindle, *Chem. Soc. Rev.,* 2010, **39**, 1600-1632.

(19) J. M. M. Verkade, L. J. C. v. Hemert, P. J. L. M. Quaedflieg and F. P. J. T. Rutjes, *Chem. Soc. Rev.,* 2008, **37**, 29-41.

(20) N. Mase, R. Thayumanavan, F. Tanaka and C. F. Barbas, *Org. Lett.,* 2004, **6**, 2527-2530.

(21) M. Gruttadauria, F. Giacalone, P. L. Meo, A. M. Marculescu, S. Riela and R. Noto, *Eur. J. Org. Chem.,* 2008, **2008**, 1589-1596.

(22) A. Dondoni and A. Massi, *Angew. Chem. Int. Ed.,* 2008, **47**, 4638-4660.

(23) A. J. A. Cobb, D. M. Shaw, D. A. Longbottom, J. B. Gold and S. V. Ley, *Org. Biomol. Chem.,* 2005, **3**, 84-96.

(24) M. Gruttadauria, F. Giacalone and R. Noto, *Chem. Soc. Rev.,* 2008, **37**, 1666-1688.

(25) L. Xu and Y. Lu, *Org. Biomol. Chem.,* 2008, **6**, 2047-2053.

(26) L. Xu, J. Luo and Y. Lu, *Chem. Commun.,* 2009, 1807-1821.

(27) Z. Jiang, Z. Liang, X. Wu and Y. Lu, *Chem. Commun.,* 2006, 2801-2803.

(28) A. Cordova, W. B. Zou, I. Ibrahem, E. Reyes, M. Engqvist and W. W. Liao, *Chem. Commun.,* 2005, 3586-3588.

(29) T. Marcelli and H. Hiemstra, *Synthesis,* 2010, **2010**, 1229-1279.

(30) S. J. Connon, *Angew. Chem. Int. Ed.,* 2006, **45**, 3909-3912.

(31) T. Akiyama, *Chem. Rev.,* 2007, **107**, 5744-5758.

(32) M. Terada, *Chem. Commun.,* 2008, 4097-4112.

(33) T. Hashimoto and K. Maruoka, *Chem. Rev.,* 2007, **107**, 5656-5682.

(34) B. Trost, *Science,* 1991, **254**, 1471-1477.

(35) B. M. Trost, *Angew. Chem. Int. Ed.,* 1995, **34**, 259-281.

(36) R. Mahrwald (ed.), *Modern Aldol Reactions*, 2 Vols, Wiley-VCH Verlag GmbH, Weinheim., 2004, 1218-1223.

(37) H. Yang and R. G. Carter, *Org. Lett.,* 2008, **10**, 4649-4652.

(38) H. Yang, S. Mahapatra, P. H. Cheong and R. G. Carter, *J. Org. Chem.,* 2010, **75**, 7279-7290.

(39) H. Gotoh, H. Ishikawa and Y. Hayashi, *Org. Lett.,* 2007, **9**, 5307-5309.

(40) H. Huang and E. N. Jacobsen, *J. Am. Chem. Soc.,* 2006, **128**, 7170-7171.

(41) H. B. Kagan and O. Riant, *Chem. Rev.,* 1992, **92**, 1007-1019.

(42) A. B. Northrup and D. W. C. MacMillan, *J. Am. Chem. Soc.,* 2002, **124**, 2458-2460.

(43) V. Von Richter, *Chem. Ber.,* 1873, **6**, 1252.

(44) J. M. Brunel, *Chem. Rev.,* 2005, **105**, 857-898.

(45) Y. Chen, S. Yekta and A. K. Yudin, *Chem. Rev.,* 2003, **103**, 3155-3212.

(46) T. Akiyama, Y. Honma, J. Itoh and K. Fuchibe, *Adv. Synth. Catal.,* 2008, **350**, 399-402.

(47) A. Bähr, A. S. Droz, M. Püntener, U. Neidlein, S. Anderson, P. Seiler and F. Diederich, *Helv. Chim. Acta,* 1998, **81**, 1931-1963.

(48) J. Bunzen, R. Hovorka and A. Lützen, *J. Org. Chem.,* 2009, **74**, 5228-5236.

(49) S. J. Dolman, K. C. Hultzsch, F. Pezet, X. Teng, A. H. Hoveyda and R. R. Schrock, *J. Am. Chem. Soc.,* 2004, **126**, 10945-10953.

(50) X. Huang, L. Wu, J. Xu, L. Zong, H. Hu and Y. Cheng, *Tetrahedron Lett.,* 2008, **49**, 6823-6826.

(51) Z. Li, J. Lin, H. Zhang, M. Sabat, M. Hyacinth and L. Pu, *J. Org. Chem.,* 2004, **69**, 6284-6293.

(52) C. A. Mulrooney, X. Li, E. S. DiVirgilio and M. C. Kozlowski, *J. Am. Chem. Soc.,* 2003, **125**, 6856-6857.

(53) Y. Yamashita, H. Ishitani, H. Shimizu and S. Kobayashi, *J. Am. Chem. Soc.,* 2002, **124**, 3292-3302.

(54) D. Uraguchi and M. Terada, *J. Am. Chem. Soc.,* 2004, **126**, 5356-5357.

(55) T. Akiyama, J. Itoh, K. Yokota and K. Fuchibe, *Angew. Chem. Int. Ed.,* 2004, **43**, 1566-1568.

(56) M. Makosza, *Pure Appl. Chem.,* 2000, **72**, 1399-1403.

(57) T. Hashimoto and K. Maruoka, *Chem. Rev.,* 2007, **107**, 5656-5682.

(58) M. J. O'Donnell, *Acc. Chem. Res.,* 2004, **37**, 506-517.

(59) M. J. O'Donnell, W. D. Bennett and S. Wu, *J. Am. Chem. Soc.,* 1989, **111**, 2353-2355.

(60) T. Ooi, M. Kameda and K. Maruoka, *J. Am. Chem. Soc.,* 1999, **121**, 6519-6520.

(61) M. Kitamura, S. Shirakawa and K. Maruoka, *Angew. Chem. In. Ed.,* 2005, **44**, 1549-1551.

(62) I. T. Horváth and P. T. Anastas, *Chem. Rev.,* 2007, **107**, 2169-2173.

(63) P. T. Anastas and J. C. Warner, *Green Chemistry: Theory and Practice*, Oxford University Press, New York, 1998.

(64) S. Lidder, P. I. Dargan, M. Sexton, J. Button, J. Ramsey, D. W. Holt and D. M. Wood, *J. Med. Toxicol*., 2008, **4**, 167-169.

(65) S. L. Hill and S. H. L. Thomas, *Clin. Toxicol*., 2011, **49**, 705-719.

(66) S. Inagaki, S. Taniguchi, H. Hirashima, T. Higashi, J. Z. Min, R. Kikura-Hanajiri, Y. Goda and T. Toyo'oka, *J. Sep. Sci.*, 2010, **33**, 3137-3143.

(67) P. S. Portoghese, T. L. Pazdernik, W. L. Kuhn, G. Hite and A. Shafi'ee, *J. Med. Chem.*, 1968, **11**, 12-15.

(68) Pyrrolidine derivatives US patent application [webpage on internet]. Patent application by Jackson PF and Guildford Pharmaceuticals; Patent number 5,650,521 [updated 1997 July 22; cited 2008 Feb 19]. Available from: http://v3.espacenet.com/origdoc?CY=gb&LG=en&DB=EPODOC&IDX=US5650521&DOC=dcb65d04ab6724e097530cc48c44ebbb62

(69) Drugs-Forum research chemicals discussion forum [webpage on internet]. Diphenyl-2-Pyrrolidinyl-Methanol (diphenylprolinol) trip reports [updated 2007 Apr 1; cited 2008 Feb 19]. Available from: http://www.drugs-forum.co.uk/forum/showthread.php?t=41534

(70) A. Kaizaki, S. Tanaka, K. Tsujikawa, S. Numazawa and T. Yoshida, *J. Toxicol. Sci.*, 2010, **35**, 375-381.

(71) R. H. Goodman, C. C Fjeld, M. D. Jackson, 1,1'-Binaphthyl-based inhibitors of NAD+ -dependent deacetylase activity and SIR2-family members. PCT Int. Appl. WO 2007124383, 2007

(72) D. Verga, M. Nadai, F. Doria, C. Percivalle, M. Di Antonio, M. Palumbo, S. N. Richter and M. Freccero, *J. Am. Chem. Soc.,* 2010, **132**, 14625-14637.

(73) S. N. Richter, S. Maggi, S. C. Mels, M. Palumbo and M. Freccero, *J. Am. Chem. Soc.,* 2004, **126**, 13973-13979.

(74) F. Doria, S. N. Richter, M. Nadai, S. Colloredo-Mels, M. Mella, M. Palumbo and M. Freccero, *J. Med. Chem.,* 2007, **50**, 6570-6579.

(75) E. Pérez-Carrera, V. M. León, P. A. Lara-Martín and E. González-Mazo, *Sci. Total Environ.,* 2010, **408**, 922-930.

(76) J. Ranke, S. Stolte, R. Störmann, J. Arning and B. Jastorff, *Chem. Rev.,* 2007, **107**, 2183-2206.

(77) D. Coleman and N. Gathergood, *Chem. Soc. Rev.,* 2010, **39**, 600-637.

(78) R. S. Boethling, E. Sommer and D. DiFiore, *Chem. Rev.,* 2007, **107**, 2207-2227.

(79) ISO 14593: Water quality, Evaluation of ultimate aerobic biodegradability of organic compounds in aqueous medium. Method by analysis of inorganic carbon in sealed vessels (CO_2 headspace test), 1999.

(80) R. Sturm, *J. Am. Oil Chem. Soc.,* 1973, **50**, 159-167.

(81) J. Struijs and J. Stoltenkamp, *Ecotoxicol. Environ. Saf.,* 1990, **19**, 204-211.

(82) R. R. Birch and R. J. Fletcher, *Chemosphere,* 1991, **23**, 855-872.

(83) N. S. Battersby, *Chemosphere,* 1997, **34**, 1813-1822.

(84) OECD *Guidelines for the testing of chemicals, Method* 310: Ready Biodegradability-CO_2 in sealed vessels (Headspace Test), 2006.

(85) H. A. Painter, P. Reynolds and S. Comber, *Chemosphere,* 2003, **50**, 29-38.

(86) T. P. Thuy Pham, C. Cho and Y. Yun, *Water Res.,* 2010, **44**, 352-372.

(87) J. R. Harjani, R. D. Singer, M. T. Garcia and P. J. Scammells, *Green Chem.*, 2009, **11**, 83-90.

(88) S. K. Samanta, O. V. Singh and R. K. Jain, *Trends Biotechnol.,* 2002, **20**, 243-248.

(89) S. M. Bamforth and I. Singleton, *J. Chem. Technol. Biotechnol.,* 2005, **80**, 723-736.

(90) S. Husain, *Remediation Journal,* 2008, **18**, 131-161.

(91) G. Mastrangelo, E. Fadda and V. Marzia, *Environ. Health Perspect.,* 1996, **104**.

(92) R. Renner, *Environ. Sci. Technol.,* 1999, **33**, 62A.

(93) A. L. Juhasz and R. Naidu, *Int. Biodeterior. Biodegrad.,* 2000, **45**, 57-88.

(94) R. A. Kanaly and S. Harayama, *J. Bacteriol.,* 2000, **182**, 2059-2067.

(95) A. Brändström and U. Junggren, *Tetrahedron Lett*., 1972, **6**, 473-474

(96) M. L. Ingalsbe, J. D. S. Denis, M. E. McGahan, W. W. Steiner and R. Priefer, *Bioorg. Med. Chem. Lett.,* 2009, **19**, 4984-4987.

(97) D. J. Couling, R. J. Bernot, K. M. Docherty, J. K. Dixon and E. J. Maginn, *Green Chem.,* 2006, **8**, 82-90.

(98) H. Miyakawa, H. Iwasaka, T. Zelles and T. Noguchi, *Brain Res. Bull.,* 2001, **56**, 517-519.

(99) Y. Huang, J. Bourreau, H. Y. Chan, C. Lau, J. W. T. Wong and X. Yao, *Life Sci.,* 2001, **69**, 1661-1672.

(100) J. C. Fiaud, *Tetrahedron Lett*., 1975, **40**, 3495-3496

(101) U. H. Dolling, P. Davis and E. J. J. Grabowski, *J. Am. Chem. Soc.,* 1984, **106**, 446-447

(102) B. Lygo and P. G. Wainwright, *Tetrahedron Lett.,* 1997, **38**, 8595-8598.

(103) E. J. Corey, F. Xu and M. C. Noe, *J. Am. Chem. Soc.,* 1997, **119**, 12414-12415.

(104) T. Akiyama, Y. Saitoh, H. Morita and K. Fuchibe, *Adv. Synth. Catal.,* 2005, **347**, 1523-1526.

(105) S. Hoffmann, A. M. Seayad and B. List, *Angew. Chem. Int. Ed.,* 2005, **44**, 7424-7427.

(106) G. B. Rowland, H. Zhang, E. B. Rowland, S. Chennamadhavuni, Y. Wang and J. C. Antilla, *J. Am. Chem. Soc.,* 2005, **127**, 15696-15697.

(107) D. Uraguchi, K. Sorimachi and M. Terada, *J. Am. Chem. Soc.,* 2005, **127**, 9360-9361.

Chapter 2: Results and Discussion

2 Antimicrobial, cytotoxicity, apoptosis, cell viability and biodegradation studies of known organocatalysts

2.1 Aim

The objective of this study was to determine the anti-microbial activity for known organocatalysts. The outcome of these results would establish the suitability of these compounds for further studies such as biodegradation. Chemicals that show potent anti-microbial activity may have limited biodegradation in the environment. Therefore, a preliminary screen of organocatalysts to determine their anti-microbial activity is necessary before proceeding to a biodegradation assay. The effect of stereochemistry on anti-microbial activity is assessed using both enantiomers of amino acids and BINOLs. Cytotoxicity, apoptosis and cell viability studies are performed to determine the effect of organocatalysts on human blood cell lines. Biodegradability of organocatalysts will be determined using the CO_2 headspace test (ISO 14593).[1]

2.2 Introduction

Data on the environmental impact of organocatalysts is lacking in the literature. In order to design and develop non-toxic, biodegradable organocatalysts that are sustainable, a structure toxicity relationship needs to be established. Our efforts are to determine which organocatalysts are biodegradable and exhibit low toxicity in microbial assays.

A selection of organocatalysts were chosen for this study, amino acids (both L and D), proline derivatives, BINOLs, TADDOL, chiral phosphoric acids, Jacobsen thioureas, MacMillan imidazolidinones, cinchona alkaloid derivatives and a Maruoka phase-transfer catalyst. All catalysts were purchased from Sigma-Aldrich and Strem chemicals.

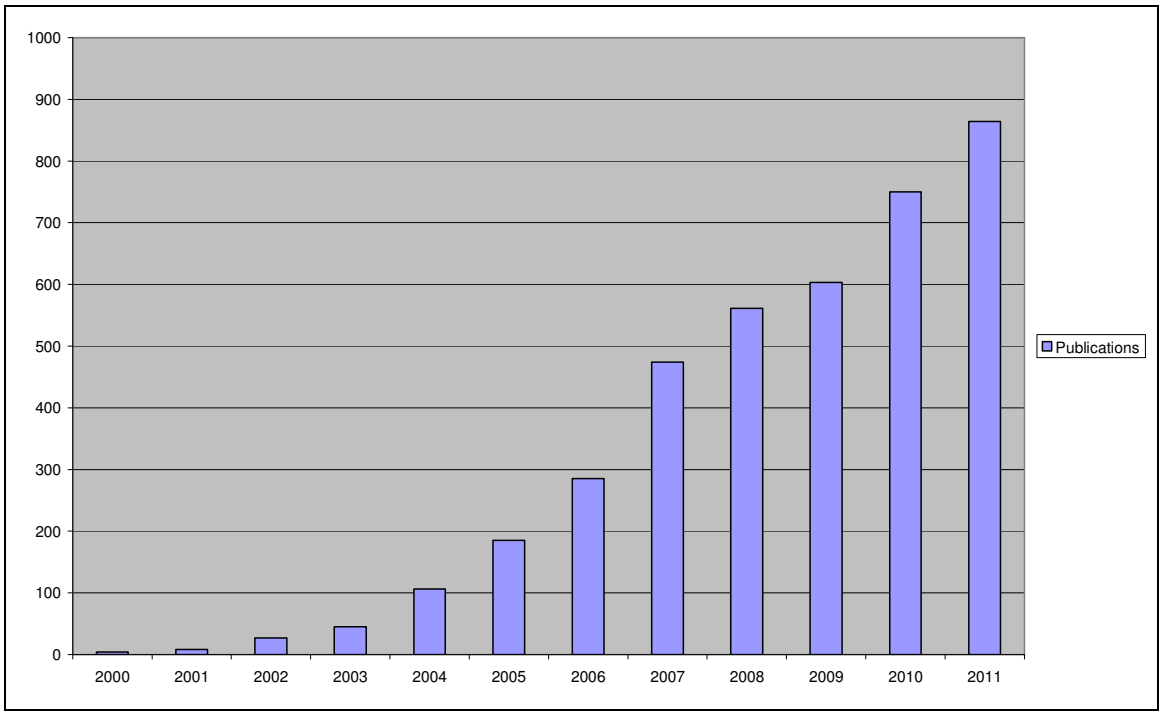

Fig. 2.1 Number of publications containing the concept organocatalysis from 2000-2011 as entered in research topic in Scifinder.

Both L and D enantiomers of amino acids were screened to determine the effect of stereochemistry on anti-microbial activity. Remaining organocatalysts were tested mainly as single enantiomers except for BINOL (**45a** and **45b**), H_8-BINOL (**48a** and **48b**), 6,6'-dibromoBINOL (**50a** and **50b**), 3,3'-dibromo-H_8-BINOL (**105a** and **105b**) and chiral phosphoric acid (**26a** and **26b**) which had both enantiomers screened for antimicrobial activity. A major benefit of organocatalysts is that both enantiomers are available. Enantiomers can exhibit different biological activities. Therefore one enantiomer of an organocatalyst could exhibit anti-microbial activity while the other enantiomer could be environmentally benign. To assess the different effects of enantiomers on anti-microbial activity, we screened both enantiomers of amino acids, BINOL and BINOL derivatives.

Initially, the amino acids (both L and D), proline derivatives, BINOLs and a TADDOL were screened for antibacterial activity (section 2.3). While subsequent antimicrobial studies of a broader range of organocatalysts were performed by our collaborator Dr

Marcel Špulák of Charles University Czech Republic (section 2.4). Antimicrobial studies in our research group were performed using the microtiter broth dilution technique.[2] This assay evaluates the minimum inhibitory concentration (MIC) for a chemical.

2.3 Microtiter broth dilution technique (DCU study)

Antibacterial screening of organocatalysts (amino acids, proline derivatives, BINOLs and TADDOL) for our study was performed using the microtiter broth dilution technique.[2] A range of Gram positive and Gram negative bacteria were screened against to determine MIC values. Bacteria used for this screening were as follows

Gram positive	**Gram negative**
Micrococcus luteus 20030	*Escherichia coli* 498
Bacillus subtilis 10	*Pseudomonas fluorescens* 50090
	Pseudomonas putida CP1

Bacillus subtilis is common in soil samples while *Pseudomonas putida CP1* is known to degrade organic compounds (toluene). These organisms were challenged at different concentrations and the MIC value was noted after 24 h incubation.

2.3.1 Antibacterial screening of amino acids

To study the effect of stereochemistry on antibacterial activity both L and D amino acids were screened. Tyrosine was excluded due to poor water solubility. The rationale behind this study was mainly to establish the effect of D-amino acids on our test set of bacteria. A set concentration of 20 mM was chosen to identify inhibitory amino acids. MIC values were determined for those amino acids showing inhibition. MIC values for the amino acid antibacterial study were defined as 100% inhibition of the growth of control. For this study, some amino acids proved non-inhibitory (Table 2.1) and others proved inhibitory for both enantiomers at 20 mM (Table 2.2). MIC values were determined for inhibitory amino acids and the results are presented in table 2.3.

L-alanine	L-threonine
D-alanine	D-threonine
L-valine	L-arginine
D-valine	D-arginine
L-leucine	L-lysine
D-leucine	D-lysine
L-isoleucine	L-proline
D-isoleucine	D-proline
L-methionine	L-glutamine
D-methionine	D-glutamine
L-serine	L-asparagine
D-serine	D-asparagine
4-*trans*-hydroxy-proline	glycine
4-*cis*-hydroxy-proline	

Table 2.1: List of non-inhibitory amino acids

	M.luteus	*B.subtilis*	*E.coli*	*P.fluorescens*	*P.putida*
L-cysteine	**20 mM**	**20 mM**	**20 mM**	**20 mM**	**20 mM**
D-cysteine	**20 mM**	**20 mM**	**20 mM**	**20 mM**	**20 mM**
L-tryptophan	**20 mM**	**20 mM**	**20 mM**	**20 mM**	**20 mM**
D-tryptophan	**20 mM**	**20 mM**	**20 mM**	**20 mM**	**20 mM**
L-glutamic acid	**20 mM**	**20 mM**	**20 mM**	**20 mM**	**20 mM**
D-glutamic acid	**20 mM**	**20 mM**	**20 mM**	**20 mM**	**20 mM**
L-aspartic acid	**20 mM**	**20 mM**	**20 mM**	**20 mM**	>20 mM
D-aspartic acid	**20 mM**	**20 mM**	**20 mM**	**20 mM**	>20 mM
L-phenylalanine	**20 mM**	>20 mM	>20 mM	>20 mM	>20 mM
D-phenylalanine	**20 mM**	>20 mM	>20 mM	>20 mM	>20 mM
L-histidine	**20 mM**	>20 mM	>20 mM	>20 mM	>20 mM
D-histidine	**20 mM**	>20 mM	>20 mM	>20 mM	>20 mM

Table 2.2: List of both L and D inhibitory amino acids at 20 mM

	M.luteus	*B.subtilis*	*E.coli*	*P.fluorescens*	*P.putida*
L-cysteine	**5 mM**	**5 mM**	**10 mM**	**10 mM**	**10 mM**
D-cysteine	**5 mM**	**5 mM**	**10 mM**	**10 mM**	**5 mM**
L-tryptophan	**5 mM**	**5 mM**	**10 mM**	**5 mM**	**5 mM**
D-tryptophan	**5 mM**	**5 mM**	**10 mM**	**5 mM**	**5 mM**
L-glutamic acid	**2.5 mM**	**5 mM**	**5 mM**	**2.5 mM**	**2.5 mM**
D-glutamic acid	**2.5 mM**	**5 mM**	**5 mM**	**2.5 mM**	**2.5 mM**
L-aspartic acid	**2.5 mM**	**5 mM**	**5 mM**	**2.5 mM**	>20 mM
D-aspartic acid	**2.5 mM**	**5 mM**	**5 mM**	**2.5 mM**	>20 mM
L-phenylalanine	**20 mM**	>20 mM	>20 mM	>20 mM	>20 mM
D-phenylalanine	**20 mM**	>20 mM	>20 mM	>20 mM	>20 mM
L-histidine	**20 mM**	>20 mM	>20 mM	>20 mM	>20 mM
D-histidine	**20 mM**	>20 mM	>20 mM	>20 mM	>20 mM

Table 2.3: MIC results for inhibitory amino acids

During the course of this screen it became apparent that other research groups had reported in the literature cases for antimicrobial inhibition using amino acids and these papers are presented in section 2.3.2.

2.3.2 Previous antimicrobial studies for amino acids

Nature has selected natural amino acids (L configuration) as building blocks for peptides and proteins in living systems.[3] However, unnatural amino acids (D configuration) have been found in living systems.[4] The natural occurrence of D-amino acids, for example, include D-alanine and D-glutamic acid containing peptidoglycans of bacterial cell walls and D-amino acid containing antimicrobial peptides such as valinomycin (D-valine present).[3,4]

Antimicrobial studies for natural and unnatural amino acids have been reported by various groups throughout the last hundred years. Early reports were confined for the inhibitory effects of a single amino acid towards a single microbe and the reversal of this inhibition by other amino acids. However, more recent reports give the inhibitory effects

for a complete set of D-amino acids against specific bacteria such as *E.coli* and discuss the possible modes of inhibition.

Growth inhibition of a number of microorganisms in minimal medium containing amino acids has been reported by various groups, such inhibition can be reversed by other amino acids.[5-8] Gladstone found that in *Bacillus anthracis* either valine or leucine alone inhibits growth at a concentration of 1 μg/ml but when both are present no inhibition occurred.[5] Tatum showed that *E. coli K12* fails to grow in minimal medium containing valine and that isoleucine counters this inhibition.[6] Beerstecher and Shive reported that the growth of *E.coli* is inhibited by tyrosine and phenylalanine reverses this inhibition in minimal medium.[7] A comprehensive screen of various amino acids against 356 *E.coli* strains was reported by Rowley.[8]

The effects for L-valine inhibition in *E. coli K12* were reviewed by De felice and coworkers.[9] Growth inhibition of *E. coli K-12* by L-valine is due to the inhibition of the enzyme acetohydroxy acid synthase. This inhibition, in turn, leads to L-isoleucine starvation which results in the inhibition of growth for *E.coli K12*.

For D-amino acids, early reports for inhibition of specific bacteria were shown using a single amino acid. Fox *et al.* reported the effects of D-leucine, an unnatural amino acid, on the growth of *Lactobacillus arabinosus*.[10] Their experiments demonstrated that D-leucine inhibited the growth of *Lactobacillus arabinosus*. D-Serine has been found to produce toxic effects in various groups of organisms. Among bacteria it prevents the growth of *Streptococcus faecalis R*,[11] *E.coli* [12] and inhibits the production of tetanus toxin by *Clostridium tetani*.[13]

Recent reports give a more comprehensive account for potential D-amino acid inhibition as a larger set of D-amino acids have been screened against specific bacteria. For cases where inhibition occurs with amino acids, the biochemical nature of this inhibition is discussed. Toxicity of D-amino acids could be due to the erroneous incorporation of D-amino acids into the peptidoglycan layer disrupting its ability to withstand osmotic

pressure.[14] It has been observed that at 20 mM concentration D-methionine, D-tryptophan and D-phenylalanine are incorporated into peptidoglycan layer.

Another mode of inhibition postulated for D-amino acids is their interference for the biosynthesis of certain amino acids. Starvation of these amino acids inhibits the growth of the microorganism. The possibility of D-amino acids being incorporated into polypeptides or proteins is unlikely due to the high fidelity of protein translation.[15]

De pedro and coworkers examined the effect various D-amino acids have on the structure and synthesis of peptidoglycan in *E. coli*.[14] They investigated the accumulation of modified muropeptides in the peptidoglycan of cells grown in the presence of D-amino acids at 20 mM concentrations. This group found that the L-isomers had no effect on the structure of peptidoglycan. Under there conditions (20 mM), D-amino acids (D-methionine, D-tryptophan and D-phenylalanine) had no apparent effect on growth or morphology for organism but caused a severe inhibition for peptidoglycan synthesis and cross-linking possibly leading to a reduction in the amount of peptidoglycan per cell.

Blanquet and coworkers reported the effects D-amino acids have on strains of *E.coli* and *Saccharomyces cerevisiae* with and without deacylase activity.[16] They discussed the role of D-Tyr-tRNA deacylase enzyme as a defence mechanism utilised by *E.coli* and *Saccharomyces cerevisiae* for combating the incorporation of D-amino acids into peptides thus preventing the development of faulty proteins that would lead to cell death. Tyrosyl-tRNA synthetase is known to esterify tRNA with tyrosine in *E.coli*. The resulting D-Tyr-tRNA can be hydrolyzed by a D-Tyr-tRNA deacylase enzyme thus preventing its incorporation into proteins.

Blanquet studied other D-amino acids for toxicity which might be exacerbated by the inactivation of the gene encoding D-Tyr-tRNA deacylase. To determine whether the D-Tyrosyl-tRNA deacylase enzyme protected *E.coli* cells from other amino acids, they studied the effect 18 D-amino acids had on the growth of *E.coli* strains K37 (dtd^+= deacylase present) and K37ΔTyrH (Δdtd= deacylase activity absent). Under there

conditions D-amino acid concentration ranged from 0-25 mM. For the two strains no inhibition of the bacterial growth was observed upon the addition of D-alanine, D-proline or D-arginine. With D-asparagine, D-histidine, D-isoleucine, D-leucine, D-methionine and D-phenylalanine the toxic effect was small and no difference could be noted between strains K37 and K37ΔTyrH. Several D-amino acids such as D-glutamic acid, D-threonine, D-lysine, D-valine and D-cysteine markedly inhibited *E.coli* growth for both strains. Inhibition caused by these amino acids is the result of another mode of action. They found a difference in the behaviours for the two strains in the presence of D-aspartic acid, D-serine, D-glutamine and D-tryptophan which implys that these amino acids attach to tRNA and with the loss of deacylase activity for *E.coli* K37ΔTyrH can exert toxicity due to the creation of faulty proteins.

For *Saccharomyces cerevisiae* (yeast) the toxicity of D-tyrosine also depends on the absence of deacylase activity. They explored the toxicity of 18 D-amino acids for *Saccharomyces cerevisiae* and it was found that only D-leucine toxicity was exacerbated by the inactivation of D-tyrosyl-tRNA deacylase activity.

Dtd-like genes that encode for D-Tyr-tRNA deacylase enzymes are widely distributed in the living world and deacylase homologs are expected to occur in many bacteria as well as in yeasts, nematodes, higher plants, mouse and man. D-amino-acyl-tRNA deacylase activity is present in cells to counteract against the harmful effects of D-amino acid transfer onto tRNA. However, the set of incorporated D-amino acids may vary from one type of cell to another.

Evidently from the papers presented above, there has been literature reported on the antimicrobial activity for amino acids. From the previous studies undertaken, it is clear that different microbes and their respective strains can be inhibited by specific amino acids in minimal medium. The causes for this activity can be due to the inhibition of biosynthesis for amino acids leading to the starvation for that respective amino acid or the erroneous incorporation of D-amino acids into the peptidoglycan layer may also result in antimicrobial toxicity.

In our study, a complete set of amino acids (both L and D enantiomers) were assessed against 5 strains of bacteria (*M.luteus, B.subtilis, E.coli, P.putida* and *P.fluorescens*). Microbial inhibitions observed in our study do not correlate with those reported in the literature. This lack of correlation could be due to different bacterial strains and medium (nutrient broth) being used for our respective assay. For instance, using a complex nutrient broth medium as opposed to a minimal medium may result in not observing antimicrobial activity resulting from the inhibition of amino acid biosynthesis. Inhibitory amino acids that are observed in our study may be the result of the erroneous incorporation of amino acids into the peptidoglycan layer resulting in the loss of cell viability or could be due to other modes of action not known.

2.3.3 Antibacterial screening of proline derivatives

A series of proline derivatives (**5**, **89**, **90**, **91**, **92**, **93**, **94**, **95**, **96** and **97**) were screened as part of our study against the test set of bacteria. Different concentration ranges were used dependant on the chemicals solubility and molecular weight. MIC values for the proline derivative antibacterial study were defined as 100% inhibition of the growth of control. The results in table 2.4 represent MIC values obtained for proline derivatives.

	M.luteus	*B.subtilis*	*E.coli*	*P.putida*	*P.fluorescens*
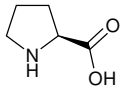 **5**	>8.7 mM	>8.7 mM	>8.7 mM	>8.7 mM	>8.7 mM
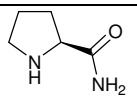 **89**	>8.8 mM	>8.8 mM	>8.8 mM	>8.8 mM	>8.8 mM
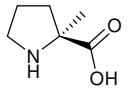 **90**	>7.7 mM	>7.7 mM	>7.7 mM	>7.7 mM	>7.7 mM
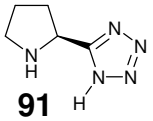 **91**	>7.2 mM	>7.2 mM	>7.2 mM	>7.2 mM	>7.2 mM
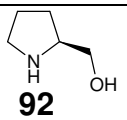 **92**	>9.9 mM	>9.9 mM	>9.9 mM	>9.9 mM	>9.9 mM
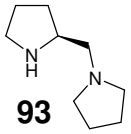 **93**	>6.5 mM	>6.5 mM	>6.5 mM	>6.5 mM	>6.5 mM
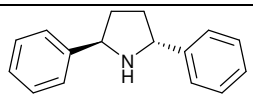 **94**	>3.9 mM	>3.9 mM	>3.9 mM	>3.9 mM	>3.9 mM
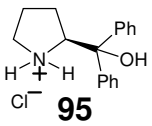 **95**	**3.45 mM**	**3.45 mM**	**3.45 mM**	>3.45 mM	>3.45 mM
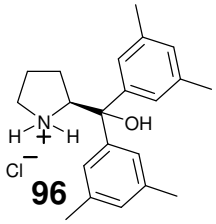 **96**	**0.18 mM**	**0.18 mM**	**1.45 mM**	>2.89 mM	>2.89 mM
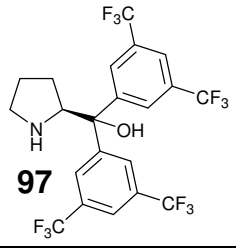 **97**	>1.9 mM	>1.9 mM	>1.9 mM	>1.9 mM	>1.9 mM

Table 2.4: Results from our antibacterial study of proline derivatives

Proline and derivatives (**5**, **89**, **90**, **91**, **92**, **93**, **94** and **97**) were found to be non-inhibitory towards bacteria. Proline derivative (**96**) was observed with the lowest MIC of 0.18 mM for *Micrococcus luteus* and *Bacillus subtilis* while an MIC of 1.45 mM was noted for *E.coli*. An MIC value of 3.45 mM was observed for **95** towards *Micrococcus luteus*, *Bacillus subtilis* and *E.coli*. The presence of methyl substituents at the *meta* position for the aromatic rings of proline derivative (**96**) are contributing to a more toxic compound.

2.3.4 Antibacterial screening of BINOLs and TADDOL

Racemic BINOL (**45**), chiral BINOL derivatives (**98** and **99**) and a TADDOL (**100**) were evaluated using the microtiter broth dilution technique against our panel of bacteria. These compounds have limited solubility in water and were screened at a low concentration. MIC values for the BINOLs and TADDOL antibacterial study were defined as 40% inhibition (IC_{40}) of the growth of control. The results in table 2.5 represent the MIC values obtained for BINOLs and TADDOL. In this study inhibition of bacteria was observed for racemic BINOL (**45**). Remaining chiral BINOL derivatives (**98** and **99**) and TADDOL (**100**) were found to be non-inhibitory for bacteria within tested concentration range. For BINOL (**45**), an MIC value of 0.107 mmol was noted for *Micrococcus luteus* and *Bacillus subtilis* after 24 h while remaining bacteria were not inhibited by BINOL (**45**) within tested concentration range.

	M.luteus	*B.subtilis*	*E.coli*	*P.putida*
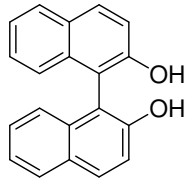 **45**	IC_{40}= 0.107 mM	IC_{40}= 0.107 mM	>1.7 mM	>1.7 mM
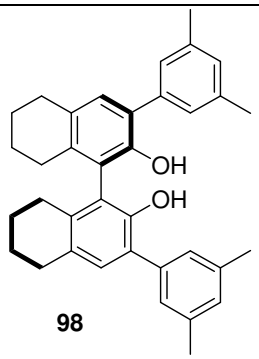 **98**	>0.9 mM	>0.9 mM	>0.9 mM	>0.9 mM
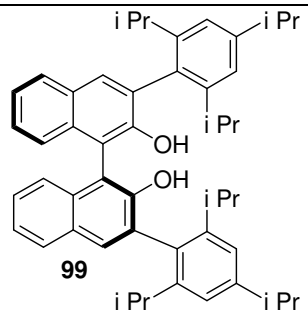 **99**	>0.7 mM	>0.7 mM	>0.7 mM	>0.7 mM
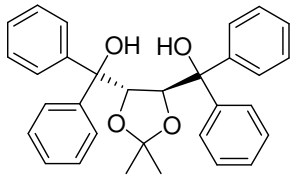 **100**	>1.045 mM	>1.045 mM	>1.045 mM	>1.045 mM

Table 2.5: Antibacterial results for BINOL (**45**), BINOL derivatives (**98** and **99**) and TADDOL (**100**)

2.4 Antimicrobial studies of organocatalysts by our collaborator in Czech Republic

In vitro antimicrobial activities of a broader range of organocatalysts (proline derivatives, chiral BINOLs, TADDOL, Jacobsen thioureas, cinchona alkaloid derived organocatalysts, MacMillan imidazolidinones, chiral phosphoric acids and a Maruoka phase-transfer catalyst) were evaluated by our collaborator Dr Marcel Špulák of Charles University Czech Republic. Organocatalysts were screened against the following bacteria

Staphylococcus aureus ATCC 6538, *Staphylococcus aureus* MRSA HK5996/08, *Staphylococcus epidermidis* HK6966/08, *Enterococcus sp.* HK14365/08, *Escherichia coli* ATCC 8739, *Klebsiella pneumoniae* HK11750/08, *Klebsiella pneumoniae*-**ESBL** positive HK14368/08 and *Pseudomonas aeruginosa* ATCC 9027. MIC values for the antibacterial study were defined as 95% inhibition (IC_{95}) of the growth of control. The highest concentration tested for all organocatalysts was 2000 μM, however, poorly soluble catalysts in test medium were screened at a lower concentration. MIC values were recorded after 24 h and 48 h incubation.

For the *in vitro* antifungal studies, all organocatalysts were screened against the following yeast strains (*Candida albicans* ATCC 44859, *Candida albicans* ATCC 90028, *Candida parapsilosis* ATCC 22019, *Candida krusei* ATCC 6258, *Candida krusei* E28, *Candida tropicalis* 156, *Candida glabrata* 20/I, *Candida lusitaniae* 2446/I, *Trichosporan asahii* 1188) and filamentous fungi (*Aspergillus fumigatus* 231, *Absidia corymbifera* 272 and Trichophyton *mentagrophytes* 445). MIC values for antifungal study were defined as 80% inhibition (IC_{80}) of the growth of control for yeast and 50% inhibition (IC_{50}) of the growth of control for filamentous fungi. The MIC values for most fungi were recorded after 24 h and 48 h except for the dermatophytic strain (*T. mentagrophytes* 445) which was determined after 72 h and 120 h.
Results for antimicrobial study are presented in sections 2.4.1-2.4.12 according to the different categories of organocatalysts.

2.4.1 Antibacterial study of proline derivatives (IC_{95})

A series of proline derivatives (**8**, **41a**, **89**, **91**, **92**, **94**, **97**, **102**, **103** and **104**) were screened by our collaborator against the test set of bacteria for the determination of IC_{95} values. All proline derivatives (Figure 2.2) for this study were tested at the highest concentration range of 2000 μM. The results in the appendix (Table 1) represent the MIC values obtained for proline derivatives (**8**, **41a**, **89**, **91**, **92**, **94** and **97**). Table 2.6 represents the MIC values for proline derivatives (**101**, **102**, **103** and **104**).

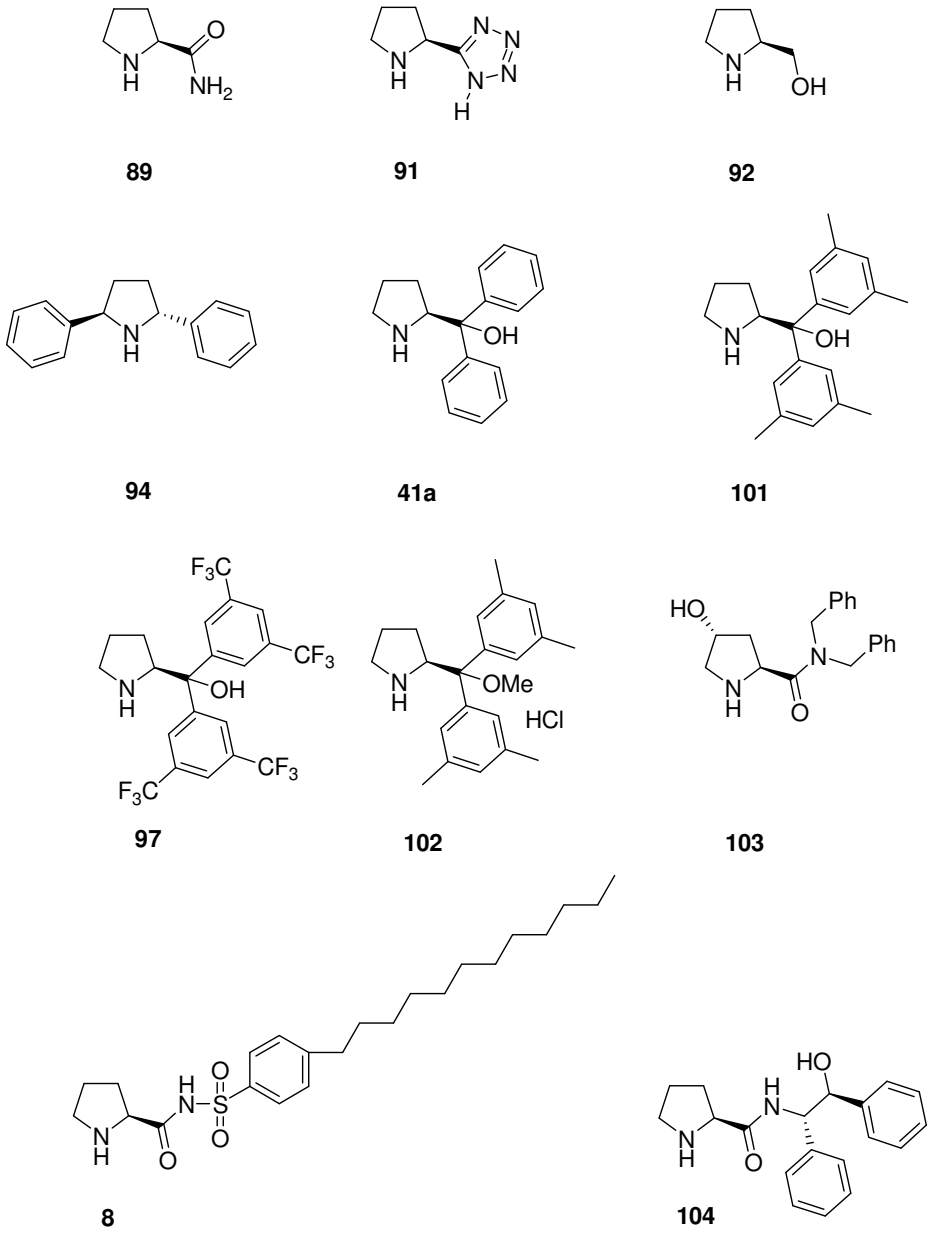

Fig. 2.2 Proline derivatives (**8**, **41a**, **89**, **91**, **92**, **94**, **97**, **101**, **102**, **103** and **104**) screened for IC_{95} antibacterial activity and IC_{80}/IC_{50} antifungal activity

Proline derived catalysts					
Organism	Time (h)	**101**	**102**	**103**	**104**
S.aureus	24 h	**500**	**250**	>2000	>2000
	48 h	**500**	**250**	>2000	>2000
MRSA	24 h	**500**	**250**	>2000	>2000
	48 h	**500**	**250**	>2000	>2000
S.epidermidis	24 h	**500**	**125**	**2000**	>2000
	48 h	**500**	**125**	**2000**	>2000
Enterococcus sp.	24 h	**500**	**125**	**2000**	**2000**
	48 h	**500**	**125**	**2000**	**2000**
E.coli	24 h	**1000**	**1000**	>2000	>2000
	48 h	**1000**	**1000**	>2000	>2000
K.pneumoniae	24 h	**2000**	**1000**	>2000	>2000
	48 h	**2000**	**1000**	>2000	>2000
K.pneumoniae **ESBL** positive	24 h	**>**2000	**2000**	>2000	>2000
	48 h	**>**2000	**2000**	>2000	>2000
P.aeruginosa	24 h	**2000**	**1000**	>2000	>2000
	48 h	**2000**	**1000**	>2000	>2000

Table 2.6: Antibacterial MIC/ IC_{95} (μM) results for proline derivatives (**101**, **102**, **103** and **104**) with antibacterial activity < 2000 μM

Proline derivatives (**8**, **41a**, **89**, **91**, **92**, **94** and **97**) were non-inhibitory for all bacteria (>2000 μM) within tested concentration range. **104** inhibited *Enterococcus sp.* with an MIC value of 2000 μM being observed after 24 h and at 48 h. All remaining bacteria showed low inhibition for **104**. *Staphylococcus epidermidis* and *Enterococcus sp.* were inhibited by **103** with an MIC value of 2000 μM recorded after 24 h and at 48 h. No cases of MIC inhibition were seen for **103** against remaining bacteria.

101 showed low inhibition for *Klebsiella pneumoniae*-**ESBL** positive (>2000 μM). An MIC value of 500 μM was observed for **101** towards Gram positive bacteria (*Staphylococcus aureus*, *MRSA*, *Staphylococcus epidermidis* and *Enterococcus sp.*) after 24 h and at 48 h. *E. coli* was inhibited by **101** with an MIC value of 1000 μM being observed after 24 h and at 48 h. *Klebsiella pneumoniae* and *Pseudomonas aeruginosa* were observed with an MIC value of 2000 μM after 24 h and at 48 h for **101**. Gram positive organisms were slightly more inhibited by **101** than the Gram negative bacteria.

102 gave an MIC value of 125 μM after 24 h and at 48 h for *Staphylococcus epidermidis* and *Enterococcus*. The highest MIC recorded for **102** was against *Klebsiella pneumoniae*-**ESBL** positive (2000 μM after 24 h and at 48 h). *Staphylococcus aureus* and *MRSA* were inhibited by **102** giving an MIC of 250 μM after 24 h and at 48 h. The remaining Gram negative organisms (*E.coli*, *Klebsiella pneumoniae* and *Pseudomonas aeruginosa*) were observed with an MIC value of 1000 μM after 24 h and at 48 h for **102**. Lower MIC values were obtained for **102** against Gram positive bacteria than against Gram negative bacteria.

2.4.2 Antifungal study of proline derivatives

Proline derivatives (**41a**, **89**, **91**, **92**, **94**, **97**, **101**, **102**, **103** and **104**) were screened at 2000 μM while **8** was screened at a lower concentration of 250 μM due to low solubility in test medium (RPMI 1640). The antifungal results in the appendix (Table 2) represent the MIC values obtained for proline derivatives (**8**, **41a**, **89**, **91**, **92**, **94** and **97**). Table 2.7 represents the MIC values for proline derivatives (**101**, **102**, **103** and **104**).

Proline derived catalysts					
Organism	Time (h)	**101**	**102**	**103**	**104**
C.albicans (ATCC44859)	24h	**1000**	**2000**	>2000	>2000
	48h	**1000**	**2000**	>2000	>2000
C.albicans (ATCC90028)	24h	**500**	**2000**	>2000	>2000
	48h	**1000**	**2000**	>2000	>2000
C.parapsilosis (ATCC22019)	24h	**1000**	**1000**	>2000	>2000
	48h	**1000**	**1000**	>2000	>2000
C.krusei (ATCC6258)	24h	**500**	**500**	>2000	>2000
	48h	**500**	**500**	>2000	>2000
C.krusei (E28)	24h	**500**	**500**	>2000	>2000
	48h	**500**	**500**	>2000	>2000
C.tropicalis (156)	24h	**1000**	**1000**	>2000	>2000
	48h	**1000**	**1000**	>2000	>2000
C.glabrata (20/I)	24h	**1000**	**2000**	>2000	>2000
	48h	**2000**	**2000**	>2000	>2000
C.lusitaniae (2446/I)	24h	**125**	**125**	>2000	>2000
	48h	**250**	**125**	>2000	>2000
Trichosporon asahii (1188)	24h	**500**	**500**	>2000	>2000
	48h	**500**	**500**	>2000	>2000
Aspergillus fumigatus (231)	24h	>2000	**2000**	>2000	>2000
	48h	>2000	**2000**	>2000	>2000
Absidia corymbifera (272)	24h	**2000**	**2000**	>2000	>2000
	48h	**2000**	**2000**	>2000	>2000
Trichophyton mentagrophytes (445)	72h	**250**	**2000**	>2000	**2000**
	120h	**250**	**2000**	>2000	**2000**

Table 2.7: Antifungal IC_{80}/IC_{50} (μM) values for proline derivatives (**101**, **102**, **103** and **104**)

89, **91**, **92**, **97** and **103** were all non-inhibitory to the fungal strains within tested concentration range (>2000 μM in RPMI 1640 medium). As well, **8** proved to be non-inhibitory towards test fungal organisms (>250 μM). *Candida albicans* ATCC 90028 and *Candida tropicalis* were inhibited by **94** after 24 h (2000 μM) but recovered at 48 h (>2000 μM). *Trichophyton mentagrophytes* gave an MIC/IC_{50} value of 2000 μM after 72 h for **94** but recovered at 120 h (>2000 μM). All remaining fungal strains were not inhibited by **94**. An MIC value of 2000 μM was noted for **41a** towards *Candida krusei* ATCC 6258 and *Candida tropicalis* after 24 h , however, a recovery was apparent after 48 h (>2000 μM). **41a** showed low inhibition towards remaining fungal strains (>2000 μM). **101** gave the lowest MIC value of 125 μM after 24 h for *Candida lusitaniae* while a recovery was noted after 48 h (250 μM). *Trichophyton mentagrophytes* was inhibited by **101** with an MIC/IC_{50} value of 250 μM being observed after 72 h and at 120 h. An MIC value of 500 μM was seen for **101** towards *Candida krusei* ATCC 6258, *Candida krusei* E28 and *Trichosporon asahii* after 24 h and at 48 h. *Candida albicans* ATCC 90028 and *Candida glabrata* were inhibited by **101** with MIC values of 500 μM and 1000 μM, respectively, after 24 h while at 48 h a recovery was seen as MIC values increased to 1000 μM and 2000 μM, respectively. *Candida albicans* ATCC 44859, *Candida parapsilosis* and *Candida tropicalis* gave an MIC of 1000 μM for **101** after 24 h and at 48 h. **101** inhibited *Absidia corymbifera* with MIC of 2000 μM after 24 h and at 48 h. *Aspergillus fumigatus* was the only fungal organism not to be inhibited by **101** (>2000 μM).

104 inhibited *Trichophyton mentagrophytes* with an MIC of 2000 μM being reported after 72 h and 120 h. All remaining fungi showed low inhibition for **104** (>2000 μM). An MIC value of 2000 μM was noted for **102** towards *Candida albicans* ATCC 44859, *Candida albicans* ATCC 90028, *Candida glabrata*, *Aspergillus fumigatus* and *Absidia corymbifera* after 24 h and at 48 h *Trichophyton mentagrophytes* was inhibited by **102** with an MIC of 2000 μM after 72 h and at 120 h. The lowest MIC value obtained for **102** was 125 μM against *Candida lusitaniae* after 24 h and at 48 h. *Candida krusei* ATCC 6258, *Candida krusei* E28 and *Trichosporon asahii* were inhibited by **102** with an MIC of 500 μM being observed after 24 h and at 48 h. An MIC value of 1000 μM was observed for **102** against *Candida parapsilosis* and *Candida tropicalis* after 24 h and at 48 h.

2.4.3 Antibacterial study of chiral BINOLs and TADDOL

BINOL (**45a** and **45b**) was screened at 500 μM, while BINOL derivatives (**98** and **99**) and TADDOL (**100**) were screened at a lower concentration of 125 μM due to low solubility in test medium (Mueller Hinton) (Figures 2.3 and 2.4). BINOL derivatives (**48a**, **48b**, **50a**, **50b**, **105a** and **105b**) were screened at 2000 μM (Figures 2.3 and 2.4). Brominated BINOL derivatives were selected for this study as they are more lipophilic than unbrominated BINOL derivatives. MIC results for this antibacterial study are presented in tables 2.8 and 2.9.

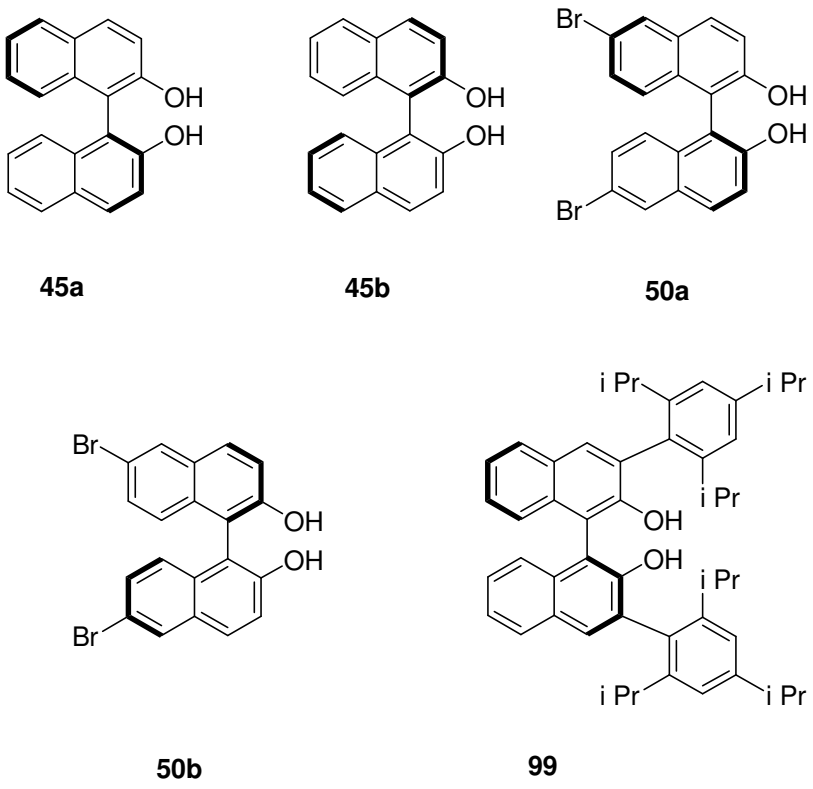

Fig. 2.3 BINOL (**45a** and **45b**) and BINOL derivatives (**50a**, **50b** and **99**)

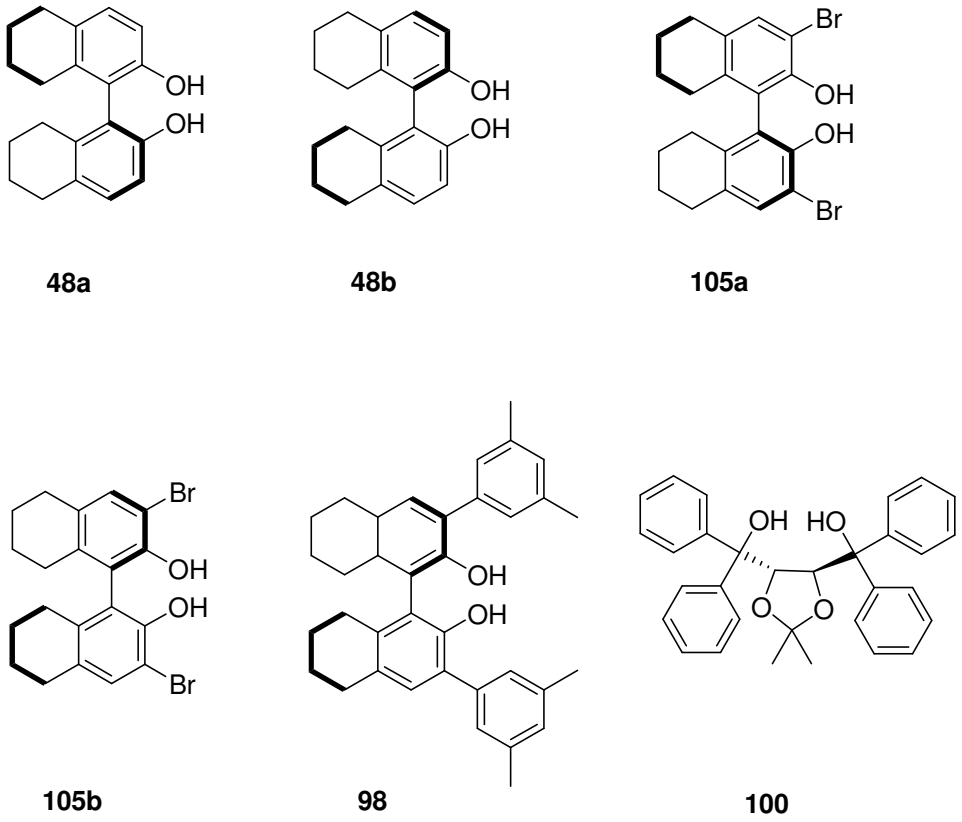

Fig. 2.4 Saturated BINOL derivatives (**48a**, **48b**, **98**, **105a** and **105b**) and TADDOL (**100**)

Chiral BINOLs						
Organism	Time (h)	**45a**	**45b**	**50a**	**50b**	**99**
S.aureus	24 h	**31.25**	**31.25**	**7.81**	**3.9**	>125
	48 h	**31.25**	**62.5**	**31.25**	**3.9**	>125
MRSA	24 h	**31.25**	**31.25**	**7.81**	**3.9**	>125
	48 h	**62.5**	**62.5**	**31.25**	**3.9**	>125
S.epidermidis	24 h	**31.25**	**31.25**	**7.81**	**3.9**	>125
	48 h	**31.25**	**31.25**	**31.25**	**3.9**	>125
Enterococcus sp.	24 h	**62.5**	**62.5**	**7.81**	**7.81**	>125
	48 h	**62.5**	**62.5**	**31.25**	**7.81**	>125
E.coli	24 h	>500	>500	>2000	>2000	>125
	48 h	>500	>500	>2000	>2000	>125
K.pneumoniae	24 h	>500	>500	>2000	>2000	>125
	48 h	>500	>500	>2000	>2000	>125
K.pneumoniae **ESBL** positive	24 h	>500	>500	>2000	>2000	>125
	48 h	>500	>500	>2000	>2000	>125
P.aeruginosa	24 h	>500	>500	>2000	>2000	>125
	48 h	>500	>500	>2000	>2000	>125

Table 2.8: Antibacterial MIC/IC_{95} (μM) results for BINOL (**45a** and **45b**) and BINOL derivatives (**50a**, **50b** and **99**)

Chiral BINOLs and TADDOL							
Organism	Time (h)	**48a**	**48b**	**105a**	**105b**	**98**	**100**
S.aureus	24 h	**62.5**	**62.5**	**15.62**	**1.98**	>125	>125
	48 h	**500**	**500**	**15.62**	**3.9**	>125	>125
MRSA	24 h	**62.5**	**125**	**15.62**	**1.98**	>125	>125
	48 h	**500**	**500**	**15.62**	**3.9**	>125	>125
S.epidermidis	24 h	**31.25**	**62.5**	**15.62**	**1.98**	>125	>125
	48 h	**62.5**	**62.5**	**15.62**	**3.9**	>125	>125
Enterococcus sp.	24 h	**31.25**	**125**	**1.98**	**1.98**	>125	>125
	48 h	**500**	**1000**	**15.62**	**3.9**	>125	>125
E.coli	24 h	>2000	>2000	>2000	>2000	>125	>125
	48 h	>2000	>2000	>2000	>2000	>125	>125
K.pneumoniae	24 h	>2000	>2000	>2000	>2000	>125	>125
	48 h	>2000	>2000	>2000	>2000	>125	>125
K.pneumoniae **ESBL** positive	24 h	>2000	>2000	>2000	>2000	>125	>125
	48 h	>2000	>2000	>2000	>2000	>125	>125
P.aeruginosa	24 h	>2000	>2000	>2000	>2000	>125	>125
	48 h	>2000	>2000	>2000	>2000	>125	>125

Table 2.9: Antibacterial MIC/IC_{95} (μM) results for saturated BINOL derivatives (**48a**, **48b**, **98**, **105a** and **105b**) and TADDOL (**100**)

98, **99** and **100** were non-inhibitory for bacteria within tested concentration range (>125 μM). (*S*)-BINOL (**45a**) and (*R*)-BINOL (**45b**) inhibited all Gram positive bacteria. *Staphylococcus epidermidis* was inhibited by (*S*)-BINOL (**45a**) and (*R*)-BINOL (**45b**) at 31.25 μM after 24 h and at 48 h. An MIC value of 31.25 μM was noted for **45a** towards *Staphylococcus aureus* after 24 h and at 48 h. **45b** inhibited *Staphylococcus aureus* at 31.25 μM after 24 h and at 62.5 μM after 48 h. Both **45a** and **45b** inhibited *MRSA* at 31.25 μM after 24 h while an MIC value of 62.5 μM was noted after 48 h. *Enterococcus sp.* was inhibited at 62.5 μM after 24 h and at 48 h for **45a** and **45b**. Gram negative bacteria showed low inhibition for (*S*)-BINOL (**45a**) and (*R*)-BINOL (**45b**) within studied concentration range (>500 μM).

The brominated BINOL derivatives (**50a** and **50b**) inhibited all Gram positive bacteria while Gram negative bacteria were noted with low inhibition (>2000 μM). (*S*)-6,6'-DibromoBINOL (**50a**) inhibited all Gram-positive bacteria (*Staphylococcus aureus*, *MRSA*, *Staphylococcus epidermidis* and *Enterococcus sp*.) at 7.81 μM after 24 h but the MIC value increased to 31.25 μM after 48 h. *Staphylococcus aureus*, *MRSA* and *Staphylococcus epidermidis* were inhibited by (*R*)-6,6'-dibromoBINOL (**50b**) at 3.9 μM after 24 h and at 48 h. *Enterococcus sp.* was noted with an MIC value of 7.81 μM after 24 h and at 48 h for **50b**. The (*R*)-6,6'-dibromoBINOL (**50b**) enantiomer exhibited lower MIC values for Gram positive bacteria when compared to the (*S*)-6,6'-dibromoBINOL (**50a**) enantiomer. It is apparent that the placement of bromine substituents at the 6-position of BINOL leads to a more toxic compound as MIC values for **50a** and **50b** are lower than those obtained for both enantiomers of BINOL (**45a** and **45b**).

Reduced BINOL derivatives (**48a**, **48b**, **105a** and **105b**) exhibited inhibition for all Gram positive bacteria while Gram negative bacteria were observed with low inhibition (>2000 μM). (*S*)-H_8-BINOL (**48a**) gave an MIC value of 62.5 μM after 24 h for *Staphylococcus aureus* and *MRSA* while after 48 h the MIC values increased to 500 μM. *Staphylococcus epidermidis* was inhibited by (*S*)-H_8-BINOL (**48a**) at 31.25 μM after 24 h and at 62.5 μM after 48 h. An MIC value of 31.25 μM was noted for (*S*)-H_8-BINOL (**48a**) towards *Enterococcus sp.* after 24 h while an MIC value of 500 μM was observed after 48 h.

(*R*)-H_8-BINOL (**48b**) gave an MIC value of 62.5 μM after 24 h for *Staphylococcus aureus* and an MIC value of 500 μM after 48 h. *MRSA* was inhibited by **48b** at 125 μM after 24 h and at 500 μM after 48 h. An MIC value of 62.5 μM was noted for **48b** towards *Staphylococcus epidermidis* after 24 h and at 48 h. **48b** inhibited *Enterococcus sp.* at 125 μM after 24 h and at 1000 μM after 48 h. Both enantiomers **48a** and **48b** did not show a clear trend with regard to inhibition of bacteria as similar MIC values were obtained for Gram positive bacteria.

Brominated H_8-BINOL derivatives (**105a** and **105b**) were observed with lower MIC values for Gram positive bacteria when compared to the parent molecules (**48a** and **48b**). (*S*)-3,3'-Dibromo-H_8-BINOL (**105a**) inhibited *Staphylococcus aureus*, *MRSA* and *Staphylococcus epidermidis* at 15.62 μM after 24 h and at 48 h. An MIC value of 1.98 μM after 24 h was observed for **105a** towards *Enterococcus sp.* and after 48 h an MIC value of 15.62 μM was noted.

(*R*)-3,3'-Dibromo-H_8-BINOL (**105b**) gave an MIC value of 1.98 μM for *Staphylococcus aureus*, *MRSA*, *Staphylococcus epidermidis* and *Enterococcus sp.* after 24 h and an MIC value of 3.9 μM after 48 h. The (*R*)-3,3'-dibromo-H_8-BINOL (**105b**) enantiomer proved more toxic towards Gram positive bacteria when compared to the (*S*)-3,3'-dibromo-H_8-BINOL enantiomer as MIC values were lower.

An overall trend can be seen for the antibacterial activity of BINOL and BINOL derivatives towards Gram positive bacteria (**105b >50b >105a**, **50a >45a**, **45b**, **48a, 48b >99**, **98** and **100**).

The *R* enantiomers of BINOL derivatives are more active (lower MICs) than the *S* enantiomers. Brominated BINOL derivatives showed more antibacterial activity when compared to the unbrominated parent molecules (**105b** is more active than **48b**). Saturated brominated BINOL derivative (**105b**) was found to be the most active antibacterial for Gram positive organisms in this study.

2.4.4 Antifungal study of chiral BINOLs and TADDOL

BINOL (**45a** and **45b**) was screened at 500 μM, while BINOL derivatives (**48a**, **48b**, **50a**, **50b**, **98**, **99**, **105a** and **105b**) and TADDOL (**100**) were screened at a lower concentration of 125 μM due to low solubility in test medium (RPMI 1640) (Figures 2.3 and 2.4). MIC results for this antifungal study are presented in tables 2.10 and 2.11.

98, **99**, **100** and **105a** were non-inhibitory for fungi within tested concentration range (>125 μM). *Trichophyton mentagrophytes* was inhibited by **45b** and **45a** at 31.25 μM and 15.62 μM, respectively, after 72 h and at 120 h. **45a** inhibited *Trichosporon asahii* at 31.25 μM after 24 h and at 125 μM after 48 h. *Candida parapsilosis* was inhibited by **45a** at 250 μM after 24 h but recovered after 48 h (>500 μM). *Candida albicans* ATCC 44859 was inhibited by **45b** at 250 μM after 24 h and recovered after 48 h (>500 μM). An MIC value of 250 μM was noted for **45b** towards *Trichosporon asahii* after 24 h and at 48 h. All remaining fungal strains showed low inhibition for **45a** and **45b** (>500 μM).

50a inhibited *Candida lusitaniae* at 1.98 μM after 24 h and at 48 h. *Candida parapsilosis*, *Candida tropicalis*, *Trichosporon asahii* and *Absidia corymbifera* were noted with an MIC value of 1.98 μM after 24 h for **50a** while the MIC increased to 3.9 μM after 48 h. An MIC value of 3.9 μM was observed for **50a** towards both strains of *Candida albicans* after 24 h and increased to 7.81 μM after 48 h. *Candida glabrata* gave an MIC of 7.81 μM after 24 h and an MIC of 15.62 μM after 48 h. Both strains of *Candida krusei* and *Aspergillus fumigatus* exhibited an MIC of 15.62 μM for **50a** after 24 h and at 48 h. *Trichophyton mentagrophytes* was inhibited by **50a** at 1.98 μM after 72 h and at 120 h.

Chiral BINOLs						
Organism	Time (h)	**45a**	**45b**	**50a**	**50b**	**99**
C.albicans (ATCC44859)	24h	>500	**250**	**3.9**	**15.62**	>125
	48h	>500	>500	**7.81**	**15.62**	>125
C.albicans (ATCC90028)	24h	>500	>500	**3.9**	**15.62**	>125
	48h	>500	>500	**7.81**	**15.62**	>125
C.parapsilosis (ATCC22019)	24h	**250**	>500	**1.98**	**7.81**	>125
	48h	>500	>500	**3.9**	**15.62**	>125
C.krusei (ATCC6258)	24h	>500	>500	**15.62**	**7.81**	>125
	48h	>500	>500	**15.62**	**15.62**	>125
C.krusei (E28)	24h	>500	>500	**15.62**	**7.81**	>125
	48h	>500	>500	**15.62**	**15.62**	>125
C.tropicalis (156)	24h	>500	>500	**1.98**	**15.62**	>125
	48h	>500	>500	**3.9**	**15.62**	>125
C.glabrata (20/I)	24h	>500	>500	**7.81**	**3.9**	>125
	48h	>500	>500	**15.62**	**7.81**	>125
C.lusitaniae (2446/I)	24h	>500	>500	**1.98**	**7.81**	>125
	48h	>500	>500	**1.98**	**15.62**	>125
Trichosporon asahii (1188)	24h	**31.25**	**250**	**1.98**	**3.9**	>125
	48h	**125**	**250**	**3.9**	**7.81**	>125
Aspergillus fumigatus (231)	24h	>500	>500	**15.62**	**15.62**	>125
	48h	>500	>500	**15.62**	**15.62**	>125
Absidia corymbifera (272)	24h	>500	>500	**1.98**	**3.9**	>125
	48h	>500	>500	**3.9**	**3.9**	>125
Trichophyton mentagrophytes (445)	72h	**15.62**	**31.25**	**1.98**	**1.98**	>125
	120h	**15.62**	**31.25**	**1.98**	**1.98**	>125

Table 2.10: Antifungal IC_{80}/IC_{50} (μM) results for BINOL (**45a** and **45b**) and BINOL derivatives (**50a**, **50b** and **99**)

Chiral BINOLs and TADDOL							
Organism	Time (h)	**48a**	**48b**	**105a**	**105b**	**98**	**100**
C.albicans (ATCC44859)	24h	>125	>125	>125	>125	>125	>125
	48h	>125	>125	>125	>125	>125	>125
C.albicans (ATCC90028)	24h	>125	>125	>125	>125	>125	>125
	48h	>125	>125	>125	>125	>125	>125
C.parapsilosis (ATCC22019)	24h	>125	>125	>125	>125	>125	>125
	48h	>125	>125	>125	>125	>125	>125
C.krusei (ATCC6258)	24h	>125	>125	>125	>125	>125	>125
	48h	>125	>125	>125	>125	>125	>125
C.krusei (E28)	24h	>125	>125	>125	>125	>125	>125
	48h	>125	>125	>125	>125	>125	>125
C.tropicalis (156)	24h	>125	>125	>125	>125	>125	>125
	48h	>125	>125	>125	>125	>125	>125
C.glabrata (20/I)	24h	>125	>125	>125	>125	>125	>125
	48h	>125	>125	>125	>125	>125	>125
C.lusitaniae (2446/I)	24h	>125	>125	>125	>125	>125	>125
	48h	>125	>125	>125	>125	>125	>125
Trichosporon asahii (1188)	24h	>125	>125	>125	>125	>125	>125
	48h	>125	>125	>125	>125	>125	>125
Aspergillus fumigatus (231)	24h	>125	>125	>125	>125	>125	>125
	48h	>125	>125	>125	>125	>125	>125
Absidia corymbifera (272)	24h	>125	>125	>125	>125	>125	>125
	48h	>125	>125	>125	>125	>125	>125
Trichophyton mentagrophytes (445)	72h	**15.62**	**62.5**	>125	**1.98**	>125	>125
	120h	**15.62**	**62.5**	>125	**1.98**	>125	>125

Table 2.11: Antifungal IC_{80}/IC_{50} (μM) results for saturated BINOLs (**48a**, **48b**, **98**, **105a** and **105b**) and TADDOL (**100**)

50b inhibited *Absidia corymbifera* at 3.9 μM after 24 h and at 48 h. An MIC value of 3.9 μM was noted for **50b** towards *Candida glabrata* and *Trichosporon asahii* after 24 h and increased to 7.81 μM after 48 h. Both strains of *Candida krusei*, *Candida parapsilosis* and *Candida lusitaniae* exhibited an MIC of 7.81 μM for **50b** after 24 h and an MIC of 15.62 μM after 48 h. **50b** inhibited both strains of *Candida albicans*, *Candida tropicalis* and *Aspergillus fumigatus* at 15.62 μM after 24 h and at 48 h.
Trichophyton mentagrophytes was inhibited by **50b** at 1.98 μM after 72 h and at 120 h.
Brominated BINOL derivatives (**50a** and **50b**) showed more growth inhibition towards fungal organisms than BINOL (**45a** and **45b**).

Trichophyton mentagrophytes was inhibited by **48a**, **48b** and **105b** at 15.62 μM, 62.5 μM and 1.98 μM after 72 h and at 120 h, respectively. All remaining fungal organisms showed low inhibition for **48a**, **48b** and **105b** (>125 μM).

An overall trend can be seen for the antifungal activity of BINOL and BINOL derivatives (**50a**, **50b >45a**, **45b >105b**, **48a**, **48b >98**, **100**, **105a** and **99**)

Brominated BINOL derivatives (**50a** and **50b**) were found to be the most active for antifungal activity (inhibited all test fungi) among the BINOLs studied. The *S* enantiomer **50a** was slightly more active than the *R* enantiomer **50b** as lower MICs were obtained for fungi in most cases. BINOL (**45a** and **45b**) were observed with 3 cases of antifungal activity each. BINOL derivatives (**48a**, **48b** and **105b**) were less active as they inhibited one fungal organism each. While BINOL derivatives (**98**, **99**, **100** and **105a**) showed no activity towards test fungal organisms.

2.4.5 Antibacterial study of Jacobsen thioureas (IC_{95})

Jacobsen thioureas (**15**, **106** and **107**) were screened against the test set of bacteria for the determination of IC_{95} values. Jacobsen thioureas (Figure 2.5) used for this study were tested at the highest concentration range of 2000 μM. The results in table 2.12 represent the MIC values obtained for Jacobsen thioureas (**15**, **106** and **107**).

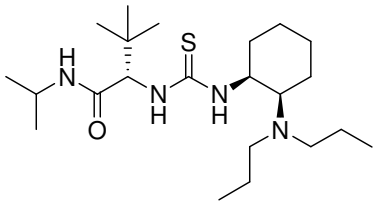

106

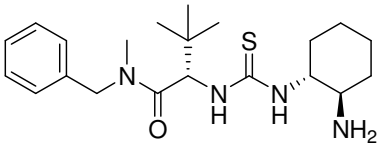

15

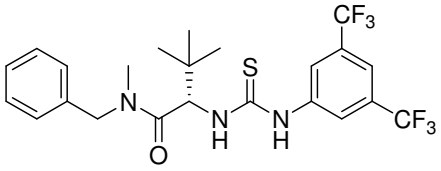

107

Fig 2.5 Jacobsen thioureas (**15, 106** and **107**) evaluated for antimicrobial activity

Organism	Time (h)	**106**	**15**	**107**
S. aureus	24	>2000	**1000**	**250**
	48	>2000	**1000**	**250**
MRSA	24	**1000**	**62.5**	**250**
	48	**1000**	**62.5**	**250**
S. epidermidis	24	**1000**	**15.62**	**250**
	48	**1000**	**15.62**	**250**
Enterococcus sp.	24	**1000**	**500**	**500**
	48	**1000**	**500**	**500**
E. coli	24	>2000	**1000**	**250**
	48	>2000	**1000**	**250**
K. pneumoniae	24	>2000	**1000**	**125**
	48	>2000	**1000**	**125**
K. pneumoniae - ***ESBL***	24	>2000	**1000**	>2000
	48	>2000	**1000**	>2000
P. aeruginosa	24	>2000	**2000**	>2000
	48	>2000	**2000**	>2000

Table 2.12: MIC/IC_{95} (μM) values of Jacobsens thioureas (**15**, **106** and **107**)

Jacobsens thioureas (**15**, **106** and **107**) showed cases of inhibition towards bacteria. **15** inhibited all bacteria. **106** was inhibitory for *MRSA*, *Staphylococcus epidermidis* and *Enterococcus sp* while **107** inhibited most bacteria except for *Klebsiella pneumoniae*-**ESBL** positive (>2000 μM) and *Pseudomonas aeruginosa* (>2000 μM).

Low MIC values were obtained for **15** against *MRSA* (62.5 μM after 24 h and at 48 h) and *Staphylococcus epidermidis* (15.62 μM after 24 h and at 48 h). The highest MIC value obtained for **15** was against *Pseudomonas aeruginosa* (2000 μM after 24 h and at 48 h). *Enterococcus sp* gave an MIC value of 500 μM after 24 h and at 48 h for **15**. All remaining bacteria (*Staphylococcus aureus*, *Escherichia coli*, *Klebsiella pneumoniae* and *Klebsiella pneumoniae*-**ESBL** positive) gave an MIC value of 1000 μM after 24 h and at 48 h for **15.**

107 showed low inhibition for *Klebsiella pneumoniae*-**ESBL** positive (>2000 μM) and *Pseudomonas aeruginosa* (>2000 μM). The highest MIC value obtained for **107** was against *Enterococcus sp* (500 μM after 24 h and at 48 h). *Klebsiella pneumoniae* was observed with the lowest MIC value of 125 μM after 24 h and at 48 h for **107**. Remaining bacteria (*Staphylococcus aureus, MRSA, Staphylococcus epidermidis* and *Escherichia coli*) were noted with an MIC value of 250 μM after 24 h and at 48 h for **107**.

106 exhibited an MIC value of 1000 μM after 24 h and at 48 h for *MRSA*, *Staphylococcus epidermidis* and *Enterococcus sp*. Remaining bacteria (*Staphylococcus aureus, Escherichia coli, Klebsiella pneumoniae, Klebsiella pneumoniae*-**ESBL** positive and *Pseudomonas aeruginosa*) were noted with low inhibition for catalyst **106** (>2000 μM).

2.4.6 Antifungal study of Jacobsen thioureas

Jacobsen thioureas (**15**, **106** and **107**) were screened at a lower concentration for antifungal screening, this was due to there respective solubility in test medium (1000 μM for **15**, 500 μM for **106** and 125 μM for **107**). MIC results for this antifungal study are presented in the appendix (Table 3).

Both **106** and **107** proved non-inhibitory for all fungal strains within studied concentration range. Some cases of antifungal inhibition were noted for **15**. *Candida parapsilosis*, *Candida tropicalis* and *Candida lusitaniae* gave an MIC value of 1000 μM after 24 h and at 48 h for **15**. The MIC value obtained for **15** against *Trichophyton mentagrophytes* was 1000 μM after 72 h and at 120 h. All remaining fungal strains gave low inhibition for **15**.

2.4.7 Antibacterial study of Cinchona alkaloid derivatives

Cinchona alkaloid derivatives **38a**, **81a** and **108** (Figure 2.6) were screened against the test set of bacteria for the determination of IC_{95} values. Both **38a** and **108** were screened at the highest concentration of 2000 μM while **81a** was tested at 500 μM. The results in the appendix (Table 4) represent the MIC values obtained for cinchona alkaloid derivatives (**38a**, **81a** and **108**).

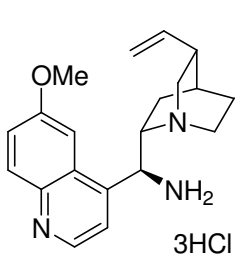

108

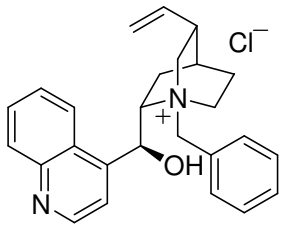

38a

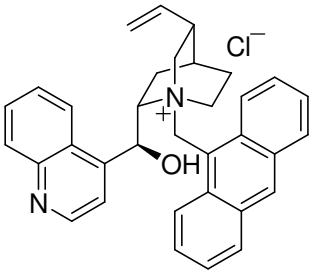

81a

Fig 2.6 Cinchona alkaloid derived catalysts (**38a**, **81a** and **108**) screened for antimicrobial activity

All cinchona alkaloid derivatives (**38a**, **81a** and **108**) were observed with low inhibition against test bacteria within the tested concentration ranges.

2.4.8 Antifungal study of Cinchona alkaloid derivatives

Both **38a** and **108** were screened at the highest concentration of 2000 μM while **81a** was tested at 500 μM. MIC results for this antifungal study are presented in the appendix (Table 5).

Cinchona alkaloid derivatives **38a** and **108** showed no inhibition towards fungal strains (>2000 μM). **81a** was screened at 500 μM due to low solubility in the test medium. Some cases of inhibition were observed with **81a** for fungal strains. *Candida parapsilosis* and *Candida lusitaniae* were noted with an MIC value of 125 μM after 24 h and at 48 h for **81a**. An MIC value of 500 μM was recorded for *Candida albicans* ATCC 44859, *Candida albicans* ATCC 90028, *Candida krusei* ATCC 6258, *Candida krusei* E28, *Candida tropicalis* and *Candida glabrata* after 24 h and at 48 h. Remaining fungal strains (*Trichosporon asahii*, *Aspergillus fumigatus*, *Absidia corymbifera* and *Trichophyton mentagrophytes*) were not inhibited by **81a** within the tested concentration range.

2.4.9 Antibacterial study of MacMillan imidazolidinones

MacMillan imidazolidinones **19**, **109** and **110** (Figure 2.7) were screened against the test set of bacteria for the determination of IC_{95} values. **19**, **109** and **110** were screened at the highest concentration of 2000 μM. MIC results for the antibacterial study of **19**, **109** and **110** are presented in the appendix (Table 6).

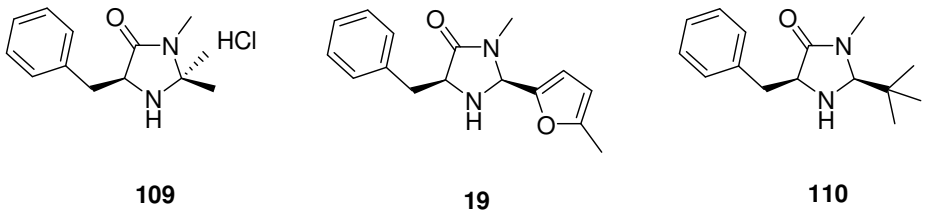

109 **19** **110**

Fig 2.7 MacMillan imidazolidinones (**19**, **109** and **110**) screened for antimicrobial activity

109 was noted with an MIC value of 2000 μM for *MRSA* after 24 h and at 48 h. All remaining bacteria showed low inhibition for **109** (>2000 μM). Macmillan imidazolidinone **110** exhibited an MIC value of 2000 μM for *Staphylococcus epidermidis* after 24 h and at 48 h while remaining bacteria were not inhibited by **110** (>2000 μM). **19** (>2000 μM) proved non-inhibitory for test bacteria within tested concentration range.

2.4.10 Antifungal study of MacMillan imidazolidinones

MacMillan imidazolidinones **19**, **109** and **110** were screened against fungal organisms at 2000 μM. MIC results for antifungal study of **19**, **109** and **110** are presented in the appendix (Table 7).

Both **19** and **109** proved non-inhibitory for fungal strains within tested concentration range. MacMillan imidazolidinone **110** inhibited *Trichosporon asahii* at 2000 μM after 24 h while a recovery was noted after 48 h (>2000 μM). *Trichophyton mentagrophytes* was inhibited at 2000 μM by **110** after 72 h and at 120 h.

2.4.11 Antibacterial study of chiral phosphoric acids and Maruoka phase-transfer catalyst

Chiral phosphoric acids (**26a** and **26b**) and Maruoka phase-transfer catalyst **40** (Figure 2.8) were screened against the test set of bacteria for the determination of IC_{95} values. **26a** and **26b** were screened at the highest concentration of 2000 μM while **40** was tested at a lower concentration of 125 μM. MIC results for the antibacterial study of **26a**, **26b** and **40** are presented in table 2.13.

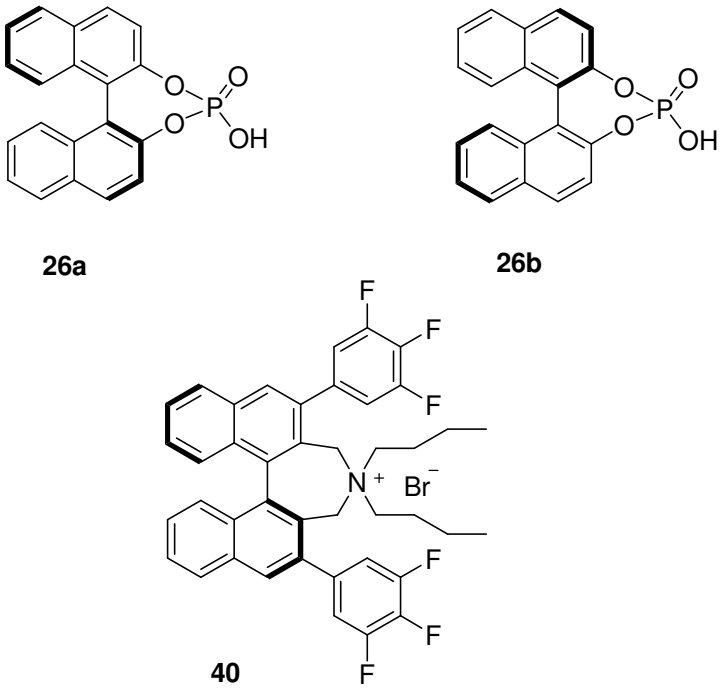

Fig. 2.8 Chiral phosphoric acids (**26a** and **26b**) and Maruoka phase-transfer catalyst (**40**) screened for antimicrobial activity

26a proved inhibitory for Gram positive organisms *Staphylococcus aureus*, *MRSA* and *Staphylococcus epidermidis* with MIC values of 2000 μM, 1000 μM and 1000 μM noted respectively after 24 h and at 48 h. *Enterococcus sp.* and remaining Gram negative bacteria (*E.coli*, *Klebsiella pneumoniae*, *Klebsiella pneumoniae*-**ESBL** positive and *Pseudomonas aeruginosa*) showed low inhibition for **26a** (>2000 μM). **26b** inhibited *Staphylococcus aureus* and *MRSA* at 2000 μM after 24 h and at 48 h. *Staphylococcus epidermidis* was inhibited by **26b** at 1000 μM after 24 h and at 2000 μM after 48 h.

Organism	Time (h)	**26a**	**26b**	**40**
S. aureus	24	**2000**	**2000**	**125**
	48	**2000**	**2000**	**125**
MRSA	24	**1000**	**2000**	**31.25**
	48	**1000**	**2000**	**31.25**
S. epidermidis	24	**1000**	**1000**	**125**
	48	**1000**	**2000**	**125**
Enterococcus sp.	24	>2000	>2000	**62.5**
	48	>2000	>2000	**62.5**
E. coli	24	>2000	>2000	>125
	48	>2000	>2000	>125
K. pneumoniae	24	>2000	>2000	>125
	48	>2000	>2000	>125
K. pneumoniae - ***ESBL***	24	>2000	>2000	>125
	48	>2000	>2000	>125
P. aeruginosa	24	>2000	>2000	>125
	48	>2000	>2000	>125

Table 2.13: MIC/IC_{95} (μM) values of **26a**, **26b** and **40**

All 4 Gram positive organisms were inhibited by **40**. *MRSA* exhibited the lowest MIC value of 31.25 μM for **40** after 24 h and at 48 h. Both *Staphylococcus aureus* and *Staphylococcus epidermidis* gave the highest MIC value of 125 μM after 24 h and at 48 h for **40**. *Enterococcus sp.* was observed with an MIC value of 62.5 μM after 24 h and at 48 h for **40**. All Gram negative bacteria (*E.coli*, *Klebsiella pneumoniae*, *Klebsiella pneumoniae*-**ESBL** positive and *Pseudomonas aeruginosa*) showed low inhibition for **40** (>125 μM).

2.4.12 Antifungal study of chiral phosphoric acids and Maruoka phase-transfer catalyst

Chiral phosphoric acids (**26a** and **26b**) and Maruoka phase-transfer catalyst **40** (Figure 2.8) were screened against the test set of fungi. **26a** and **26b** were screened at the highest concentration of 2000 μM while **40** was tested at a lower concentration of 125 μM. MIC results for the antifungal study of **26a**, **26b** and **40** are presented in table 2.14. **26a** showed low antifungal activity (>2000 μM) for all fungal strains. *Trichophyton mentagrophytes* was inhibited by **26b** at 500 μM after 72 h and at 2000 μM after 120 h. An MIC value of 2000 μM was observed for **26b** towards *Absidia corymbifera* after 24 h and at 48 h. **40** was screened at 125 μM. *Candida lusitaniae* exhibited the lowest MIC value of 3.9 μM after 24 h and at 48 h for **40**. An MIC value of 7.81 μM was obtained for **40** towards *Candida albicans* ATCC 44859 after 24 h and at 48 h. *Candida albicans* ATCC 90028 and *Candida parapsilosis* were inhibited by **40** with an MIC value of 15.62 μM after 24 h and at 48 h. An MIC value of 31.25 μM for **40** was noted for *Candida krusei* ATCC 6258 and *Candida tropicalis* after 24 h and at 48 h. *Trichosporon asahii* gave an MIC value of 62.5 μM for **40** after 24 h and at 48 h. All remaining fungi (*Candida krusei* E28, *Candida glabrata*, *Aspergillus fumigatus*, *Absidia corymbifera* and *Trichophyton mentagrophytes*) were observed with low inhibition (>125 μM).

Organism	Time (h)	**26a**	**26b**	**40**
C. albicans (ATCC44859)	24	>2000	>2000	**7.81**
	48	>2000	>2000	**7.81**
C. albicans (ATCC90028)	24	>2000	>2000	**15.62**
	48	>2000	>2000	**15.62**
C. parapsilosis (ATCC22019)	24	>2000	>2000	**15.62**
	48	>2000	>2000	**15.62**
C. krusei (ATCC6258)	24	>2000	>2000	**31.25**
	48	>2000	>2000	**31.25**
C. krusei (E28)	24	>2000	>2000	>125
	48	>2000	>2000	>125
C. tropicalis (156)	24	>2000	>2000	**31.25**
	48	>2000	>2000	**31.25**
C. glabrata (20/I)	24	>2000	>2000	>125
	48	>2000	>2000	>125
C. lusitaniae (2446/I)	24	>2000	>2000	**3.9**
	48	>2000	>2000	**3.9**
T. asahii (1188)	24	>2000	>2000	**62.5**
	48	>2000	>2000	**62.5**
A. fumigatus (231)	24	>2000	>2000	>125
	48	>2000	>2000	>125
A. corymbifera (272)	24	>2000	**2000**	>125
	48	>2000	**2000**	>125
T. mentagrophytes (445)	72	>2000	**500**	>125
	120	>2000	**2000**	>125

Table 2.14: Antifungal IC_{80}/IC_{50} (μM) values for **26a**, **26b** and **40**

2.5 Cytotoxicity, apoptosis and cell viability studies of organocatalysts

Cytotoxicity, apoptosis and cell viability studies of organocatalysts were performed by our collaborator Dr. Petr Bartunek in the Czech Republic. These studies were carried out on human erythroid progenitors, HL-60 and K-562 blood cell lines in the presence of various concentrations of organocatalysts (0-10 μM). Human erythroid progenitors are normal blood cells while HL-60 (ATCC CCL-240) is a human promyelocytic leukemia cell line and K-562 (ATCC CCL-243) is a human myelogenous leukemia cell line.

2.5.1 Cytotoxicity of organocatalysts

Cytotoxic effects on all cell lines were determined using the CytoTox-ONE homogeneous membrane integrity assay (G7892, promega).[17] This assay is a homogeneous, fluorometric method for estimating the number of non-viable cells present in multiwell plates.[17] Non-viable cells generate a fluorescent signal for this assay and the emitted fluorescence is proportional to the number of non-viable cells present. The principle for this assay is that non-viable cells have a damaged plasma membrane that allows cellular contents to leak out which results in cell death. Viable cells will not emit a fluorescent signal for this assay. The cytotoxicity results for **8**, **15**, **26a**, **38a**, **40**, **81a**, **102**, **103**, **104**, **106**, **107**, **108** and **109** against human erythroid progenitors, HL-60 and K-562 cell lines are presented in Figures 2.9, 2.10 and 2.11 respectively. Fold induction for the cytotoxicity assay is the ratio between experimental fluorescence (cells + test substance) and control fluorescence (cells without test substance). An increase in fold induction for test compound indicates the presence of non-viable cells (cytotoxicity).

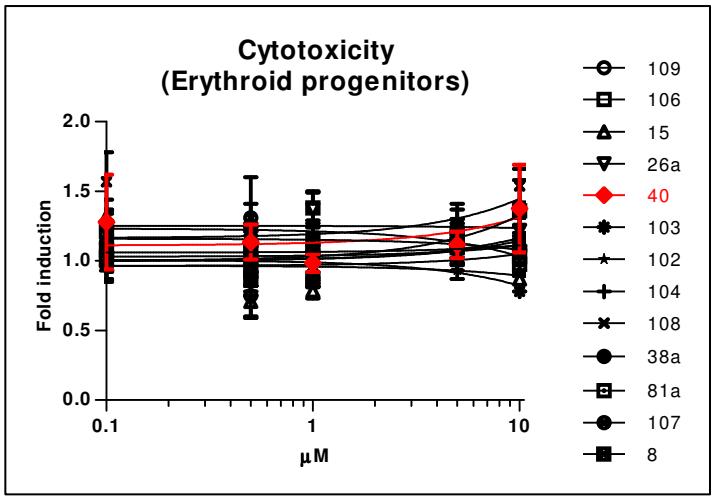

Fig. 2.9 Cytotoxicity results for erythroid progenitors

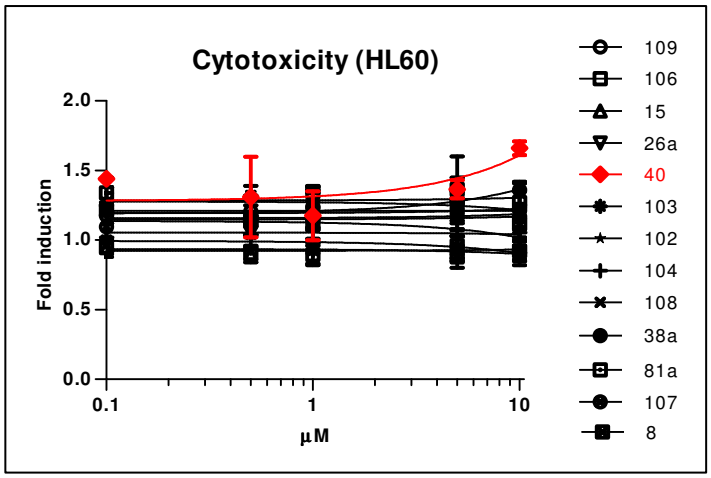

Fig. 2.10 Cytotoxicity results for HL-60

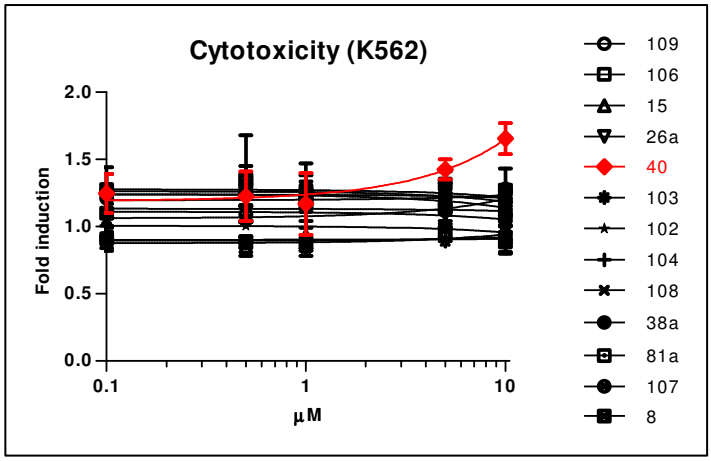

Fig. 2.11 Cytotoxicity results for K-562

Organocatalysts (**8**, **15**, **26a**, **38a**, **40**, **81a**, **102**, **103**, **104**, **106**, **107**, **108** and **109**) exhibited no cytotoxicity towards test cell lines under the parameters of the CytoTox-ONE homogeneous membrane integrity assay within the studied concentration range (0.1-10 μM). These compounds failed to disrupt the plasma membranes which would lead to non-viable cells.

2.5.2 Apoptosis induced by organocatalysts

Apoptosis for cell lines was monitored using the Caspase-Glo 3/7 assay (G8091, promega).[18] The Caspase-Glo 3/7 assay is a homogeneous, luminescent assay that measures caspase-3 and -7 activities.[18] Caspases are proteases that are implicated in apoptosis.[19] Apoptosis is a process of programmed cell death that is accomplished by specialized cellular machinery. In apoptosis, caspases function in both cell disassembly and the initiation of cell disassembly in response to pro-apoptotic signals.[19] This assay determines cell death induced by apoptosis by measuring caspase-3 and -7 activities. The luminescent signal readout for this assay only occurs when caspase-3 and -7 become activated, therefore luminescence is proportional to caspase-3 and -7 activities. Viable cells that contain inactive caspase-3 and -7 enzymes will not give a luminescent signal.

The apoptosis results for **8**, **15**, **26a**, **38a**, **40**, **81a**, **102**, **103**, **104**, **106**, **107**, **108** and **109** against human erythroid progenitors, HL-60 and K-562 cell lines are presented in Figures 2.12, 2.13 and 2.14 respectively. Fold induction for the apoptosis assay is the ratio between experimental luminescence (cells + test substance) and control luminescence (cells without test substance). An increase in fold induction for test compounds indicates the activation of caspase-3 and -7.

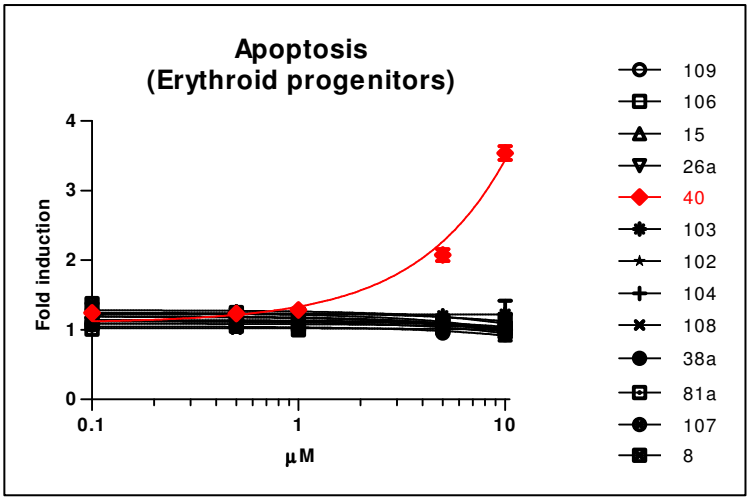

Fig. 2.12 Apoptosis results for erythroid progenitors

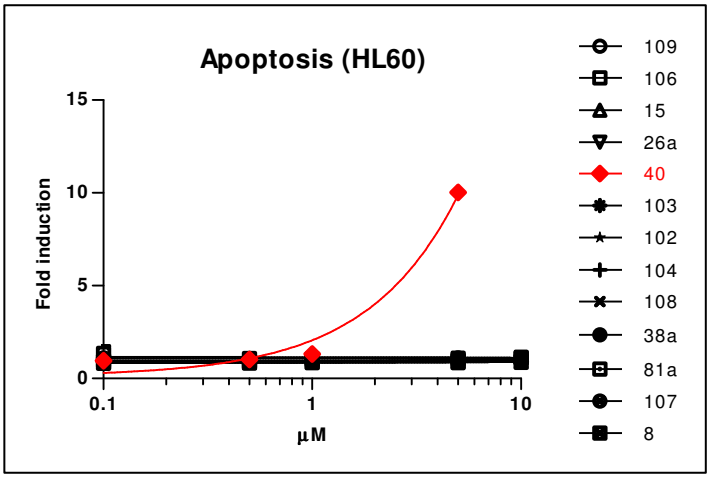

Fig. 2.13 Apoptosis results for HL-60

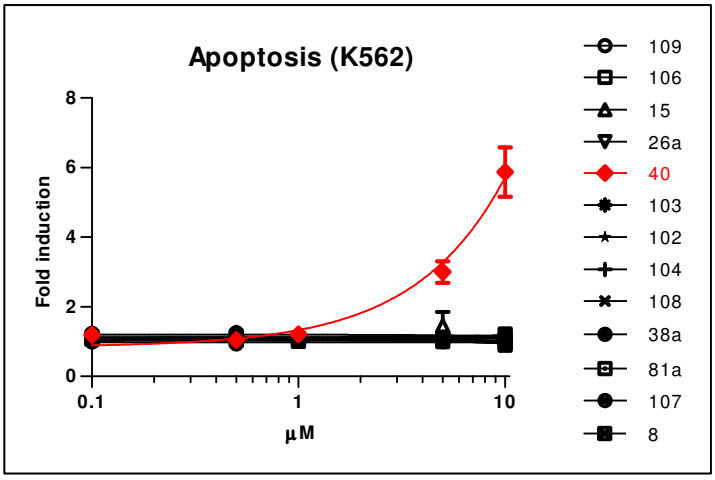

Fig. 2.14 Apoptosis results for K-562

Organocatalysts (**8**, **15**, **26a**, **38a**, **81a**, **102**, **103**, **104**, **106**, **107**, **108** and **109**) did not induce apoptosis for test cell lines under the parameters of the Caspase-Glo 3/7 assay within the concentration range (0.1-10 μM). These compounds failed to damage the cells which would in turn activate caspase-3 and -7 activities. However, **40** did produce apoptosis for all 3 cell lines within the concentration range (0.1-10μM). An increase in fold induction was noted for **40** against all 3 cell lines (Figures 2.12, 2.13 and 2.14).

2.5.3 Cell viability study with organocatalysts

Cell viability was measured using the CellTiter-Blue cell viability assay (G8082, promega).[20] This assay is a homogeneous, fluorometric method for estimating the number of viable cells present in multiwell plates.[20] Viable cells are metabolically active and will emit a fluorescent signal for this assay. The number of viable cells is proportional to the fluorescence signal. Non-viable cells are not metabolically active therefore these cells will not emit a fluorescent signal for this assay. A decrease in fold induction indicates a loss in cell viability.

The cell viability results for **8**, **15**, **26a**, **38a**, **40**, **81a**, **102**, **103**, **104**, **106**, **107**, **108** and **109** against erythroid progenitors, HL-60 and K-562 cell lines are presented in Figures 2.15, 2.16 and 2.17 respectively. Fold induction for the cell viability assay is the ratio between experimental fluorescence (cells + test substance) and control fluorescence (cells without test substance).

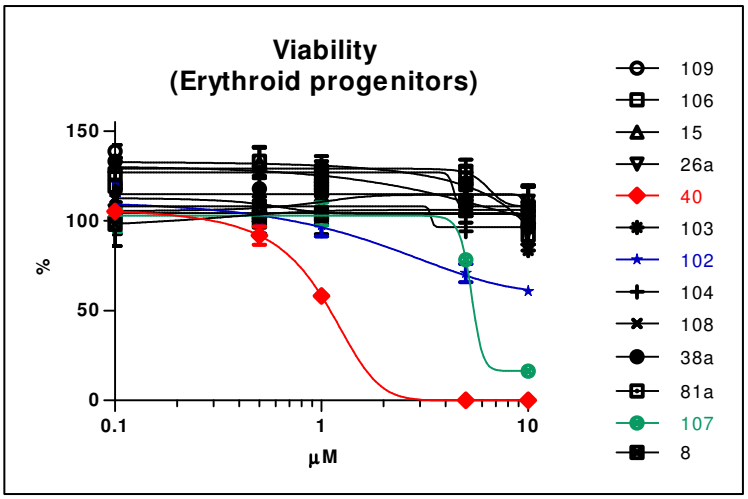

Fig. 2.15 Cell viability results for erythroid progenitors

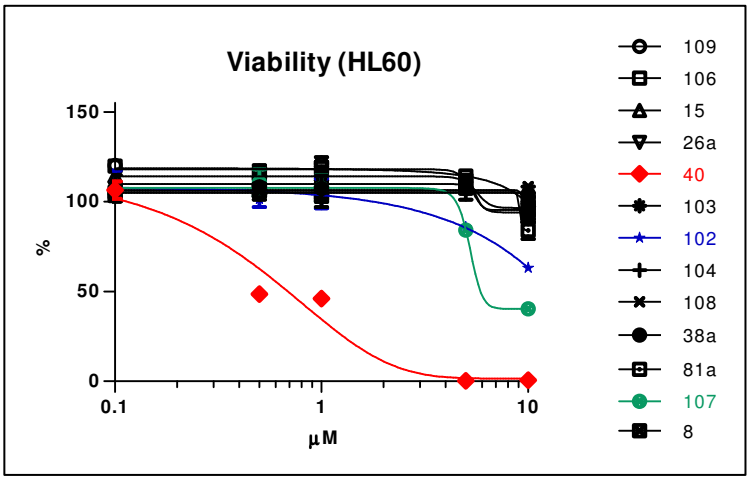

Fig. 2.16 Cell viability results for HL-60

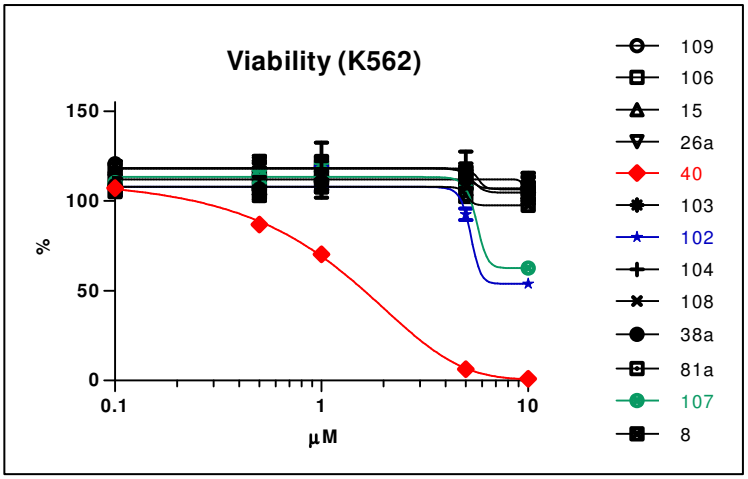

Fig. 2.17 Cell viability results for K-562

Organocatalysts (**8**, **15**, **26a**, **38a**, **81a**, **103**, **104**, **106**, **108** and **109**) did not result in loss of cell viability for test cell lines. **102** and **107** reduced cell viability by less than 50% for all 3 cell lines at 10 µM.

40 resulted in a loss of cell viability for all 3 cell lines within the studied concentration range (0.1-10 µM). A decrease in fold induction was noted for **40** against all 3 cell lines (Figures 2.15, 2.16 and 2.17).

2.5.4 EC_{50} and IC_{50} values for Maruoka phase-transfer catalyst (40)

EC_{50} values were determined for the affect **40** has on apoptosis (Figure 2.18). An EC_{50} value of 6.0 µM was observed for **40** against erythroid progenitors. Both HL-60 and K-562 gave an EC_{50} value of 2.1 µM and 5.5 µM, respectively.

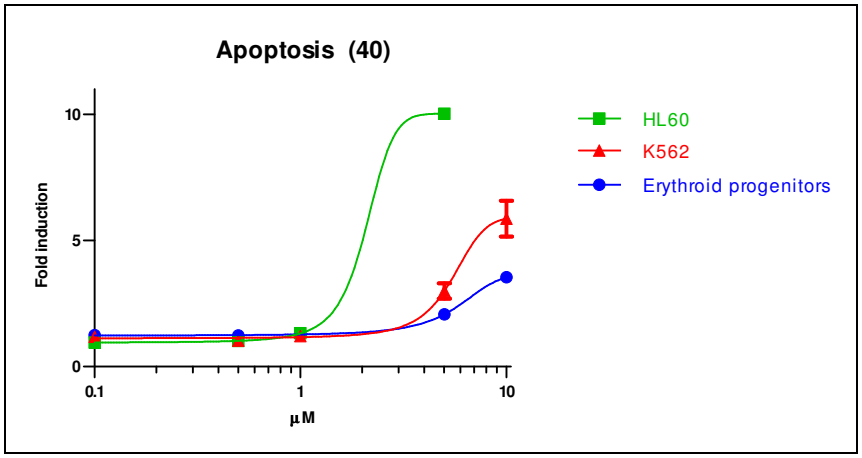

Fig. 2.18 Apoptosis results for **40** against all 3 cell lines (erythroid progenitors, HL-60 and K-562)

IC_{50} values were determined for the affect **40** has on cell viability (Figure 2.19). An IC_{50} value of 1.2 μM was observed for **40** against erythroid progenitors. Both HL-60 and K-562 gave an IC_{50} value of 0.8 μM and 1.7 μM, respectively.

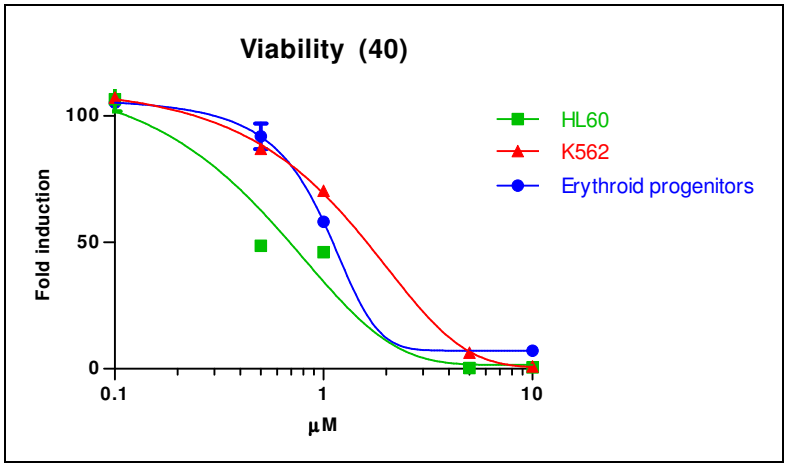

Fig. 2.19 Cell viability results for **40** against all 3 cell lines (erythroid progenitors, HL-60 and K-562)

From the apoptosis and cell viability studies it is apparent that **40** is toxic to erythroid progenitors, HL-60 and K-562 cell lines for those test parameters.

2.6 Biodegradation study of known organocatalysts

Jacobsen thioureas, cinchona alkaloid derivatives, proline derivatives, MacMillan imidazolidinones, Maruoka phase-transfer catalyst and chiral phosphoric acids (Figures 2.20 and 2.22) were evaluated for biodegradation using the CO_2 headspace test (ISO 14593).[1] This study was performed by our collaborator Dr Teresa Garcia at the department of surfactant technology in Barcelona, Spain. General procedure for this assay was discussed in section 1.3.4. Results from this study are presented in Tables 2.15 and 2.17.

Compound	**% Biodegradation**			
	6 d	**14 d**	**21 d**	**28 d**
SDS	76	93	93	94
8	1	5	4	5
15	0	0	0	0
26a	0	0	2	3
38a	0	4	0	2
40	0	3	0	0
81a	0	0	0	0
106	0	0	0	0
107	0	0	0	0
108	0	0	0	0
109	1	1	3	6

Table 2.15: Biodegradation results for organocatalysts (**8**, **15**, **26a**, **38a**, **40**, **81a**, **106**, **107**, **108** and **109**)

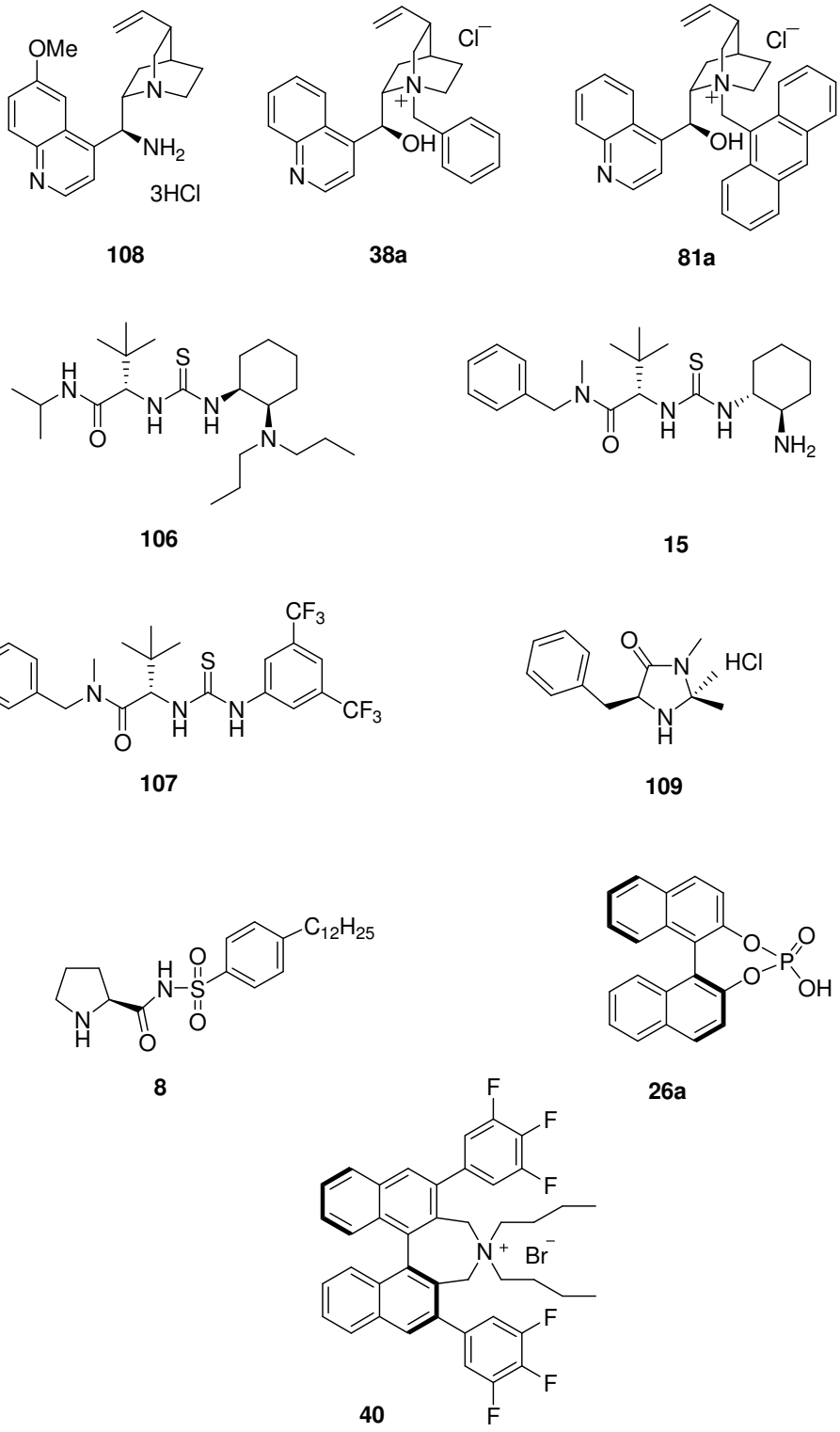

Fig 2.20 Organocatalysts (**8**, **15**, **26a**, **38a**, **40**, **81a**, **106**, **107**, **108** and **109**) evaluated for biodegradation using the CO_2 headspace test (ISO 14593)

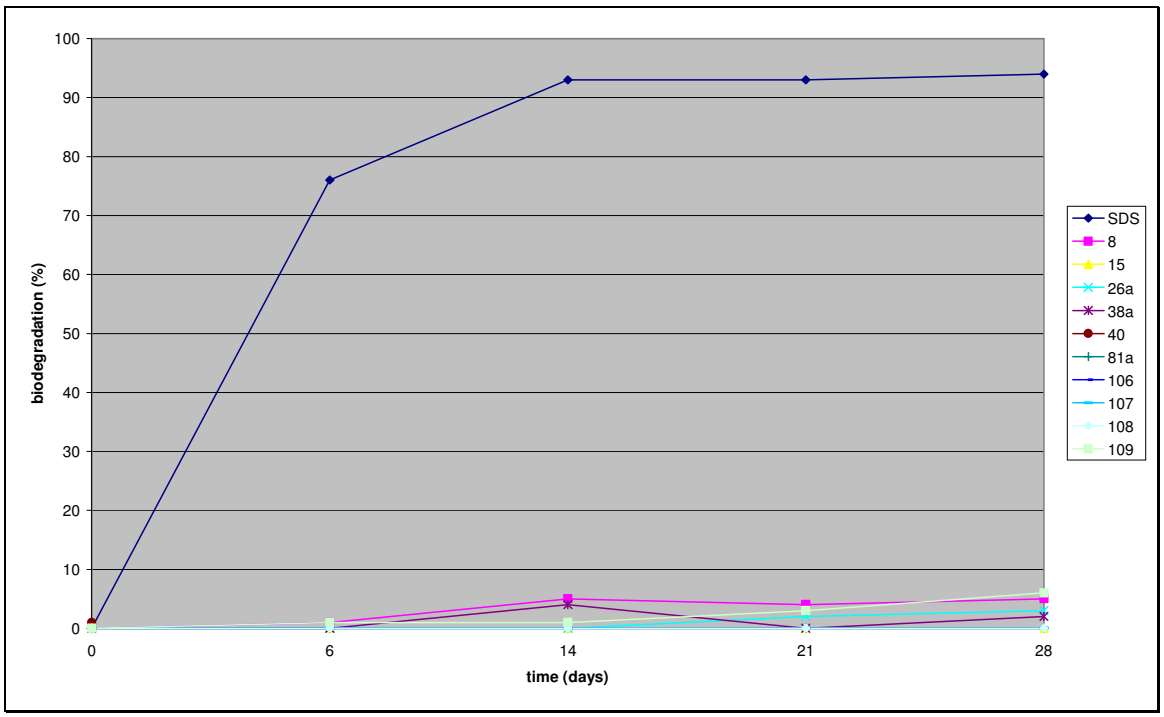

Fig 2.21 Biodegradation curves for organocatalysts (**8**, **15**, **26a**, **38a**, **40**, **81a**, **106**, **107**, **108** and **109**)

The readily biodegradable reference substance SDS was evaluated as the control experiment and exhibited 76% biodegradation after 6 days. Days 14, 21 and 28 gave biodegradation values of 93%, 93% and 94%, respectively. These data points verify that the inoculum is active and capable of mineralising biodegradable organic chemicals. Organocatalysts (**8**, **15**, **26a**, **38a**, **40**, **81a**, **106**, **107**, **108** and **109**) were non-biodegradable as less than 7% CO_2 output was measured for these molecules (Table 2.15). In order for a chemical to be deemed readily biodegradable it must evolve >60% CO_2 over a period of 28 days. Therefore, organocatalysts (**8**, **15**, **26a**, **38a**, **40**, **81a**, **106**, **107**, **108** and **109**) failed the CO_2 headspace test (ISO 14593) and can be classified as being non-biodegradable as negligible CO_2 output occurred (Figure 2.21). As no biodegradation was apparent for organocatalysts (**8**, **15**, **26a**, **38a**, **40**, **81a**, **106**, **107**, **108** and **109**), a control experiment was run to determine if compounds were having an inhibitory effect on the activity of the inoculum. For this experiment reference substance (SDS) and test substance (organocatalysts) were added together to the inoculum and if inhibition of SDS biodegradation occurred (>25% inhibition is required for a positive

result), this implied that the test substance is inhibiting the inoculum. Results from this experiment are presented in Table 2.16. Maruoka phase-transfer catalyst (**40**) gave the largest % inhibition (30%) for the inhibitory control assay at a concentration of 40 μM. Cinchona alkaloid derived phase-transfer catalyst (**81a**) gave a % inhibition value of 19% at 49 μM. Compounds **40** and **81a** showed cases of inhibition for the antimicrobial screening. Proline derived organocatalyst (**8**) was noted with an inhibition of 8% for the inhibitory control biodegradation assay at a concentration of 72 μM. Remaining organocatalysts (**15**, **26a**, **38a**, **106**, **107**, **108** and **109**) were observed with low inhibition to the inoculum (Table 2.16).

Compound	Concentration (mgC/L)	Molar concentration of test sample	Inhibition (%)
8 + SDS	20 + 20	72 μM	8
15 + SDS	20 + 20	79 μM	3
26a + SDS	20 + 20	83 μM	0
38a + SDS	20 + 20	64 μM	3
40 + SDS	20 + 20	40 μM	30
81a + SDS	20 + 20	49 μM	19
106 + SDS	20 + 20	76 μM	0
107 + SDS	20 + 20	72 μM	0
108 + SDS	20 + 20	83 μM	1
109 +SDS	20 + 20	128 μM	0

Table 2.16: Inhibition of SDS biodegradation by **8**, **15**, **26a**, **38a**, **40**, **81a**, **106**, **107**, **108** and **109**

The % inhibition values for organocatalysts (**8**, **15**, **26a**, **38a**, **81a**, **106**, **107**, **108** and **109**) are lower than the limit (>25% inhibition) generally accepted to consider an inhibitory effect on the activity of the inoculum. However, Maruoka phase-transfer catalyst (**40**) gave a % inhibition value of 30%, as a result this compound has an inhibitory effect on the activity of the inoculum.

Organocatalysts **19**, **89**, **103**, **104** and **110** (Figure 2.22) gave biodegradation values >10 % (Table 2.17).

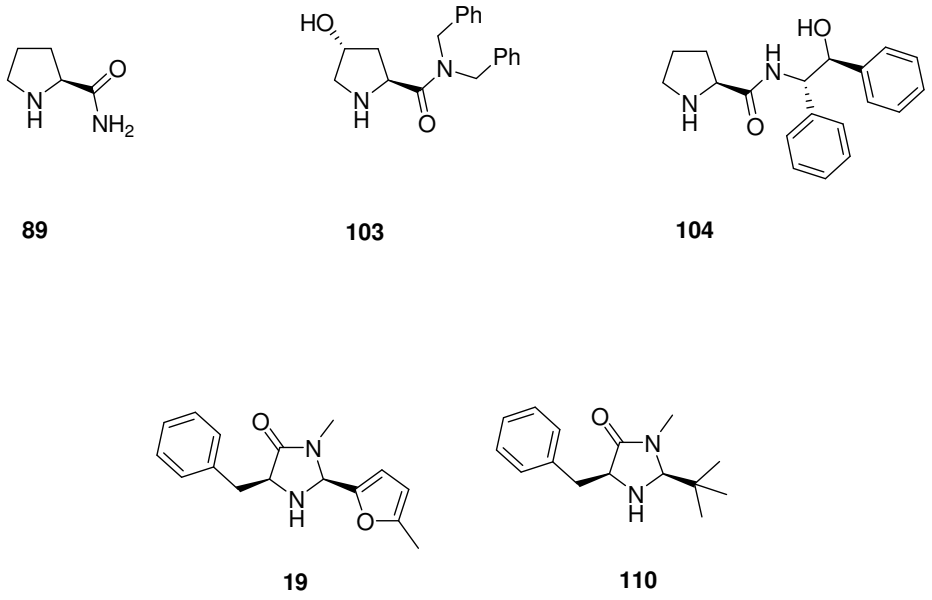

Fig 2.22 Organocatalysts (**19**, **89**, **103**, **104** and **110**) giving >10% biodegradation

Compound	% Biodegradation			
	6 d	**14 d**	**21 d**	**28 d**
SDS	78	86	85	90
19	20	19	19	30
89	72	75	81	77
103	11	10	8	11
104	14	16	36	38
110	13	24	25	30

Table 2.17: Organocatalysts (**19**, **89**, **103**, **104** and **110**) showing >10% biodegradation after 28 days

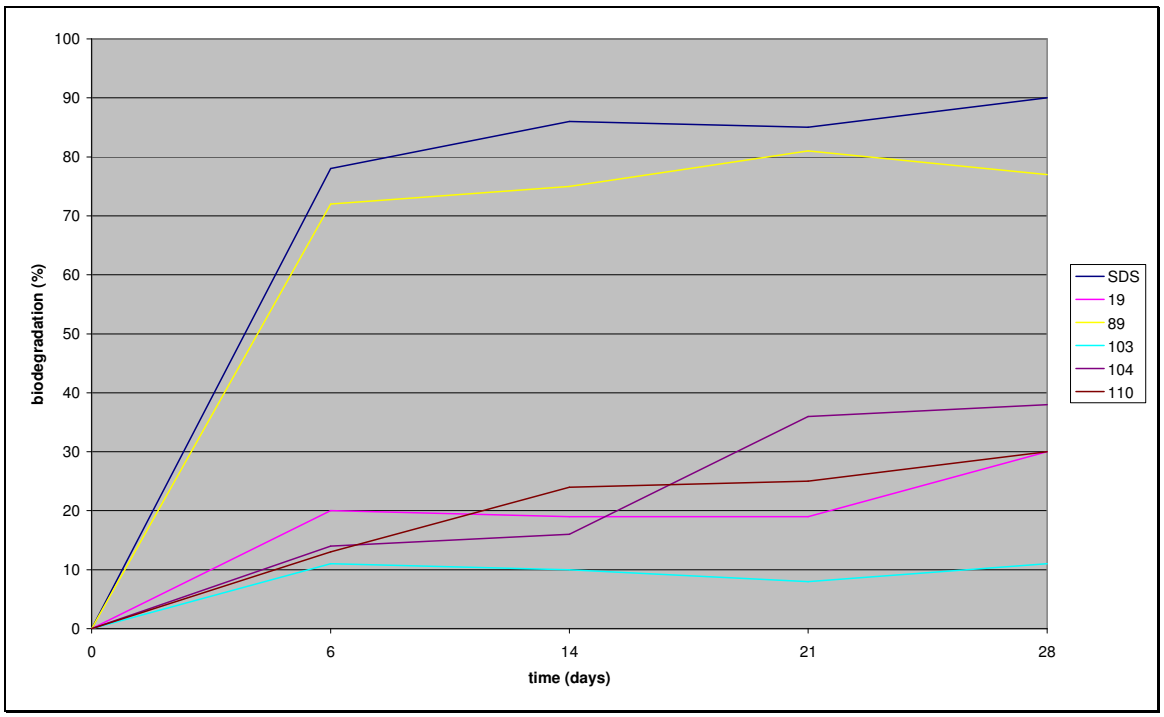

Fig 2.23 Biodegradation curves for organocatalysts (**19**, **89**, **103**, **104** and **110**) showing >10% biodegradation after 28 days

L-Prolinamide (**89**) passed the CO_2 headspace test (ISO 14593) as it gave a biodegradation value of 77% after 28 days (Figure 2.23). Compound **89** is readily biodegradable under the parameters of the CO_2 headspace test (ISO 14593). Proline derivatives **103** and **104** showed biodegradation values of 11 % and 38%, respectively, after 28 days. Both MacMillan imidazolidinones **19** and **110** gave a biodegradation value of 30% after 28 days. Compounds **19**, **103**, **104** and **110** are not readily biodegradable under the parameters of the CO_2 headspace test (ISO 14593).

Organocatalysts (**19**, **89**, **103**, **104** and **110**) showed no inhibitory effect on the activity of the inoculum (Table 2.18).

Compound	Concentration (mgC/L)	Molar concentration of test sample	Inhibition (%)
19 + SDS	20 + 20	104 μM	0
89 + SDS	20 + 20	333 μM	0
103 + SDS	20 + 20	88 μM	0
104 + SDS	20 + 20	88 μM	0
110 + SDS	20 + 20	111 μM	0

Table 2.18: Inhibition of SDS biodegradation by organocatalysts (**19**, **89**, **103**, **104** and **110**)

Biodegradation data for other organocatalysts (**26b**, **41a**, **45a**, **45b**, **48a**, **48b**, **50a**, **50b**, **92**, **97**, **100**, **101**, **102**, **105a** and **105b**) studied, showed negligible CO_2 output (see appendix table 8 and figure 1), these catalysts are non-biodegradable under the parameters of the CO_2 headspace test (ISO 14593).

2.7 Conclusions

A range of known organocatalysts including amino acids, proline derivatives, BINOL, BINOL derivatives, TADDOL, Jacobsen thioureas, Cinchona alkaloid derivatives, MacMillan imidazolidinones, chiral phosphoric acids and a Maruoka phase-transfer catalyst were studied for antimicrobial activity. Studies performed in DCU showed a number of amino acids inhibiting test bacteria. MIC values for inhibitory amino acids were found to be high (>2.5 mM). Proline derivatives (**95** and **96**) inhibited Gram positive *M.luteus*, *B.subtilis* and Gram negative *E.coli*. Remaining proline derivatives proved non-inhibitory within tested concentration range (3.45 mM-0.007 mM). BINOL (**45**) exhibited inhibition towards *M.luteus* and *B.subtilis* (0.107 mM) while BINOL derivatives and TADDOL proved to be non-inhibitory for test organisms within studied concentration range.

Antimicrobial studies performed by our collaborator Dr Marcel Špulák showed a number of organocatalysts inhibiting test microorganisms. A number of cases of inhibition were found with proline derivatives (**101** and **102**) for both bacterial and fungal organisms. Jacobsen thioureas inhibited different bacteria with **15** being the most active. **15** was the only Jacobsen thiourea found to inhibit fungal strains (4 in total). Cinchona alkaloid derivatives were observed with low inhibition for bacteria, with only **81a** exhibiting antifungal activity in some cases. MacMillan imidazolidinones were found to be mostly non-inhibitory towards both bacterial and fungal strains (>2000 μM). The only exceptions were **109** which inhibited *MRSA* at 2000 μM after 24 h and at 48 h and **110** was found to inhibit *Staphylococcus epidermidis* at 2000 μM after 24 h and at 48 h. **110** inhibited 2 fungal strains. Chiral phosphoric acids (**26a** and **26b**) and Maruoka phase-transfer catalyst (**40**) proved inhibitory for most Gram positive bacteria while Gram negative bacteria showed low inhibition. **26b** was observed with two cases of inhibition for fungal organisms while **40** inhibited a number of fungal organisms. TADDOL (**100**) and BINOL derivatives (**98** and **99**) showed low inhibition towards all bacterial and fungal organisms. (*S*)-BINOL (**45a**) and (*R*)-BINOL (**45b**) inhibited all Gram positive bacteria while Gram negative bacteria showed low inhibition. **45a** and **45b** showed a few cases of anti-fungal activity. Brominated BINOL derivatives (**50a** and **50b**) were found to be more toxic than BINOL (**45a** and **45b**) as lower MIC values were obtained for Gram positive bacteria. **50a** and **50b** inhibited all Gram positive bacteria while Gram negative bacteria showed low inhibition (>2000 μM). A trend noted was that the *R* enantiomer (**50b**) was more active than the *S* enantiomer (**50a**). H_8-BINOLs (**48a** and **48b**) inhibited all Gram positive bacteria while Gram negative bacteria were not inhibited (>2000 μM). Brominated H_8-BINOL derivatives (**105a** and **105b**) were found to be more toxic towards Gram positive bacteria than the non-brominated H_8-BINOLs (**48a** and **48b**). (*R*)-3,3'-Dibromo-H_8-BINOL (**105b**) was observed with lower MIC values when compared to (*S*)-3,3'-dibromo-H_8-BINOL (**105a**). Cytotoxicity, apoptosis and cell viability studies showed most organocatalysts to be non-toxic towards erythroid progenitors, HL-60 and K-562 blood cell lines. However, **102** and **107** were found to reduce cell viability by less than 50% for all 3 cell lines at 10 μM. **40** proved toxic for all 3 blood cell lines as it was found to induce cell death by apoptosis and resulted in a loss of cell viability.

Organocatalysts (**8**, **15**, **19**, **26a**, **26b**, **38a**, **40**, **41a**, **45a**, **45b**, **48a**, **48b**, **50a**, **50b**, **81a**, **92**, **97**, **100**, **101**, **102**, **103**, **104**, **105a**, **105b**, **106**, **107**, **108**, **109** and **110**) were found to be non-biodegradable under the parameters of the CO_2 headspace test (ISO 14593). L-Prolinamide (**89**) passed the CO_2 headspace test (ISO 14593) with a biodegradation value of 77% after 28 days. Compounds (**8**, **15**, **19**, **26a**, **26b**, **38a**, **41a**, **45a**, **45b**, **48a**, **48b**, **50a**, **50b**, **81a**, **89**, **92**, **97**, **100**, **101**, **102**, **103**, **104**, **105a**, **105b**, **106**, **107**, **108**, **109** and **110**) did not have a significant inhibitory effect on the activity of the inoculum. Maruoka phase-transfer catalyst (**40**) had an inhibitory effect on the activity of the inoculum as a % inhibition value of 30% was noted. Persistence in the environment for organocatalysts (**8**, **15**, **19**, **26a**, **26b**, **38a**, **40**, **41a**, **45a**, **45b**, **48a**, **48b**, **50a**, **50b**, **81a**, **92**, **97**, **100**, **101**, **102**, **103**, **104**, **105a**, **105b**, **106**, **107**, **108**, **109** and **110**) is a concern.

2.8 References

(1) ISO 14593: Water quality, Evaluation of ultimate aerobic biodegradability of organic compounds in aqueous medium. Method by analysis of inorganic carbon in sealed vessels (CO_2 headspace test), 1999.

(2) D. Amsterdam, *Antibiotics in Laboratory Medicine,* 4th ed. V. Lorian, Williams & Wilkins, Baltimore, MD, 1996.

(3) M. Friedman, *J. Agric. Food Chem.,* 1999, **47**, 3457-3479.

(4) H. Yang, G. Zheng, X. Peng, B. Qiang and J. Yuan, *FEBS Lett.,* 2003, **552**, 95-98.

(5) G. P. Gladstone, *Brit. J. Exptl. Path.,* 1939, **20**, 189-200.

(6) E. L. Tatum, *Cold Spring Harb. Symp. Quant. Biol.,* 1946, **11**, 278-284.

(7) E. Beerstecher and W. Shive, *J. Biol. Chem.,* 1947, **167**, 527-534.

(8) D. Rowley, *J. Gen. Microbiol.,* 1953, **9**, 37-43.

(9) M. De Felice, M. Levinthal, M. Iaccarino and J. Guardiola, *Microbiol. Mol. Biol. Rev.,* 1979, **43**, 42-58.

(10) S. W. Fox, M. Fling and G. N. Bollenback, *J. Biol. Chem.,* 1944, **155**, 465-468.

(11) E. E. Snell and B. M. Guirard, *Proc. Natl. Acad. Sci.,* 1943, **29**, 66-73.

(12) B. D. Davis and W. K. Maas, *J. Am. Chem. Soc.,* 1949, **71**, 1865.

(13) J. H. Mueller and P. A. Miller, *J. Am. Chem. Soc.,* 1949, **71**, 1865-1866.

(14) M. Caparros, A. G. Pisabarro and M. A. de Pedro, *J. Bacteriol.,* 1992, **174**, 5549-5559.

(15) S. Wydau, G. van der Rest, C. Aubard, P. Plateau and S. Blanquet, *J. Biol. Chem.,* 2009, **284**, 14096-14104.

(16) O. Soutourina, J. Soutourina, S. Blanquet and P. Plateau, *J. Biol. Chem.,* 2004, **279**, 42560-42565.

(17) CytoTox-ONE homogeneous membrane integrity assay (G7892, Promega)

(18) Caspase-Glo 3/7 assay (G8091, Promega)

(19) N. A. Thornberry and Y. Lazebnik, *Science.,* 1998, **281**, 1312-1316

(20) CellTiter-Blue cell viability assay (G8082, Promega)

Chapter 3: Results and Discussion

Chapter 3: Results and Discussion

3 Polysubstituted BINOL derivatives

3.1 Aim

The aim for this part of the project was to design and synthesise a library of novel polysubstituted BINOLs which contained structural features that are known to improve biodegradability of a chemical ('rules of thumb'). We anticipated poor biodegradability for BINOL due to the presence of quaternary carbons, fused rings and poor water solubility. Initially, the biodegradability of (+/−)-BINOL (**45**) and (+/−)-3,3'-diphenyl-2,2'-dihydroxy-1,1'-binaphthyl (**122**) were determined using the CO_2 headspace test (ISO 14593). Subsequent to those findings the synthesis of polysubstituted BINOLs was initiated.

3.2 Introduction

For our design of polysubstituted BINOLs, the placement of bulky substituents at the 3,3'-position of the BINOL scaffold was necessary, as bulky groups have been found as a requirement for effective asymmetric induction.[1] As a result, a phenyl group was placed at the 3,3'-position of the BINOL scaffold which should have a lesser effect on biodegradability compared to more bulkier groups e.g. anthracene, naphthalene, triphenylsilyl and phenanthrene. The 6,6'-position was selected for the attachment of molecular features with a positive effect for biodegradability. Substituents to be placed at the 6,6'-position were *n*-butyl, hydroxyl, methoxy, ethoxy, carboxylic acid and an alkylcarbonyl group (Figure 3.1). Our hypothesis is these functionalities will provide a site for microbial attack, allow for ring cleavage which could result in the biodegradation of the compound.

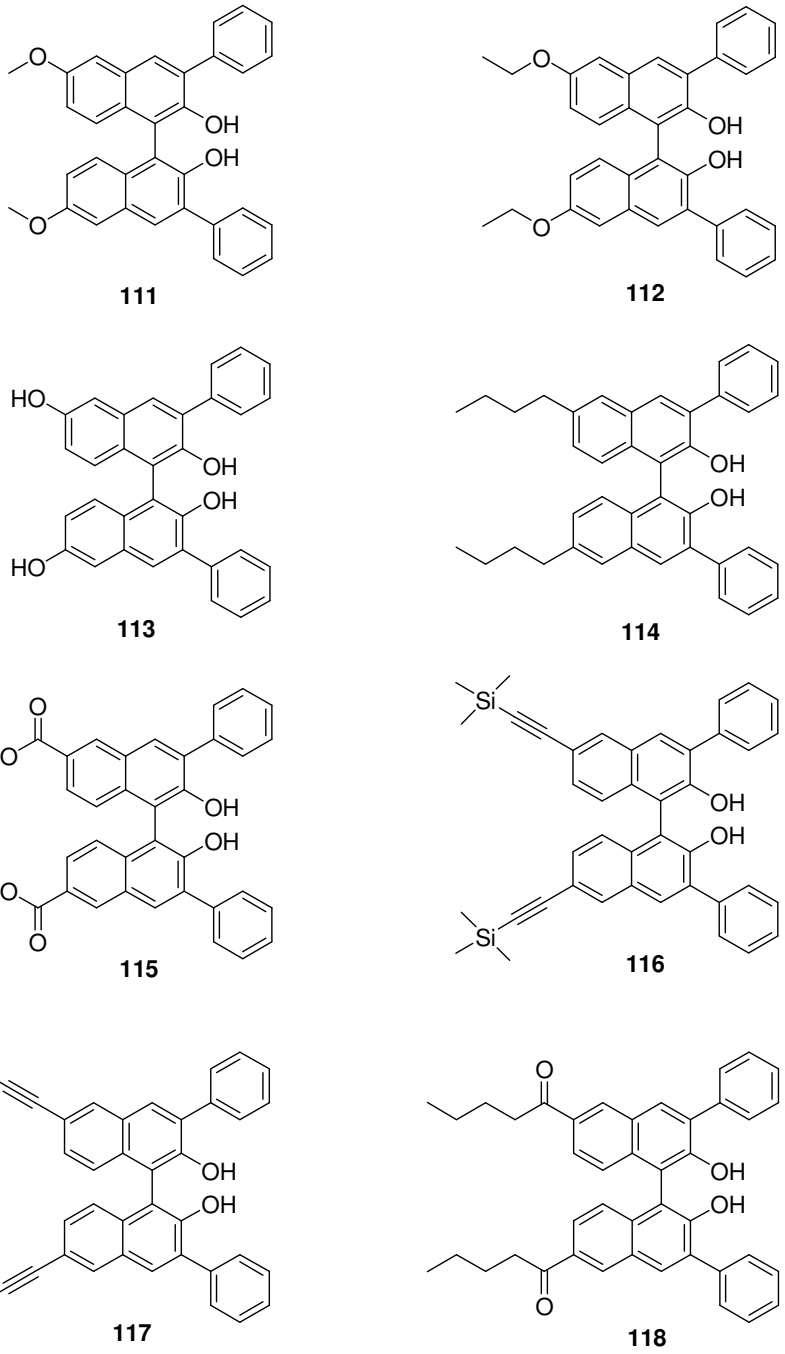

Fig. 3.1 Target compounds

3.3 Synthesis of achiral polysubstituted BINOL derivatives

In order to make these polysubstituted BINOLs (Figure 3.1), a key intermediate (**123**) had to be prepared from BINOL (**45**) in 5 steps following a literature procedure (Scheme 3.1).[2]

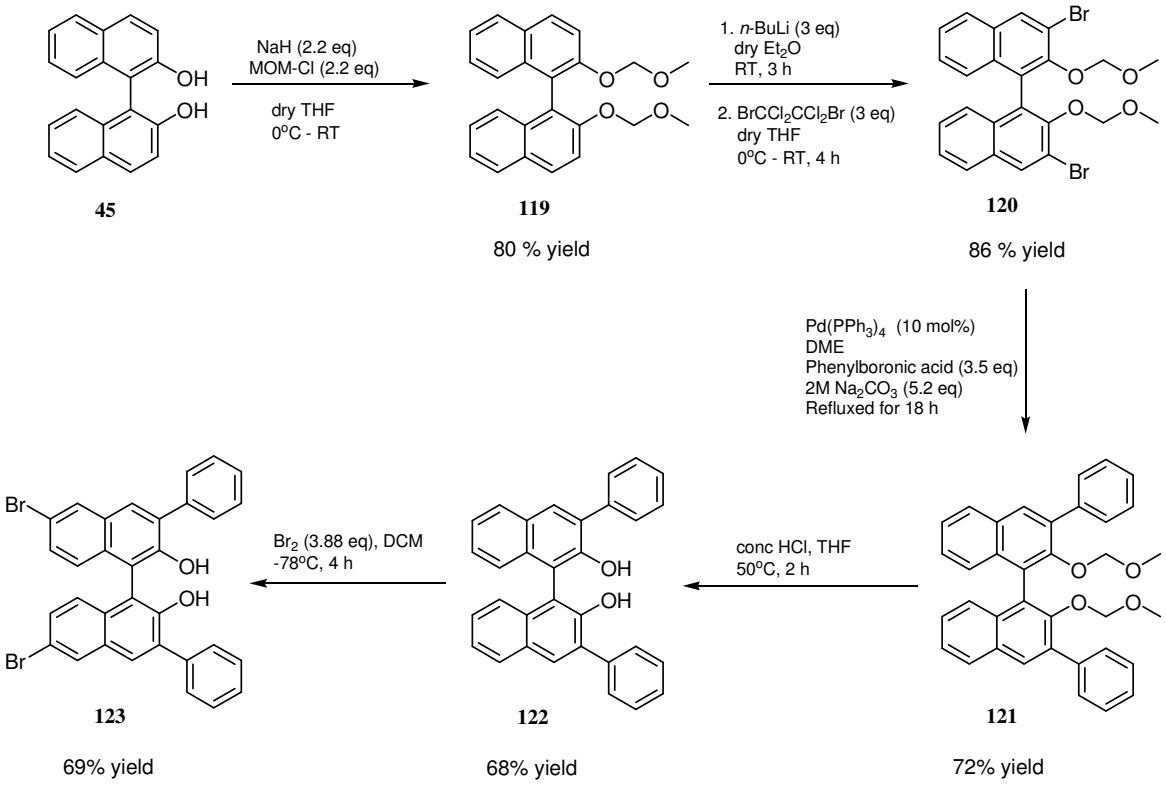

Scheme 3.1: Synthesis of key intermediate (+/−)-6,6'-dibromo-3,3'-diphenyl-2,2'-dihydroxy-1,1'-binaphthyl (**123**)

First step in the synthesis of key intermediate (**123**) involved the protection of (+/−)-BINOL (**45**) hydroxyl groups with chloromethyl methyl ether to yield (+/−)-2,2'-*bis*(methoxymethoxy)-1,1'-binaphthyl (**119**) as a white solid in 80% yield after column chromatography. Next step was to introduce Br atoms at the 3,3'-position of compound (**119**). These bromine atoms were introduced by a directed *ortho*-lithiation reaction followed by bromination. Firstly, the dilithiated (+/−)-2,2'-*bis*(methoxymethoxy)-1,1'-

binaphthyl intermediate was formed by the addition of an excess (3 equivalents) of 1.6 M *n*-butyllithium in hexanes to a solution of (**119**) in dry diethyl ether. The MOM-protecting group acts as a directing metalating group thereby facilitating the deprotonation of the *ortho* C-H bond by co-ordinating *n*-butyllithium.[3] This functionality also facilitates in the break up of lithium aggregates thus eliminating the need for TMEDA in this reaction. After the dilithiated intermediate was allowed to form, it was quenched with the appropriate electrophile 1,2-dibromo-tetrachloroethane to yield (+/−)-3,3'-dibromo-2,2'-*bis*(methoxymethoxy-1,1'-binaphthyl (**120**).

At first, the dibrominated intermediate (**120**) was obtained in a range of yields (25-86%), dependant on the addition step of the electrophile. It was found that the method that the electrophile 1,2-dibromo-tetrachloroethane was added had an impact on the yield being obtained for the dibrominated product (**120**). Initially, 1,2-dibromo-tetrachloroethane was pre-dissolved in THF and was then added slowly to the dilithiated intermediate. A mixture of mono- and dibrominated products were obtained when the brominating reagent was added this way, the monobrominated product (**124**) was obtained in 48% yield and dibrominated product (**120**) was obtained in a lower yield of 25% (Figure 3.2).

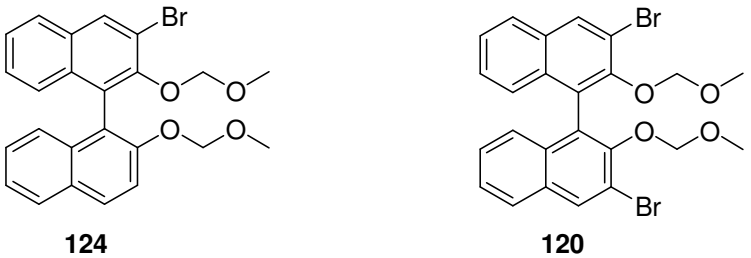

124 **120**

Fig. 3.2 Mono and dibrominated products (**124** and **120**)

Further compounding this result was the fact that both products (**120** and **124**) eluted as very close spots on the TLC (R_f = 0.39 for **120**, R_f = 0.34 for **124** in Hex/EA 10/1) which gave poor separation by column chromatography. In addition a mix fraction of the two compounds (27% yield) was also obtained after column chromatography. By changing the method of addition for the electrophile as reported by Chong and coworkers,[4] it was found that no monobrominated product (**124**) resulted when THF was added directly to the dilithiated intermediate and allowed to stir for 1 h followed by the addition of 1,2-dibromo-tetrachloroethane, only the dibrominated product (**120**) was formed and obtained in 86% yield after column chromatography.

Following the synthesis of (**120**), phenyl groups were attached to the 3,3'-position of the BINOL scaffold *via* Suzuki coupling. For this step, (**120**) was reacted with phenylboronic acid using 2M sodium carbonate and *tetrakis*(triphenylphosphine)palladium(0) as catalyst to yield (+/−)-3,3'-diphenyl-2,2'-*bis*(methoxymethoxy)-1,1'-binaphthyl (**121**) in 72% yield. The MOM protecting group was removed by acidic hydrolysis using concentrated HCl to yield (+/−)-3,3'-diphenyl-2,2'-dihydroxy-1,1'-binaphthyl (**122**) in 68% yield.

The final step towards the key intermediate (**123**) involved the bromination of (**122**) with molecular bromine to yield (+/−)-6,6'-dibromo-3,3'-diphenyl-2,2'-dihydroxy-1,1'-binaphthyl (**123**). However, it was not possible to obtain (**123**) pure when 2.09 equivalents of bromine was used for this reaction as reported in the literature.[2] Additional signals relating to an impurity were apparent in the proton NMR spectrum (Figure 3.3) that did not correlate with the reported proton data for compound (**123**).

.

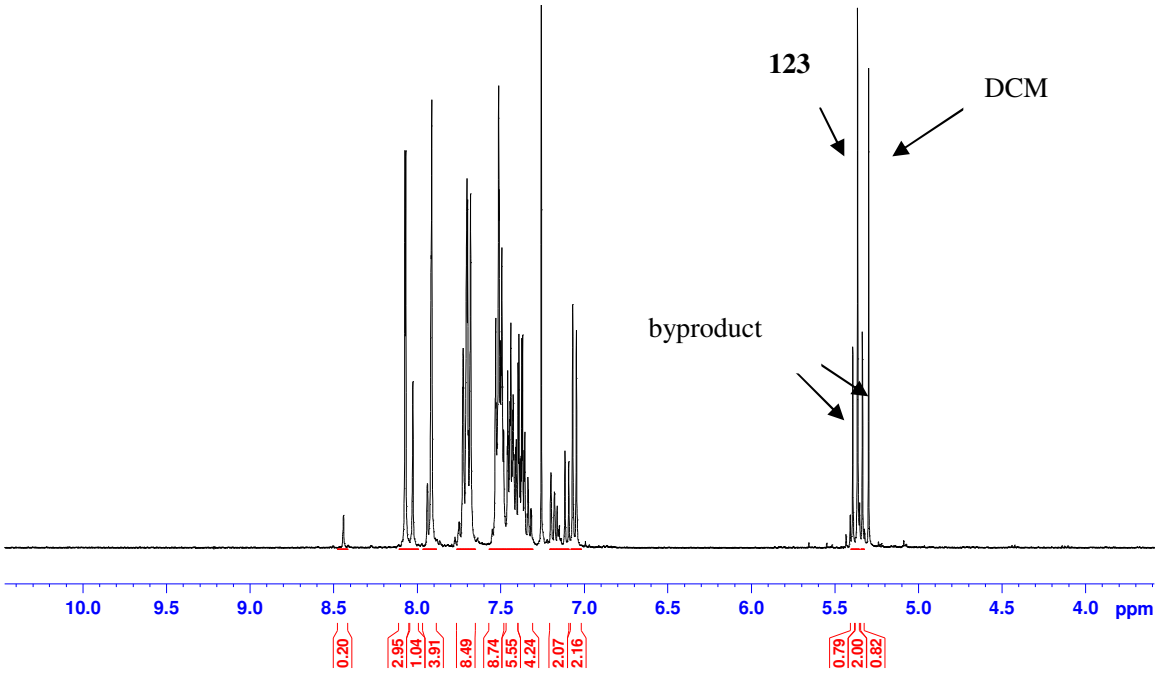

Fig. 3.3 Proton spectrum of key intermediate (**123**) after 2.09 equivalents of bromine

Unfortunately, the impurity was overlapping with the product (**123**) on TLC and it was not possible to achieve separation with different mobile phases (Hex/EA, Hex/DCM, Tol). The addition of extra equivalents of bromine did help to improve the bromination reaction, for instance, 3.08 and 3.88 equivalents of bromine were all tried for this step. Best results were obtained with 3.88 equivalents of bromine, however, some impurity still remained and following recrystallisation it was possible to obtain (**123**) in 97 % purity (by ^{1}H NMR) in 69% yield. As can be seen from the proton spectra, the impurity was more prevalent for 3.08 equivalents (Figure 3.4) than for 3.88 equivalents (Figure 3.5). As the addition of extra equivalents of bromine reduced the impurity, this suggests that underbromination of **122** occurred when 2.09 equivalents of bromine was used. The postulated structure of the impurity is the monobrominated product.

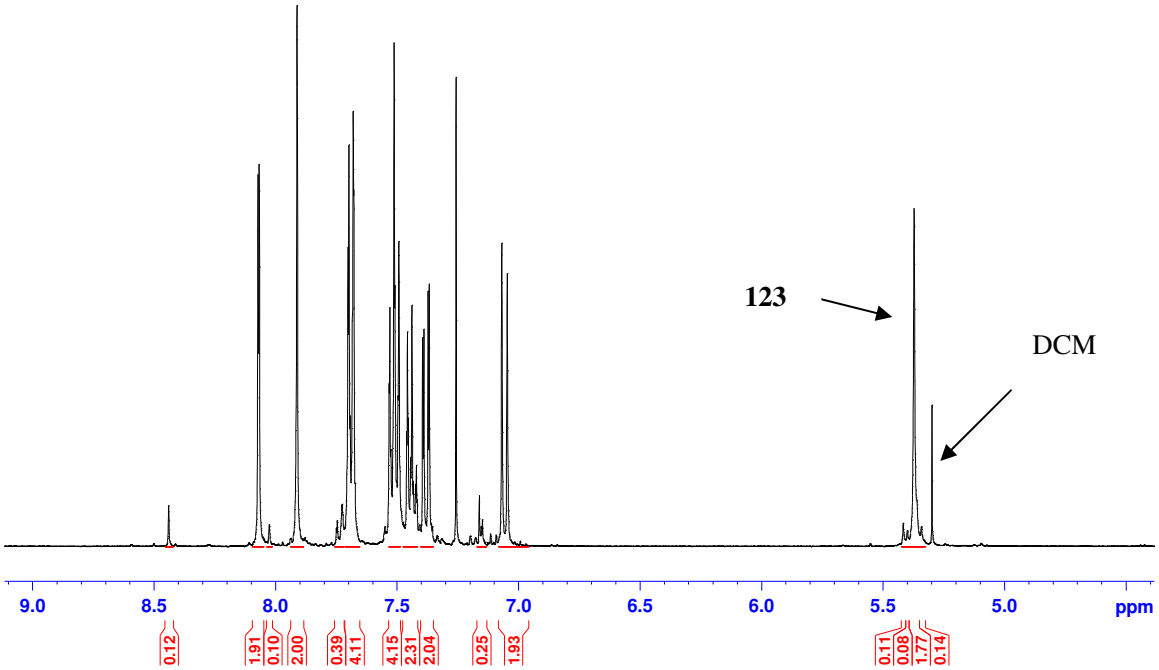

Fig. 3.4 Proton spectrum of key intermediate (**123**) after 3.08 equivalents of bromine

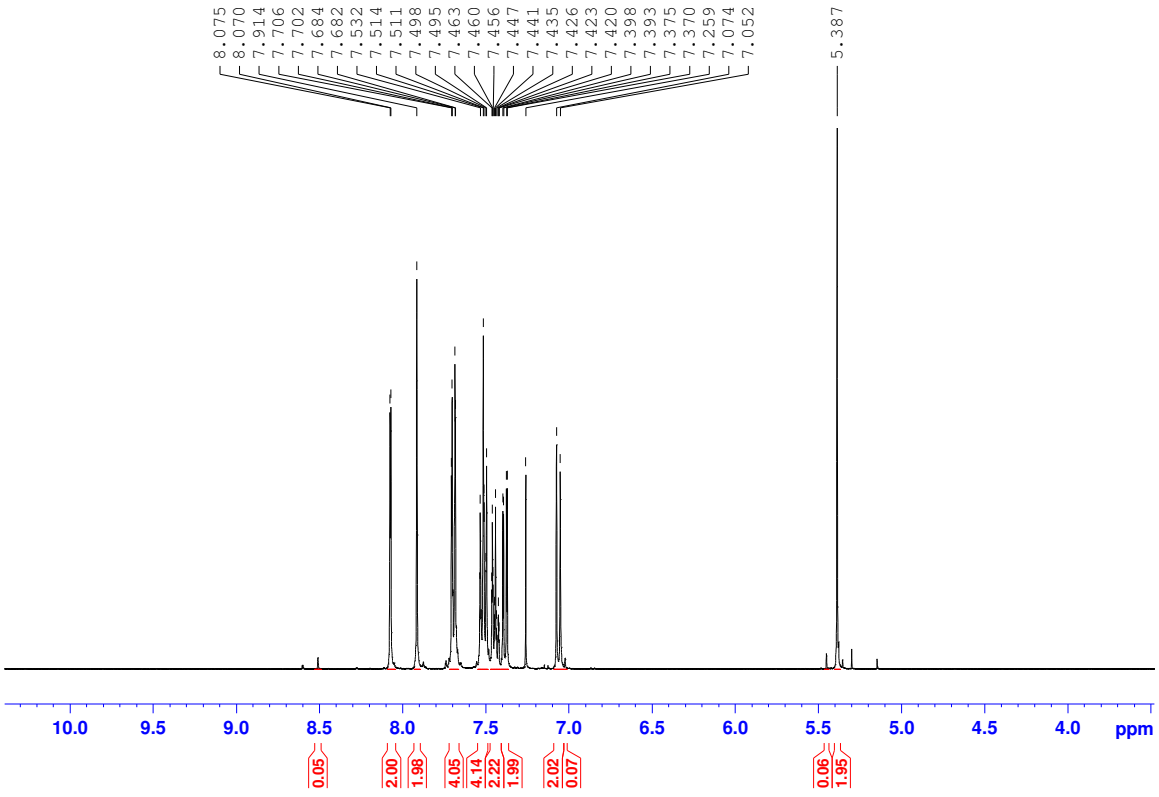

Fig. 3.5 Proton spectrum of key intermediate (**123**) after 3.88 equivalents of bromine

Bromination of (**121**) was also attempted, but due to the generation of HBr during the reaction, the deprotection of the MOM groups occurred.

Following the preparation of key intermediate (**123**) the synthesis of target compounds (Figure 3.1) was started. Initially, (+/−)-6,6'-dimethoxy-3,3'-diphenyl-2,2'-dihydroxy-1,1'-binaphthyl (**111**) and (+/−)-6,6'-diethoxy-3,3'-diphenyl-2,2'-dihydroxy-1,1'-binaphthyl (**112**) were synthesised from (**123**) by a copper coupling reaction (Ullmann-type condensation).[5,6] By refluxing the key intermediate (**123**) in DMF with 4.4 M sodium methoxide in methanol and copper(I) iodide as catalyst, it was possible to obtain compound (**111**) in 65% yield after work-up and column chromatography. Substituting the sodium methoxide base for this reaction with 2.2 M sodium ethoxide allowed for the synthesis of (**112**) in 55% yield after work-up and column chromatography.

For the synthesis of (+/−)-6,6'-dihydroxy-3,3'-diphenyl-2,2'-dihydroxy-1,1'-binaphthyl (**113**), a demethylation of (**111**) using 1 M boron tribromide in DCM was necessary to produce free hydroxyl groups in position 6.[6] A yield of 49% was obtained for this reaction, however, degradation of the compound was apparent during column chromatography as a purple band was observed on silica and tailing fractions showed signs of an impurity in ^{1}H NMR spectrum. Future studies should optimise the isolation method.

The route selected for introducing a carboxylic acid group at the 6,6'-position, was to perform a halogen metal exchange of the bromine substituents and quench the resulting dilithiated intermediate with dry ice (Solid CO_2). Before performing this reaction it was necessary to protect the hydroxyl groups of diol (**123**) with MOM-Cl to generate (+/−)-6,6-dibromo-3,3'-diphenyl-2,2'-*bis*(methoxymethoxy)-1,1'-binaphthyl (**125**) in 68% yield after column chromatography. With the MOM-protected intermediate (**125**) a halogen metal exchange of bromine substituents was performed using 1.6 M *n*-butyllithium in hexanes as base and the resultant dilithiated intermediate was reacted with dry ice to furnish (+/−)-6,6'-dicarboxyl-3,3'-diphenyl-2,2'-*bis*(methoxymethoxy)-1,1'-binaphthyl (**126**) in 44% yield after column chromatography. Next step involved the

removal of MOM protecting groups by acidic hydrolysis to yield (+/−)-6,6'-dicarboxyl-3,3'-diphenyl-2,2'-dihydroxy-1,1'-binaphthyl (**115**) in 77% yield as final product.

For the introduction of *n*-butyl substituents, a Kumada metal coupling reaction[7] was performed using the MOM-protected (**125**). This coupling procedure involved reacting MOM-protected (**125**) with a nickel catalyst (1,3-dppp)$NiCl_2$ and a Grignard reagent (2 M *n*-butylmagnesiumchloride in THF) to yield (+/−)-6,6'-dibutyl-3,3'-diphenyl-2,2'-*bis*(methoxymethoxy)-1,1'-binaphthyl (**127**) in 35 % yield after column chromatography. The monosubstituted compound (**128**) and intermediate (**121**) were also obtained as side products for this reaction (Figure 3.6).

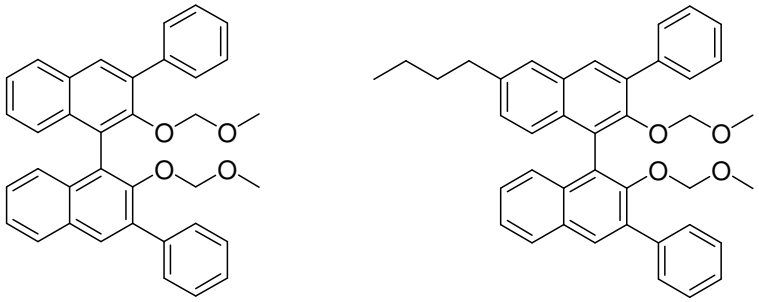

121 **128**

Fig. 3.6 Side products obtained from Kumada coupling reaction

Purification of **127** (R_f = 0.79, Hex/EA 5/1) was tedious due to the monosubstituted product (**128**) (R_f = 0.71, Hex/EA 5/1) eluting very close on the TLC. Monosubstituted product (**128**) was obtained in 27% yield and compound (**121**) was isolated in 18% yield. In addition a mix fraction of 11% yield was obtained containing both **127** and **128**. Subsequent removal of the MOM groups for **127** by acidic hydrolysis yielded (+/−)-6,6'dibutyl-3,3'-diphenyl-2,2'-dihydroxy-1,1'-binaphthyl (**114**) in 74% yield after column chromatography.

An attempt to make **127** *via* a halogen-metal exchange of bromine substitutents on **125** to generate a dilithiated intermediate and the subsequent quenching with bromobutane[8]

proved unsuccessful for the synthesis of **127** as only **121** was obtained after work-up and column chromatography.

The acyl functional group was to be introduced at the 6,6'-position *via* hydration of an alkyne substituent. Using the Sonogashira coupling reaction,[9] the introduction of an alkyne substituent at the 6,6'- position was possible. The Sonogashira methodology reported by Beller and coworkers was adopted for this reaction.[10] For this metal coupling reaction the MOM protection of the hydroxyl groups for key intermediate (**123**) was not necessary.

Initially, to ensure that the conditions used by Beller for the Sonogashira reaction worked for the polysubstituted BINOL key intermediate (**123**), the preparation of (+/−)-6,6'-*bis*(2-(trimethylsilyl)ethynyl)-3,3'-diphenyl-2,2'-dihydroxy-1,1'-binaphthyl (**116**) was investigated. Synthesis of (+/−)-6,6'-*bis*(2-(trimethylsilyl)ethynyl)-3,3'-diphenyl-2,2'-dihydroxy-1,1'-binaphthyl (**116**) involved reacting (**123**) in TMEDA with ethynyltrimethylsilane using sodium tetrachloropalladate(II), 2-(di-*tert*-butylphosphino)-1-phenylindole (PIntB) and copper(I) iodide as catalytic reagents. Product (**116**) was obtained in 60% yield after column chromatography. Similarly, (+/−)-6,6'-dipentynyl-3,3'-diphenyl-2,2'-dihydroxy-1,1'-binaphthyl (**117**) was prepared by reacting (**123**) in TMEDA with 1-pentyne using sodium tetrachloropalladate(II), PIntB and copper(I) iodide as catalytic reagents to give a 50% yield after work-up and column chromatography.

Alami and coworkers have reported the use of PTSA for the hydration of internal arylalkynes.[11] Since PTSA is a greener alternative compared to the mercury based catalysts, it was applied for the hydration of (+/−)-6,6'-dipentynyl-3,3'-diphenyl-2,2'-dihydroxy-1,1'-binaphthyl (**117**). For this step (**117**) was hydrated using 1 equivalent of PTSA monohydrate in refluxing ethanol and the desired product (+/−)-6,6'-dipentan-1-one-3,3'-diphenyl-2,2'-dihydroxy-1,1'-binaphthyl (**118**) was obtained in 59% yield after column chromatography.

Overall the synthesis of racemic key intermediate (**123**) was accomplished in 5 steps with an overall yield of 23%. The synthetic steps of intermediate **120** and key intermediate **123**

were optimised as problems arose in the reported method. Novel polysubstituted BINOLs (Figure 3.1) were successfully synthesised.

As well, optically pure BINOL derivatives were required for asymmetric catalysis studies. The synthesis of chiral key intermediate (+)-(*R*)-(**123b**) was needed before chiral polysubstituted BINOLs could be made.

3.4 Synthesis of chiral polysubstituted BINOL derivatives

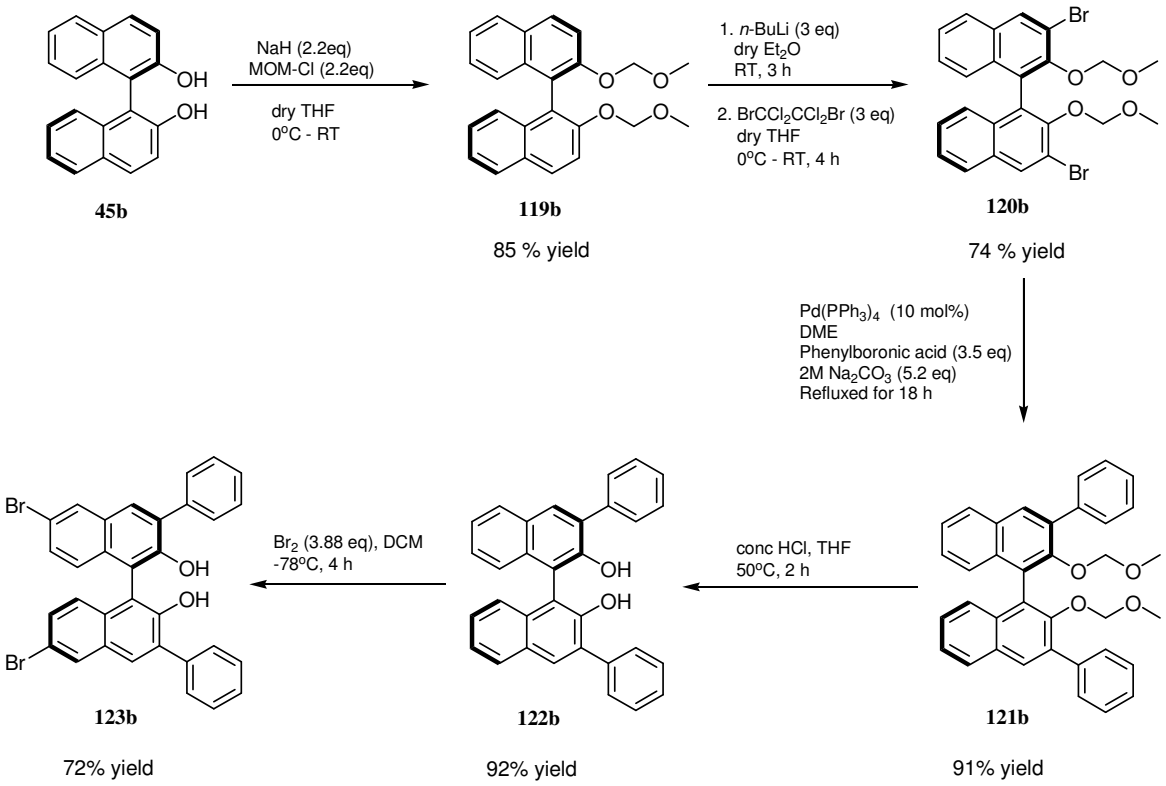

Scheme 3.2: Synthesis of key chiral intermediate (+)-(*R*)-6,6'-dibromo-3,3'-diphenyl-2,2'-dihydroxy-1,1'-binaphthyl (**123b**)

First step in the synthesis of key chiral intermediate (+)-(*R*)-(**123b**) involved the protection of (+)-(*R*)-BINOL (**45b**) hydroxyl groups with chloromethyl methyl ether to

yield (+)-(*R*)-(**119b**) as a white solid in 85% yield after column chromatography. Next step was to introduce Br atoms at the 3,3'-position of compound (+)-(*R*)-(**119b**). These bromine atoms were introduced by a directed *ortho*-lithiation reaction followed by bromination. Firstly, the dilithiated (*R*)-2,2'-*bis*(methoxymethoxy)-1,1'-binaphthyl intermediate was formed by the addition of an excess (3 equivalents) 1.6 M *n*-butyllithium in hexanes to a solution of (+)-(*R*)-(**119b**) in dry diethyl ether. After the dilithiated intermediate was allowed to form for 3 h, THF was added and after additional 1 h of stirring, the reaction was quenched with the electrophile 1,2-dibromo-tetrachloroethane to yield (+)-(*R*)-(**120b**) in 74% yield after work-up and column chromatography.

Following the synthesis of (+)-(*R*)-(**120b**), phenyl groups were attached to the 3,3'-position of the BINOL scaffold *via* Suzuki coupling. For this step, (+)-(*R*)-(**120b**) was reacted with phenylboronic acid using 2M sodium carbonate and *tetrakis*(triphenylphosphine)palladium(0) as catalyst to yield (−)-(*R*)-(**121b**) in 91% yield. The MOM protecting group was removed by acidic hydrolysis using concentrated HCl to yield (+)-(*R*)-(**122b**) in 92% yield. The final step towards the key intermediate (+)-(*R*)-(**123b**) involved the bromination of (+)-(*R*)-(**122b**) with molecular bromine (3.88 equivalents) to yield (+)-(*R*)-(**123b**) in 72% yield after recrystallisation. Next step was to synthesise the novel chiral polysubstituted BINOLs ((−)-(*R*)-**125b**, (+)-(*R*)-**111b** and (+)-(*R*)-**114b**) (Figure 3.7).

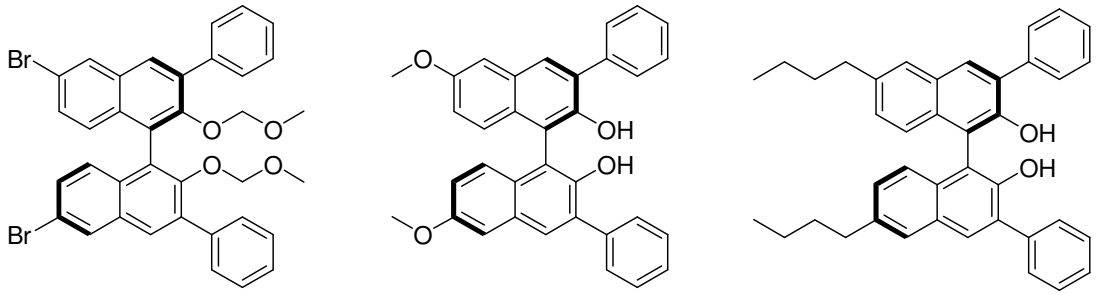

125b **111b** **114b**

Fig 3.7 Novel chiral polysubstituted BINOLs ((+)-(*R*)-**111b**, (+)-(*R*)-**114b** and (−)-(*R*)-**125b**)

(+)-(*R*)-6,6'-Dimethoxy-3,3'-diphenyl-2,2'-dihydroxy-1,1'-binaphthyl (**111b**) was synthesised from (+)-(*R*)-(**123b**) by a copper coupling reaction (Ullmann-type condensation).[5,6] By refluxing the key intermediate (+)-(*R*)-(**123b**) in DMF with 4.4 M sodium methoxide in methanol and copper(I) iodide as catalyst, it was possible to obtain compound (+)-(*R*)-(**111b**) in 67% yield after work-up and column chromatography.

Synthesis of intermediate (−)-(*R*)-(**125b**) involved MOM protection of the diol (+)-(*R*)-(**123b**) with chloromethyl methyl ether to yield (−)-(*R*)-6,6'-dibromo-3,3'-diphenyl-2,2'-*bis*(methoxymethoxy)-1,1'-binaphthyl (**125b**) in 56% yield after column chromatography. For the introduction of *n*-butyl substituents, a Kumada metal coupling reaction[7] was performed using the MOM-protected (−)-(*R*)-(**125b**). This coupling procedure involved reacting MOM-protected (−)-(*R*)-(**125b**) with a nickel catalyst (1,3-dppp)$NiCl_2$ and a Grignard reagent (2 M *n*-butylmagnesiumchloride in THF) to give crude (*R*)-6,6'-dibutyl-3,3'-diphenyl-2,2'-*bis*(methoxymethoxy)-1,1'-binaphthyl which was not isolated and directly deprotected by acidic hydrolysis to yield (+)-(*R*)-6,6'-dibutyl-3,3'-diphenyl-2,2'-dihydroxy-1,1'-binaphthyl (**114b**) in 42 % yield after column chromatography. The monosubstituted compound (**129b**) and intermediate (**122b**) were also obtained as side products for this reaction (Figure 3.8).

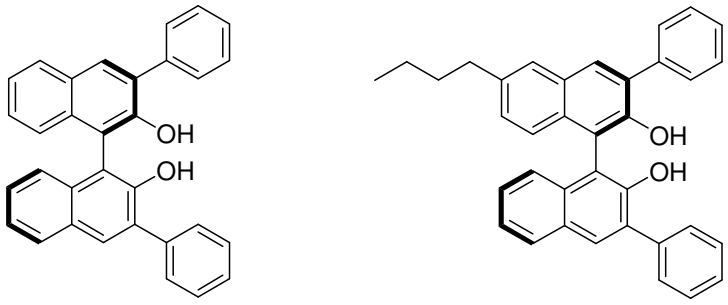

122b **129b**

Fig. 3.8 Side products obtained from Kumada coupling reaction

Chiral key intermediate (+)-(*R*)-(**123b**) was synthesised in 5 steps with an overall yield of 38%. Intermediates (+)-(*R*)-(**119b**), (+)-(*R*)-(**120b**), (−)-(*R*)-(**121b**), (+)-(*R*)-(**122b**) and (+)-(*R*)-(**123b**) were prepared in yields of 85%, 74%, 91%, 92% and 72%, respectively. The overall yield obtained for the chiral key intermediate (+)-(*R*)-(**123b**) (38%) is higher than the overall yield obtained for the racemic key intermediate **123** (23%).

The literature synthesis for (+)-(*R*)-(**123b**) was accomplished in 5 steps with an overall yield of 94%.[2] Reported yields for intermediates (+)-(*R*)-(**119b**), (+)-(*R*)-(**120b**), (+)-(*R*)-(**122b**) and (+)-(*R*)-(**123b**) in the literature were 100% (without column chromatography), 96%, 100% and 98%, respectively. Intermediate (−)-(*R*)-(**121b**) was not isolated in the literature procedure. The overall yield obtained in our laboratory for (+)-(*R*)-(**123b**) (38%) is lower than that obtained in the literature (94%). The reason for the overall yield being lower could be due to additional column chromatography performed on the first step to remove the residual dispersion oil and also the intermediate (−)-(*R*)-(**121b**) was isolated. The other group did not perform column chromatography on the first step therefore residual dispersion oil may have been taken into account for their reported yield, unless an extra step in the work-up was omitted in the method reported. Problems arose in the reported method for the synthesis of (+)-(*R*)-(**123b**) and also the required recrystallisation step resulted in a lower yield of 72% being obtained. These differences contributed to a lower overall yield being obtained for (+)-(*R*)-(**123b**).

Final chiral compounds **111b** and **114b** were successfully synthesised in 67% and 42% yield, respectively, and applied as catalysts in the Morita-Baylis-Hillman reaction (Chapter 5).

3.5 Optical rotations of chiral BINOL derivatives

The optical rotation values were recorded for chiral BINOL derivatives at 20 °C in THF at a concentration of 1 gram per 100 mL (C=1). Optical rotation values obtained for chiral BINOL derivatives are presented in Table 3.1. Most compounds gave a positive sign for optical rotation. However, an inversion for optical rotation was noted for MOM-protected

BINOLs (−)-(*R*)-**121b** and (−)-(*R*)-**125b** which resulted in a negative sign for optical rotation values. Slight variations were noted for optical rotation values compared to those reported in the literature, probably due to the differences in conditions used for measuring the optical rotation values (temperature).

Compound	Optical rotation from literature	Optical rotation from our study
(+)-(*R*)-(**45b**)	$[\alpha]^{21}_{D}$ = +34 ° (1.0 c, THF)	$[\alpha]^{20}_{D}$= +34.5 ° (1.0 c, THF)
(+)-(*R*)-(**119b**)	$[\alpha]^{25}_{589}$ = +95.0 ° (1.0 c, THF)[4]	$[\alpha]^{20}_{D}$ = +84.2 ° (1.0 c, THF)
(+)-(*R*)-(**120b**)	$[\alpha]^{25}_{589}$ = +28.3 ° (1.0 c, THF)[4]	$[\alpha]^{20}_{D}$ = +25.7 ° (1.0 c, THF)
(−)-(*R*)-(**121b**)	Not reported	$[\alpha]^{20}_{D}$ = −67.7 ° (1.0 c, THF)
(+)-(*R*)-(**122b**)	$[\alpha]_{D}$= +69.1 ° (1.0 c, $CHCl_3$)[12]	$[\alpha]^{20}_{D}$= +64.3 ° (1.0 c, $CHCl_3$)
(+)-(*R*)-(**123b**)	$[\alpha]^{25}_{589}$ = +96.6 ° (1.0 c, THF)[2]	$[\alpha]^{20}_{D}$ = +85.1 ° (1.0 c, THF)
(−)-(*R*)-(**125b**)	Novel compound	$[\alpha]^{20}_{D}$ = −2.0 ° (1.0 c, THF)
(+)-(*R*)-(**111b**)	Novel compound	$[\alpha]^{20}_{D}$ = +68.1 ° (1.0 c, THF)
(+)-(*R*)-(**114b**)	Novel compound	$[\alpha]^{20}_{D}$ = +53.2 ° (1.0 c, THF)

Table 3.1: Optical rotation values for chiral BINOL derivatives

Optical purity for chiral intermediate (+)-(*R*)-(**122b**) was further verified by chiral HPLC. An ee of 99.5 % was determined for (+)-(*R*)-(**122b**) *via* chiral HPLC analysis (Figure 3.9).

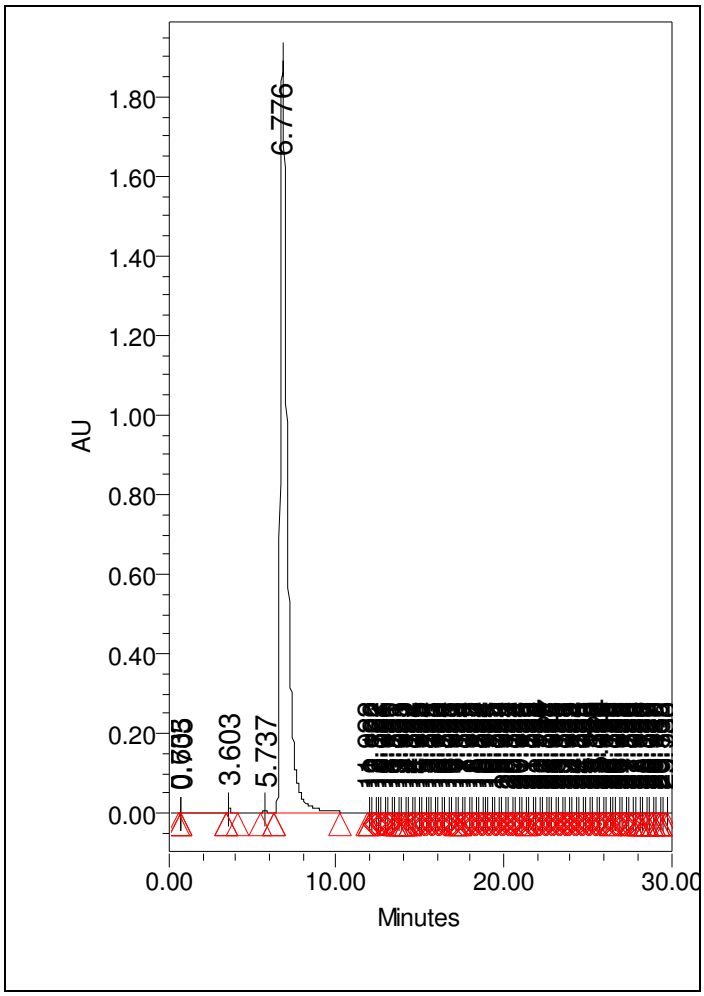

(+)-(*R*)-**122b**	**Peak**	**Retention time**	**% Area**	**Area**	**%ee**
	1	5.737 min	0.25	139444	99.5
	2	6.776 min	99.13	54773920	

Fig 3.9 HPLC chromatogram for chiral (+)-(*R*)-**122b** (Lux 2 column, 9:1 hexane:i-PrOH, 1.0 mL/min, 240 nm)

3.6 Antimicrobial screening of BINOL and polysubstituted derivatives

The antimicrobial activities of **45**, **122**, **111**, **114**, **115** and **118** were evaluated by our collaborator Dr Marcel Špulák of Charles University Czech Republic. Bacteria screened against were the four Gram positive organisms *Staphylococcus aureus* ATCC 6538, *Staphylococcus aureus* MRSA HK5996/08, *Staphylococcus epidermidis* HK6966/08, *Enterococcus sp.* HK14365/08 and four Gram negative organisms *Escherichia coli* ATCC 8739, *Klebsiella pneumoniae* HK11750/08, *Klebsiella pneumoniae*-**ESBL** positive HK14368/08 and *Pseudomonas aeruginosa* ATCC 9027. MIC values for antibacterial study were defined as 95 % inhibition (IC_{95}) of the growth of control. The results in Table 3.2 represent the MIC values obtained for BINOL and polysubstituted BINOLs (Figure 3.10). Antimicrobial screening of BINOL and derivatives is an essential preliminary screen before compounds can be evaluated for biodegradation.

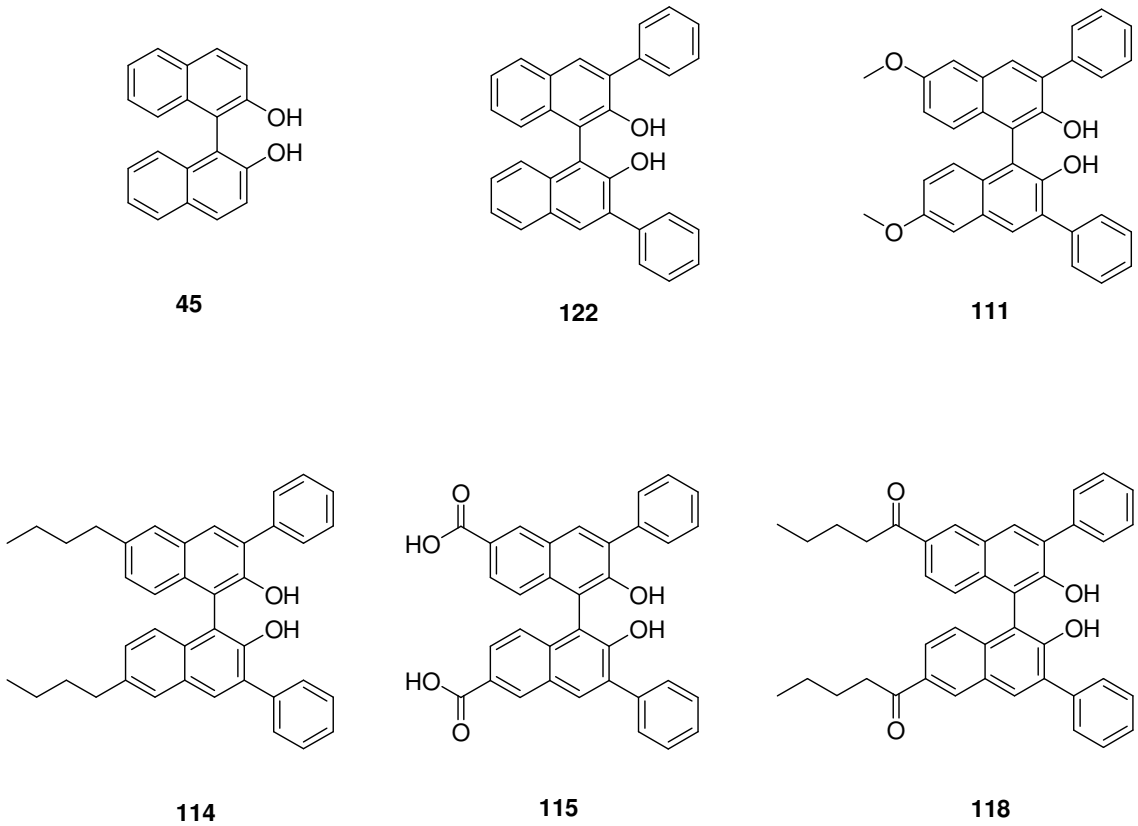

Fig 3.10 BINOL (**45**) and substituted derivatives (**111, 114, 115, 118** and **122**) screened for antimicrobial activity

		BINOL and derivatives					
Organism	Time (h)	**45**	**122**	**111**	**114**	**115**	**118**
S.aureus	24 h	**31.25**	>2000	>125	>125	>250	>125
	48 h	**125**	>2000	>125	>125	>250	>125
MRSA	24 h	**31.25**	>2000	>125	>125	>250	>125
	48 h	**125**	>2000	>125	>125	>250	>125
S.epidermidis	24 h	**31.25**	**500**	>125	>125	>250	>125
	48 h	**62.5**	**500**	>125	>125	>250	>125
Enterococcus sp.	24 h	**62.5**	**250**	>125	>125	>250	>125
	48 h	**125**	**250**	>125	>125	>250	>125
E.coli	24 h	>500	>2000	>125	>125	>250	>125
	48 h	>500	>2000	>125	>125	>250	>125
K.pneumoniae	24 h	>500	>2000	>125	>125	>250	>125
	48 h	>500	>2000	>125	>125	>250	>125
K.pneumoniae **ESBL** positive	24 h	>500	>2000	>125	>125	>250	>125
	48 h	>500	>2000	>125	>125	>250	>125
P.aeruginosa	24 h	>500	>2000	>125	>125	>250	>125
	48 h	>500	>2000	>125	>125	>250	>125

Results obtained by collaborator

Table 3.2: MIC/IC_{95} (μM) values of BINOL (**45**) and substituted derivatives (**111**, **114, 115, 118** and **122**)

(+/−)-1,1'-Bi-2-naphthol (**45**) was screened at 500 μM, (+/−)-3,3'-diphenyl-2,2'-dihydroxy-1,1'-binaphthyl (**122**) was screened at the highest concentration of 2000 μM, while compounds **111**, **114** and **118** were screened at a lower concentration of 125 μM due to the low solubility for these molecules in test medium (Mueller Hinton broth). Derivative **115** was screened at 250 μM as it was slightly more soluble in the test medium. MIC (minimum inhibitory concentration)/IC_{95} results for BINOL (**45**) and derivatives (**111, 114, 115, 118** and **122**) are displayed in Table 3.2.

BINOL (**45**) proved inhibitory for all Gram positive bacteria while Gram negative bacteria showed low inhibition (>500 μM). *Enterococcus sp.* was noted with an MIC value of 62.5 μM after 24 h and a value of 125 μM was observed after 48 h for **45**. *Staphylococcus aureus* and *MRSA* exhibited an MIC value of 31.25 μM after 24 h and a value of 125 μM after 48 h for BINOL (**45**). An MIC value of 31.25 μM was noted for **45** towards *Staphylococcus epidermidis* after 24 h while at 48 h the MIC value was 62.5 μM. A trend is noted for the MIC values of **45** whereby a lower MIC is recorded after 24 h than at 48 h. This is due to the fact that viable cells are still present at 24 h and the remaining viable bacterial cells grow substantial over the addtional 24 h period to increase the IC_{95} value observed after 48 h. Among the inhibited bacteria, *Escherichia coli* and *Enterococcus sp.* showed the greatest recovery.

(+/−)-3,3'-Diphenyl-2,2'-dihydroxy-1,1'-binaphthyl (**122**) proved inhibitory for 2 bacteria, *Staphylococcus epidermidis* (MIC value of 500 μM after 24 h and 48 h) and *Enterococcus sp.* (MIC value of 250 μM after 24 h and 48 h). Remaining bacteria proved non-inhibitory for **122** (>2000 μM).

MIC values were not observed for polysubstituted BINOLs **111**, **114**, **118** (>125 μM) and **115** (>250 μM). Polysubstituted BINOLs (**111**, **114**, **115** and **118**) were observed with low antimicrobial activity compared to **45** and **122**. Unsubstituted BINOL (**45**) proved the most toxic for bacteria. A trend noted for this case of antibacterial screening is that MIC values are lower at 24 h than at 48 h. Novel polysubstituted BINOLs (**111**, **114**, **115** and

118) and BINOL derivative (**99**) are less toxic towards test bacteria when compared to brominated BINOLs (**50b** and **50a**) and BINOL (**45b** and **45a**) (Figure 3.11).

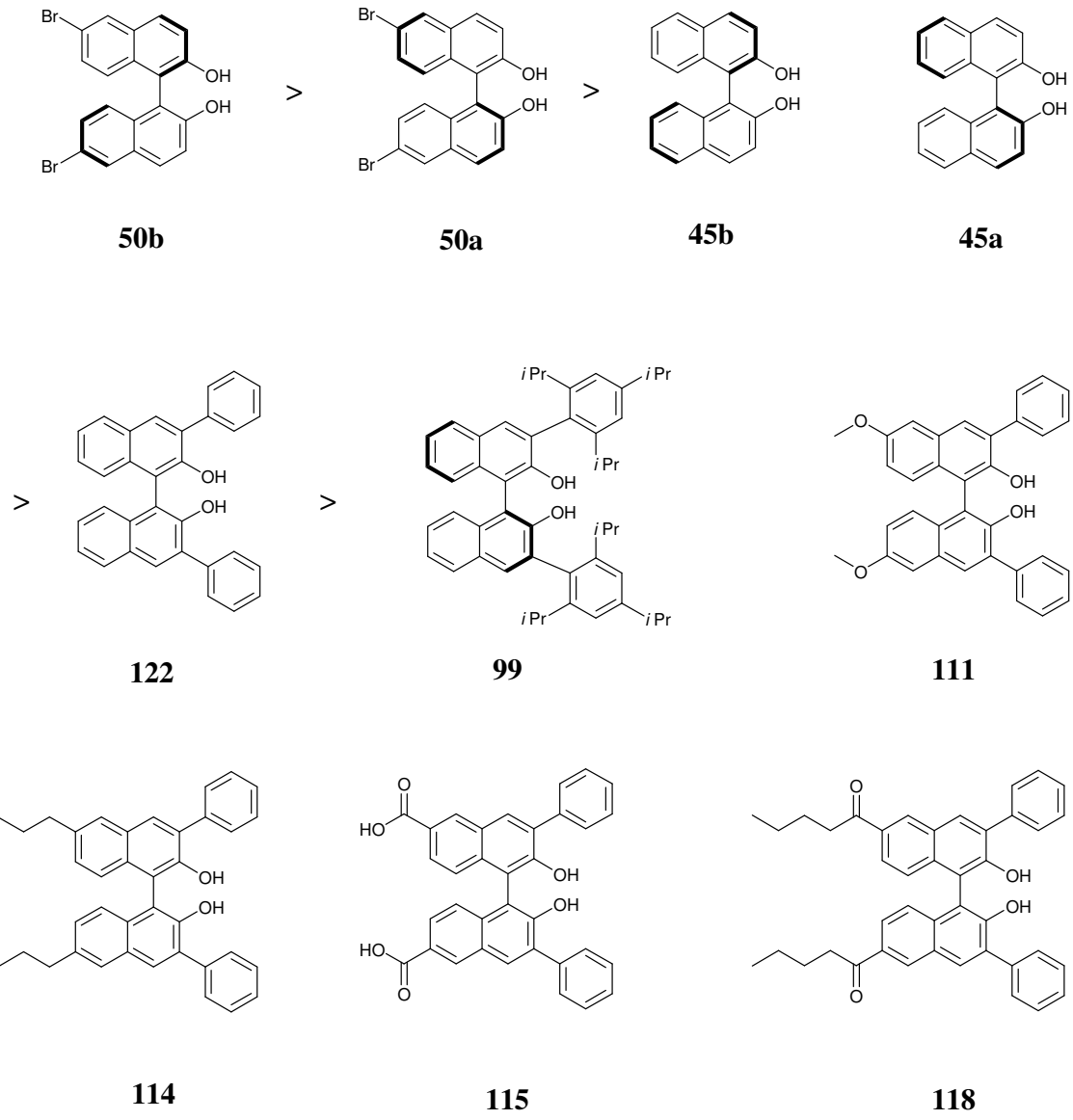

Fig 3.11 Overall trend for antibacterial activity of BINOL, BINOL derivatives and novel polysubstituted BINOLs (**50b >50a >45b**, **45a >122 >99**, **111**, **114**, **115** and **118**)

For the antifungal studies, compounds were screened against the following yeast strains (*Candida albicans* ATCC 44859, *Candida albicans* ATCC 90028, *Candida parapsilosis* ATCC 22019, *Candida krusei* ATCC 6258, *Candida krusei* E28, *Candida tropicalis* 156, *Candida glabrata* 20/I, *Candida lusitaniae* 2446/I, *Trichosporan asahii* 1188) and filamentous fungi (*Aspergillus fumigatus* 231, *Absidia corymbifera* 272, *Trichophyton mentagrophytes* 445). MIC values for antifungal study were defined as 80% inhibition (IC_{80}) of the growth of control for yeast and 50% inhibition (IC_{50}) of the growth of control for filamentous fungi. The MIC values for most fungi were recorded after 24 h and 48 h except for the dermatophytic strain (*T. mentagrophytes* 445) which was determined after 72 h and 120 h.

BINOL (**45**) was screened at 500 μM, while BINOL derivatives **111**, **114**, **115**, **118** and **122** were screened at 125 μM due to low solubility in the test medium.

BINOL derivatives **111**, **114**, **115**, **118** and **122** all proved non-inhibitory for the fungal strains tested (Table 3.3). BINOL (**45**) inhibited *Trichosporon asahii* at 62.5 μM after 24 h and an MIC value of 500 μM was noted after 48 h. *Trichophyton mentagrophytes* gave an MIC value of 31.25 μM after 72 h and at 120 h for BINOL (**45**). An MIC value of 250 μM was noted for BINOL (**45**) towards *Candida albicans* ATCC 44859 after 24 h while at 48 h no inhibition was observed (>500 μM).

BINOL and derivatives							
Organism	Time(h)	**45**	**122**	**111**	**114**	**115**	**118**
C.albicans (ATCC44859)	24 h	**250**	>125	>125	>125	>125	>125
	48 h	>500	>125	>125	>125	>125	>125
C.albicans (ATCC90028)	24 h	>500	>125	>125	>125	>125	>125
	48 h	>500	>125	>125	>125	>125	>125
C.parapsilosis (ATCC22019)	24 h	>500	>125	>125	>125	>125	>125
	48 h	>500	>125	>125	>125	>125	>125
C.krusei (ATCC6258)	24 h	>500	>125	>125	>125	>125	>125
	48 h	>500	>125	>125	>125	>125	>125
C.krusei (E28)	24 h	>500	>125	>125	>125	>125	>125
	48 h	>500	>125	>125	>125	>125	>125
C.tropicalis (156)	24 h	>500	>125	>125	>125	>125	>125
	48 h	>500	>125	>125	>125	>125	>125
C.glabrata (20/I)	24 h	>500	>125	>125	>125	>125	>125
	48 h	>500	>125	>125	>125	>125	>125
C.lusitaniae (2446/I)	24 h	>500	>125	>125	>125	>125	>125
	48 h	>500	>125	>125	>125	>125	>125
T. asahii (1188)	24 h	**62.5**	>125	>125	>125	>125	>125
	48 h	**500**	>125	>125	>125	>125	>125
A.fumigatus (231)	24 h	>500	>125	>125	>125	>125	>125
	48 h	>500	>125	>125	>125	>125	>125
A.corymbifera (272)	24 h	>500	>125	>125	>125	>125	>125
	48 h	>500	>125	>125	>125	>125	>125
T.mentagrophytes (445)	72 h	**31.25**	>125	>125	>125	>125	>125
	120 h	**31.25**	>125	>125	>125	>125	>125

Table 3.3: Antifungal IC_{80}/IC_{50} (μM) values of BINOL (**45**) and derivatives (**111**, **114**, **115**, **118** and **122**)

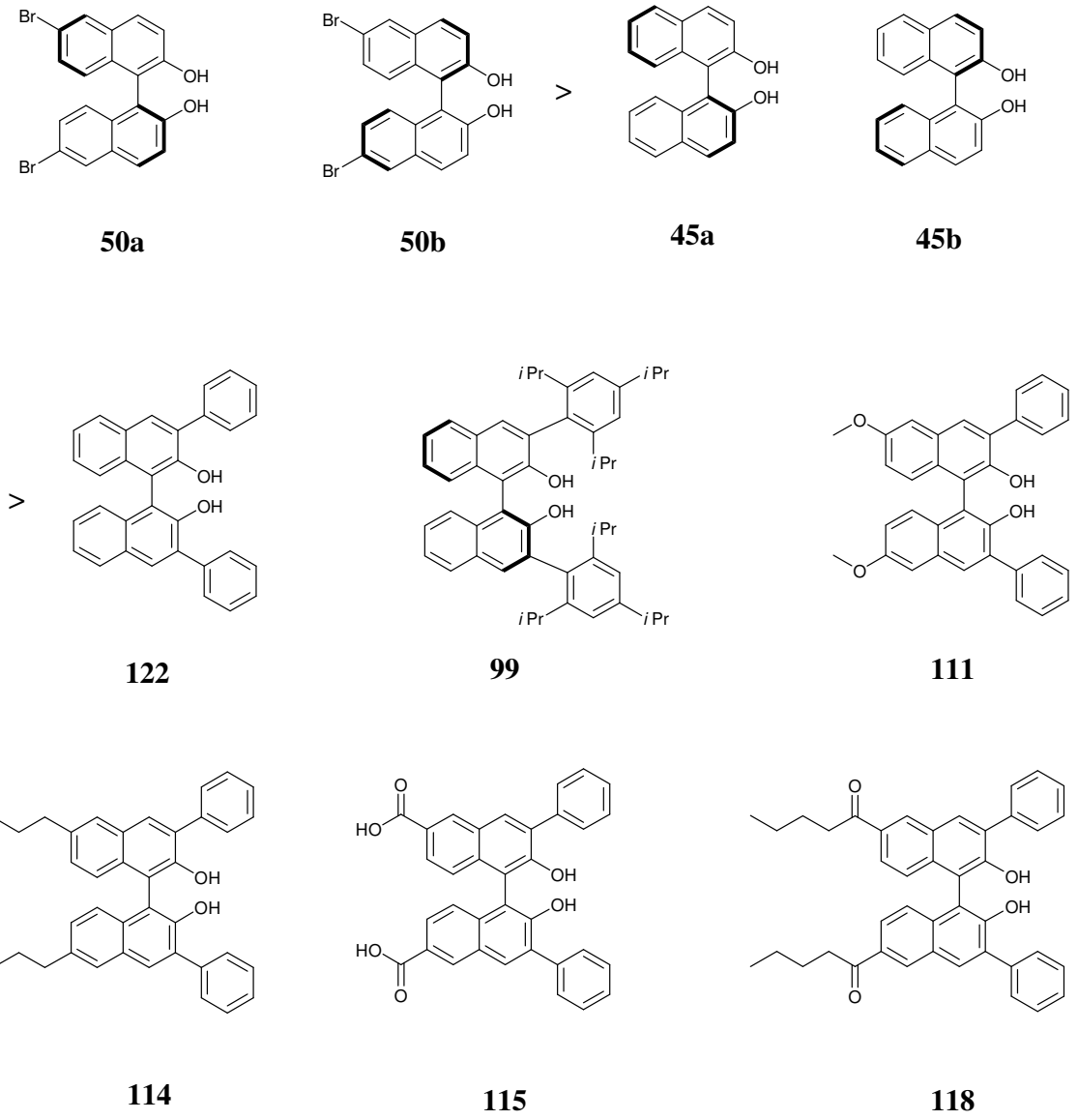

Fig 3.12 Overall trend for antifungal activity of BINOL, BINOL derivatives and novel polysubstituted BINOLs (**50a**, **50b** >**45a**, **45b** >**122**, **99**, **111**, **114**, **115** and **118**)

Novel polysubstituted BINOLs (**111**, **114**, **115** and **118**) and BINOL derivatives (**99** and **122**) showed low inhibition towards fungal organisms (> 125 μM) and were less toxic when compared to BINOLs (**45a**, **45b**, **50a** and **50b**) (Figure 3.12). Chiral BINOL (**45a** and **45b**) was observed with a number of cases of antifungal activity. Brominated BINOLs (**50a** and **50b**) proved inhibitory for all test fungi.

3.7 Biodegradation study of BINOL and polysubstituted derivatives

BINOL (**45**) and derivatives (**111**, **113**, **114**, **115**, **118** and **122**) were evaluated for biodegradation using the CO_2 headspace test (ISO 14593). This study was performed by our collaborator Dr Teresa Garcia at the department of surfactant technology in Barcelona, Spain. General procedure for this assay was discussed in section 1.3.4. Results from this study are presented in Table 3.4 and the biodegradation curve is displayed in Figure 3.13.

Compound	**% Biodegradation**			
	6 d	**14 d**	**21 d**	**28 d**
SDS	75	87	93	93
45	0	0	2	0
111	0	0	1	3
113	1	0	2	4
114	0	0	0	1
115	0	0	0	3
118	0	0	0	1
122	1	0	1	1

Table 3.4: Biodegradation results for BINOL (**45**) and derivatives (**111**, **113**, **114**, **115**, **118** and **122**)

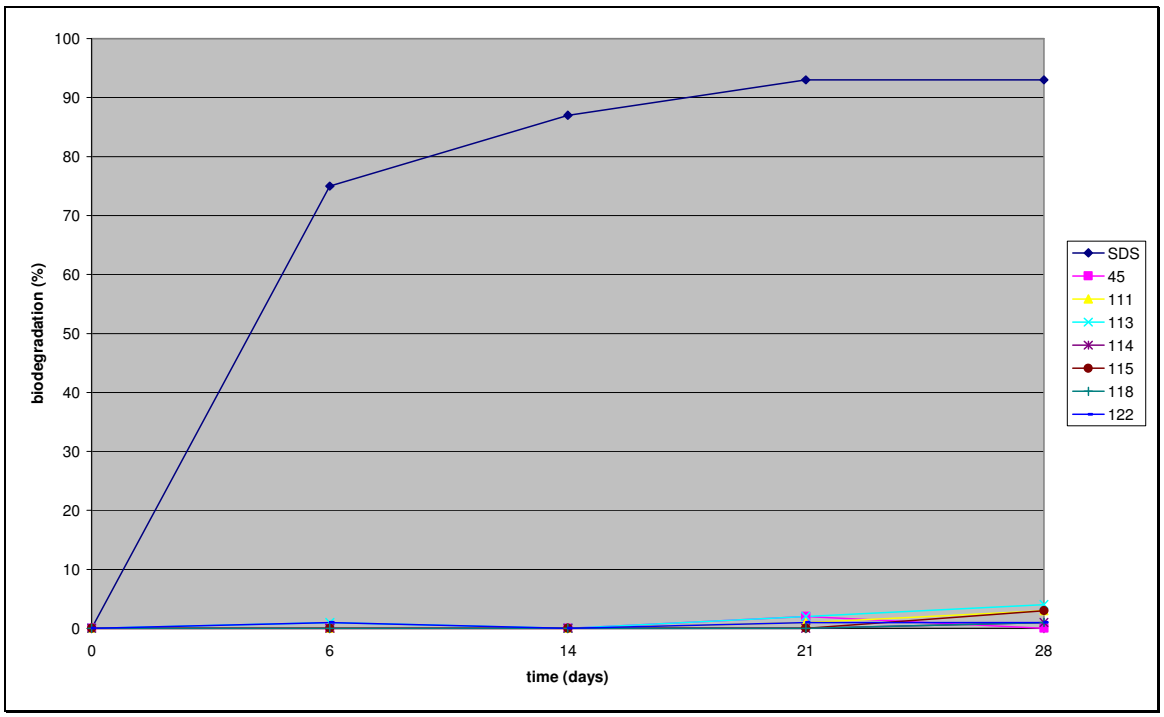

Figure 3.13 Biodegradation curves for BINOL (**45**), **111**, **113**, **114**, **115**, **118** and **122**

The readily biodegradable reference substance SDS was evaluated as the control experiment and exhibited 75% biodegradation after 6 days. Days 14, 21 and 28 gave biodegradation values of 87%, 93% and 93%, respectively. These data points verify that the inoculum is active and capable of mineralising biodegradable organic chemicals. BINOL (**45**) and derivatives (**111**, **113**, **114**, **115**, **118** and **122**) were non-biodegradable as less than 5% CO_2 output was measured for these molecules (Table 3.4). In order for a chemical to be deemed readily biodegradable it must evolve >60% CO_2 over a period of 28 days. Therefore, BINOL (**45**) and derivatives (**111**, **113**, **114**, **115**, **118** and **122**) failed the CO_2 headspace test and can be classified as being non-biodegradable as negligible CO_2 output occurred (Figure 3.13). These results suggest that biodegradation of BINOL is a considerable task, as well the modified BINOL derivatives failed to enhance biodegradation.

As no biodegradation was apparent for BINOL (**45**) and derivatives (**111**, **113**, **114**, **115**, **118** and **122**), a control experiment was run to determine if compounds were having an

inhibitory effect on the activity of the inoculum. For this experiment reference substance (SDS) and test substance (BINOL and derivatives individually) were added together to the inoculum and if inhibition of SDS biodegradation occurred, this implied that the test substance is inhibiting the inoculum. Results from this experiment are presented in Table 3.5. BINOL (**45**) gave the largest % inhibition (9%) for the inhibitory control biodegradation assay. This is not surprising as BINOL proved to be inhibitory for the preliminary antimicrobial screening. The concentration of 83.26 μM used for BINOL (**45**) in the inhibitory control biodegradation assay lies within the inhibitory concentration range observed in the antibacterial screen. Remaining derivatives (**111**, **113**, **114**, **115**, **118** and **122**) were observed with low inhibition to the inoculum (Table 3.5).

Compound	Concentration (mgC/L)	Molar concentration of test sample	Inhibition (%)
45 + SDS	20 + 20	83.26 μM	9
111 + SDS	20 + 20	48.98 μM	1
113 + SDS	20 + 20	52.0 μM	0
114 + SDS	20 + 20	41.63 μM	1
115 + SDS	20 + 20	48.98 μM	1
118 + SDS	20 + 20	39.65 μM	0
122 + SDS	20 + 20	52.04 μM	1

Table 3.5: Inhibition of SDS biodegradation by **45**, **111**, **113**, **114**, **115**, **118** and **122**

These % inhibition values for BINOL (**45**) and derivatives (**111**, **113**, **114**, **115**, **118** and **122**) are lower than the limit (>25% inhibition) generally accepted to consider an inhibitory effect on the activity of the inoculum. Therefore, BINOL (**45**) and derivatives

(**111**, **113**, **114**, **115**, **118** and **122**) can be classified as being non-biodegradable chemicals within the parameters of the CO_2 headspace test (ISO 14593).

3.8 Conclusions

The synthesis and characterisation of a series of novel polysubstituted BINOLs has been carried out. Eleven novel achiral polysubstituted BINOLs and three novel chiral polysubstituted BINOLs were synthesised from the key intermediates (+/−)-(**123**) and (+)-(*R*)-(**123b**) respectively. The five step synthesis towards both key intermediates has been discussed. Target compounds (Figure 3.1) were synthesised in low to moderate yields. Final compounds obtained were verified by ^{1}H and ^{13}C NMR. Antimicrobial studies were performed with **45**, **111**, **114**, **115**, **118** and **122**. BINOL derivatives (**111**, **114**, **115**, **118** and **122**) were non-inhibitory (within concentration range) towards the fungal strains tested. BINOL (**45**) was observed with three cases of antifungal activity. Some cases of anti-bacterial activity were noted for BINOL (**45**) and **122**. BINOL (**45**) proved to be the most toxic with inhibition being observed for all Gram positive bacteria. (+/−)-3,3'-Diphenyl-2,2'-dihydroxy-1,1'-binaphthyl (**122**) showed inhibition for two bacteria, *Staphylococcus epidermidis* (MIC value of 500 μM after 24 h and 48 h) and *Enterococcus sp.* (MIC value of 250 μM after 24 h and 48 h). The remaining polysubstituted BINOLs (**111**, **114**, **115** and **118**) exhibited low anti-bacterial activity with no MIC values being observed within tested concentration range. Known BINOL derivative (**99**) and novel polysubstituted BINOL derivatives (**111**, **114**, **115** and **118**) were found to be less toxic towards test bacteria when compared to BINOL (**45**, **45a** and **45b**). The CO_2 headspace test (ISO 14593) was applied for evaluating the biodegradation of BINOL and derivatives. Both BINOL (**45**) and derivatives (**111**, **114**, **115**, **118** and **122**) were found to be non-biodegradable within the parameters of the CO_2 headspace test (ISO 14593).

3.9 References

(1) Y. Chen, S. Yekta and A. K. Yudin, *Chem. Rev.,* 2003, **103**, 3155-3212.

(2) S. Kobayashi, K. Kusakabe, S. Komiyama and H. Ishitani, *J. Org. Chem.,* 1999, **64**, 4220-4221.

(3) V. Snieckus, *Chem. Rev.,* 1990, **90**, 879-933.

(4) T. R. Wu, L. Shen and J. M. Chong, *Org. Lett.,* 2004, **6**, 2701-2704.

(5) F. Monnier and M. Taillefer, *Angew. Chem. Int. Ed.,* 2009, **48**, 6954-6971.

(6) H. Yu, Q. Hu and L. Pu, *J. Am. Chem. Soc.,* 2000, **122**, 6500-6501.

(7) N. M. Brunkan and M. R. Gagna, *J. Am. Chem. Soc.,* 2000, **122**, 6217-6225.

(8) S. Zhang, Y. Liu, H. Huang, L. Zheng, L. Wu and Y. Cheng, *Synlett,* 2008, **6**, 853-856.

(9) R. Chinchilla and C. Najera, *Chem. Soc. Rev.,* 2011, **40**, 5084-5121.

(10) C. Torborg, A. Zapf and M. Beller, *ChemSusChem,* 2008, **1**, 91-96.

(11) G. Le Bras, L. Provot, J. Peyrat, M. Alami and J. Brion, *Tetrahedron Lett,* 2006, **47**, 5497.

(12) K. B. Simonsen, K. V. Gothelf and K. A. Jørgensen, *J. Org. Chem.,* 1998, **63**, 7536-7538.

Chapter 4: Results and Discussion

Chapter 4: Results and Discussion

4 Biquinoline derivatives

4.1 Aim

The objective for this part of the project was to synthesise biquinoline compounds with substituents that are known to promote biodegradation in accordance with the 'rules of thumb' (section 1.3.3). Stemming from work already completed by the Scammells research group on biodegradable pyridinium ionic liquids (see section 1.3.5), we decided to adopt those features that were applied for the design and development of biodegradable pyridinium ionic liquids. Such features included the *N*-alkylation of pyridine with ethyl bromoacetate and the introduction of an ester group on the heteroaromatic ring (Figure 4.1). For instance, compounds **60** and **64** proved to be readily biodegradable giving >60% biodegradation after 28 days in the CO_2 Headspace test (ISO 14593).[1]

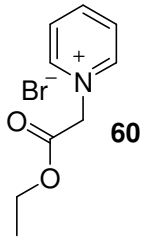

60

71% biodegradation after 7 days,
87% biodegradation after 28 days

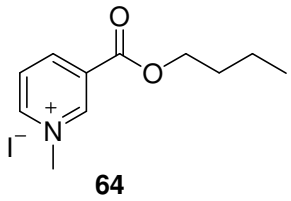

64

>60% biodegradation after 7 days,
72% biodegradation after 28 days

Fig 4.1 Readily biodegradable pyridinium ionic liquids

These modifications incorporate ester groups that are susceptible to enzymatic hydrolysis and also provide a site for cleavage of the heterocycle thus allowing for the microbial degradation of **60** and **64**.

4.2 Introduction

Using (+/−)-6,6'-dihydroxy-5,5'-biquinoline (BIQOL) (**130**) as a scaffold, it was decided to alkylate the nitrogen position with methyl, *n*-butyl and ethoxycarbonylmethyl substituents generating *N*-alkylated salts that should be water soluble. Also the introduction of an ester group at the C3 position was investigated.

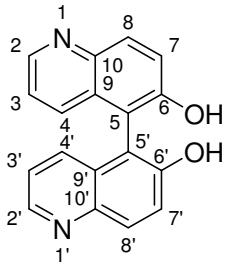

Fig 4.2 (+/−)-6,6'-dihydroxy-5,5'-biquinoline (BIQOL) (**130**) with numbering

BIQOL has been resolved and applied as an asymmetric catalyst for the enantioselective addition of diethylzinc to a variety of aldehydes in the literature.[2] The resolution of this compound was achieved by converting the phenolic hydroxyl groups to triflates, then separation of the racemic triflated BIQOL (**132**) *via* HPLC on a chiral preparative OD column and subsequent hydrolysis of enantiopure triflated BIQOL to yield both (*R*)-BIQOL and (*S*)-BIQOL enantiomers in 91% yield (Scheme 4.1). As a ligand (*R*)-BIQOL was added to titanium tetraisopropoxide to generate a titanium-BIQOL catalyst, which promoted enantioselective addition of diethylzinc to a range of aldehydes. Excellent conversions and high enantioselectives were obtained with aromatic aldehydes while for the aliphatic aldehyde, heptanal, a lower conversion of 61.7% with an ee of 83% was reported (Scheme 4.2).

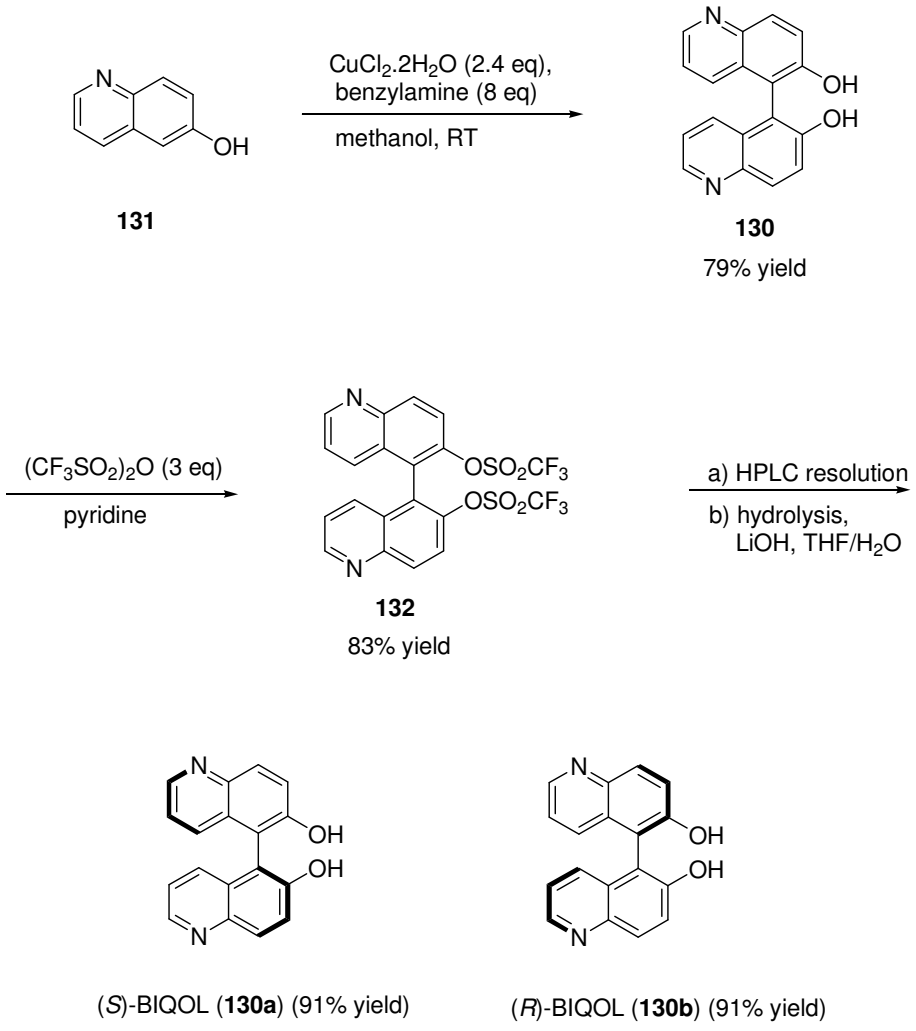

Scheme 4.1: Synthesis and resolution of BIQOL [2]

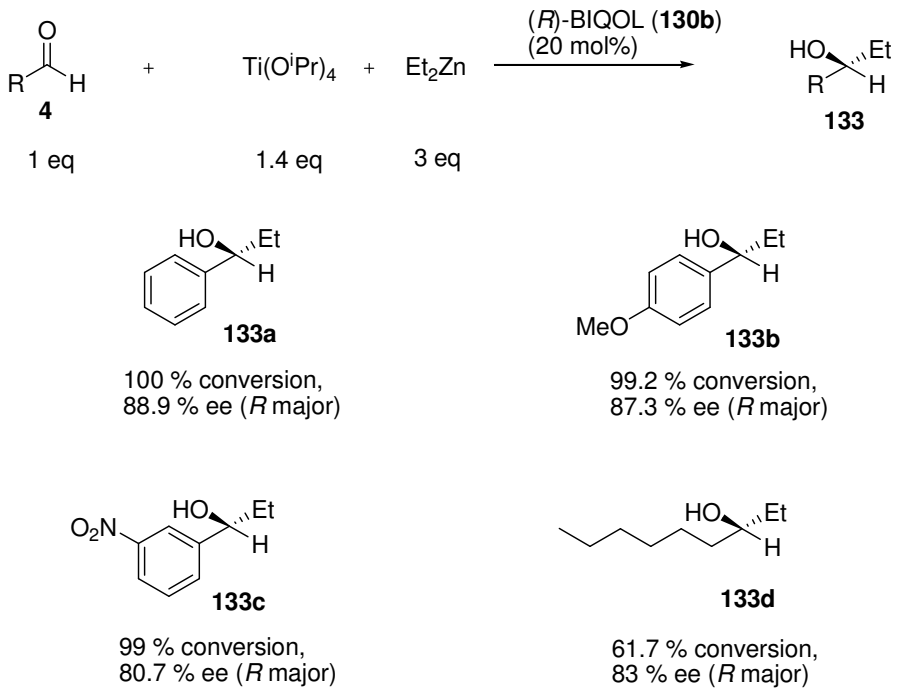

Scheme 4.2: Enantioselective addition of diethylzinc to aldehydes [2]

4.3 Synthesis of biquinoline derivatives

Firstly, it was possible to synthesise (+/−)-6,6'-dihydroxy-5,5'-biquinoline (**130**) *via* a copper mediated oxidative coupling of 6-hydroxyquinoline (**131**) in 65% yield.

(+/−)-6,6'-Dihydroxy-5,5'-biquinoline (**130**) can be modified by alkylation of the nitrogen position. *N*-alkylated biquinoline derivatives that were synthesised can be seen in Figure 4.3.

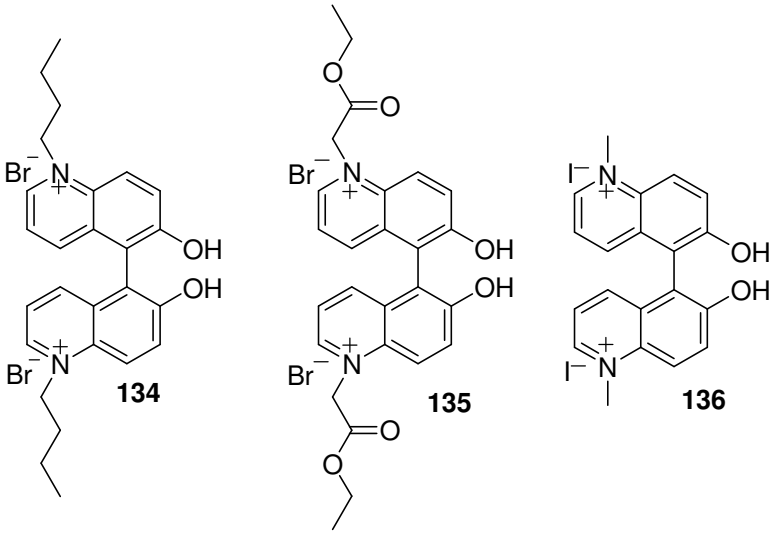

Fig 4.3 *N*-alkylated biquinoline derivatives synthesised (**134**, **135** and **136**)

Initially, the *N*-alkylation of BIQOL (**130**) with methyl iodide was tried using DMF as solvent. The reaction was attempted at room temperature, however, due to incompletion of reaction as confirmed by TLC, it was heated to 90°C and after 24 h the reaction was complete. Desired product (**136**) was obtained and verified by proton and carbon NMR, however, it was found to contain a significant impurity. In the proton spectrum a signal at 3.12 ppm with an integration of 24 protons was noticeable (Figure 4.4) and in the carbon spectrum a strong signal at 54.38 ppm was present (Figure 4.5), these additional signals did not correlate with the structure.

This signal could be attributed to dimethylamine and the source of this impurity is due to the decomposition of DMF during the reaction. DMF decomposes slightly at its boiling point to give dimethylamine and carbon monoxide, in addition decomposition can occur at room temperature in the presence of some acidic or basic materials.[3]

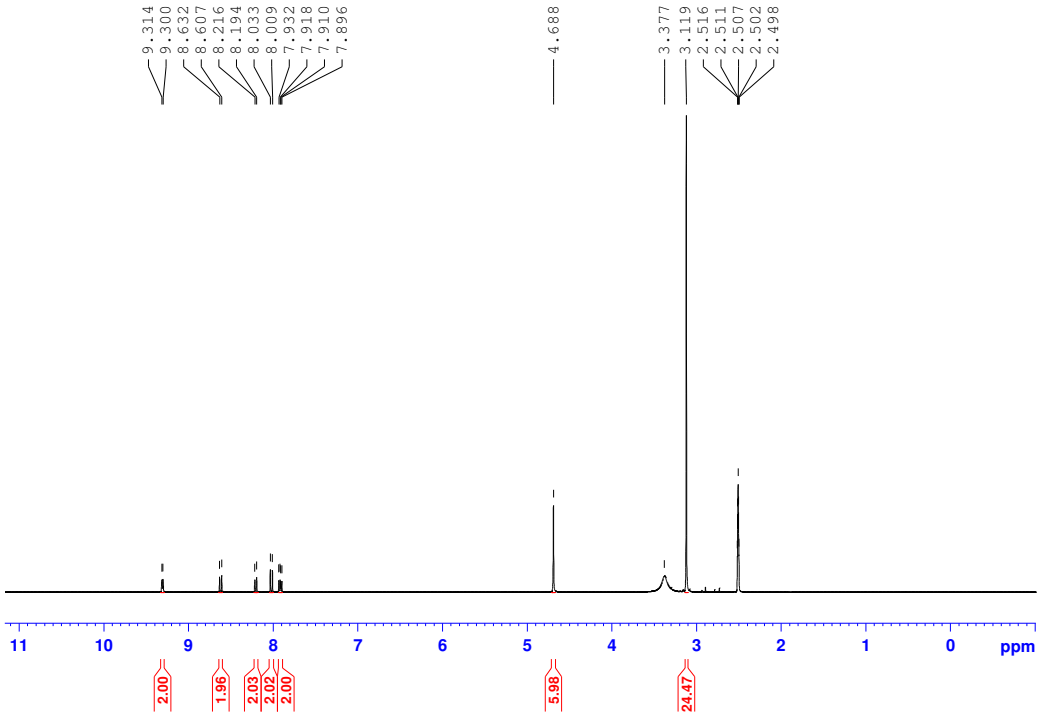

Fig. 4.4 ^{1}H NMR spectrum of impure (+/–)-1,1'-dimethyl-6,6'-dihydroxy-5,5'-biquinoline (**136**)

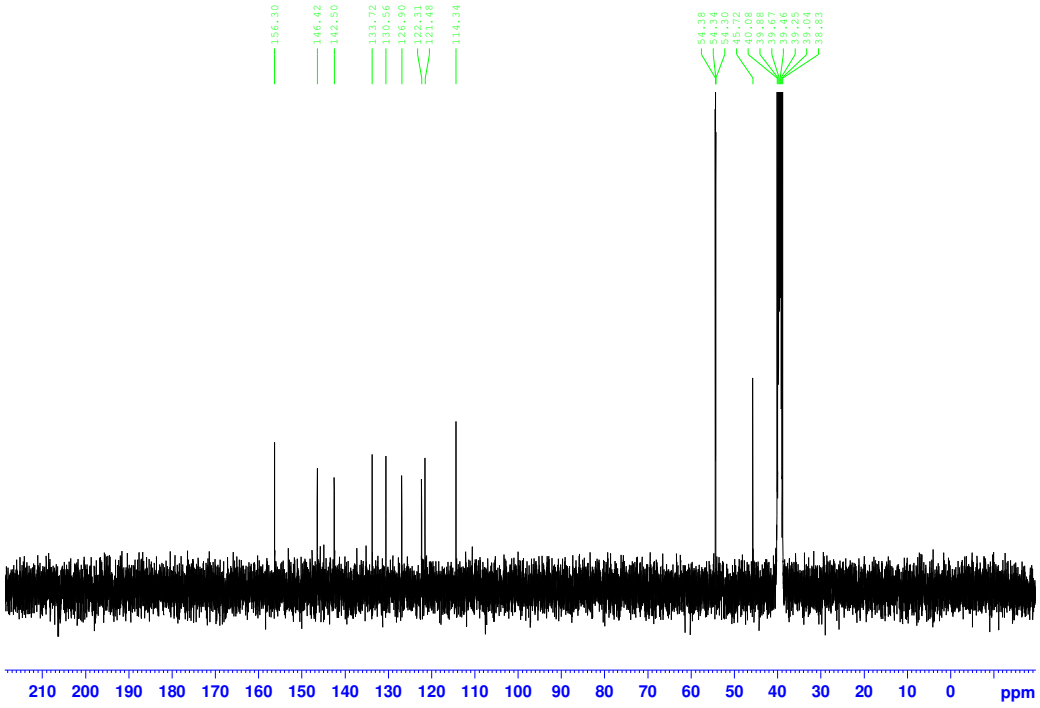

Fig. 4.5 ^{13}C NMR spectrum of impure (+/–)-1,1'-dimethyl-6,6'-dihydroxy-5,5'-biquinoline (**136**)

On TLC it was not possible to move the product (**136**) from the baseline using methanol as mobile phase, therefore column chromatography was not attempted. Removal of dimethylamine by doing an aqueous wash was not possible as the compound (**136**) was water soluble. Drying under high vacuum for a period of 3 days at room temperature also failed to remove the impurity. Next we decided to switch solvent for the alkylation step. The choice of solvent was NMP, which dissolves (+/−)-6,6'-dihydroxy-5,5'-biquinoline (**130**) and can facilitate alkylation reactions. *N*-alkylation of (+/−)-6,6'-dihydroxy-5,5'-biquinoline (**130**) with methyl iodide in NMP was tried at room temperature but the reaction did not go to completion. However, the reaction went to completion when heated at 90 °C for 2 h to give a yield of 79% for (+/−)-1,1'-dimethyl-6,6'-dihydroxy-5,5'-biquinoline (**136**) after work-up.

Alkylation of (+/−)-6,6'-dihydroxy-5,5'-biquinoline (**130**) with ethyl bromoacetate was achieved at room temperature after 72 h with a yield of 86% for (+/−)-1,1'-diethoxycarbonylmethyl-6,6'-dihydroxy-5,5'-biquinoline (**135**) after work up. The reason for this reaction occurring without heating is due to ethyl bromoacetate being a more reactive electrophile. As well, alkylation of (+/−)-6,6'-dihydroxy-5,5'-biquinoline (**130**) with ethyl bromoacetate was tried under neat conditions, as ethyl bromoacetate could dissolve the starting material and play the role as a solvent. But the reaction did not go to completion even upon heating at 110 °C for 4 days. Purification of *N*-alkylated salts **135** and **136** involved precipitating out the product with diethyl ether, the resulting suspension was filtered and washed with diethyl ether to give the desired compounds.

Alkylation of BIQOL (**130**) with bromobutane was tried in NMP at room temperature but no conversion was noted on TLC. When heated at 110 °C for 48 h, conversion was observed but an additional faint spot was also present on the TLC that did not correlate with starting material or the product, the addition of extra equivalents (36 in total) of bromobutane did not help to drive the reaction to completion. Previously, it was possible to obtain the dibutylated product (+/−)-1,1'-dibutyl-6,6'-dihydroxy-5,5'-biquinoline (**134**) when the reaction was carried out in DMF at 110 °C for 48 h using 14 equivalents of bromobutane with 30 mol% of potassium iodide and after filtration compound **134** was

obtained with a yield of 26%. A low yield was obtained due to the presence of residual DMF in the crude product prior to filtration which resulted in a loss of product to the filtrate. The residual impurity from DMF decomposition was also observable in the ^{1}H and ^{13}C NMR spectra for compound **134**. However, for (+/−)-1,1'-dibutyl-6,6'-dihydroxy-5,5'-biquinoline (**134**) it was possible to remove the residual impurity by heating the compound at 150 °C under high vacuum for 36 h.

All salts (**134**, **135** and **136**) were soluble in polar media such as water, DMSO and methanol.

Also the biquinoline derivatives with an ester group at the 3-position (**137a** and **137b**) were proposed as targets (Figure 4.6).

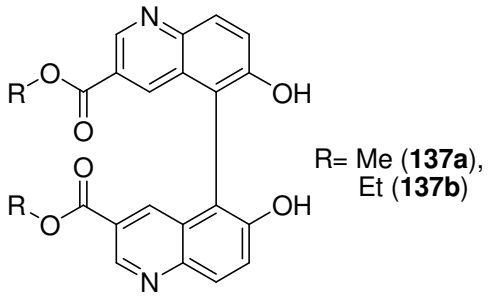

Fig. 4.6 Proposed targets **137a** and **137b**

In order to make this class of compound, a 6-hydroxyquinoline derivative (**140**) with an ester group at the 3-position was required. Recently reported in the literature was that the introduction of an ethyl ester at the 3 position is possible by making the substituted quinoline *via* a modified Friedländer synthesis.[4] Venkatesan and coworkers reported the one step procedure for the synthesis of 2,4-unsubstituted quinoline-3-carboxylic acid ethyl esters. They performed a reductive cyclization by treating various substituted *ortho*-nitro-benzaldehydes with 3,3-diethoxypropionic acid ethyl ester (**139**) and tin(II)

chloride dihydrate in refluxing ethanol. 6-Hydroxy-quinoline-3-carboxylic acid ethyl ester (**140**) was one of the reported products with a 46% yield (Scheme 4.3).

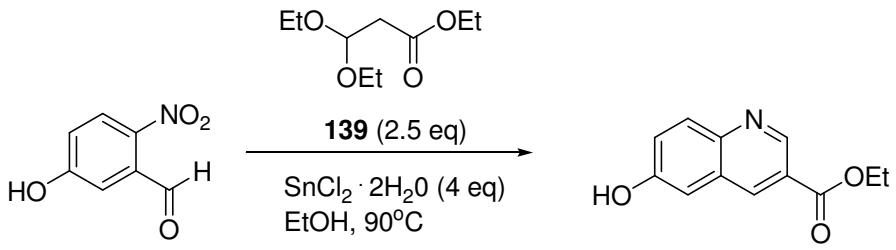

138 **140**

46% yield

Scheme 4.3: Modified Friedländer synthesis of **140** [4]

This product (**140**) contains an ester group at the 3-position which should enhance biodegradation and the hydroxyl group at the 6-position (β-position) is required for the oxidative coupling reaction. As a result, 6-hydroxy-quinoline-3-carboxylic acid ethyl ester (**140**) was synthesised in 44% yield. Attempts were made to dimerise this compound following the previous methodology employed for the synthesis of (+/−)-6,6'-dihydroxy-5,5'-biquinoline.[2] However, due to the use of methanol as solvent, a transesterified compound was proposed to be obtained as additional signals were present in the proton and carbon NMR spectra. Next the reaction was performed in ethanol, however, the desired product (**137b**) was never obtained. No conversion was noted on TLC, only the remaining starting material**.** From the literature, methanol is the only solvent that has been used for oxidative coupling reactions involving copper(II) chloride dihydrate and benzylamine as reagents.[5,6] Therefore, for methanol to be employed as solvent for the dimerisation reaction, synthesis of the quinoline derivative with the methyl ester (**142**) was embarked upon. 6-Hydroxy-quinoline-3-carboxylic acid methyl ester (**142**) was made in 46% yield by reacting 5-hydroxy-2-nitro-benzaldehyde (**138**) with 3,3-dimethoxypropionic acid methyl ester (**141**) and tin(II) chloride dihydrate in refluxing methanol.

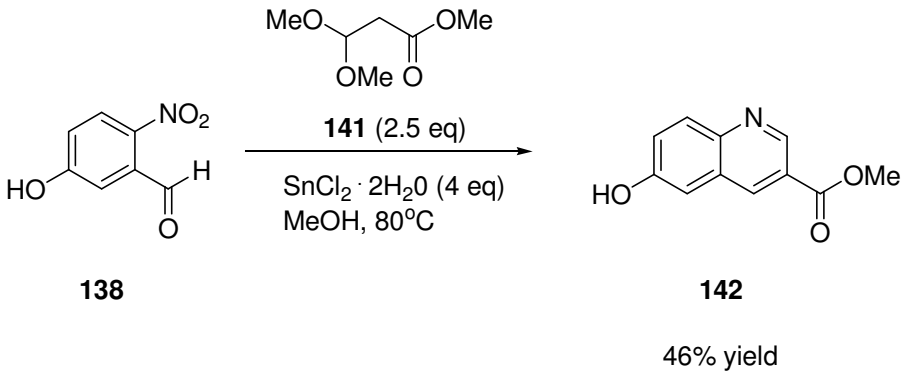

Scheme 4.4: Modified Friedländer synthesis of **142**

6-Hydroxy-quinoline-3-carboxylic acid methyl ester (**142**) was tested for the dimerisation reaction employing copper(II) dihydrate and benzylamine as catalyst in refluxing methanol and after work-up, the target molecule **137a** was obtained in 21% yield as verified by proton and carbon NMR. However, due to the broadness of some proton signals, one possibility is that residual copper salts are present. The remaining copper could be bound to the nitrogen atoms, giving broad proton signals in the ^{1}H NMR spectrum (Appendix: Figure 17). As a result of low yield and possible copper contamination it was decided not to send this sample for antimicrobial and biodegradation analysis.

4.4 Antimicrobial study of biquinoline and derivatives

The antimicrobial activities of biquinoline (**130**) and *N*-biquinoline salts (**134**, **135** and **136**) were evaluated by our collaborator Dr Marcel Špulák of Charles University Czech Republic. Bacteria screened against were *Staphylococcus aureus* ATCC 6538, *Staphylococcus aureus* MRSA HK5996/08, *Staphylococcus epidermidis* HK6966/08, *Enterococcus sp.* HK14365/08, *Escherichia coli* ATCC 8739, *Klebsiella pneumoniae* HK11750/08, *Klebsiella pneumoniae*-**ESBL** positive HK14368/08 and *Pseudomonas aeruginosa* ATCC 9027. MIC values for antibacterial study were defined as 95 % inhibition (IC_{95}) of the growth of control. The results in table 4.1 represent the MIC/IC_{95} values obtained for biquinoline and *N*-alkylated salts (Figure 4.7).

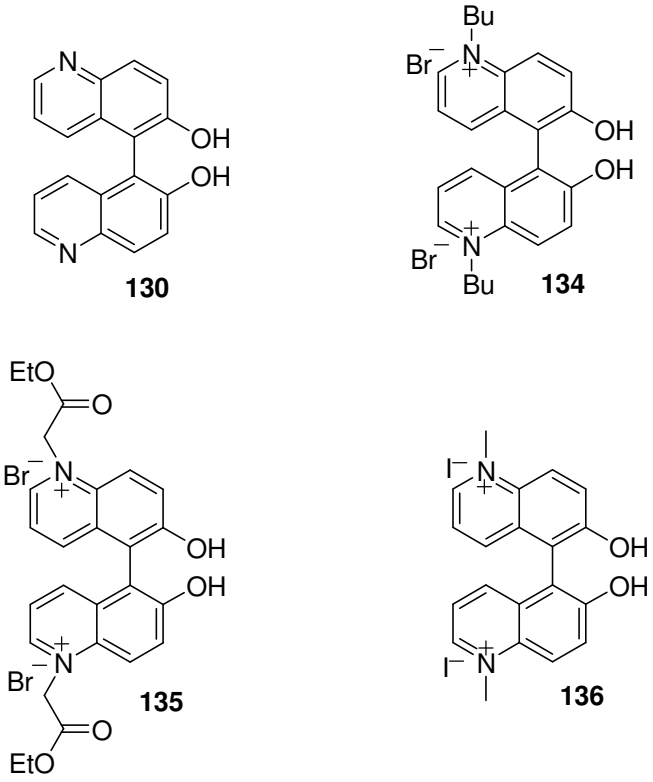

Fig 4.7 Biquinoline (**130**) and *N*-alkylated salts (**134, 135, 136**) screened for antimicrobial activity

Biquinoline and derivatives					
Organism	Time (h)	**130**	**134**	**135**	**136**
S. aureus	24	>2000	>1000	>2000	>2000
	48	>2000	>1000	>2000	>2000
MRSA	24	>2000	>1000	>2000	>2000
	48	>2000	>1000	>2000	>2000
S. epidermidis	24	>2000	>1000	>2000	>2000
	48	>2000	>1000	>2000	>2000
Enterococcus sp.	24	**250**	**125**	>2000	>2000
	48	**500**	**500**	>2000	>2000
E. coli	24	**250**	>1000	>2000	>2000
	48	**500**	>1000	>2000	>2000
K. pneumoniae	24	**15.62**	>1000	>2000	>2000
	48	**125**	>1000	>2000	>2000
*K. pneumoniae -**ESBL***	24	>2000	>1000	>2000	>2000
	48	>2000	>1000	>2000	>2000
P. aeruginosa	24	>2000	>1000	>2000	>2000
	48	>2000	>1000	>2000	>2000

Results obtained by collaborator

Table 4.1: MIC/IC_{95} (μM) values of biquinoline (**130**) and *N*-alkylated salts (**134**, **135** and **136**)

N-alkylated salts **135** and **136** displayed low antimicrobial activity to all bacteria (>2000 μM) as a MIC/IC_{95} was not observed within the tested concentration range. Biquinoline (**130**) proved inhibitory for *Enterococcus sp*, *E. coli* and *K. pneumoniae* with MIC values of 250 μM, 250 μM and 15.62 μM after 24 h, respectively, and after 48 h MIC values were 500 μM, 500 μM and 125 μM. A trend is seen as MIC value is lower at 24 h than 48 h. While this is slight for *Enterococcus sp* and *E. coli*, it is very significant for *K. pneumoniae*. A change in MIC value after 48 h signifies that viable bacteria are present at 24 h and grow substantial over a 24 h period which increases the MIC/IC_{95} value. Remaining bacteria were not inhibited by **130**. Inhibition of *Enterococcus sp* was also noted for **134** at 125 μM after 24 h and at 500 μM after 48 h. The highest concentration screened for **134** was 1000 μM as the compound was less soluble in test medium.

For the antifungal studies, compounds were screened against the following yeast strains (*Candida albicans* ATCC 44859, *Candida albicans* ATCC 90028, *Candida parapsilosis* ATCC 22019, *Candida krusei* ATCC 6258, *Candida krusei* E28, *Candida tropicalis* 156, *Candida glabrata* 20/I, *Candida lusitaniae* 2446/I, *Trichosporan asahii* 1188) and filamentous fungi (*Aspergillus fumigatus* 231, *Absidia corymbifera* 272 and *Trichophyton mentagrophytes* 445). MIC values for antifungal study were defined as 80% inhibition (IC_{80}) of the growth of control for yeast and 50% inhibition (IC_{50}) of the growth of control for filamentous fungi. The MIC values for most fungi were recorded after 24 h and 48 h except for the dermatophytic strain (*T. mentagrophytes* 445) which was determined after 72 h and 120 h. Biquinoline (**130**) and derivatives (**134**, **135** and **136**) all proved non-inhibitory for the fungal strains tested (Table 4.2). *N*-alkylated salt (**134**) was screened at a lower concentration of 1000 μM as it was less soluble in test medium.

Biquinoline derivatives					
Organism	Time(h)	**130**	**134**	**135**	**136**
C. albicans (ATCC44859)	24	>2000	>1000	>2000	>2000
	48	>2000	>1000	>2000	>2000
C. albicans (ATCC90028)	24	>2000	>1000	>2000	>2000
	48	>2000	>1000	>2000	>2000
C. parapsilosis (ATCC22019)	24	>2000	>1000	>2000	>2000
	48	>2000	>1000	>2000	>2000
C. krusei (ATCC6258)	24	>2000	>1000	>2000	>2000
	48	>2000	>1000	>2000	>2000
C. krusei (E28)	24	>2000	>1000	>2000	>2000
	48	>2000	>1000	>2000	>2000
C. tropicalis (156)	24	>2000	>1000	>2000	>2000
	48	>2000	>1000	>2000	>2000
C. glabrata (20/I)	24	>2000	>1000	>2000	>2000
	48	>2000	>1000	>2000	>2000
C. lusitaniae (2446/I)	24	>2000	>1000	>2000	>2000
	48	>2000	>1000	>2000	>2000
T. asahii (1188)	24	>2000	>1000	>2000	>2000
	48	>2000	>1000	>2000	>2000
A. fumigatus (231)	24	>2000	>1000	>2000	>2000
	48	>2000	>1000	>2000	>2000
A. corymbifera (272)	24	>2000	>1000	>2000	>2000
	48	>2000	>1000	>2000	>2000
T. mentagrophytes (445)	72	>2000	>1000	>2000	>2000
	120	>2000	>1000	>2000	>2000

Table 4.2: Antifungal IC_{80}/IC_{50} (μM) values of biquinoline (**130**) and *N*-alkylated salts (**134, 135** and **136**)

4.5 Biodegradation study of biquinoline and derivatives

Biquinoline (**130**) and derivatives **135** and **136** were evaluated using the CO_2 headspace test (ISO 14593). General procedure for this assay was mentioned in Section 1.3.4. The results from this study are presented in Table 4.3 and the biodegradation curve is displayed in Figure 4.8.

Compound	% Biodegradation			
	6 d	14 d	21 d	28 d
SDS	75	87	93	93
130	0	1	1	1
135	9	8	19	15
136	0	0	0	0

Table 4.3: CO_2 Headspace test results for biquinoline (**130**) and derivatives (**135** and **136**)

The readily biodegradable reference substance SDS was evaluated as the control experiment and exhibited % biodegradation values of 75%, 87%, 93% and 93% after 6 days, 14 days, 21 days and 28 days, respectively. These results ensure that the inoculum is viable and capable of mineralising biodegradable organic chemicals. Biquinoline (**130**) and derivative **136** were found to be non-biodegradable as negligible CO_2 evolution was recorded. For **135** a value of 15% biodegradation was recorded after 28 days. This degradation can be attributed to the hydrolysis of the ester group. Biquinoline (**130**) and derivatives **135** and **136** failed the CO_2 headspace test (ISO 14593) as both compounds did not attain the pass rate of >60% CO_2 output within the 28 day timescale.

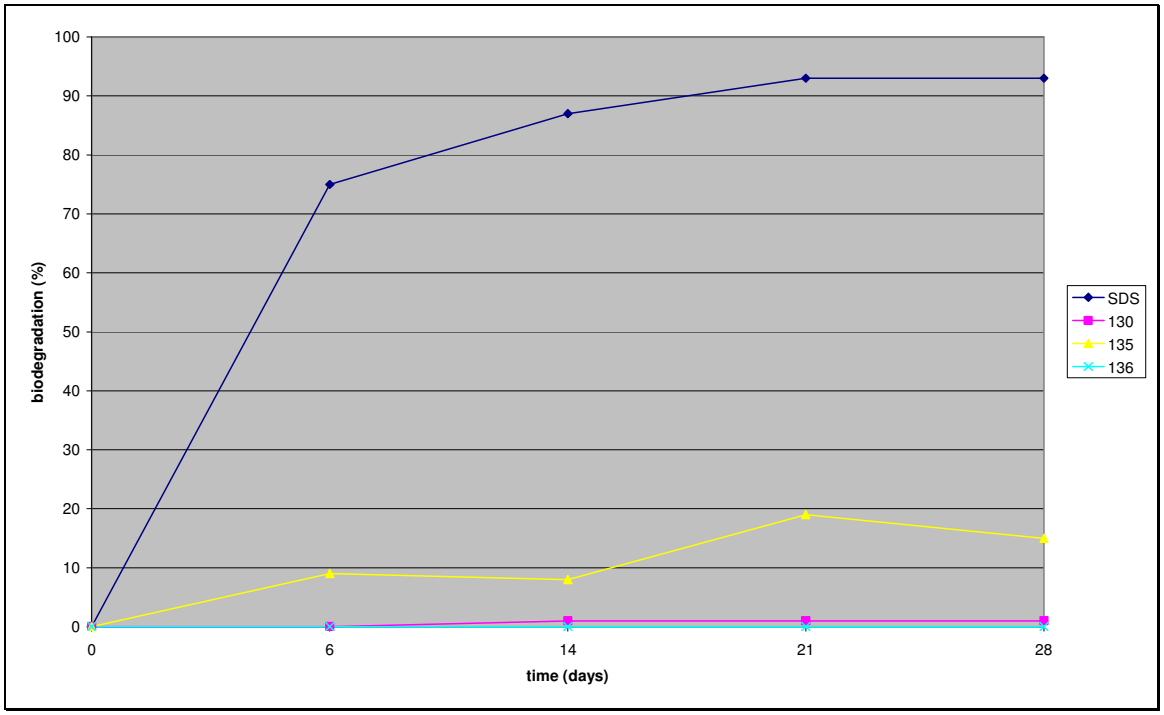

Figure 4.8 Biodegradation curve for SDS, biquinoline (**130**) and derivatives (**135** and **136**)

An inhibitory control experiment was run to determine if biquinoline (**130**) and derivatives **135** and **136** were having an inhibitory effect on the activity of the inoculum. For this experiment reference substance (SDS) and test substance (biquinoline and derivatives individually) were added together to the inoculum and if inhibition of SDS biodegradation occurred, this implied that the test substance is inhibiting the inoculum. Results from this experiment are presented in Table 4.4.

For **130** and **135** no inhibition was observed towards the inoculum while for **136** a 5% inhibition of the inoculum was noted, however, this is not significant enough to prevent the inoculum from mineralising biodegradable organic chemicals. Therefore, **130**, **135** and **136** are non-biodegradable within the parameters of the CO_2 headspace test (ISO 14593).

Compound	Concentration (mgC/L)	Molar concentration of sample	Inhibition (%)
SDS + **130**	20 + 20	92.5 μM	0
SDS + **135**	20 + 20	64.05 μM	0
SDS + **136**	20 + 20	83.3 μM	5

Table 4.4: Inhibition of SDS biodegradation by **130**, **135** and **136**

4.6 Conclusion

N-alkylated biquinoline salts **134**, **135** and **136** were synthesised in moderate to good yields. As well, the synthesis of a biquinoline compound (**137a**) with a methyl ester at the 3 position was achieved. However, low yield and possible copper contamination prevented further antimicrobial and biodegradation studies. Antimicrobial studies were performed for biquinoline (**130**) and *N*-alkylated biquinoline salts (**134, 135** and **136**). Some cases of antibacterial inhibition were noted for **130** (*Enterococcus sp, E.coli* and *K.pneumoniae*) and **134** (*Enterococcus sp*). A trend was observed for antibacterial inhibition as MIC value was lower at 24 h than 48 h for both compounds.

No case of anti-fungal activity was observed for biquinoline (**130**) and *N*-alkylated biquinoline salts (**134, 135** and **136**).

For the biodegradation studies, **130**, **135** and **136** were evaluated using the CO_2 headspace test (ISO 14593) and all molecules failed the test indicating that they are non-biodegradable within the parameters of the test.

4.7 References

(1) J. R. Harjani, R. D. Singer, M. T. Garcia and P. J. Scammells, *Green Chem.*, 2009, **11**, 83-90.

(2) Y. Chen, L. Yang, Y. Li, Z. Zhou, K. Lam, A. S. C. Chan and H. Kwong, *Chirality*, 2000, **12**, 510-513.

(3) M. Jacques, *Tetrahedron*, 2009, **65**, 8313-8323.

(4) H. Venkatesan, F. M. Hocutt, T. K. Jones and M. H. Rabinowitz, *J. Org. Chem.*, 2010, **75**, 3488-3491.

(5) M. Smrcina, S. Vyskocil, B. Maca, M. Polasek, T. A. Claxton, A. P. Abbott and P. Kocovsky, *J. Org. Chem.*, 1994, **59**, 2156-2163.

(6) S. Vyskocil, M. Smrcina, M. Lorenc, I. Tislerova, R. D. Brooks, J. J. Kulagowski, V. Langer, L. J. Farrugia and P. Kocovsky, *J. Org. Chem.*, 2001, **66**, 1359-1365.

Chapter 5: Results and Discussion

5 Morita-Baylis-Hillman reaction

5.1 Aim

The aim for this part of the project was to evaluate novel chiral polysubstituted BINOLs as asymmetric catalysts for the Morita-Baylis-Hillman reaction. A model reaction from the literature, which can be promoted by BINOL, was selected for a preliminary screening of catalysts.[1]

5.2 Introduction

The Morita-Baylis-Hillman (MBH) reaction involves the addition of electrophilic alkenes to carbonyl electrophiles and is catalyzed by nucleophilic amines or phosphines to generate β-hydroxy-α-methylene carbonyl products.[2]

Enantiomerically enriched β-hydroxy-α-methylene carbonyl compounds are useful building blocks for natural product synthesis.[3] The usage of organocatalysts to catalyse the MBH reaction has been investigated by many research groups.[4,5,6] Newly designed organocatalysts are overcoming the drawbacks that have been associated with the asymmetric MBH reaction such as long reaction times (a week to a month), low conversion and low enantioselectivity.[3] Organocatalysts are assisting in the development of a more efficient asymmetric MBH reaction. The proposed mechanism for the MBH reaction is presented in Scheme 5.1. Initially, the nucleophilic catalyst either a tertiary amine or a tertiary phosphine undergoes a reversible 1,4-Michael addition with the electron deficient alkene **143** (Step 1) to generate a nucleophilic zwitterionic enolate intermediate **144** which then undergoes an Aldol reaction with the carbonyl electrophile **145** to give the zwitterionic intermediate **146** (Step 2). Step 2 is considered to be the rate determining step for the MBH reaction.[3] Step 3 involves a proton shift from the α-carbon atom to the β-alkoxide within intermediate **146** to give the zwitterionic intermediate **147**. Subsequent β-elimination of the organic catalyst (tertiary amine or phosphine) from

intermediate **147** yields the β-hydroxy-α-methylene carbonyl product **148** (Step 4). The regenerated organic catalyst undergoes further cycles to generate many β-hydroxy-α-methylene carbonyl products. Overall the MBH can be considered an atom economic reaction as atoms in both starting materials end up in the product.

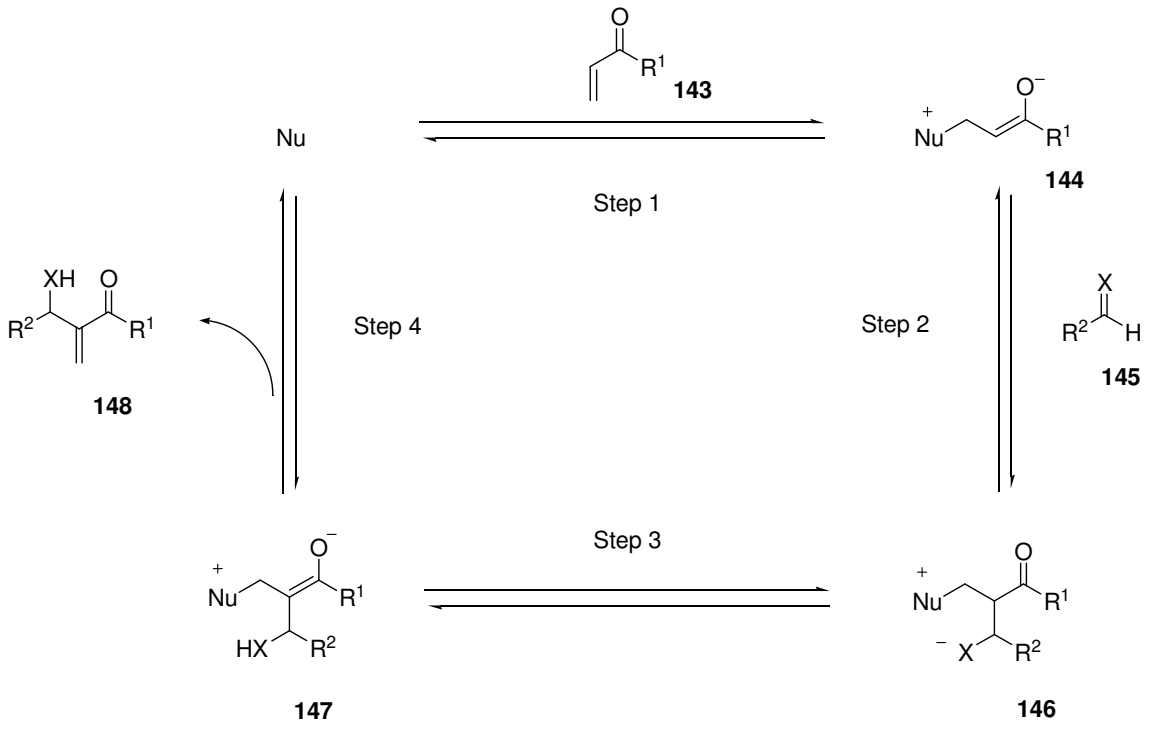

Scheme 5.1: Proposed mechanism for the MBH reaction[3]

5.3 Morita-Baylis-Hillman reaction promoted by diols

In 2000 Ikegami and Yamada reported a catalytic Morita-Baylis-Hillman (MBH) reaction that was promoted by tributylphosphine and (+/–)-1,1'-bi-2-naphthol (BINOL) in THF to furnish β-hydroxy-α-methylene carbonyl products in high yields.[7] Ikegami and coworkers envisioned that a mild Brønsted acid as co-catalyst would activate the carbonyl groups of the enolate intermediate and the aldehyde to accelerate the reaction rate for the MBH

reaction. Initially, test substrates **149a** and **150a** were selected for their preliminary study (Scheme 5.2). Tributylphosphine was found to catalyse the MBH reaction furnishing a yield of 23% for the MBH adduct **151a** while the Lewis bases DABCO and triphenylphosphine failed to give any conversion (Table 5.1). A variety of mild Brønsted acids were examined as co-catalysts for this reaction and quantitative yields for **151a** were obtained in the presence of BINOL, 2-napthol and phenol. It was found that free hydroxyl groups are necessary for promoting the MBH reaction as BINOL derivatives **153** and **154** (Figure 5.1) gave lower yields of 80% and 24%, respectively, for **151a**.

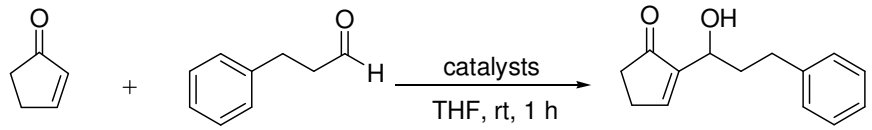

149a **150a** (1.5 eq) **151a**

Scheme 5.2: MBH reaction for test substrates **149a** and **150a**

Catalyst	Co-catalyst	Yield (%)
DABCO (20 mol %)	–	no reaction
Bu_3P (**152**) (20 mol %)	–	23
(**152**) (20 mol %)	methanol (20 mol %)	23
(**152**) (20 mol %)	(+/–)-1,1'-bi-2-naphthol (**45**) (10 mol %)	quantitative
(**152**) (20 mol %)	2-naphthol (20 mol %)	quantitative
(**152**) (20 mol %)	**153** (10 mol %)	80
(**152**) (20 mol %)	**154** (10 mol %)	24
DABCO (20 mol %)	**45** (10 mol %)	no reaction
Ph_3P (20 mol %)	**45** (10 mol %)	no reaction
(**152**) (20 mol %)	phenol (20 mol %)	quantitative

Table 5.1: Results from Ikegami preliminary study of MBH reaction.[7]

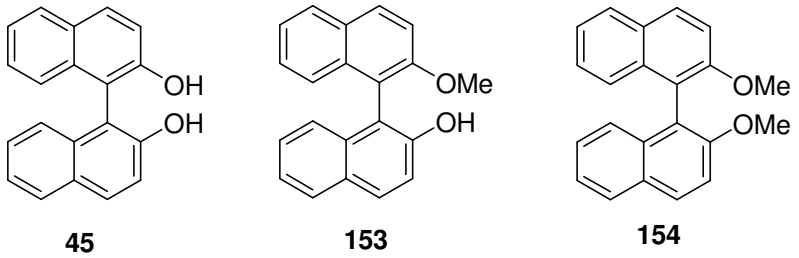

45 **153** **154**

Fig. 5.1 BINOL (**45**) and BINOL derivatives (**153** and **154**) evaluated for MBH reaction

For their extensive study, tributylphosphine (**152**) and (+/−)-BINOL (**45**) were evaluated as catalysts against a broad range of Michael acceptors and aldehydes (Table 5.2).[7] 2-Cyclopenten-1-one (**149a**) was reacted with benzaldehyde (**150b**) and propanal (**150c)** with yields of 92% and 91% being obtained, respectively. 2-Cyclohexen-1-one (**149b**) was reacted with hydrocinnamaldehyde (**150a**) and benzaldehyde (**150b**) with yields of 88% and 57%, respectively. Methyl acrylate (**149c**) was found to give a lower yield of 52% when reacted with heptanal (**150d**). From their results, cyclic enones performed better than acyclic enones for the MBH reaction.

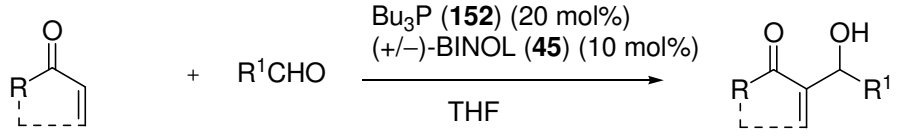

149 **150** (1.5 eq) **151**

Scheme: 5.3 Generic scheme for Ikegami extended study

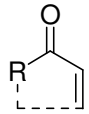	R^1CHO	Time (h)	Temp (°C)	Product	Yield (%)
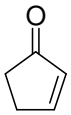 **149a**	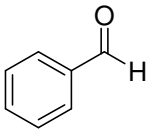 **150b**	2	rt	**151b**	92
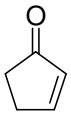 **149a**	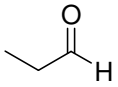 **150c**	24	rt	**151c**	91
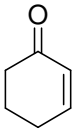 **149b**	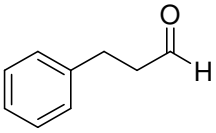 **150a**	19	rt	**151d**	88
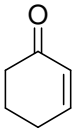 **149b**	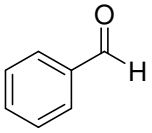 **150b**	48	rt	**151e**	57
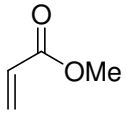 **149c**	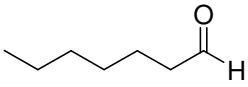 **150d**	5	50	**151f**	52

Table 5.2: Results for Ikegami extended study.[7]

Schaus and coworkers extended the idea of Brønsted acid catalysis for the asymmetric Morita-Baylis-Hillman using chiral BINOL derived organocatalysts.[1] They reported the addition of a cyclic enone to aldehydes and found chiral saturated BINOLs to be superior

catalysts for promoting the asymmetric MBH reaction. Test substrates used for their preliminary study were cyclohexeneone (**149b**) and hydrocinnamaldehyde (**150a**) (Scheme 5.4).

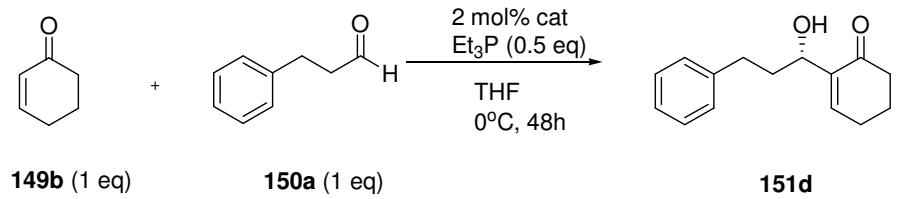

Scheme 5.4: Schaus MBH reaction of test substrate **149b** and **150a**

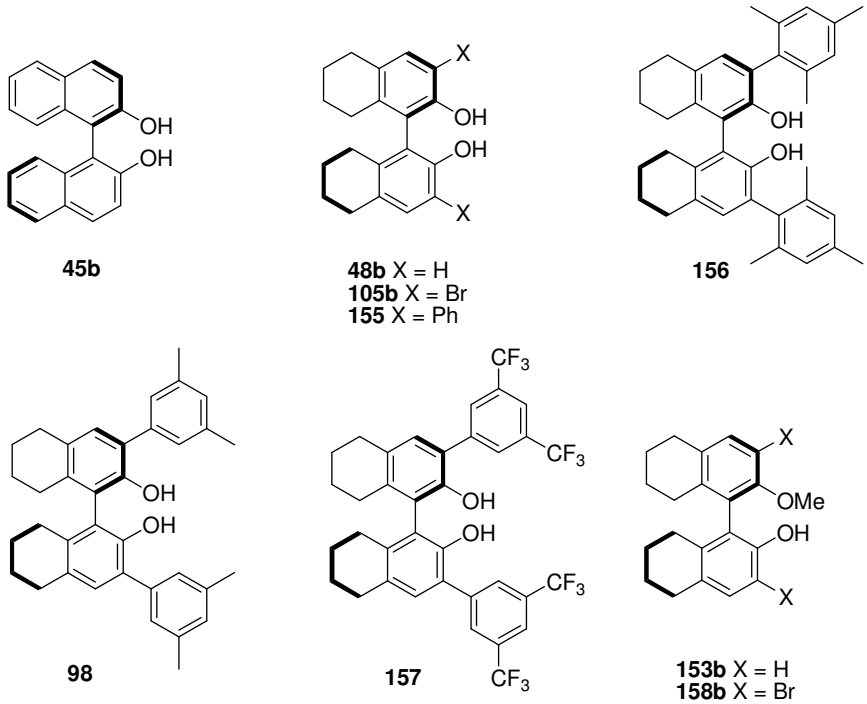

Fig 5.2 BINOL derivatives used in Schaus study.[1]

catalyst	% yield	% ee
no catalyst	5	not applicable
45b	74	32
48b	73	48
105b	73	79
155	69	86
156	9	31
98	70	88
157	84	86
153b	43	3
158b	15	3

Table 5.3: Results for Schaus preliminary study of MBH reaction.[1]

A variety of chiral diols (**45b**, **48b**, **98**, **105b**, **153b**, **155**, **156**, **157** and **158b**) (Figure 5.2) along with the catalyst triethylphosphine were screened for the MBH reaction with test substrates **149b** and **150a** (Table 5.3).

Triethylphosphine as catalyst afforded a low yield of 5% for the MBH adduct (**151d**) (Table 5.3). The addition of BINOL (**45b**) increased the yield substantial to 74% and gave an ee of 32% for **151d**. This is not surprising considering the report made by Ikegami.[7] However, saturation of the BINOL scaffold (**48b**) was found to increase the ee to 48% for **151d**. Further modification of the reduced BINOL scaffold at the 3,3'-position with bulky substituents was found to enhance the ee substantial.

Catalysts **98**, **105b**, **155** and **157** yielded the MBH adduct (**151d**) with high ee, with catalyst **98** giving the highest ee (88%) and **157** generating the highest yield (84%)**.** They found that removal of one Brønsted acid equivalent from the BINOL-derived catalyst (**153b** and **158b**) resulted in diminished catalytic activity. Interestingly, the addition of methyl substituents at the *ortho* position of the phenyl substituent at position 3 for catalyst **156** resulted in a detrimental low yield of 9% and gave an ee of 31% for **151d**. Triethylphosphine was the optimal catalyst for their MBH reaction as trimethylphosphine and tributylphosphine gave similar yields for **151d** but lower enantioselectivities. From there preliminary study, it is apparent that key structural features like saturation of the

BINOL scaffold, substitution at the 3,3'-position and free diols are required for an efficient BINOL derived catalyst in the asymmetric MBH reaction.

Catalysts **98** and **157** were selected for further study and were evaluated against a range of aldehydes to assess substrate scope (Table 5.4). Catalyst **157** proved to be the optimal catalyst for aliphatic aldehydes while catalyst **98** gave the best results for more hindered aldehydes. Conjugated aldehydes performed poorly for their MBH reaction as low yields and low enantioselectivities were obtained. For their further study, 2 equivalents of triethylphosphine and cyclohexenone (**149b**), 10-20 mol% of catalyst **98** and **157** at -10 °C in THF were found to be the optimum conditions for affording the MBH adduct in high yield.

5.4 Our study of MBH reaction

The MBH reaction was selected for our study as BINOL and other related diols have been reported to promote this reaction by Ikegami and Schaus. Therefore, it was ideal to validate our catalysts against the MBH reaction.

It was decided to adopt the model reaction used by Schaus for our investigation of chiral polysubstituted BINOL as catalysts for the asymmetric MBH reaction. Similar conditions were employed to those that Schaus used for his preliminary study such as 2-cyclohexen-1-one (**149b**) (1 equivalent) and hydrocinnamaldehyde (**150a**) (1 equivalent) as test substrates, triethylphosphine (0.5 equivalent) as nucleophilic promoter and THF as solvent. The only exception was that the reaction could not be performed at 0 °C for the full 48 h. Therefore, reaction was run at 0 °C for 3 h and the remaining 45 hrs were at room temperature. Each catalyst was screened at a loading of 2 mol%.

Our hypothesis for using polysubstituted BINOLs were that they shared similar features to those identified in Schaus study such as substitution at the 3,3'-position and free chiral diols. However, they do not contain a saturated ring. We feel that the placement of substituents at the 6,6'-position will have an affect on the bite angle, whether this would have a positive effect on the MBH reaction was the main reason for investigating these catalysts.

aldehyde	catalyst	Yield (%)	% ee
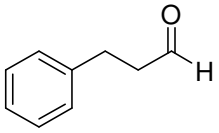	**157**	**151d** (88)	90
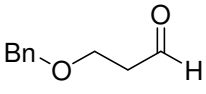	**157** (20 mol%)	**151g** (74)	82
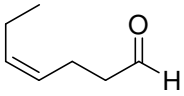	**98**	**151h** (72)	96
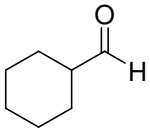	**98**	**151i** (71)	96
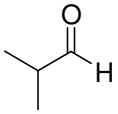	**98**	**151j** (82)	95
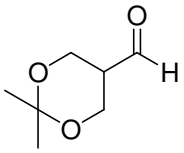	**98** (20 mol%)	**151k** (70)	92
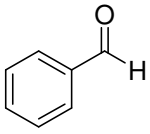	**157**	**151e** (40)	67
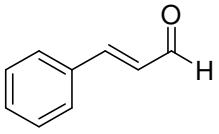	**98**	**151L** (39)	81

Table 5.4: Schaus extended study of MBH reaction.[1]

Initially, a racemic sample of the MBH adduct (+/−)-2-(1-hydroxy-3-phenylpropyl)cyclohex-2-enone (**151d**) was required. This was synthesised by reacting 2-cyclohexen-1-one (**149b**) and hydrocinnamaldehyde (**150a**), catalyzed by 1M triethylphosphine in THF and (+/−)-BINOL (**45**) to yield MBH adduct **151d** in 59% yield after column chromatography. A sample of **151d** was used to identify conditions for separating the enantiomers *via* chiral High Performance Liquid Chromatography (HPLC) analysis. Optimum conditions for separating enantiomers are presented in Chapter 7 (section 7.9).

The results obtained from our MBH study are presented in Table 5.5. Chiral (+)-(*R*)-BINOL (**45b**) was evaluated at a loading of 2 mol% and furnished the MBH adduct **151d** with a yield of 57% and an ee of 32.5% (Table 5.5, entry 1). In the literature (+)-(*R*)-BINOL (**45b**) has been reported to generate the MBH adduct **151d** with a yield of 74% and an ee of 32%. In our laboratory the yield is slightly lower than that reported but the ee is the same. The commercial available Schaus catalyst (+)-(*R*)-(**98**) was also evaluated and gave a yield of 59% and an ee of 87% for **151d** (Table 5.5, entry 5). Schaus reported a yield of 70% and an ee of 88% with catalyst (+)-(*R*)-(**98**). Our yield is slightly lower but the ee is similar to that reported in the literature with catalyst (+)-(*R*)-(**98**). Next intermediate (+)-(*R*)-**122b** was screened and the MBH adduct **151d** was obtained in 43% yield with an ee of 44% (Table 5.5, entry 2). A slight decrease in yield is noted for (+)-(*R*)-**122b** compared to (+)-(*R*)-BINOL (**45b**) (entry 1 vs 2), however, an increase in ee was obtained for the product **151d**. The reason for the increase in enantioselectivity could be due to the bulky phenyl substituent present in (+)-(*R*)-**122b**.

Polysubstituted derivative (+)-(*R*)-**123b** gave a low yield of 28% and a low ee of 9% for **151d** (entry 3). A dramatic loss in yield and ee for **151d** is apparent for the catalyst (+)-(*R*)-**123b**. Novel polysubstituted BINOL (+)-(*R*)-**111b** afforded **151d** with a yield of 15% and an ee of 7% (entry 4). Novel polysubstituted (+)-(*R*)-**114b** furnished the MBH adduct **151d** in 24% yield and with an ee of 29% (entry 8). Derivative (+)-(*R*)-**114b** gave better results in terms of yield and ee for **151d** compared to (+)-(*R*)-**111b** (entry 4 vs 8).

Overall polysubstituted derivatives gave a low yield and a lower ee for the MBH adduct **151d** compared to chiral (+)-(*R*)-BINOL (**45b**). Another commercial catalyst (−)-(*S*)-**159** was evaluated and this yielded **151d** with a 35% yield and with an ee of 12% (entry 7). Racemic biquinoline (+/−)-(**130**) was evaluated for the conversion of **151d** and a yield of 58% was obtained for adduct **151d** (entry 6). From our study it is apparent that saturation of the BINOL scaffold is necessary in order to obtain high yields and high ee for the MBH adduct **151d**. Due to time constraints and unpromising results further catalysis studies were not carried out. Priority was now given to completing the toxicity and biodegradation studies of the saturated BINOL examples, as positive results from those studies would be a significant development.

Entry	Catalyst	Loading	Yield	ee
1	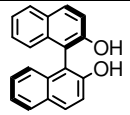 **(+)-(*R*)-45b**	2 mol%	57%	32.5% ee
2	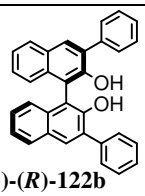 **(+)-(*R*)-122b**	2 mol%	43%	44%ee
3	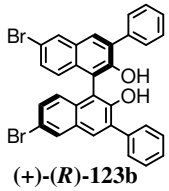 **(+)-(*R*)-123b**	2 mol%	28%	9%ee
4	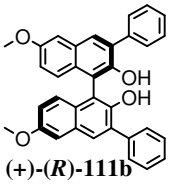 **(+)-(*R*)-111b**	2 mol%	15%	7%ee
5	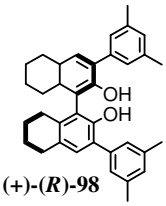 **(+)-(*R*)-98**	2 mol%	59%	87% ee
6	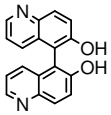 **(+/-)-(*R*)-130**	2 mol%	58%	
7	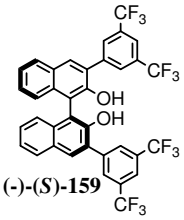 **(-)-(*S*)-159**	2 mol%	35%	12% ee
8	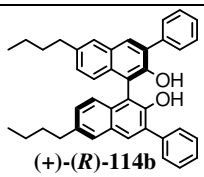 **(+)-(*R*)-114b**	2 mol%	24%	29% ee

Table 5.5: Catalysts screened for MBH reaction with yields and ee for compound **151d**

5.5 Conclusion

A range of chiral diols have been evaluated as catalysts for the MBH reaction. Novel polysubstituted BINOLs (+)-(*R*)-**111b** and (+)-(*R*)-**114b** were assessed for the MBH reaction as part of a preliminary study. Results for novel catalysts (+)-(*R*)-**111b** and (+)-(*R*)-**114b** compared poorly with (+)-(*R*)-BINOL (**45b**) and the Schaus catalyst (+)-(*R*)-(**98**). Further studies are needed in the future to determine if other substrates work better for these catalysts ((+)-(*R*)-**111b** and (+)-(*R*)**-114b**). As the saturated BINOL examples are known to give high enantioselectivity, priority was now given to completing the toxicity and biodegradation studies of these saturated BINOL examples, as positive results from those studies would be a significant development.

5.6 References

(1) N. T. McDougal and S. E. Schaus, *J. Am. Chem. Soc.,* 2003, **125**, 12094-12095.

(2) K. Morita, Z. Suzuki and H. Hirose, *Bull. Chem. Soc. Jpn.,* 1968, **41**, 2815.

(3) G. Masson, C. Housseman, J. Zhu, *Angew. Chem. Int. Ed.,* 2007, **46**, 4614-4628.

(4) D. Basavaiah, B. S. Reddy and S. S. Badsara, *Chem. Rev.,* 2010, **110**, 5447-5674.

(5) D. Basavaiah, K. Venkateswara Rao and R. Jannapu Reddy, *Chem. Soc. Rev.,* 2007, **36**, 1581-1588.

(6) N. McDougal, W. Trevellini, S. Rodgen, L. Kliman and S. Schaus, *Adv. Synth. Catal.,* 2004, **346**, 1231-1240.

(7) Y. M. A. Yamada and S. Ikegami, *Tetrahedron Lett.,* 2000, **41**, 2165-2169.

Chapter 6: Conclusion and Future work

6 Conclusion and Future work

6.1 Conclusion

Toxicity and biodegradation data for organocatalysts was lacking in the literature prior to starting this project. Our objectives for this work was to establish the environmental impact for commercial organocatalysts by obtaining their antimicrobial data, affect on human blood cell lines and biodegradation data. This thesis presents the first comprehensive toxicity and biodegradation study for organocatalysts. New organocatalysts with improved biodegradation and lower toxicity was a primary target. By working with our collaborators we have managed to assess novel and commercial organocatalysts for toxicity and biodegradation

The antimicrobial activity for a range of known organocatalysts was established by growth inhibition assays. Antimicrobial screening was carried out both in DCU and by our collaborator Dr. Marcel Špulák of Charles University Czech Republic. Amino acids, proline derivatives, BINOL, BINOL derivatives, TADDOL, Jacobsen thioureas, Cinchona alkaloid derivatives, MacMillan imidazolidinones, chiral phosphoric acids and a Maruoka phase-transfer catalyst are the classes of organocatalysts that were studied for antimicrobial activity.

The data obtained from the screening studies of amino acids exhibited some cases of anti-microbial activity. However, the MIC values determined for inhibitory amino acids proved high (>2.5 mM). For proline derivatives, compounds **95** and **96** were shown to exhibit anti-microbial activity for *M.luteus, B.subtilis* and *E.coli* using the microtiter broth dilution technique. Other proline derivatives proved non-inhibitory within tested concentration range (3.45 mM-0.007 mM). BINOL (**45**) exhibited inhibition towards *M.luteus* and *B.subtilis* (0.107 mM) while BINOL derivatives and TADDOL proved to be non-inhibitory for test organisms within studied concentration range.

Antimicrobial studies performed by our collaborator Dr Marcel Špulák showed a number of organocatalysts inhibiting test microorganisms. Growth inhibition was found with

proline derivatives (**101** and **102**) for both bacterial and fungal organisms. **102** was found to be more toxic (lower MIC values) than **101** towards test microorganisms. Jacobsen thioureas showed more inhibition for bacteria than for fungi. All three Jacobsen thioureas inhibited different bacteria with **15** being the most active. **15** was the only Jacobsen thiourea found to inhibit fungal strains (4 in total). Cinchona alkaloid derivatives were observed with low inhibition for bacteria, with only **81a** exhibiting antifungal activity in some cases. MacMillan imidazolidinones were found to be mostly non-inhibitory towards both bacterial and fungal strains (>2000 μM). The only exceptions were **109** which inhibited *MRSA* at 2000 μM after 24 h and at 48 h and **110** was found to inhibit *Staphylococcus epidermidis* at 2000 μM after 24 h and at 48 h. **110** inhibited 2 fungal strains. Chiral phosphoric acids (**26a** and **26b**) proved inhibitory for most Gram positive bacteria while Gram negative bacteria showed low inhibition. **26b** was observed with two cases of inhibition for fungal organisms. Maruoka phase-transfer catalyst (**40**) inhibited all Gram positive bacteria but Gram negative bacteria were not inhibited (>125 μM). **40** inhibited a number of fungal organisms with MIC values ranging from 3.9 μM to 62.5 μM.

TADDOL (**100**) and BINOL derivatives (**98** and **99**) showed low inhibition towards all bacterial and fungal organisms (>125 μM). (*S*)-BINOL (**45a**) and (*R*)-BINOL (**45b**) inhibited all Gram positive bacteria while Gram negative bacteria showed low inhibition. Both **45a** and **45b** showed a few cases of anti-fungal activity. However, most fungal organisms were not inhibited by **45a** and **45b** (>500 μM). Brominated BINOL derivatives (**50a** and **50b**) were found to be more toxic than BINOL (**45a** and **45b**) as lower MIC values were obtained for Gram positive bacteria. **50a** and **50b** inhibited all Gram positive bacteria while Gram negative bacteria showed low inhibition (>2000 μM). A trend noted was that the *R* enantiomer (**50b**) was more active than the *S* enantiomer (**50a**). H_8-BINOLs (**48a** and **48b**) inhibited all Gram positive bacteria while Gram negative bacteria were not inhibited (>2000 μM). Brominated H_8-BINOL derivatives (**105a** and **105b**) were found to be more toxic towards Gram positive bacteria than the non-brominated H_8-BINOLs (**48a** and **48b**). (*R*)-3,3'-Dibromo-H_8-BINOL (**105b**) was observed with lower MIC values when compared to (*S*)-3,3'-dibromo-H_8-BINOL (**105a**).

Cytotoxicity, apoptosis and cell viability studies were performed for organocatalysts (**8**, **15**, **26a**, **38a**, **40**, **81a**, **102**, **103**, **104**, **106**, **107**, **108** and **109**) against 3 blood cell lines (erythroid progenitors, HL-60 and K-562). These studies were carried out by our collaborator Dr. Petr Bartunek in the Czech Republic. **102** and **107** reduced cell viability by less than 50% for all 3 cell lines at 10 μM. Maruoka catalyst (**40**) was found to induce apoptosis for all three cell lines. A loss of cell viability for all three cell lines was observed with **40**. The integrity of the plasma membranes for the blood cell lines was not disrupted by **40**. EC_{50} values were determined for the affect **40** has on apoptosis. Erythroid progenitors, HL-60 and K-562 cell lines gave EC_{50} values of 6.0 μM, 2.1 μM and 5.5 μM, respectively for **40**. IC_{50} values were determined for the affect **40** has on cell viability. Erythroid progenitors, HL-60 and K-562 cell lines gave IC_{50} values of 1.2 μM, 0.8 μM and 1.7 μM, respectively for **40**. Remaining organocatalysts were found to be non-toxic for all 3 cell lines within the studied concentration range (0.1 – 10 μM).

Biodegradation studies were performed on organocatalysts (**8**, **15**, **19**, **26a**, **26b**, **38a**, **40**, **41a**, **45a**, **45b**, **48a**, **48b**, **50a**, **50b**, **81a**, **89**, **92**, **97**, **100**, **101**, **102**, **103**, **104**, **105a**, **105b**, **106**, **107**, **108**, **109** and **110**) using the CO_2 headspace test (ISO 14593). Organocatalysts (**8**, **15**, **19**, **26a**, **26b**, **38a**, **40**, **41a**, **45a**, **45b**, **48a**, **48b**, **50a**, **50b**, **81a**, **92**, **97**, **100**, **101**, **102**, **103**, **104**, **105a**, **105b**, **106**, **107**, **108**, **109** and **110**) failed the test and cannot be classified as readily biodegradable. L-Prolinamide (**89**) passed the CO_2 headspace test (ISO 14593) with a biodegradation value of 77% after 28 days. **81a** and **8** were found to have a slight inhibitory effect on the inoculum (19% and 8% respectively), however, these % inhibitions are lower than the limit (>25% inhibition) generally accepted to consider a significant inhibitory effect on the activity of the inoculum. Maruoka phase-transfer catalyst (**40**) had an inhibitory effect on the activity of the inoculum, as a % inhibition value of 30% is higher than the limit (>25% inhibition) accepted for an inhibitory effect on the inoculum.

The synthesis of novel polysubstituted BINOLs from the key intermediate (**123**) were performed in 1 to 2 steps. Key intermediate (**123**) was synthesised in 5 steps according to a literature known procedure. Each step provided intermediates (**119**, **120**, **121**, **122**, **123**)

in moderate to good yields. However, difficulty was initially encountered for the synthesis of **120,** as a low yield of 25% was obtained. By changing the addition of electrophile, an improvement in yield to 86% was obtained (A yield that is more comparable to that reported in literature). The procedure for the synthesis of key intermediate (**123**) was modified as the addition of extra equivalents of bromine was required to drive the reaction to completion. Using the key intermediate (**123**), synthesis of polysubstituted BINOLs was achieved. A range of polysubstituted BINOLs were prepared *via* different synthetic methods. Target molecules **111** and **112** were made with yields of 65% and 55% respectively using an Ullmann-type condensation reaction. Demethylation of **111** yielded compound **113** in 49%. **127** was obtained using a modified Kumada metal coupling reaction in 35% yield and subsequent MOM deprotection furnished **114** in 74% yield. **126** was made in 44% yield *via* a halogen metal exchange route and subsequent MOM deprotection gave **115** in 77% yield. Using a Sonogashira coupling reaction, compounds **116** and **117** were obtained in 60% and 50% yields respectively. Hydration of **117** furnished **118** in 59% yield.

Optically pure BINOL derivatives were synthesised in 1-2 steps from the chiral key intermediate (+)-(*R*)-(**123b**). BINOL derivative (+)-(*R*)-(**111b**) was synthesised from (+)-(*R*)-(**123b**) by an Ullmann-type condensation in 67% yield. A modified Kumada metal coupling reaction was performed using (−)-(*R*)-(**125b**) and subsequent MOM deprotection yielded (+)-(*R*)-(**114b**) in 42% yield.

Achiral BINOL (**45**) and BINOL derivatives (**111**, **114**, **115**, **118** and **122**) were screened for antibacterial and antifungal activity. Achiral polysubstituted BINOLs (**111**, **114**, **115** and **118**) showed low inhibition towards bacteria and fungi. BINOL derivative (**122**) inhibited *Staphylococcus epidermidis* (500 μM) and *Enterococcus sp.* (250 μM) while remaining bacteria showed low inhibition (>2000 μM). BINOL (**45**) was found to be active against all Gram positive bacteria. MIC values ranging from 31.25 μM to 125 μM were noted for **45**. A number of fungal organisms showed inhibition for **45**.

Achiral BINOL (**45**) and BINOL derivatives (**111**, **114**, **115**, **118** and **122**) failed the CO_2

headspace test (ISO 14593) and can be classified as non-biodegradable. BINOL (**45**) was found to have a slight inhibitory effect on the inoculum (9%), however, this % inhibition is lower than the limit (>25% inhibition) generally accepted to consider a significant inhibitory effect on the activity of the inoculum.

Biquinoline derivatives **134**, **135** and **136** were synthesised in one step from BIQOL (**130**) *via N*-alkylation reactions to furnish yields of 26%, 86% and 79% respectively. The quinoline derivatives **140** and **142** were prepared by a modified Friedländer synthesis with yields of 44% and 46% being obtained respectively. Dimerisation of these intermediates was investigated by employing an oxidative copper coupling reaction. **142** dimerised under reaction conditions, however, the synthesis needs further optimization due to low yields and the possibility that residual copper salts are still present.

The antimicrobial activities of **130** and *N*-biquinoline salts (**134**, **135** and **136**) were determined for bacteria and fungi. These compounds showed low inhibition for all fungal organisms studied. Biquinoline (**130**) inhibited *Enterococcus sp*., *E.coli* and *Klebsiella pneumoniae* while remaining bacteria were not inhibited (>2000 μM). *N*-biquinoline salt (**134**) inhibited *Enterococcus sp.* but remaining bacteria showed low inhibition (>1000 μM). Test bacteria were not inhibited by **135** and **136** (>2000 μM).

The asymmetric Morita-Baylis-Hillman reaction was investigated using chiral (+)-(*R*)-BINOL (**45b**) and substituted BINOL derivatives ((+)-(*R*)-(**111b**), (+)-(*R*)-(**114b**), (+)-(*R*)-(**122b**) and (+)-(*R*)-(**123b**),). Catalysts performed poorly for the model reaction as low yields and ee were obtained for the MBH adduct **151d**. Due to time constraints and unpromising results further catalysis studies were not carried out.

6.2 Future work

From our biodegradation studies of BINOL and novel polysubstituted BINOL derivatives, it is apparent that biodegradation for these scaffolds is a considerable task. Work towards a more biodegradable biaryl scaffold should be continued. For instance the placement of an ester or a methyl group on the 3-position of biquinoline (**137**) may lead

to a more biodegradable scaffold (Figure 6.1). Optimization for the dimerisation of **142** needs further investigation. Reduced BINOL derivatives (**160**) that are modified with substituents to enhance biodegradation are another possibility. Evaluation of biphenyl atropisomers (**161**) may lead to a more biodegradable scaffold as these compounds contain less aromatic rings which would make it easier for microorganisms to degrade. Modification of the biphenyl scaffold with substituents that are in line with the 'rules of thumb' could enhance biodegradation for that respective scaffold.

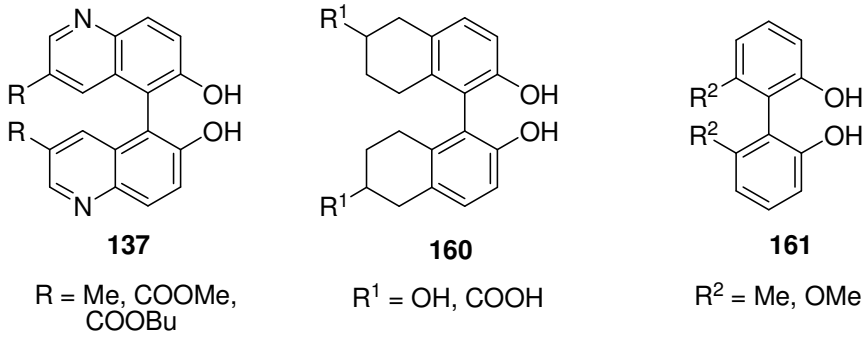

Fig. 6.1 Potential biaryl scaffolds for future biodegradation studies.

Further ecotoxicity studies with known organocatalysts should be done to determine their toxicity towards algae and aquatic organisms.

Chapter 7: Experimental

7.1 Introduction

7.1.1 Chemicals

All chemicals used in Chapters 2, 3, 4 and 5 were purchased from Sigma-Aldrich and Strem chemicals. THF and diethyl ether were dried over sodium wire and benzophenone and distilled before use. DMF and DME were purchased in anhydrous form from Sigma-Aldrich. Merck silica 60 (particle size 0.063-0.200 nm) was used for flash chromatography. Thin layer chromatography (TLC) was performed on aluminium sheets coated with 0.20 mm of fluka silica gel containing fluorescent indicator 254 nm.

Müeller Hinton broth and nutrient broth were obtained from Sigma-Aldich and Oxoid. Well plates were sourced from Corning.

7.1.2 NMR Spectroscopy

All NMR analysis was performed on a Bruker AC 400 MHz spectrometer in either deuterated chloroform, DMSO, acetone and methanol, operating at 400 MHz for ^{1}H NMR and 100 MHz for ^{13}C NMR. A 600 MHz spectrometer, operating at 600 MHz for ^{1}H NMR and 150 MHz for ^{13}C NMR, was also used for the analysis of some compounds. Chemical shifts are reported in parts per million (ppm) are relative to the internal standard TMS and coupling constants (*J*) are reported in Hertz (Hz). When stating multiplicity of peaks in NMR the following abbreviations are used; s-singlet, d-doublet, t-triplet, q-quartet, qt-quintet, dd-doublet of doublets, dt-doublet of triplets, dq-doublet of quartets, tt-triplet of triplets, tq-triplet of quartets, m-multiplet, br-broad.

7.1.3 Optical Rotation

Optical rotations were measured using a Perkin Elmer 343 Polarimeter in THF or methanol at 20 °C.

7.1.4 Melting point

Melting points were determined using a Griffin melting point apparatus and the values are expressed in degrees Celcius (°C) uncorrected.

7.1.5 IR analysis

All IR analysis was carried out on a Perkin Elmer 100 FT-IR spectrometer with ATR.

7.1.6 Mass spectrometry

High resolution mass spectrometry was obtained for all novel compounds using the Waters LCT premier time of flight instrument.

7.2 Experimental for antimicrobial studies

7.2.1 Microtiter broth dilution technique

Minimum inhibitory concentrations (MICs) for compounds were determined by serial two-fold dilutions in Mueller-hinton or nutrient broth using the microtiter broth dilution technique described by Amsterdam.[1] All assays were done in triplicate.

Method

Test strains were grown in nutrient broth at 30 °C overnight. Next day, cultures were centrifuged at 5000 rpm for 10 minutes. Pellet was washed twice with 10 ml 0.01 M sodium phosphate buffer (pH 7). Optical density of cultures was adjusted to give an optical density of 0.07 at 660 nm.

The compound solution and 96 well plates were ready before the cultures were adjusted to the desired optical density.

For stock solution of chemical, the compound to be tested was dissolved in 1 ml of sterile water or organic solvents such as methanol and DMSO dependant on the chemicals solubility.

For microplate preparation, 190 µl of Mueller-hinton broth was dispensed into wells in column 1. 100 µl of Mueller-hinton broth was dispensed into all wells from column 2 to column 12. 10 µl of the compound solution was pipetted into wells in column 1 (far left of plate). The compound was mixed into the wells in column 1 by pipetting up and down 6-8 times. 100 µl was withdrawn from column 1 and added to column 2. This made column 2 a two-fold dilution of column 1. This was mixed up and down 6-8 times. 100 µl was transferred to column 3. This procedure was repeated down to column 10 only. 100 µl was discarded from column 10 rather than putting it in column 11. 5 µl of the strain to be tested was dispensed into wells in columns 11 to 1 in that order. Column 11 was used as a growth control and column 12 was the sterility control. The plates were incubated at 30 °C overnight. Growth on the plates was noted and optical density measured after 24 hours.

Results from this screening are presented in chapter 2 (Section 2.3).

7.2.2 Antibacterial and antifungal procedure for Czech screening

7.2.2.1 Antibacterial activity – experimental method

In vitro antibacterial activities[2] of the compounds were evaluated on a panel of three ATCC strains (*Staphylococcus aureus* ATCC 6538, *Escherichia coli* ATCC 8739, *Pseudomonas aeruginosa* ATCC 9027) and five clinical isolates (*Staphylococcus aureus* MRSA HK5996/08, *Staphylococcus epidermidis* HK6966/08, *Enterococcus* sp. HK14365/08, *Klebsiella pneumoniae* HK11750/08, *Klebsiella pneumoniae* ESBL HK14368/08) from the collection of bacterial strains deposited at the Department of Biological and Medical Sciences, Faculty of Pharmacy, Charles University, Hradec Králové, Czech Republic. The above-mentioned ATCC strains also served as the quality control strains. All the isolates were maintained on Mueller-Hinton agar prior to being tested.

Dimethyl sulfoxide (100 %) served as a diluent for all compounds; the final concentration did not exceed 2 %. Mueller-Hinton broth (MH, HiMedia, Čadersky-Envitek, Czech Republic) buffered to pH 7.4 (±0.2) was used as the test medium. The wells of the microdilution tray contained 200 µl of the Mueller-Hinton medium with 2-fold serial dilutions of the compounds (2000 to 0.488 µmol/l) and 10 µl of inoculum suspension. Inoculum in MH medium was prepared to give a final concentration of 0.5 McFarland scale (1.5×10^8 cfu.ml^{-1}). The trays were incubated at 37°C and MICs were read visually after 24 h and 48 h. The MICs were defined as 95 % inhibition of the growth of control. MICs were determined twice and in duplicate. The deviations from the usually obtained values were no higher than the nearest concentration value up and down the dilution scale.

7.2.2.2 Antifungal activity – experimental method

In vitro antifungal activities[3,4] of the compounds were evaluated on a panel of four ATCC strains (*Candida albicans* ATCC 44859, *Candida albicans* ATCC 90028, *Candida parapsilosis* ATCC 22019, *Candida krusei* ATCC 6258) and eight clinical isolates of

yeasts (*Candida krusei* E28, *Candida tropicalis* 156, *Candida glabrata* 20/I, *Candida lusitaniae* 2446/I, *Trichosporon asahii* 1188) and filamentous fungi (*Aspergillus fumigatus* 231, *Absidia corymbifera* 272, *Trichophyton mentagrophytes* 445) from the collection of fungal strains deposited at the Department of Biological and Medical Sciences, Faculty of Pharmacy, Charles University, Hradec Králové, Czech Republic. Three ATCC strains were used as the quality control strains. All the isolates were maintained on Sabouraud dextrose agar prior to being tested.

Minimum inhibitory concentrations (MICs) were determined by modified CLSI standard of microdilution format of the M27-A3 and M38-A2 documents.[3,4] Dimethyl sulfoxide (100 %) served as a diluent for all compounds; the final concentration did not exceed 2 %. RPMI 1640 (Sevapharma, Prague) medium supplemented with *L*-glutamine and buffered with 0.165 M morpholinepropanesulfonic acid (Serva) to pH 7.0 by 10 M NaOH was used as the test medium. The wells of the microdilution tray contained 200 µl of the RPMI 1640 medium with 2-fold serial dilutions of the compounds (2000 to 0.488 µmol/l for the new compounds) and 10 µl of inoculum suspension. Fungal inoculum in RPMI 1640 was prepared to give a final concentration of $5 \times 10^3 \pm 0.2$ cfu.ml^{-1}. The trays were incubated at 35°C and MICs were read visually after 24 h and 48 h. The MIC values for the dermatophytic strain (*T. mentagrophytes*) were determined after 72 h and 120 h. The MICs were defined as 80 % inhibition (IC_{80}) of the growth of control for yeasts and as 50 % inhibition (IC_{50}) of the growth of control for filamentous fungi. MICs were determined twice and in duplicate. The deviations from the usually obtained values were no higher than the nearest concentration value up and down the dilution scale.

7.3 Experimental for cytotoxicity, apoptosis and cell viability studies

Normal human erythroid progenitor cells were grown according to a previous report.[5]

HL-60 (ATCC CCL-240) and K-562 (ATCC CCL-243) were grown in DMEM (D5546, Sigma) with 10% fetal bovine serum (10270, Gibco) supplemented with 2 mM glutamine (25030, Gibco) and PenStrep: Penicillin 100 units/mL + Streptomycin 100 µg/mL (15140, Gibco) in a humidified atmosphere (95%) with 5% CO_2 at 37 ºC. Assays were performed as follows: Cells were plated at 5000 (for HL-60 and K-562) or 10000 (for erythroid

progenitor cells) cells per well per 25 μL in 384-well plates immediately before compound addition. Cell viability and cytotoxicity have a fluorescent readout, and cells were plated into black 384-well plates (Corning, Cat. No.3571). Apoptosis has a luminescent readout and cells were plated into white 384-well plates (Corning, Cat. No. 3570). Test compounds diluted in DMSO were acoustically transferred to the cell supernatant (Echo 520, Labcyte). Cytotoxicity and apoptosis were measured 3 h after compound addition using the CytoTox-ONE homogeneous membrane integrity assay (G7892, Promega)[6] and the Caspase-Glo 3/7 assay (G8091, Promega)[7], respectively. Cell viability was measured using the CellTiter-Blue cell viability assay (G8082. Promega)[8] 48 h after compound addition. All assays were measured using the EnVision plate reader (PerkinElmer). Data were analyzed using GraphPad Prism 5.0 statistical software.

7.4 Experimental for biodegradation studies -CO_2 headspace test (ISO 14593)

To evaluate the biodegradability of the compounds, the 'CO_2 Headspace' test (ISO 14593) was applied.[9] This method allows the evaluation of the ultimate aerobic biodegradability of an organic compound in aqueous medium at a given concentration of microorganisms by analysis of inorganic carbon. The test compound, as the only source of carbon and energy, was added to a buffer-mineral salts medium which had been inoculated with a mixed population of microorganisms derived from an activated sludge collected from a sewage treatment plant to give a final organic carbon concentration of 20 mg/L. These solutions were incubated in sealed vessels with a headspace of air, which provided a reservoir of oxygen for aerobic biodegradation. Biodegradation (mineralization to carbon dioxide) was determined by measuring the net increase in total inorganic carbon (TIC) levels over time compared to unamended blanks. Sodium *n*-dodecyl sulfate (SDS) was used as a reference substance. The test ran for 28 days. The extent of biodegradation was expressed as a percentage of the theoretical amount of inorganic carbon (ThID) based on the amount of test compound added initially. Assuming 100% mineralization of the test compound, the theoretical amount of inorganic carbon (ThID) in excess of that produced in the blank controls equals the amount of total organic carbon (TOC) added as the test compound to each vessel at the start of the test, that is:

ThIC = TOC

Percentage biodegradation D_t in each case is given by :

$$D_t = \frac{(TIC_t - TIC_b)}{TOC_i} \times 100$$

where:

TIC_t is the TIC, in milligrams, in vessel at time t;

TIC_b is the mean TIC, in milligrams, in blank control vessels at time t

TOC_i is the TOC, in milligrams, initially added to the test vessel

7.5 Preparation of achiral polysubstituted BINOL derivatives

(+/−)-6,6'-Dimethoxy-3,3'-diphenyl-2,2'-dihydroxy-1,1'-binaphthyl (111)

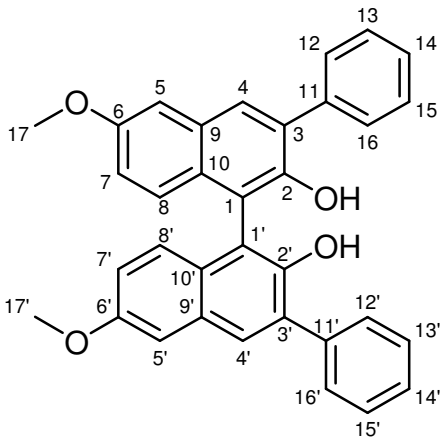

(+/−)-6,6'-Dibromo-3,3'-diphenyl -2,2'-dihydroxy-1,1'-binaphthyl (**123**) (260 mg, 0.44 mmol) and copper (I) iodide (348 mg, 1.83 mmol) were stirred in dry DMF (1.30 mL) at room temperature under nitrogen for 10 minutes. 4.4 M Sodium methoxide in methanol (2.62 mL, 11.53 mmol) was added and the reaction mixture was refluxed for 24 h, then allowed cool to room temperature. Ice-water mixture (6 mL) was added, followed by 4N HCl (2 mL) and mixture was allowed to stir for 10 minutes. Mixture was filtered and remaining solid was washed with ethyl acetate. Filtrate was extracted with ethyl acetate (3 x 10 mL) and the combined organic phase was washed with brine (10 mL), dried over anhydrous magnesium sulfate, filtered and volatiles removed *via* rotary evaporation to yield the crude product. Crude product was purified by column chromatography (SiO_2, hexane/ethyl acetate 10:1) to yield the title compound as a beige solid in 65% yield (142 mg, 0.29 mmol).

Mpt = 230-232 °C

Molecular formula $C_{34}H_{26}O_4$

Molecular weight 498.57 $gmol^{-1}$

^{1}H NMR (400 MHz, $CDCl_3$) δ ppm 7.96 (s, 2H, *H4, H4'*), 7.78 (dd, *J*= 7.2 Hz, 1.4 Hz, 4H, *H12, H12', H16, H16'*), 7.54 (dd, *J*= 7.2 Hz, 1.4 Hz, 4H, *H13, H13', H15, H15'*), 7.45 (tt, *J*= 7.2 Hz, 1.4 Hz, 2H, *H14, H14'*), 7.28 (d, *J*= 2.8 Hz, 2H, *H5, H5'*), 7.19 (d, *J*= 9.0 Hz, 2H, *H8, H8'*), 7.04 (dd, *J*= 9.0 Hz, 2.8 Hz, 2H, *H7, H7'*), 5.31 (s, 2H, *OH*), 3.94 (s, 6H, *H17, H17'*)

^{13}C NMR (100 MHz, $CDCl_3$) δ ppm

156.59 (C, *C6, C6'*), 148.38 (C, *C2, C2'*), 137.69 (C, *C11, C11'*), 131.07 (C, *C3, C3'*), 130.38 (C, *C9/C10, C9'/C10'*), 130.12 (CH, *C4, C4'*), 129.65 (2CH, *C12, C12', C16 C16'*), 128.51 (2CH, *C13, C13',C15, C15'*), 128.24 (C, *C9/C10, C9'/C10'*), 127.76 (CH,

C14, C14'), 125.98 (CH, *C8, C8'*), 119.88 (CH, *C7, C7'*), 112.91 (C, *C1, C1'*), 106.72 (CH, *C5, C5'*), 55.44 (CH_3, *C17, C17'*)

IR (neat) (cm^{-1}) 3509, 2932, 2836, 1624, 1603, 1504, 1461, 1371, 1225, 1173, 1124, 1029

HRMS (EI, 70 eV, *m/z*) Found $[M+H]^+$ 499.1900, $C_{34}H_{27}O_4^+$ requires 499.1909

(+/–)-6,6'-Diethoxy-3,3'-diphenyl-2,2'-dihydroxy-1,1'-binaphthyl (112)

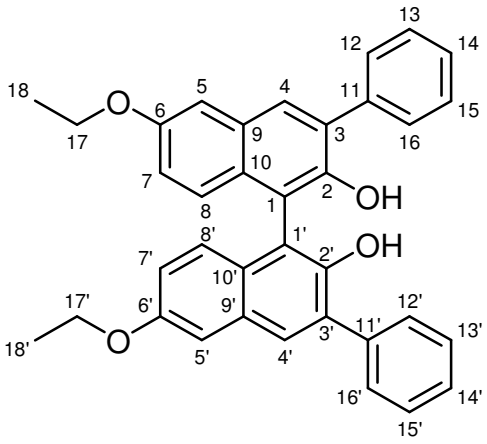

(+/–)-6,6'-Dibromo -3,3'-diphenyl -2,2'-dihydroxy-1,1'-binaphthyl (**123**) (250 mg, 0.42 mmol) and copper (I) iodide (331 mg, 1.74 mmol) were stirred in dry DMF (1 mL) at room temperature under nitrogen for 10 minutes. 2.2 M Sodium ethoxide in ethanol (5.24 mL, 11.54 mmol) was added and the reaction mixture was refluxed for 24 h, then allowed cool to room temperature. Ice-water mixture (6 mL) was added, followed by 4N HCl (2 mL) and allowed to stir for 10 minutes. Mixture was filtered and the remaining solid was washed with ethyl acetate. Filtrate was extracted with ethyl acetate (3 x 10 mL) and the combined organic phase was washed with brine (10 mL), dried over anhydrous magnesium sulfate, filtered and the solvent was removed *via* rotary evaporation to yield the crude product. Crude product was purified by column chromatography (SiO_2, hexane/ethyl acetate 10:0.3) to yield the title compound as beige solid in 55 % yield (122 mg, 0.23 mmol).

Mpt = 211-213 °C

Molecular formula $C_{36}H_{30}O_4$

Molecular weight 526.62 $gmol^{-1}$

^{1}H NMR (400 MHz, $CDCl_3$) δ ppm 7.90 (s, 2H, *H4, H4'*), 7.74 (dd, *J*= 7.0 Hz, 1.4 Hz, 4H, *H12, H12', H16, H16'*), 7.49 (dd, *J*= 7.0 Hz, 1.4 Hz, 4H, *H13, H13', H15, H15'*),

7.41 (tt, *J*= 7.0 Hz, 1.4 Hz, 2H, *H14, H14'*), 7.23 (d, *J*= 2.4 Hz, 2H, *H5, H5'*), 7.14 (d, *J*= 9.2 Hz, 2H, *H8, H8'*), 7.00 (dd, *J*= 9.2 Hz, 2H, *H7, H7'*), 5.23 (s, 2H, *OH*), 4.15 (q, *J*= 7.0 Hz, 4H, *H17, H17'*), 1.47 (t, *J*= 7.0 Hz, 6H, *H18, H18'*)

^{13}C NMR (100 MHz, $CDCl_3$) δ ppm

155.90 (C, *C6, C6'*), 148.28 (C, *C2, C2'*), 137.71 (C, *C11, C11'*), 130.97 (C, *C3, C3'*), 130.40 (C, *C9/C10, C9'/C10'*), 130.05 (CH, *C4, C4'*), 129.62 (2CH, *C12, C12', C16, C16'*), 128.46 (2CH, *C13, C13', C15, C15'*), 128.13 (C, *C9/C10, C9'/C10'*), 127.70 (CH, *C14, C14'*), 125.92 (CH, *C8, C8'*), 120.14 (CH, *C7, C7'*), 112.82 (C, *C1, C1'*), 107.50 (CH, *C5, C5'*), 63.58 (CH_2, *C17, C17'*), 14.88 (CH_3, *C18, C18'*)

IR (neat) (cm^{-1}) 3480, 3361, 3034, 2923, 1626, 1600, 1506, 1473, 1351, 1226, 1172, 1130, 1112, 1039, 1028

HRMS (EI, 70 eV, *m/z*) Found $[M+H]^+$ 527.2214, $C_{36}H_{31}O_4^+$ requires 527.2222

(+/–)-6,6'-Dihydroxy-3,3'-diphenyl-2,2'-dihydroxy-1,1'-binaphthyl (113)

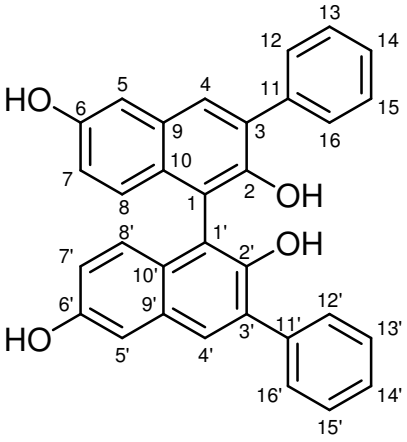

To a stirred solution of (+/–)-6,6'-dimethoxy-3,3'-diphenyl-2,2'-dihydroxy-1,1'-binaphthyl (**111**) (100 mg, 0.19 mmol) in DCM (4 mL) at 0 °C under a nitrogen atmosphere was added dropwise 1 M boron tribromide in DCM (1.77 mL, 440 mg, 1.77 mmol). Reaction mixture was allowed to reach room temperature and stirred overnight. Reaction was quenched at 0 °C by the slow addition of deionised water (5 mL). Product was extracted with DCM (3 x 5 mL) and the combined organic phase was washed with brine (5 mL), dried over anhydrous magnesium sulfate, filtered and volatiles removed to yield crude product. Crude product was purified by column chromatography (SiO_2, hexane/ethyl acetate 1.25:1) to yield the title compound as a white solid in 49% yield (46 mg, 0.10 mmol)

Mpt = 239-240 °C

Molecular formula $C_{32}H_{22}O_4$

Molecular weight 470.51 $gmol^{-1}$

^{1}H NMR (400 MHz, $(CD_3)_2SO$) δ ppm 9.43 (s, 2H, *OH*), 7.92 (s, 2H, *OH*), 7.78 (s, 2H, *H4, H4'*), 7.77 (d, *J*= 7.4 Hz, 4H, *H12, H12', H16, H16'*), 7.54 (dd, *J*= 7.4 Hz, 7.4 Hz, 4H, *H13, H13', H15, H15'*), 7.43 (t, *J*= 7.4 Hz, 2H, *H14, H14'*), 7.25 (d, *J*= 2.2 Hz, 2H, *H5, H5'*), 6.90 (dd, *J*= 9.0 Hz, 2.2 Hz, 2H, *H7, H7'*), 6.86 (d, *J*= 9.0 Hz, 2H, *H8, H8'*)

^{13}C NMR (100 MHz, $(CD_3)_2CO$) δ ppm 154.53 (C, *C6, C6'*), 150.36 (C, *C2, C2'*), 140.14 (C, *C11, C11'*), 132.95 (C, *C3, C3'*), 131.43 (C, *C9/C10, C9'/C10'*) 130.64 (2CH, *C12, C12', C16, C16'*), 129.70 (CH, *C4, C4'*), 129.41 (C, *C9/C10, C9'/C10'*), 128.79 (2CH, *C13, C13', C15, C15'*), 127.84 (CH, *C14, C14'*), 126.91 (CH, *C8, C8'*), 119.55 (CH, *C7, C7'*), 115.16 (C, *C1, C1'*), 110.58 (CH, *C5, C5'*)

IR (neat) (cm^{-1}) 3342, 3051, 1607, 1505, 1379, 1199, 1180, 1129, 1072

HRMS (EI, 70 eV, *m/z*) Found $[M+H]^+$ 471.1578, $C_{32}H_{23}O_4^+$ requires 471.1596

(+/–)-6,6'-Dibutyl-3,3'-diphenyl-2,2'-dihydroxy-1,1'-binaphthyl (114)

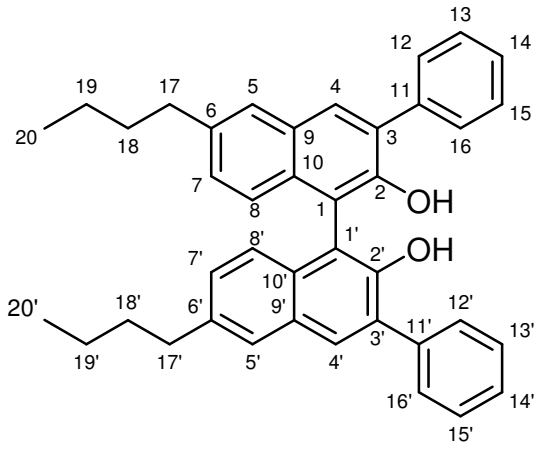

To a stirred solution of (+/–)-6,6'-dibutyl-3,3'-diphenyl-2,2'-*bis*(methoxymethoxy)- 1 ,1'-binaphthyl (**127**) (232 mg, 0.36 mmol) in THF (11 mL) at room temperature, was added concentrated hydrochloric acid (0.25 mL, 32%, 10.17 M). Reaction mixture was warmed to 50 °C and after 24 h allowed to cool to room temperature. Solvent was removed *via* rotary evaporation. Deionised water (5 mL) was added and the product was extracted with DCM (3 x 10 mL) and the combined organic phase was washed with brine (10 mL), dried over anhydrous magnesium sulfate, filtered and solvent removed *via* rotary evaporation to yield the crude product. Crude product was purified by column chromatography (SiO_2, hexane/ethyl

acetate 10:0.3) to yield the title compound as a yellow solid in 74% yield (148 mg, 0.27 mmol).

Mpt = 130-131 °C

Molecular formula $C_{40}H_{38}O_2$

Molecular weight 550.73 $gmol^{-1}$

^{1}H NMR (400 MHz, $CDCl_3$) δ ppm 7.98 (s, 2H, *H4, H4'*), 7.76 (dd, *J*= 7.2 Hz, 1.4 Hz, 4H, *H12, H12', H16, H16'*), 7.71 (s, 2H, *H5, H5'*), 7.51 (dd, *J*= 7.2 Hz, 1.4 Hz, 4H, *H13, H13', H15, H15'*), 7.42 (tt, *J*= 7.2 Hz, 1.4 Hz, 2H, *H14, H14'*), 7.20 (d, *J*= 1.2 Hz, 4H, *H7, H7', H8, H8'*), 5.32 (s, 2H, *OH*), 2.76 (t, *J*= 7.4 Hz, 4H, *H17, H17'*), 1.69 (tt, *J*= 7.4 Hz, 7.4 Hz, 4H, *H18, H18'*), 1.41 (qt, *J*= 7.4 Hz, 7.4 Hz, 4H, *H19, H19'*), 0.96 (t, *J*= 7.4 Hz, 6H, *H20, H20'*)

^{13}C NMR (100 MHz, $CDCl_3$) δ ppm

149.52 (C, *C2, C2'*), 138.90 (C, *C6, C6'*), 137.77 (C, *C11, C11'*), 131.32 (C, *C9/C10, C9'/C10'*), 130.90 (CH, *C4, C4'*), 130.58 (C, *C3, C3'*), 129.66 (2CH, *C12, C12', C16, C16'*), 129.63 (C, *C9/C10, C9'/C10'*), 128.99 (CH, *C7, C7'*), 128.46 (2CH, *C13, C13', C15, C15'*), 127.67 (CH, *C14, C14'*), 126.93 (CH, *C5, C5'*), 124.27 (CH, *C8, C8'*), 112.39 (C, *C1, C1'*), 35.56 (CH_2, *C17, C17'*), 33.59 (CH_2, *C18, C18'*), 22.43 (CH_2, *C19, C19'*), 14.05 (CH_3, *C20, C20'*)

IR (neat) (cm^{-1}) 3517, 2955, 2925, 2856, 1604, 1496, 1457, 1428, 1369, 1235, 1178, 1136

HRMS (EI, 70 eV, *m/z*) Found $[M+H]^+$ 551.2953, $C_{40}H_{39}O_2^+$ requires 551.2950

(+/−)-6,6'-Dicarboxyl-3,3'-diphenyl-2,2'-dihydroxy-1,1'-binaphthyl (115)

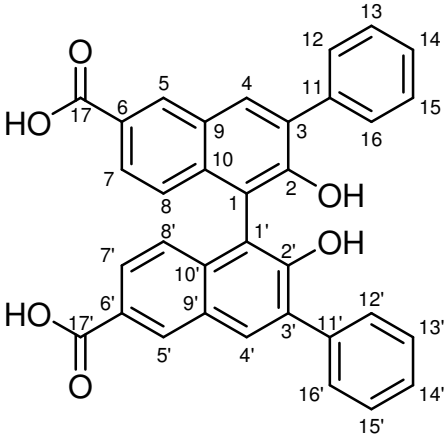

To a stirred mixture of (+/−)-6,6'-dicarboxyl-3,3'-diphenyl-2,2'-*bis*(methoxymethoxy)-1,1'-binaphthyl (**126**) (79 mg, 0.13 mmol) in THF (1 mL) at room temperature, was added concentrated hydrochloric acid (0.03 mL, 32%, 10.17 M). Reaction mixture was warmed to 50 °C and after 4 h allowed to cool to room temperature. Solvent was removed *via* rotary evaporation. Deionised water (1 mL) was added and product was extracted with DCM (3 x 1 mL) and the combined organic phase was washed with brine (1 mL), dried over anhydrous magnesium sulfate, filtered and solvent removed *via* rotary evaporation to yield crude product. Crude product was purified by column chromatography (SiO_2, ethyl acetate/ethanol 10:0.2) to yield title compound as a white solid in 77% yield (52 mg, 0.10 mmol).

Mpt = 254-255 °C

Molecular formula $C_{34}H_{22}O_6$

Molecular weight 526.53 $gmol^{-1}$

^{1}H NMR (400 MHz, $(CD_3)_2SO$) δ ppm 12.84 (s, 2H, *OH*), 8.85 (s, 2H, *OH*) 8.65 (s, 2H, *H5, H5'*), 8.18 (s, 2H, *H4, H4'*), 7.73 (d, *J* = 8.0 Hz, 2H, *H7, H7'*), 7.73 (d, *J*= 7.6 Hz, 4H, *H12, H12', H16, H16'*), 7.50 (dd, *J*= 7.6 Hz, 7.6 Hz, 4H, *H13, H13', H15, H15'*), 7.40 (t, *J*= 7.6 Hz, 2H, *H14, H14'*), 6.98 (d, *J*= 9.2 Hz, 2H, *H8, H8'*)

^{13}C NMR (100 MHz, $(CD_3)_2SO$) δ ppm 172.83 (C, *C17, C17'*), 158.95 (C, *C2, C2'*), 143.58 (C, *C11, C11'*), 141.02 (C, *C10, C10'*), 137.85 (C, *C3, C3'*), 136.92 (CH, *C4, C4'*), 136.36 (CH, *C5, C5'*), 134.88 (2CH, *C12, C12', C16, C16'*), 133.27 (2CH, *C13, C13', C15, C15'*), 132.94 (C, *C6/C9, C6'/C9'*), 132.45 (CH, *C14, C14'*), 130.99 (CH, *C7, C7'*), 130.39 (C, *C6/C9, C6'/C9'*), 129.23 (CH, *C8, C8'*), 119.79 (C, *C1, C1'*)

IR (neat) (cm^{-1}) 3436, 2923, 2532, 1678 (COOH), 1618, 1458, 1431, 1263, 1197, 1165, 1133, 1065, 1030

HRMS (EI, 70 eV, *m/z*) Found $[M+H]^+$ 527.1481, $C_{34}H_{23}O_6^+$ requires 527.1495

(+/−)-6,6'-*Bis*(2-(trimethylsilyl)ethynyl)-3,3'-diphenyl-2,2'-dihydroxy-1,1'-binaphthyl (116)

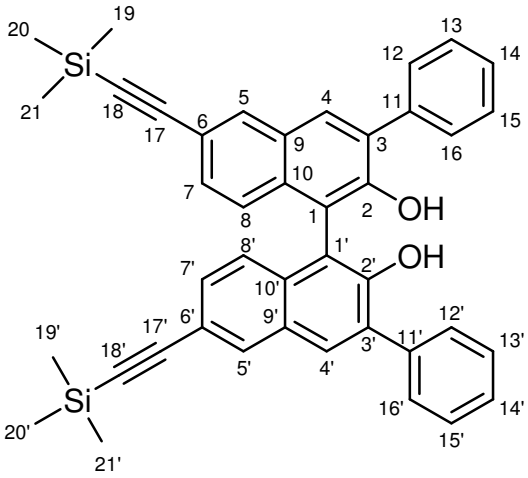

(+/−)-6,6'-Dibromo -3,3'-diphenyl- 2,2'-dihydroxy-1,1'-binaphthyl (**123**) (550 mg, 0.92 mmol) was dissolved in TMEDA (3 mL) under a nitrogen atmosphere and allowed to stir for 5 minutes. Sodium tetrachloropalladate (II) (54 mg, 0.19 mmol), 2-(di-*tert*-butylphosphino) -1-phenylindole (PIntB) (93 mg, 0.28 mmol) and copper (I) iodide (44 mg, 0.23 mmol) were added under nitrogen and the solution was warmed to 70 °C. Under a slow flow of nitrogen, ethynyltrimethylsilane (0.55 mL, 362 mg, 3.69 mmol) was added quickly and the reaction mixture was heated at 80 °C for 4 h. Dry THF (10 mL) was added and the reaction was allowed to reflux at 80 °C overnight. The reaction mixture was allowed cool to room temperature and concentrated *in vacuo*. Deionised water (10 mL) was added and the product was extracted with ethyl acetate (3 x 10 mL). The combined organic phase was washed with brine (10 mL), dried over anhydrous magnesium sulfate, filtered and the solvent was evaporated to yield crude product. Crude product was purified by column chromatography (SiO_2, hexane/ethyl acetate 10:0.3) to yield the title compound as a yellow solid in 60% yield (347 mg, 0.55 mmol).

Mpt = 215-216 °C

Molecular formula $C_{42}H_{38}O_2Si_2$

Molecular weight 630.92 $gmol^{-1}$

^{1}H NMR (400 MHz, $CDCl_3$) δ ppm 8.10 (d, *J*= 1.4 Hz, 2H, *H5, H5'*), 7.97 (s, 2H, *H4, H4'*), 7.73 (dd, *J*= 7.4 Hz, 1.2 Hz, 4H, *H12, H12', H16, H16'*), 7.53 (dd, *J*= 7.4 Hz, 1.2 Hz, 4H, *H13, H13', H15, H15'*), 7.45 (tt, *J*= 7.4 Hz, 1.2 Hz, 2H, *H14, H14'*), 7.38 (dd, *J*= 8.8 Hz, 1.4 Hz, 2H, *H7, H7'*), 7.14 (d, *J*= 8.8 Hz, 2H, *H8, H8'*), 5.45 (s, 2H, *OH*), 0.31 (s, 18H, *H19, H19', H20, H20', H21, H21'*)

^{13}C NMR (100 MHz, $CDCl_3$) δ ppm

150.77 (C, *C2, C2'*), 136.90 (C, *C11, C11'*), 132.47 (C, *C6/C9/C10, C6'/C9'/C10'*), 132.43 (CH, *C5, C5'*), 131.30 (C, *C3, C3'*), 131.14 (CH, *C4, C4'*), 130.06 (CH, *C7, C7'*), 129.48 (2CH, *C12, C12', C16, C16'*), 128.83 (C, *C6/C9/C10, C6'/C9'/C10'*), 128.61 (2CH, *C13, C13', C15, C15'*), 128.00 (CH, *C14, C14'*), 124.22 (CH, *C8, C8'*), 118.91 (C, *C6/C9/C10, C6'/C9'/C10'*), 112.44 (C, *C1, C1'*), 105.20 (C, *C17, C17'*), 94.45 (C, *C18, C18'*), 0.00 ($3CH_3$, *C19, C19', C20, C20', C21, C21'*)

IR (neat) (cm^{-1}) 3486, 3355, 2956, 2154, 1605, 1498, 1455, 1432, 1248, 1210, 1186, 1139, 1075

HRMS (EI, 70 eV, *m/z*) Found $[M+H]^+$ 631.2478, $C_{42}H_{39}O_2Si_2^+$ requires 631.2489

(+/−)-6,6'-Dipentynyl-3,3'-diphenyl-2,2'-dihydroxy-1,1'-binaphthyl (117)

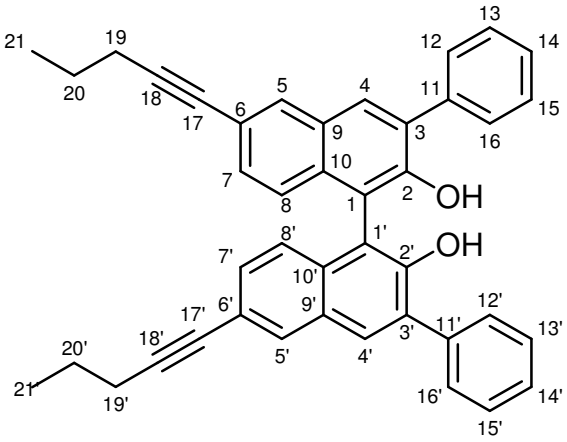

(+/−)-6,6'-Dibromo -3,3'-diphenyl -2,2'-dihydroxy-1,1'-binaphthyl (**123**) (751 mg, 1.26 mmol) was dissolved in TMEDA (5 mL) under a nitrogen atmosphere and allowed to stir for 5 minutes. Sodium tetrachloropalladate (II) (74 mg, 0.25 mmol), 2-(di-*tert*-butylphosphino)-1-phenylindole (PIntB) (127 mg, 0.38 mmol), copper (I) iodide (60 mg, 0.32

mmol) and 1-pentyne (0.75 mL, 515 mg, 7.56 mmol) were added. The reaction mixture was refluxed at 80 °C overnight, then allowed cool to room temperature and concentrated *in vacuo*. Deionised water (25 mL) was added and the product was extracted with ethyl acetate (3 x 25 mL). The combined organic phase was washed with brine (25 mL), dried over anhydrous magnesium sulfate, filtered and the solvent was evaporated to yield crude product. Crude product was purified by column chromatography (SiO_2, hexane/ethyl acetate 10:0.3) to yield the title compound as a yellow solid in 50 % yield (358 mg, 0.63 mmol).

Mpt = 119-121 °C

Molecular formula $C_{42}H_{34}O_2$

Molecular weight 570.72 $gmol^{-1}$

^{1}H NMR (400 MHz, $CDCl_3$) δ ppm 7.99 (d, *J*= 1.6 Hz, 2H, *H5, H5'*), 7.95 (s, 2H, *H4, H4'*), 7.72 (dd, *J*= 7.2 Hz, 1.6 Hz, 4H, *H12, H12', H16, H16'*), 7.51 (dd, *J*= 7.2 Hz, 1.6 Hz, 4H, *H13, H13', H15, H15'*), 7.43 (tt, *J*= 7.2 Hz, 1.6 Hz, 2H, *H14, H14'*), 7.32 (dd, *J*= 8.8 Hz, 1.6 Hz, 2H, *H7, H7'*), 7.13 (d, *J*= 8.8 Hz, 2H, *H8, H8'*), 5.40 (s, 2H, *OH*), 2.44 (t, *J*= 7.2 Hz, 4H, *H19, H19'*), 1.67 (qt, *J*= 7.2 Hz, *J*= 7.2 Hz, 4H, *H20, H20'*), 1.08 (t, *J*= 7.2 Hz, 6H, *H21, H21'*)

^{13}C NMR (100 MHz, $CDCl_3$) δ ppm150.45 (C, *C2, C2'*), 137.16 (C, *C11, C11'*), 132.02 (C, *C6/C9/C10, C6'/ C9'/C10'*), 131.53 (CH, *C5, C5'*), 131.18 (C, *C3, C3'*), 131.05 (CH, *C4, C4'*), 130.33 (CH, *C7, C7'*), 129.60 (2CH, *C12, C12', C16, C16'*), 129.12 (C, *C6/C9/C10, C6'/C9'/C10'*), 128.63 (2CH, *C13, C13', C15, C15'*), 127.99 (CH, *C14, C14'*), 124.26 (CH, *C8, C8'*), 119.98 (C, *C6/C9/C10, C6'/C9'/C10'*), 112.43 (C, *C1, C1'*), 90.63 (C, *C18, C18'*), 80.85 (C, *C17, C17'*), 22.30 (CH_2, *C20, C20'*), 21.55 (CH_2, *C19, C19'*) , 13.67 (CH_3, *C21, C21'*)

IR (neat) (cm^{-1}) 3506, 3050, 2960, 2930, 2188, 1601, 1495, 1455, 1425, 1365, 1232, 1162, 1133, 1070, 1030

HRMS (EI, 70 eV, *m/z*) Found $[M+H]^+$ 571.2646, $C_{42}H_{35}O_2^+$ requires 571.2637

(+/−)-6,6'-Dipentan-1-one-3,3'-diphenyl-2,2'-dihydroxy-1,1'-binaphthyl (118)

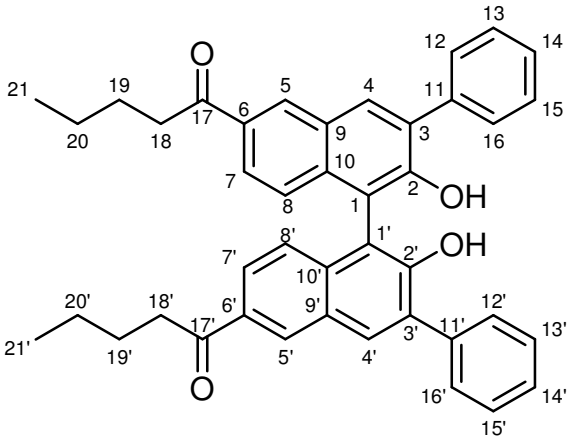

(+/−)-6,6'-Dipentynyl -3,3'-diphenyl-2,2'-dihydroxy-1,1'-binaphthyl (**117**) (358 mg, 0.63 mmol) was dissolved in ethanol (2.5 mL) and PTSA monohydrate (119 mg, 0.63 mmol) was added. Reaction mixture was refluxed at 80 °C for 36 h, allowed to cool to room temperature and volatiles were removed *via* rotary evaporation. Residual solid was dissolved in ethyl acetate (25 mL), washed with deionised water (10 mL), brine (10 mL), dried over anhydrous magnesium sulfate, filtered and volatiles were removed *via* rotary evaporation to yield the crude product. Crude product was purified by column chromatography (SiO_2, hexane/ethyl acetate 10:1) to yield the title compound as a yellow solid in 59% yield (225 mg, 0.37 mmol).

Mpt = 133-135 °C

Molecular formula $C_{42}H_{38}O_4$

Molecular weight 606.75 $gmol^{-1}$

^{1}H NMR (400 MHz, $CDCl_3$) δ ppm 8.51 (d, *J*= 1.6 Hz, 2H, *H5, H5'*), 8.12 (s, 2H, *H4, H4'*), 7.82 (dd, *J*= 8.8 Hz, 1.6 Hz, 2H, *H7, H7'*), 7.73 (dd, *J*= 7.2 Hz, 1.4 Hz, 4H, *H12, H12', H16, H16'*), 7.51 (dd, *J*= 7.2 Hz, 1.4 Hz, 4H, *H13, H13', H15, H15'*), 7.44 (tt, *J*= 7.2 Hz, 1.4 Hz, 2H, *H14, H14'*), 7.21 (d, *J*= 8.8 Hz, 2H, *H8, H8'*) 5.84 (s, 2H, *OH*), 3.01 (t, *J*= 7.4 Hz, 4H, *H18, H18'*), 1.72 (tt, *J*= 7.4 Hz, 7.4 Hz, 4H, *H19, H19'*), 1.41 (qt, *J*= 7.4 Hz, 7.4 Hz, 4H, *H20, H20'*), 0.95 (t, *J*= 7.4 Hz, 6H, *H21, H21'*)

^{13}C NMR (100 MHz, $CDCl_3$) δ ppm 200.17 (CO, *C17, C17'*), 152.20 (C, *C2, C2'*), 136.62 (C, *C11, C11'*), 135.42 (C, *C10, C10'*), 133.01 (C, *C6/C9, C6'/C9'*), 132.97 (CH, *C4, C4'*), 131.69 (C, *C3, C3'*), 130.24 (CH, *C5, C5'*), 129.53 (2CH, *C12, C12', C16, C16'*), 128.80 (2CH, *C13, C13', C15, C15'*), 128.47 (C, *C6/C9, C6'/C9'*), 128.27 (CH, *C14, C14'*), 125.64 (CH, *C7, C7'*), 124.60 (CH, *C8, C8'*), 112.73 (C, *C1, C1'*), 38.36

(CH_2, *C18, C18'*), 26.72 (CH_2, *C19, C19'*), 22.55 (CH_2, *C20, C20'*), 13.99 (CH_3, *C21, C21'*)

IR (neat) (cm^{-1}) 3313, 2956, 2925, 2865, 1664 (C=O), 1614, 1456, 1428, 1374, 1325, 1153

HRMS (EI, 70 eV, *m/z*) Found $[M+H]^+$ 607.2858, $C_{42}H_{39}O_4^+$ requires 607.2848

(+/–)-2,2'-*Bis*(methoxymethoxy)-1,1'-binaphthyl (119)

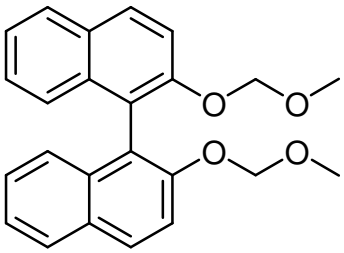

To a stirred solution of sodium hydride (2.680 g, 60% in mineral oil, 66.88 mmol) in dry THF (100 mL) at 0 °C under a nitrogen atmosphere was added dropwise a solution containing (+/–)-1,1'-bi-2-naphthol (**45**) (6.000 g, 20.95 mmol) in dry THF (50 mL). After stirring at 0 °C for 1 h, chloromethyl methyl ether (3.49 mL, 3.700 g, 45.96 mmol) was added dropwise. Upon complete addition, the reaction mixture was allowed to warm up to room temperature and stirred for 4 h. Saturated aqueous ammonium chloride (30 mL) was added slowly to quench the reaction and volatiles removed *in vacuo*. Residue was extracted with DCM (3 x 30 mL) and the combined organic phase was washed with brine (30 mL), dried over anhydrous magnesium sulfate, filtered and solvent removed *via* rotary evaporation to yield the crude product. Crude product was purified by column chromatography (SiO_2, using a gradient solvent system of hexane, hexane/ethyl acetate 10:0.5) to yield the title compound as a white solid in 80% yield (6.290 g, 16.80 mmol).

Mpt = 82-84 °C, **Lit Mpt** = 89-92 ºC[11]

Molecular formula $C_{24}H_{22}O_4$

Molecular weight 374.43 $gmol^{-1}$

^{1}H NMR (400 MHz, $CDCl_3$) δ ppm 7.97 (d, *J*= 9.2 Hz, 2H), 7.89 (d, *J*= 8.2 Hz, 2H), 7.60 (d, *J*= 9.2 Hz, 2H), 7.38-7.34 (m, 2H), 7.26-7.22 (m, 2H), 7.18 (d, *J*= 8.2 Hz, 2H), 5.10 (d, J_{AB}= 6.6 Hz, 2H), 4.99 (d, J_{AB}= 6.6 Hz, 2H), 3.16 (s, 6H)

^{13}C NMR (100 MHz, $CDCl_3$) δ ppm 152.65 (C), 134.03 (C), 129.89 (C), 129.42 (CH), 127.90 (CH), 126.33 (CH), 125.57 (CH), 124.10 (CH), 121.30 (C), 117.29 (CH), 95.20 (CH_2), 55.86 (CH_3)

^{1}H and ^{13}C NMR data in agreement with the literature.[10,11]

(+/−)-3,3'-Dibromo-2,2'-*bis*(methoxymethoxy)-1,1'-binaphthyl (120)

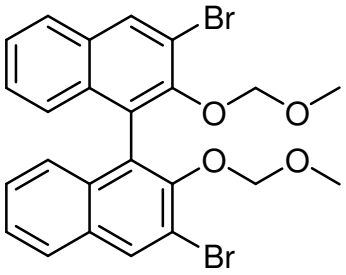

To a stirred solution of (+/−)-2,2'-*bis*(methoxymethoxy)-1,1'-binaphthyl (**119**) (5.276 g, 14.11 mmol) in dry diethyl ether (220 mL) at room temperature under a nitrogen atmosphere was added dropwise *n*-butyllithium (1.6 M in hexanes, 26.50 mL, 42.32 mmol). After stirring at room temperature for 3 h, THF (100 mL) was added. After 1 h, reaction mixture was cooled to 0 °C and dibromotetrachloroethane (13.780 g, 42.32 mmol) was added in one portion. Reaction mixture was allowed to reach room temperature over 2 h. Saturated aqueous ammonium chloride (60 mL) was added to quench the reaction and phases separated. Aqueous layer was extracted with diethyl ether (3 x 60 mL) and the combined organic phase was washed with brine (60 mL), dried over anhydrous magnesium sulfate, filtered and solvent removed *via* rotary evaporation to yield the crude product. Crude product was purified by column chromatography (SiO_2, hexane/ethyl acetate 10:0.3) to yield the title compound as a white solid in 86% yield (6.459 g, 12.14 mmol).

Mpt = 118-120 °C, **Lit Mpt** = 125-126 °C[11]

Molecular formula $C_{24}H_{20}Br_2O_4$

Molecular weight 532.22 $gmol^{-1}$

^{1}H NMR (400 MHz, $CDCl_3$) δ ppm 8.28 (s, 2H), 7.81 (d, *J*= 8.4 Hz, 2H), 7.47-7.43 (m, 2H), 7.33-7.29 (m, 2H), 7.19 (d, *J*= 8.4 Hz, 2H), 4.84 (d, J_{AB}= 5.6 Hz, 2H), 4.82 (d, J_{AB}= 5.6 Hz, 2H), 2.57 (s, 6H)

^{13}C NMR (100 MHz, $CDCl_3$) δ ppm 150.14 (C), 133.09 (C), 133.03 (CH), 131.50 (C), 127.41 (C), 126.93 (2CH), 126.58 (CH), 126.09 (CH), 117.37 (C), 99.18 (CH_2), 56.31 (CH_3)

^{1}H and ^{13}C NMR data in agreement with the literature.[10,11]

(+/−)-3,3'-Diphenyl-2,2'-*bis*(methoxymethoxy)-1,1'-binaphthyl (121)

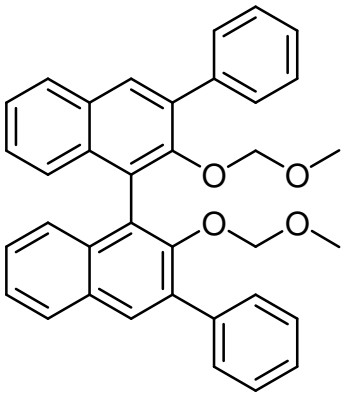

(+/−)-3,3'-Dibromo-2,2' -*bis*(methoxymethoxy)- 1,1'-binaphthyl (**120**) (300 mg, 0.56 mmol) and *tetrakis*(triphenylphosphine)palladium(0) (60 mg, 0.06 mmol) were added to dry DME (3.70 ml) at room temperature under a nitrogen atmosphere. To the stirred mixture was added phenylboronic acid (240 mg, 1.96 mmol) and 2 M aqueous sodium carbonate (1.5 mL). Reaction mixture was refluxed for 18 h, allowed cool to room temperature and filtered through a pad of celite. Solvent was removed *via* rotary evaporation to give a crude residue. Residue was dissolved in DCM (15 mL), washed with saturated aqueous ammonium chloride (15 mL), deionised water (15 mL), brine (15 mL), dried over anhydrous magnesium sulfate, filtered and solvent removed *via* rotary evaporation to yield crude product. Crude product was purified by column chromatography (SiO_2, hexane/ethyl acetate 10:1) to yield the title compound as a white solid in 72% yield (212 mg, 0.40 mmol).

Mpt = 119-121 °C

Molecular formula $C_{36}H_{30}O_4$

Molecular weight 526.62 $gmol^{-1}$

^{1}H NMR (400 MHz, $CDCl_3$) δ ppm 7.99 (s, 2H), 7.93 (d, *J*= 8.2 Hz, 2H), 7.80 (d, *J*= 8.2 Hz, 4H), 7.52-7.49 (m, 4H), 7.47-7.39 (m, 4H), 7.36-7.30 (m, 4H), 4.45 (d, J_{AB}= 6 Hz, 2H), 4.41 (d, J_{AB}= 6 Hz, 2H), 2.38 (s, 6H)

^{13}C NMR (100 MHz, $CDCl_3$) δ ppm 151.36 (C), 139.07 (C), 135.50 (C), 133.64 (C),

130.87 (C), 130.60 (CH), 129.67 (2CH), 128.36 (2CH), 127.89 (CH), 127.33 (CH), 126.55 (C), 126.46 (CH), 126.34 (CH), 125.21 (CH), 98.66 (CH_2), 55.87 (CH_3)

^{1}H and ^{13}C NMR data in agreement with the literature.[10,11]

(+/−)-3,3'-Diphenyl-2,2'-dihydroxy-1,1'-binaphthyl (122)

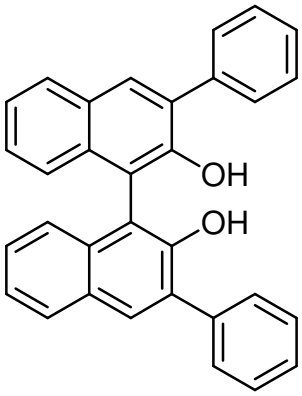

To a stirred mixture of (+/−)-3,3'-diphenyl-2,2'-*bis*(methoxymethoxy)-1,1'-binaphthyl (212 mg, 0.40 mmol) (**121**) in THF (2 mL) at room temperature, was added concentrated hydrochloric acid (0.06 mL, 32%, 10.17 M). Reaction mixture was warmed to 50 °C and after 4 h allowed cool to room temperature. Solvent was removed *via* rotary evaporation. Deionised water (2 mL) was added and product was extracted with DCM (3 x 2 mL). The combined organic phase was washed with brine (2 mL), dried over anhydrous magnesium sulfate, filtered and solvent removed *via* rotary evaporation to yield the crude product. Crude product was purified by column chromatography (SiO_2, hexane/ ethyl acetate 10:1) to yield the title compound as a white solid in 68% yield (119 mg, 0.27 mmol).

Mpt = 204-205 °C, **Lit Mpt** = 209-210 ºC[11]

Molecular formula $C_{32}H_{22}O_2$

Molecular weight 438.52 $gmol^{-1}$

^{1}H NMR (400 MHz, $CDCl_3$) δ ppm 8.05 (s, 2H), 7.95 (d, *J*= 8.2 Hz, 2H), 7.76 (d, *J*= 7.0 Hz, 4H), 7.52 (t, *J*= 7.0 Hz, 4H), 7.45-7.39 (m, 4H), 7.36-7.32 (m, 2H), 7.26 (d, *J*= 8.2 Hz, 2H), 5.40 (s, 2H)

^{13}C NMR (100 MHz, $CDCl_3$) δ ppm 150.18 (C), 137.50 (C), 132.99 (C), 131.45 (CH), 130.71 (C), 129.65 (2CH), 129.48 (C), 128.54 (2CH), 128.50 (CH), 127.82 (CH), 127.40 (CH), 124.38 (CH), 124.33 (CH), 112.43 (C)

^{1}H and ^{13}C NMR data in agreement with the literature.[10,11]

(+/−)-6,6'-Dibromo-3,3'-diphenyl-2,2'-dihydroxy-1,1'-binaphthyl (123)

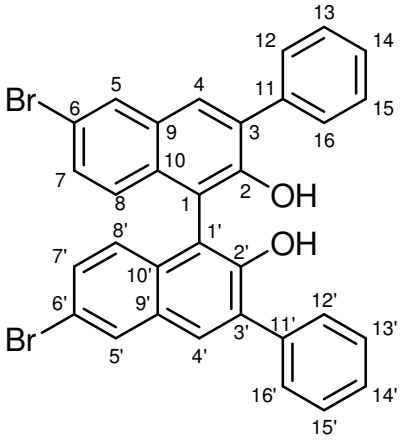

To a stirred solution of (+/−)-3,3'-diphenyl-2,2'-dihydroxy-1,1'-binaphthyl (**122**) (1.320 g, 3.01 mmol) in DCM (46 mL) at −78 °C under a nitrogen atmosphere was added slowly a solution of bromine (598 μL, 1.867 g, 11.68 mmol) in DCM (8 mL) over a period of 60 minutes. Reaction mixture was allowed to reach room temperature over 2 h, then allowed to stir at room temperature for 2 h. The reaction was quenched with 10% sodium bisulfite (40 mL). Product was extracted with DCM (3 x 50 mL) and the combined organic extracts were washed with brine (30 mL), dried over anhydrous magnesium sulfate, filtered and solvent was removed *via* rotary evaporation to yield crude product. Crude product was purified by recrystallisation from hexane/DCM at room temperature and filtered to yield the title compound as a light yellow solid in 69% yield (1.238 g, 2.08 mmol).

Mpt = 207-208 °C

Molecular formula $C_{32}H_{20}Br_2O_2$

Molecular weight 596.31 $gmol^{-1}$

^{1}H NMR (400 MHz, $CDCl_3$) δ ppm 8.07 (d, *J*= 2.0 Hz, 2H, *H5, H5'*), 7.91 (s, 2H, *H4, H4'*), 7.69 (dd, *J*= 7.6 Hz, 1.2 Hz, 4H, *H12, H12', H16, H16'*), 7.51 (dd, *J*= 7.6 Hz, 1.2 Hz, 4H, *H13, H13', H15, H15'*), 7.44 (tt, *J*= 7.6 Hz, 1.2 Hz, 2H, *H14, H14'*), 7.38 (dd, *J*= 9.0 Hz, 2.0 Hz, 2H, *H7, H7'*), 7.06 (d, *J*= 9.0 Hz, 2H, *H8, H8'*), 5.39 (s, 2H, *OH*)

^{13}C NMR (100 MHz, $CDCl_3$) δ ppm 150.26 (C), 136.73 (C), 131.85 (C), 131.48 (C), 130.64 (CH, *C7, C7'*), 130.53 (C), 130.41 (CH, *C4/C5, C4'/C5'*), 130.37 (CH, *C4/C5, C4'/C5'*), 129.54 (2CH, *C12, C12', C16, C16'*), 128.78 (2CH, *C13, C13', C15, C15'*), 128.25 (CH, *C14, C14'*), 126.08 (CH, *C8, C8'*), 118.18 (C), 112.63 (C)

^{1}H and ^{13}C NMR data in agreement with the literature.[10,11]

(+/–)-6,6'-Dibromo-3,3'-diphenyl-2,2'-*bis*(methoxymethoxy)-1,1'-binaphthyl (125)

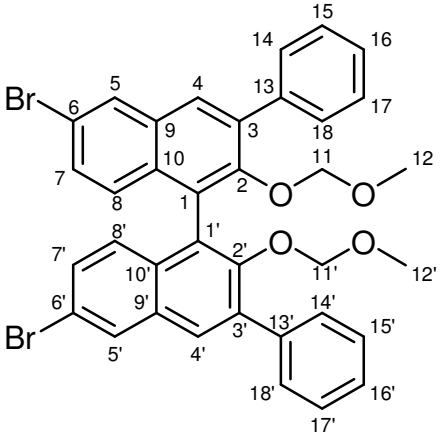

To a stirred solution of sodium hydride (230 mg, 60% in mineral oil, 5.80 mmol) in dry THF (10 mL) at 0 °C under a nitrogen atmosphere was added dropwise a solution of (+/–)-6,6'-dibromo-3,3'-diphenyl-2,2'-dihydroxy-1,1'-binaphthyl (**123**) (1.24 g, 1.93 mmol) in dry THF (4 mL). After stirring at 0 °C for 1 h, chloromethyl methyl ether (0.44 mL, 0.467 g, 5.80 mmol) was added dropwise. Upon complete addition, the reaction mixture was allowed to warm up to room temperature and stirred for 4 h. Saturated aqueous ammonium chloride (10 mL) was added slowly to quench the reaction and volatiles removed *in vacuo*. Residue was extracted with DCM (3 x 10 mL) and the combined organic phase was washed with brine (10 mL), dried over anhydrous magnesium sulfate, filtered and solvent removed *via* rotary evaporation to yield the crude product. Crude product was purified by column chromatography (SiO_2, hexane/ethyl acetate 10:0.3) to yield the title compound as a white solid in 68% yield (0.894 g, 1.31 mmol).

Mpt = 66-68 °C

Molecular formula $C_{36}H_{28}Br_2O_4$

Molecular weight 684.41 $gmol^{-1}$

^{1}H NMR (400 MHz, $CDCl_3$) δ ppm 8.06 (d, *J*= 2.0 Hz, 2H, *H5, H5'*), 7.87 (s, 2H, *H4, H4'*), 7.73 (dd, *J*= 7.2 Hz, 1.6 Hz, 4H, *H14, H14', H18, H18'*), 7.49 (dd, *J*= 7.2 Hz, 1.6 Hz, 4H, *H15, H15', H17, H17'*), 7.40 (tt, *J*= 7.2 Hz, 1.6 Hz, 2H, *H16, H16'*), 7.37 (dd, *J*= 9.0 Hz, 2.0 Hz, 2H, *H7, H7'*), 7.14 (d, *J*= 9.0 Hz, 2H, *H8, H8'*), 4.38 (s, 4H, *H11, H11'*), 2.34 (s, 6H, *H12, H12'*)

^{13}C NMR (100 MHz, $(CD_3)_2CO$) δ ppm

152.84 (C, *C2, C2'*), 139.38 (C, *C13, C13'*), 137.69 (C, *C3, C3'*), 133.09 (C, *C6/C10, C6'/C10'*), 132.85 (C, *C6/C10, C6'/C10'*), 130.88 (CH, *C4/C5, C4'/C5'*), 130.80, (CH,

C4/C5, C4'/C5') 130.41, (CH, *C7, C7'*), 130.34 (2CH, *C14, C14', C18, C18'),* 129.39 (2CH, *C15, C15', C17, C17'*), 129.20 (CH, *C16, C16'*), 128.59 (CH, *C8, C8'*), 127.22 (C, *C9, C9'*), 119.66 (C, *C1, C1'*), 99.21 (CH_2, *C11, C11'*), 56.06 (CH_3, *C12, C12'*)

IR (neat) (cm^{-1}) 2924, 2823, 1600, 1584, 1480, 1422, 1350, 1180, 1155, 1140

HRMS (EI, 70 eV, *m/z*) Found $[M+NH_4]^+$ 700.0720, $C_{36}H_{32}NO_4Br_2^+$ requires 700.0698

(+/−)-6,6'-Dicarboxyl-3,3'-diphenyl-2,2'-*bis*(methoxymethoxy)-1,1'-binaphthyl (126)

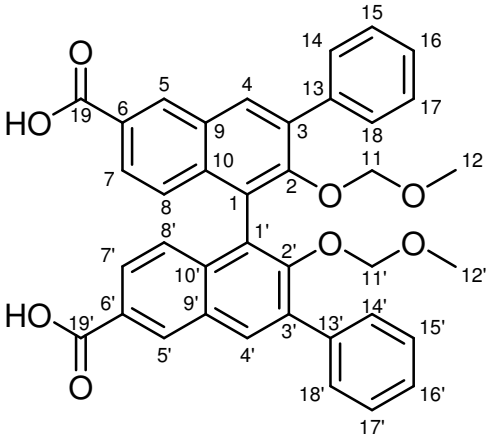

To a stirred solution of (+/−)-6,6'-dibromo-3,3'-diphenyl -2,2'-*bis*(methoxymethoxy)- 1,1'-binaphthyl (**125**) (200 mg, 0.29 mmol) in dry diethyl ether (7 mL) at room temperature under a nitrogen atmosphere was added dropwise *n*-butyllithium (1.6M in hexanes, 0.73 mL, 1.17 mmol). After stirring for 2 h at room temperature, pellets of dry ice were added to the reaction mixture at 0 °C and the reaction mixture was left to stir for 2 h. Reaction was quenched by the addition of deionised water (5 mL) and phases separated. Aqueous layer was washed with diethyl ether (3 x 50 mL) and then was acidified to pH 2 with 5% aqueous HCl. Acidified aqueous layer was extracted with ethyl acetate (3 x 50 mL) and the combined organic phase was washed with brine (20 mL), dried over anhydrous magnesium sulphate, filtered and volatiles removed to yield crude product. Crude product was purified by column chromatography (SiO_2, ethyl acetate) to yield the product as a pale yellow solid in 44 % yield (79 mg, 0.13 mmol).

Mpt = 207-209 °C

Molecular formula $C_{38}H_{30}O_8$

Molecular weight 614.64 $gmol^{-1}$

^{1}H NMR (400 MHz, $(CD_3)_2SO$) δ ppm 13.13 (s, 2H, *OH*), 8.75 (s, 2H, *H5, H5'*), 8.34

(s, 2H, *H4, H4'*), 7.84 (dd, *J* = 8.8 Hz, 1.0 Hz, 2H, *H7, H7'*), 7.73 (d, *J* = 7.4 Hz, 4H, *H14, H14', H18, H18'*), 7.54 (dd, *J* = 7.4 Hz, 7.4 Hz, 4H, *H15, H15', H17, H17'*), 7.45 (t, *J*= 7.4 Hz, 2H, *H16, H16'*), 7.23 (d, *J*= 8.8 Hz, 2H, *H8, H8'*), 4.35 (d, J_{AB}= 5.6 Hz, 2H, *H11/H11'*), 4.29 (d, J_{AB}= 5.6 Hz, 2H, *H11/H11'*), 2.25 (s, 6H, *H12, H12'*)

^{13}C NMR (100 MHz, $CDCl_3$) δ ppm 172.16 (CO, *C19, C19'*), 154.06 (C, *C2, C2'*), 138.23 (C, *C11, C11'*), 136.47 (C, *C3, C3'*), 136.14 (C, *C6/C9/C10*, *C6'/C9'/C10'*), 132.43 (CH, *C4, C*4'), 132.18 (CH, *C5, C5'*), 129.91 (C, *C6/C9/C10*, *C6'/C9'/C10'*), 129.54 (2CH, *C14, C14', C18, C18'*), 128.60 (2CH, *C15, C15', C17, C17'*), 127.80 (CH, *C16, C16'*), 126.71 (CH, *C8, C8'*), 126.32 (C, *C6/C9/C10*, *C6'/C9'/C10'*), 126.14 (C, *C1, C1'*), 126.04 (CH, *C7, C7'*), 98.73 (CH_2, *C11, C11'*), 55.96 (CH_3, *C12, C12'*)

IR (neat) (cm^{-1}) 2923, 2852, 2532, 1679 (COOH), 1619, 1496, 1456, 1427, 1261, 1241, 1179, 1137

HRMS (EI, 70 eV, *m/z*) Found $[M+NH_4]^+$ 632.2310, $C_{38}H_{34}NO_8^+$ requires 632.2284

(+/–)-6,6'-Dibutyl-3,3'-diphenyl-2,2'-*bis*(methoxymethoxy)-1,1'-binaphthyl (127)

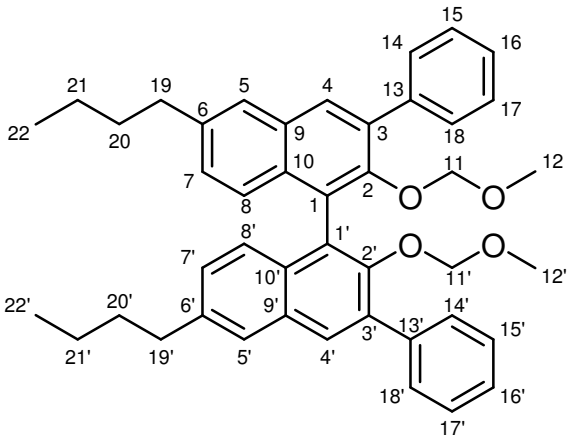

To a stirred solution of (+/–)-6,6'-dibromo -3,3'-diphenyl-2,2'-*bis*(methoxymethoxy)-1,1'-binaphthyl (**125**) (300 mg, 0.44 mmol) in THF (6 mL) was added (1,3-dppp)$NiCl_2$ (24 mg, 0.044 mmol) under a nitrogen atmosphere. Reaction mixture was allowed to stir for 10 minutes. 2 M Butylmagnesium chloride in THF (2.26 mL, 528 mg, 4.52 mmol) was added dropwise and the reaction mixture was refluxed at 60 °C for 24 h. The reaction mixture was allowed cool to room temperature and quenched with 1 M HCL (8 mL). Volatiles were removed *in vacuo*. Residue was dissolved in DCM (10 mL), washed with deionised water (5 mL), brine (5 mL), dried over anhydrous magnesium sulfate, filtered and solvent

removed *via* rotary evaporation to yield crude product. Crude product was purified by column chromatography (SiO_2, hexane/ethyl acetate 5:1) to yield the title compound as a greasy solid in 35% yield (97 mg, 0.15 mmol).

Mpt = 56-58 °C

Molecular formula $C_{44}H_{46}O_4$

Molecular weight 638.83 $gmol^{-1}$

^{1}H NMR (400 MHz, $CDCl_3$) δ ppm 7.79 (s, 2H, *H4, H4'*), 7.67 (d, *J*= 7.2 Hz, 4H, *H14, H14', H18, H18'*), 7.57 (s, 2H, *H5, H5'*), 7.38 (dd, *J*= 7.2 Hz, 7.2 Hz, 4H, *H15, H15', H17, H17'*) 7.28 (t, *J*= 7.2 Hz, 2H, *H16, H16'*), 7.15 (d, *J*= 8.6 Hz, 2H, *H8, H8'*), 7.06 (dd, *J*= 8.6 Hz 1.6 Hz, 2H, *H7, H7'*), 4.32 (d, J_{ab} = 5.8 Hz, 2H, *H11, H11'*), 4.28 (d, J_{ab} = 5.8 Hz, 2H, *H11, H11'*), 2.65 (t, *J*= 7.6 Hz, 4H, *H19, H19'*), 2.27 (s, 6H, *H12, H12'*), 1.59 (tt, *J*= 7.6 Hz, 7.6 Hz, 4H, *H20, H20'*), 1.30 (qt, *J*= 7.6 Hz, 7.6 Hz, 4H, *H21, H21'*), 0.86 (t, *J*= 7.6 Hz, 6H, *H22, H22'*)

^{13}C NMR (100 MHz, $CDCl_3$) δ ppm

150.56 (C, *C2, C2'*), 139.70 (C, *C6, C6'*), 139.28 (C, *C13, C13'*), 135.39 (C, *C3, C3'*), 132.08 (C, *C9/C10, C9'/C10'*), 131.05 (C, *C9/C10, C9'/C10'*), 130.02 (CH, *C4, C4'*), 129.68 (2CH, *C14, C14', C18, C18'*), 128.31 (2CH, *C15, C15', C17, C17'*), 127.99 (CH, *C16, C16'*), 127.20 (CH, *C7, C7'*), 126.50 (C, *C1, C1'*), 126.37 (CH, *C8, C8'*), 126.21 (CH, *C5, C5'*), 98.51 (CH_2, *C11, C11'*), 55.87 (CH_3, *C12, C12'*), 35.61 (CH_2, *C19, C19'*), 33.41 (CH_2, *C20, C20'*), 22.47 (CH_2, *C21, C21'*), 14.04 (CH_3, *C22, C22'*)

IR (neat) (cm^{-1}) 2954, 2925, 2869, 1602, 1493, 1454, 1425, 1186, 1156, 1142, 1077, 1005

HRMS (EI, 70 eV, *m/z*) Found $[M+NH_4]^+$ 656.3715, $C_{44}H_{50}NO_4^+$ requires 656.3740

7.6 Preparation of chiral polysubstituted BINOL derivatives and prolinol hydrochloride salts

(*S*)-α,α-Diphenyl-2-pyrrolidinemethanol hydrochloride salt (95)

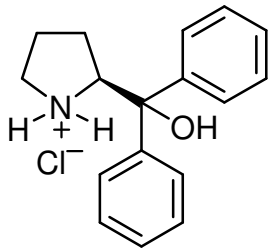

To a stirred solution of (*S*)-α,α-diphenyl-2-pyrrolidinemethanol (**41a**) (79 mg, 0.31 mmol) in diethyl ether (1 mL) at room temperature was added dropwise 1M HCl in diethyl ether (932 µL, 0.93 mmol). Reaction mixture was allowed to stir for 4 h, product was filtered and washed with diethyl ether (3 × 4 mL) to yield the title compound as a white solid in 83% yield (75 mg, 0.26 mmol).

Mpt = >270 °C

$[\alpha]^{20}_{D}$= +71.0 ° (0.1 c, MeOH)

Molecular formula $C_{17}H_{20}ClNO$

Molecular weight 289.80 $gmol^{-1}$

^{1}H NMR (400 MHz, $(CD_3)_2SO$) δ ppm 9.27 (s, *NH*, 1H), 8.17 (s, *NH,* 1H), 7.62 (d, *J*= 7.6 Hz, 2H), 7.53 (d, *J*= 7.6 Hz, 2H), 7.37-7.31 (m, 4H), 7.27-20 (m, 2H), 6.57 (s, *OH*, 1H), 4.88 (m, 1H), 3.13 (m, 2H), 1.92-1.79 (m, 4H)

^{13}C NMR (100 MHz, $(CD_3)_2SO$) δ ppm 145.04 (C), 144.61 (C), 128.35 (2CH), 128.18 (2CH), 127.14 (CH), 126.89 (CH), 125.83 (2CH), 125.36 (2CH), 77.08 (C), 64.92 (CH), 46.66 (CH_2), 25.98 (CH_2), 24.04 (CH_2)

IR (neat) (cm^{-1}) 3346, 2909, 2827, 2723, 1603, 1586, 1492, 1449, 1387, 1362, 1216, 1178, 1067, 1032

HRMS (EI, 70 eV, *m/z*) Found $[M]^+$ 254.1546, $C_{17}H_{20}NO^+$ requires 254.1545

(*S*)-α,α-*Bis*(3,5-dimethyl-phenyl)-2-pyrrolidinemethanol hydrochloride salt (96)

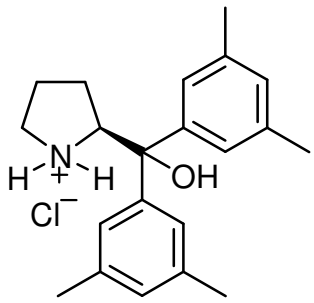

To a stirred solution of (*S*)-α,α-*bis*(3,5-dimethyl-phenyl)-2-pyrrolidinemethanol (**101**) (95 mg, 0.31 mmol) in diethyl ether (1 mL) at room temperature was added dropwise 1M HCl in diethyl ether (932 μL, 0.93 mmol). Reaction mixture was allowed to stir for 4 h, product was filtered and washed with diethyl ether (3 × 4 mL) to yield the title compound as a white solid in 89% yield (94 mg, 0.27 mmol).

Mpt = >270 °C

$[\alpha]^{20}_D$= +86.0 ° (0.1 c, MeOH)

Molecular formula $C_{21}H_{28}ClNO$

Molecular weight 345.906 $gmol^{-1}$

^{1}H NMR (400 MHz, $(CD_3)_2SO$) δ ppm 9.76 (s, *NH*, 1H), 8.21 (s, *NH*, 1H), 7.25 (s, 2H), 7.09 (s, 2H), 6.86 (s, 1H), 6.82 (s, 1H), 6.31 (s, *OH*, 1H), 4.79-4.74 (m, 1H), 3.14-3.06 (m, 2H), 2.26 (s, 6H), 2.23 (s, 6H), 1.88-1.69 (m, 4H)

^{13}C NMR (100 MHz, $(CD_3)_2SO$) δ ppm 145.00 (C), 144.51 (C), 137.20 (2C), 137.03 (2C), 128.47 (CH), 128.22 (CH), 123.60 (2CH), 123.00 (2CH), 76.89 (C), 64.90 (CH), 46.63 (CH_2), 26.01 (CH_2), 24.11 (CH_2), 21.14 ($2CH_3$), 21.10 ($2CH_3$)

IR (neat) (cm^{-1}) 3225, 2978, 2948, 2920, 1606, 1597, 1552, 1454, 1407, 1305, 1294, 1181, 1149, 1104, 1032

HRMS (EI, 70 eV, *m/z*) Found $[M]^+$ 310.2185, $C_{21}H_{28}NO^+$ requires 310.2171

(+)-6,6'-Dimethoxy-3,3'-diphenyl-2,2'-dihydroxy-1,1'-binaphthyl (111b)

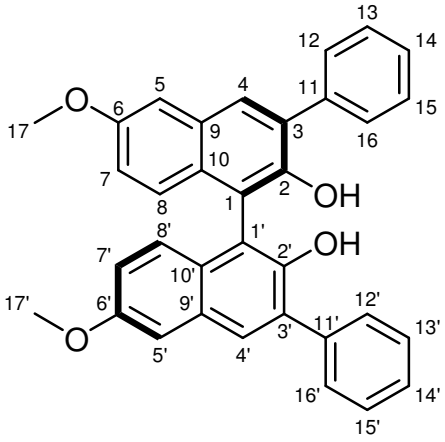

(+)-6,6'-Dibromo- 3,3'-diphenyl -2,2'-dihydroxy-1,1'-binaphthyl (**123b**) (789 mg, 1.32 mmol) and copper (I) iodide (1.04 g, 5.48 mmol) were stirred in dry DMF (6 mL) at room temperature under nitrogen for 10 minutes. 4.4 M Sodium methoxide in methanol (8.00 mL, 34.42 mmol) was added and the reaction mixture was refluxed for 24 h, then allowed cool to room temperature. Ice-water mixture (18 mL) was added, followed by 4N HCl (6 mL) and mixture was allowed to stir for 10 minutes. Mixture was filtered and remaining solid was washed with ethyl acetate. Filtrate was extracted with ethyl acetate (3 x 30 mL) and the combined organic phase was washed with brine (30 mL), dried over anhydrous magnesium sulfate, filtered and volatiles removed *via* rotary evaporation to yield the crude product. Crude product was purified by column chromatography (SiO_2, hexane/ethyl acetate 10:1) to yield the title compound as a yellow solid in 67% yield (442 mg, 0.89 mmol).

Mpt = 208-210 °C

$[\alpha]^{20}_D$ = +68.1 ° (1.0 c, THF)

Molecular formula $C_{34}H_{26}O_4$

Molecular weight 498.57 $gmol^{-1}$

^{1}H NMR (400 MHz, $CDCl_3$) δ ppm 7.92 (s, 2H, *H4, H4'*), 7.74 (dd, *J*= 7.2 Hz, 1.4 Hz, 4H, *H12, H12', H16, H16'*), 7.50 (dd, *J*= 7.2 Hz, 1.4 Hz, 4H, *H13, H13', H15, H15'*), 7.42 (tt, *J*= 7.2 Hz, 1.4 Hz, 2H, *H14, H14'*), 7.25 (d, *J*= 2.6 Hz, 2H, *H5, H5'*), 7.15 (d, *J*= 9.2 Hz, 2H, *H8, H8'*), 7.01 (dd, *J*= 9.2 Hz, 2.6 Hz, 2H, *H7, H7'*), 5.26 (s, 2H, *OH*), 3.92 (s, 6H, *H17, H17'*)

^{13}C NMR (100 MHz, $CDCl_3$) δ ppm

156.59 (C, *C6, C6'*), 148.36 (C, *C2, C2'*), 137.67 (C, *C11, C11'*), 131.06 (C, *C3, C3'*),

130.36 (C, *C9/C10, C9'/C10'*), 130.09 (CH, *C4, C4'*), 129.62 (2CH, *C12, C12', C16 C16'*), 128.49 (2CH, *C13, C13',C15, C15'*), 128.23 (C, *C9/C10, C9'/C10'*), 127.74 (CH, *C14, C14'*), 125.96 (CH, *C8, C8'*), 119.85 (CH, *C7, C7'*), 112.90 (C, *C1, C1'*), 106.71 (CH, *C5, C5'*), 55.42 (CH_3, *C17, C17'*)

IR (neat) (cm^{-1}) 3506, 2954, 2926, 2869, 1600, 1502, 1460, 1422, 1401, 1371, 1224, 1196, 1169, 1123, 1029

HRMS (EI, 70 eV, *m/z*) Found $[M+H]^+$ 499.1915, $C_{34}H_{27}O_4^+$ requires 499.1909

(+)-6,6'-Dibutyl-3,3'-diphenyl-2,2'-dihydroxy-1,1'-binaphthyl (114b)

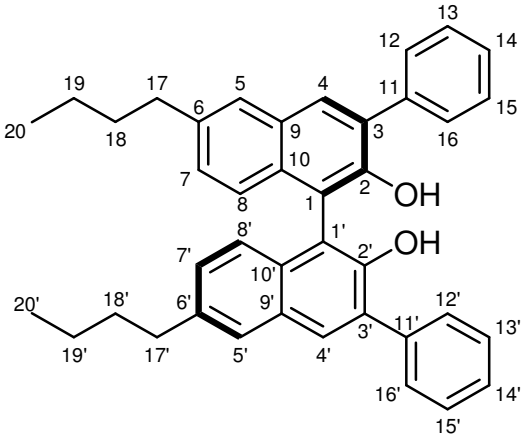

To a stirred solution of (−)-6,6'-dibromo-3,3'-diphenyl -2,2'-*bis*(methoxymethoxy)-1,1'-binaphthyl (**125b**) (444 mg, 0.65 mmol) in THF (20 mL) was added (1,3-dppp)$NiCl_2$ (70 mg, 0.13 mmol) under a nitrogen atmosphere. Reaction mixture was allowed to stir for 10 minutes. 2 M Butylmagnesium chloride in THF (7.23 mL, 1.668 g, 14.27 mmol) was added dropwise and the reaction mixture was refluxed at 60 °C for 24 h. The reaction mixture was allowed cool to room temperature and quenched with 1 M HCL (10 mL). Volatiles were removed *in vacuo*. Residue was dissolved in DCM (15 mL) washed with deionised water (5 mL), brine (5 mL), dried over anhydrous magnesium sulfate, filtered and solvent removed *via* rotary evaporation to yield crude product. Crude product was dissolved in THF (5 mL) at room temperature and concentrated hydrochloric acid (0.5 mL, 32%, 10.17 M) was added. Reaction mixture was warmed to 50 °C and after 24 h allowed to cool to room temperature. Solvent was removed *via* rotary evaporation. Deionised water (5 mL) was added, the product was extracted with DCM (3 x 10 mL) and the combined organic phase was washed with brine (10 mL), dried over anhydrous magnesium sulfate, filtered and solvent removed *via*

rotary evaporation to yield the final crude product. Final crude product was purified by column chromatography (SiO_2, hexane/ethyl acetate 10:0.3) to yield the title compound as a yellow solid in 42% yield (150 mg, 0.27 mmol).

Mpt = 104-106 °C

$[\alpha]^{20}_D$= +53.2 ° (1.0 c, THF)

Molecular formula $C_{40}H_{38}O_2$

Molecular weight 550.73 $gmol^{-1}$

^{1}H NMR (400 MHz, $CDCl_3$) δ ppm 7.97 (s, 2H, *H4, H4'*), 7.75 (dd, *J*= 7.4 Hz, 1.6 Hz, 4H, *H12, H12', H16, H16'*), 7.71 (s, 2H, *H5, H5'*), 7.50 (dd, *J*= 7.4 Hz, 1.6 Hz, 4H, *H13, H13', H15, H15'*), 7.42 (tt, *J*= 7.4 Hz, 1.6 Hz, 2H, *H14, H14'*), 7.19 (d, *J*= 1.2 Hz, 4H, *H7, H7', H8, H8'*), 5.31 (s, 2H, *OH*), 2.76 (t, *J*= 7.4 Hz, 4H, *H17, H17'*), 1.68 (tt, *J*= 7.4 Hz, 7.4 Hz, 4H, *H18, H18'*), 1.41 (qt, *J*= 7.4 Hz, 7.4 Hz, 4H, *H19, H19'*), 0.96 (t, *J*= 7.4 Hz, 6H, *H20, H20'*)

^{13}C NMR (100 MHz, $CDCl_3$) δ ppm

149.52 (C, *C2, C2'*), 138.90 (C, *C6, C6'*), 137.77 (C, *C11, C11'*), 131.32 (C, *C9/C10, C9'/C10'*), 130.90 (CH, *C4, C4'*), 130.58 (C, *C3, C3'*), 129.66 (2CH, *C12, C12', C16, C16'*), 129.63 (C, *C9/C10, C9'/C10'*), 128.99 (CH, *C7, C7'*), 128.46 (2CH, *C13, C13', C15, C15'*), 127.67 (CH, *C14, C14'*), 126.93 (CH, *C5, C5'*), 124.27 (CH, *C8, C8'*), 112.39 (C, *C1, C1'*), 35.56 (CH_2, *C17, C17'*), 33.59 (CH_2, *C18, C18'*), 22.43 (CH_2, *C19, C19'*), 14.05 (CH_3, *C20, C20'*)

IR (neat) (cm^{-1}) 3500, 3055, 2953, 2926, 2862, 1620, 1601, 1497, 1455, 1425, 1382, 1361, 1236, 1198, 1168, 1145, 1126, 1068, 1027

HRMS (EI, 70 eV, *m/z*) Found $[M+H]^+$ 551.2950, $C_{40}H_{39}O_2^+$ requires 551.2950

(+)-2,2'-*Bis*(methoxymethoxy)-1,1'-binaphthyl (119b)

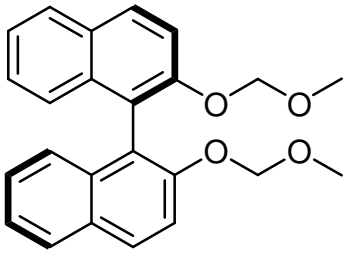

To a stirred solution of sodium hydride (2.154 g, 60% in mineral oil, 53.79 mmol) in dry THF (175 mL) at 0 °C under a nitrogen atmosphere was added dropwise a solution containing (*R*)-1,1'-bi-2-naphthol (**45b**) (7.000 g, 24.45 mmol) in dry THF (60 mL). After stirring at 0 °C for 1 h, chloromethyl methyl ether (4.09 mL, 4.327 g, 53.79 mmol) was added dropwise. Upon complete addition, the reaction mixture was allowed to warm up to room temperature and stirred for 4 h. Saturated aqueous ammonium chloride (30 mL) was added slowly to quench the reaction and volatiles were removed *in vacuo*. Residue was extracted with DCM (3 x 30 mL) and the combined organic phase was washed with brine (30 mL), dried over anhydrous magnesium sulfate, filtered and solvent removed *via* rotary evaporation to yield the crude product. Crude product was purified by column chromatography (SiO_2, using a gradient solvent system of hexane, hexane/ethyl acetate 10:0.5) to yield the title compound as a white solid in 85% yield (7.781 g, 20.78 mmol).

Mpt = 88-89°C, **Lit Mpt** = 98-100ºC[11]

$[\alpha]^{20}_{D}$ = +84.2 ° (1.0 c, THF), **Lit $[\alpha]^{25}_{589}$** = +95.0 º (1.0 c, THF)[11]

Molecular formula $C_{24}H_{22}O_4$

Molecular weight 374.43 $gmol^{-1}$

^{1}H NMR (400 MHz, $CDCl_3$) δ ppm 7.97 (d, *J*= 9.2 Hz, 2H), 7.89 (d, *J*= 8.2 Hz, 2H), 7.60 (d, *J*= 9.2 Hz, 2H), 7.38-7.34 (m, 2H), 7.26-7.22 (m, 2H), 7.18 (d, *J*= 8.2 Hz, 2H), 5.10 (d, J_{AB}= 6.6 Hz, 2H), 4.99 (d, J_{AB}= 6.6 Hz, 2H), 3.16 (s, 6H)

^{13}C NMR (100 MHz, $CDCl_3$) δ ppm 152.65 (C), 134.03 (C), 129.89 (C), 129.42 (CH), 127.90 (CH), 126.33 (CH), 125.57 (CH), 124.10 (CH), 121.30 (C), 117.29 (CH), 95.20 (CH_2), 55.86 (CH_3)

^{1}H and ^{13}C NMR data in agreement with the literature.[10,11]

(+)-3,3'-Dibromo-2,2'-*bis*(methoxymethoxy)-1,1'-binaphthyl (120b)

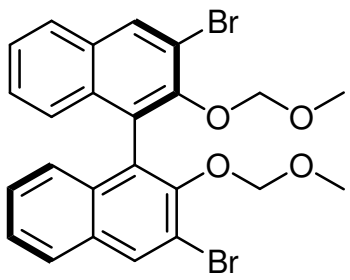

To a stirred solution of (+)-2,2'-*bis*(methoxymethoxy)-1,1'-binaphthyl (**119b**) (4.677 g, 12.51 mmol) in dry diethyl ether (220 mL) at room temperature under a nitrogen atmosphere was added dropwise *n*-butyllithium (1.6 M in hexanes, 23.45 mL, 37.52 mmol). After stirring at room temperature for 3 h, THF (140 mL) was added. After 1 h, reaction mixture was cooled to 0 °C and dibromotetrachloroethane (12.220 g, 37.52 mmol) was added in one portion under a nitrogen atmosphere. Reaction mixture was allowed to reach room temperature over 2 h. Saturated aqueous ammonium chloride (60 mL) was added to quench the reaction and phases were separated. Aqueous layer was extracted with diethyl ether (3 x 60 mL) and the combined organic phase was washed with brine (60 mL), dried over anhydrous magnesium sulfate, filtered and solvent removed *via* rotary evaporation to yield the crude product. Crude product was purified by column chromatography (SiO_2, hexane/ethyl acetate 10:0.3) to yield the title compound as a white solid in 74% yield (4.950 g, 9.30 mmol).

Mpt = 119-120 °C, **Lit Mpt** = 123-124ºC[11]

$[\alpha]^{20}_{D}$ = +25.7 ° (1.0 c, THF), **Lit $[\alpha]^{25}_{589}$** = +28.3 º (1.0 c, THF)[11]

Molecular formula $C_{24}H_{20}Br_2O_4$

Molecular weight 532.22 $gmol^{-1}$

^{1}H NMR (400 MHz, $CDCl_3$) δ ppm 8.28 (s, 2H), 7.81 (d, *J*= 8.0 Hz, 2H), 7.47-7.43 (m, 2H), 7.33-7.29 (m, 2H), 7.20 (d, *J*= 8.0 Hz, 2H), 4.85 (d, J_{AB}= 5.6 Hz, 2H), 4.83 (d, J_{AB}= 5.6 Hz, 2H), 2.57 (s, 6H)

^{13}C NMR (100 MHz, $CDCl_3$) δ ppm 150.16 (C), 133.09 (C), 133.04 (CH), 131.51 (C), 127.41 (C), 126.94 (2CH), 126.58 (CH), 126.10 (CH), 117.38 (C), 99.18 (CH_2), 56.31 (CH_3)

^{1}H and ^{13}C NMR data in agreement with the literature.[10,11]

(–)-3,3'-Diphenyl-2,2'-*bis*(methoxymethoxy)-1,1'-binaphthyl (121b)

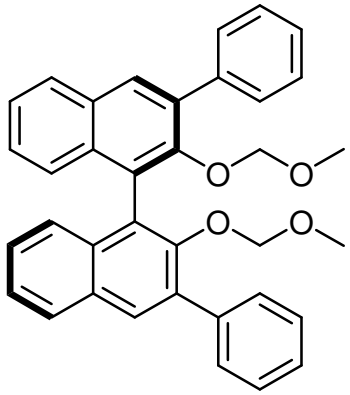

(+)-3,3'-Dibromo-2,2' -*bis*(methoxymethoxy)- 1,1'-binaphthyl (**120b**) (4.500 g, 8.46 mmol) and *tetrakis*(triphenylphosphine)palladium(0) (0.977 g, 0.85 mmol) were added to dry DME (60 mL) at room temperature under a nitrogen atmosphere. To the stirred mixture was added phenylboronic acid (3.609 g, 29.60 mmol) and 2 M aqueous sodium carbonate (22.5 mL). Reaction mixture was refluxed for 18 h, allowed cool to room temperature and filtered through a pad of celite. Solvent was removed *via* rotary evaporation to give a crude residue. Residue was dissolved in DCM (150 mL), washed with saturated aqueous ammonium chloride (50 mL), deionised water (50 mL), brine (50 mL), dried over anhydrous magnesium sulfate, filtered and solvent removed *via* rotary evaporation to yield crude product. Crude product was purified by column chromatography (SiO_2, hexane/ethyl acetate 10:1) to yield the title compound as a white solid in 91% yield (4.052 g, 7.69 mmol).

Mpt = 135-137 °C

$[\alpha]^{20}_D$ = −67.7 ° (1.0 c, THF)

Molecular formula $C_{36}H_{30}O_4$

Molecular weight 526.62 $gmol^{-1}$

^{1}H NMR (400 MHz, $CDCl_3$) δ ppm 7.97 (s, 2H), 7.91 (d, *J*= 8.0 Hz, 2H), 7.78 (d, *J*= 8.4 Hz, 4H), 7.51-7.47 (m, 4H), 7.45-7.37 (m, 4H), 7.32-7.30 (m, 4H), 4.43 (d, J_{AB}= 5.6 Hz, 2H), 4.39 (d, J_{AB}= 5.6 Hz, 2H), 2.35 (s, 6H)

^{13}C NMR (100 MHz, $CDCl_3$) δ ppm 151.35 (C), 139.04 (C), 135.48 (C), 133.63 (C), 130.87 (C), 130.62 (CH), 129.67 (2CH), 128.38 (2CH), 127.90 (CH), 127.34 (CH), 126.55 (C), 126.46 (CH), 126.35 (CH), 125.22 (CH), 98.55 (CH_2), 55.87 (CH_3)

^{1}H and ^{13}C NMR data in agreement with the literature.[10,11]

(+)-3,3'-Diphenyl-2,2'-dihydroxy-1,1'-binaphthyl (122b)

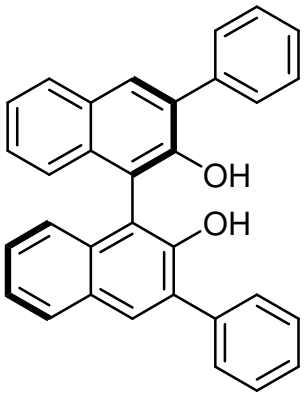

To a stirred mixture of (–)-3,3'-diphenyl-2,2'-*bis*(methoxymethoxy)-1,1'-binaphthyl (4.198 g, 7.98 mmol) (**121b**) in THF (40 mL) at room temperature, was added concentrated hydrochloric acid (0.7 mL, 32%, 10.17 M). Reaction mixture was warmed to 50 °C and after 24 h allowed cool to room temperature. Solvent was removed *via* rotary evaporation. Deionised water (40 mL) was added and the product was extracted with DCM (3 x 50 mL). The combined organic phase was washed with brine (50 mL), dried over anhydrous magnesium sulfate, filtered and the solvent was removed *via* rotary evaporation to yield the crude product. Crude product was purified by column chromatography (SiO_2, toluene) to yield the title compound as a white solid in 92% yield (3.23 g, 7.37 mmol).

Mpt = 193-195 °C, **Lit Mpt** = 200-202 °C[11]

$[\alpha]^{20}_{D}$ = +92.4 ° (1.0 c, THF), **Lit $[\alpha]^{25}_{589}$** = +135.0 (1.0 c, THF)[11]

Molecular formula $C_{32}H_{22}O_2$

Molecular weight 438.52 $gmol^{-1}$

^{1}H NMR (400 MHz, $CDCl_3$) δ ppm 8.10 (s, 2H), 7.99 (d, *J*= 8.0 Hz, 2H), 7.82 (d, *J*= 7.2 Hz, 4H), 7.57 (t, *J*= 7.2 Hz, 4H), 7.50-7.44 (m, 4H), 7.41-7.37 (m, 2H), 7.32 (d, *J*= 8.4 Hz, 2H), 5.45 (s, 2H)

^{13}C NMR (100 MHz, $CDCl_3$) δ ppm 150.23 (C), 137.55 (C), 133.03 (C), 131.49 (CH), 130.76 (C), 129.70 (2CH), 129.52 (C), 128.58 (2CH), 128.55 (CH), 127.86 (CH), 127.44 (CH), 124.43 (CH), 124.37 (CH), 112.48 (C)

^{1}H and ^{13}C NMR data in agreement with the literature.[10,11]

(+)-6,6'-Dibromo-3,3'-diphenyl-2,2'-dihydroxy-1,1'-binaphthyl (123b)

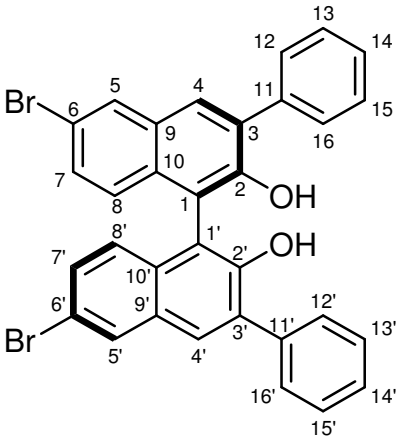

To a stirred solution of (+)-3,3'-diphenyl-2,2'-dihydroxy-1,1'-binaphthyl (**122b**) (600 mg, 1.37 mmol) in DCM (21 mL) at −78 °C under a nitrogen atmosphere was added slowly a solution of bromine (270 μL, 848 mg, 5.31 mmol) in DCM (3.8 mL) over a period of 60 minutes. Reaction mixture was allowed to reach room temperature over 2 h and to stir for a further 2 h at room temperature. The reaction was quenched with 10% sodium bisulfite (20 mL). Product was extracted with DCM (3 x 30 mL) and the combined organic extracts were washed with brine (30 mL), dried over anhydrous magnesium sulfate, filtered and solvent was removed *via* rotary evaporation to yield crude product. Crude product was purified by recrystallisation from hexane/DCM at room temperature and filtered to yield the title compound as a light yellow solid in 72% yield (588 mg, 0.99 mmol).

Mpt = 249-251 °C, **Lit Mpt** = 262-264 ºC[10]

$[\alpha]^{20}_{D}$ = +85.1 ° (1.0 c, THF), **Lit $[\alpha]^{25}_{589}$** = +96.6 º (1.0 c, THF)[10]

Molecular formula $C_{32}H_{20}Br_2O_2$

Molecular weight 596.31 $gmol^{-1}$

^{1}H NMR (400 MHz, $CDCl_3$) δ ppm 8.07 (d, *J*= 2.0 Hz, *H5, H5'*, 2H), 7.91 (s, *H4, H4'*, 2H), 7.69 (dd, *J*= 7.2 Hz, *H12, H12', H16, H16'*, 1.4 Hz, 4H), 7.51 (dd, *J*= 7.2 Hz, 1.4 Hz, *H13, H13', H15, H15'*, 4H), 7.44 (tt, *J*= 7.2 Hz, 1.4 Hz, *H14, H14'*, 2H), 7.38 (dd, *J*= 9.0 Hz, 2.0 Hz, *H7, H7'*, 2H), 7.06 (d, *J*= 9.0 Hz, *H8, H8'*, 2H), 5.38 (s, *OH*, 2H)

^{13}C NMR (100 MHz, $CDCl_3$) δ ppm 150.26 (C), 136.73 (C), 131.85 (C), 131.48 (C), 130.64 (CH, *C7, C7'*), 130.53 (C), 130.41 (CH, *C4/C5, C4'/C5'*), 130.37 (CH, *C4/C5, C4'/C5'*), 129.54 (2CH, *C12, C12', C16, C16'*), 128.78 (2CH, *C13, C13', C15, C15'*), 128.25 (CH, *C14, C14'*), 126.08 (CH, *C8, C8'*), 118.18 (C), 112.63 (C)

^{1}H and ^{13}C NMR data in agreement with the literature.[10,11]

(–)-6,6'-Dibromo-3,3'-diphenyl-2,2'-*bis*(methoxymethoxy)-1,1'-binaphthyl (125b)

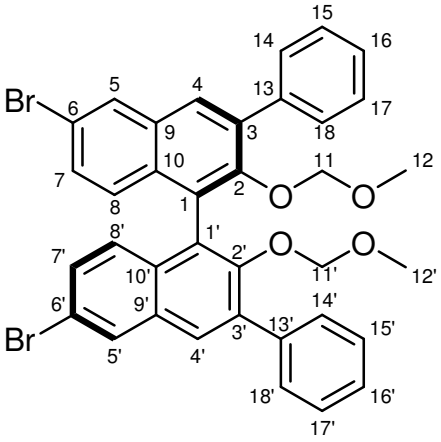

To a stirred solution of sodium hydride (112 mg, 60% in mineral oil, 2.80 mmol) in dry THF (10 mL) at 0 °C under a nitrogen atmosphere was added dropwise a solution of (+)-6,6'-dibromo-3,3'-diphenyl-2,2'-dihydroxy-1,1'-binaphthyl (**123b**) (697 mg, 1.17 mmol) in dry THF (4 mL). After stirring at 0 °C for 1 h, chloromethyl methyl ether (0.21 mL, 226 mg, 2.80 mmol) was added dropwise. Upon complete addition, the reaction mixture was allowed to warm up to room temperature and stirred for 4 h. Saturated aqueous ammonium chloride (10 mL) was added to quench the reaction and volatiles removed *in vacuo*. Residue was extracted with DCM (3 x 10 mL) and the combined organic phase was washed with brine (10 mL), dried over anhydrous magnesium sulfate, filtered and solvent removed *via* rotary evaporation to yield the crude product. Crude product was purified by column chromatography (SiO_2, hexane/ethyl acetate 10:0.3) to yield the title compound as a white solid in 56% yield (444 mg, 0.65 mmol).

Mpt = 87-88 °C

$[\alpha]^{20}_D$ = –2.0 ° (1.0 c, THF)

Molecular formula $C_{36}H_{28}Br_2O_4$

Molecular weight 684.41 $gmol^{-1}$

^{1}H NMR (400 MHz, $CDCl_3$) δ ppm 8.05 (d, *J*= 2.0 Hz, 2H, *H5, H5'*), 7.86 (s, 2H, *H4, H4'*), 7.72 (dd, *J*= 7.4 Hz, 1.2 Hz, 4H, *H14, H14', H18, H18'*), 7.48 (dd, *J*= 7.4 Hz, 1.2 Hz, 4H, *H15, H15', H17, H17'*), 7.40 (tt, *J*= 7.4 Hz, 1.2 Hz, 2H, *H16, H16'*), 7.36 (dd, *J*= 8.8 Hz, 2.0 Hz, 2H, *H7, H7'*), 7.14 (d, *J*= 8.8 Hz, 2H, *H8, H8'*), 4.37 (s, 4H, *H11, H11'*), 2.33 (s, 6H, *H12, H12'*)

^{13}C NMR (100 MHz, $(CD_3)_2CO$) δ ppm

152.84 (C, *C2, C2'*), 139.38 (C, *C13, C13'*), 137.69 (C, *C3, C3'*), 133.09 (C, *C6/C10, C6'/C10'*), 132.85 (C, *C6/C10, C6'/C10'*), 130.88 (CH, *C4/C5, C4'/C5'*), 130.80, (CH, *C4/C5, C4'/C5'*) 130.41, (CH, *C7, C7'*), 130.34 (2CH, *C14, C14', C18, C18'*), 129.39 (2CH, *C15, C15', C17, C17'*), 129.20 (CH, *C16, C16'*), 128.59 (CH, *C8, C8'*), 127.22 (C, *C9, C9'*), 119.66 (C, *C1, C1'*), 99.21 (CH_2, *C11, C11'*), 56.06 (CH_3, *C12, C12'*)

IR (neat) (cm^{-1}) 2924, 2823, 1600, 1584, 1480, 1422, 1350, 1180, 1155, 1140

HRMS (EI, 70 eV, *m/z*) Found $[M+NH_4]^+$ 700.0703, $C_{36}H_{32}NO_4Br_2^+$ requires 700.0698

7.7 Preparation of biquinoline derivatives

(+/–)-6,6'-Dihydroxy-5,5'-biquinoline (130)

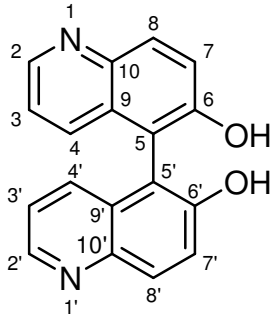

To a stirred mixture of copper (II) chloride dihydrate (8.589 g, 50.38 mmol) in methanol (420 mL) under a nitrogen atmosphere was added a solution of benzylamine (18.33 mL, 17.982 g, 167.81 mmol) in methanol (70 mL) and the solution was stirred for 10 minutes. A solution of 6-hydroxylquinoline (**131**) (3.045, 20.98 mmol) in methanol (70 mL) was added and the reaction mixture was stirred at room temperature for 48 h. The reaction mixture was filtered and the brown precipitate was washed with methanol (3 x 10 mL) and allowed to dry. Brown precipitate was dissolved in concentrated hydrochloric acid (44 mL, 32%, 10.17 M), followed by the addition of concentrated ammonia (220 mL) at 0 °C and the product precipitated on the addition of deionised water (660 mL). Mixture was filtered to yield the title compound as a brown solid in 65% yield (1.973 g, 6.84 mmol).

Mpt = >270 °C, **Lit Mpt** = 174-176 ºC[12]

Molecular formula $C_{18}H_{12}N_2O_2$

Molecular weight 288.30 $gmol^{-1}$

^{1}H NMR (400 MHz, $(CD_3)_2SO$) δ ppm 8.90 (br, 2H, *OH*), 8.66 (s, 2H, *H2, H2'*), 8.01 (d, *J*= 9.0 Hz, 2H, *H8, H8'*), 7.60 (d, *J*= 9.0 Hz, 2H, *H7, H7'*), 7.35 (d, *J*= 8.4 Hz, 2H, *H4, H4'*), 7.25 (dd, *J*= 8.4 Hz, 3.8 Hz, 2H, *H3, H3'*)

^{13}C NMR (100 MHz, $(CD_3)_2SO$) δ ppm 153.29 (C), 146.71 (CH, *C2, C2'*), 143.32 (C), 132.29 (CH, *C4, C4'*), 130.01 (CH, *C8, C8'*), 128.84 (C), 121.81 (CH, *C7, C7'*), 121.30 (CH, *C3, C3'*), 114.08 (C)

IR (neat) (cm^{-1}) 3052, 2820, 1606, 1573, 1590, 1480, 1460, 1418, 1373, 1332, 1192, 1154, 1122, 1134

^{1}H and ^{13}C NMR data in agreement with the literature. [12]

(+/–)-1,1'-Dibutyl-6,6'-dihydroxy-5,5'-biquinoline (134)

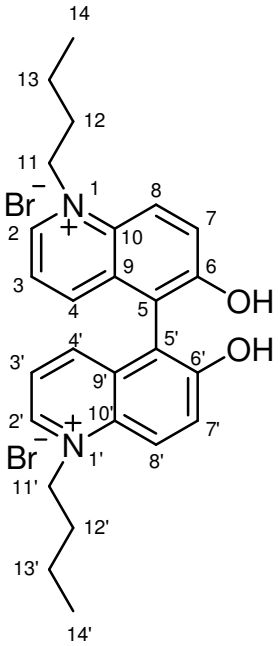

To a stirred solution of (+/–)-6,6'-dihydroxy-5,5'-biquinoline (**130**) (274 mg, 1.0 mmol) in DMF (6 mL) was added bromobutane (1.56 mL, 1.950 g, 13.8 mmol) and potassium iodide (47 mg, 0.3 mmol). Reaction mixture was refluxed for 48 h and allowed cool to room temperature. Volatiles were removed *via* rotary evaporation to yield a crude residue. Residue was filtered and washed with diethyl ether (3 x 10 mL) to yield a light brown solid. Brown solid was dried under high vacuum at 150 °C for 36 h to yield the title compound in 26% yield (139 mg, 0.25 mmol).

Mpt = >270 °C

Molecular formula $C_{26}H_{30}Br_2N_2O_2$

Molecular weight 562.34 $gmol^{-1}$

^{1}H NMR (400 MHz, $(CD_3)_2SO$) δ ppm 11.14 (s, 2H, *OH*), 9.41 (d, *J*= 5.6 Hz, 2H, *H2, H2'*), 8.74 (d, *J*= 10.0 Hz, 2H, *H8, H8'*), 8.26 (d, *J*= 8.8 Hz, 2H, *H4, H4'*), 8.09 (d, *J*= 10.0 Hz, 2H, *H7, H7'*), 7.92 (dd, *J*= 8.8 Hz, 5.6 Hz, 2H, *H3, H3'*), 5.12 (t, *J*= 7.4 Hz, 4H, *H11, H11'*), 2.01 (tt, *J*= 7.4 Hz, 7.4 Hz, 4H, *H12, H12'*), 1.48 (tq, *J*= 7.4 Hz, 7.4 Hz, 4H, *H13, H13'*), 0.98 (t, *J*= 7.4 Hz, 6H, *H14, H14'*)

^{13}C NMR (100 MHz, $(CD_3)_2SO$) δ ppm 156.13 (C, *C6, C6'*), 145.82 (CH, *C2, C2'*), 142.82 (CH, *C4, C4'*), 132.84 (C, *C10, C10'*), 131.14 (C, *C9, C9'*), 127.12 (CH, *C7, C7'*), 122.36 (CH, *C3, C3'*), 121.37 (CH, *C8, C8'*), 114.58 (C, *C5, C5'*), 57.46 (CH_2, *C11, C11'*), 31.84 (CH_2, *C12, C12'*), 19.22 (CH_2, *C13, C13'*), 13.49 (CH_3, *C14, C14'*)

IR (neat) (cm^{-1}) 3042, 2967, 2597, 1609, 1596, 1528, 1493, 1425, 1380, 1357, 1299, 1277, 1234, 1035

HRMS (EI, 70 eV, *m/z*) Found $[M-H]^+$ 401.2222, $C_{26}H_{29}N_2O_2^+$ requires 401.2229

(+/–)-1,1'-Diethoxycarbonylmethyl-6,6'-dihydroxy-5,5'-biquinoline (135)

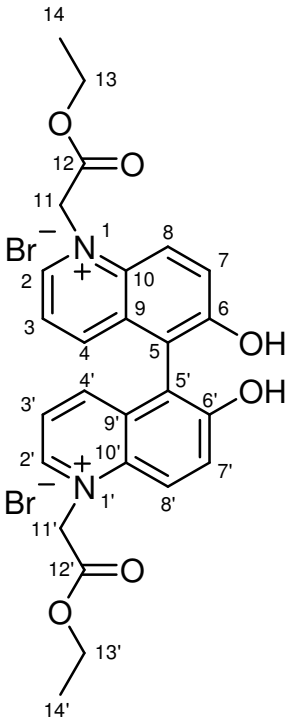

To a stirred solution of (+/–)-6,6'-dihydroxy-5,5'-biquinoline (**130**) (400 mg, 1.39 mmol) in NMP (1.20 mL) was added ethyl bromoacetate (0.80 mL, 1.21 g, 7.22 mmol). Reaction mixture was allowed to stir at room temperature for 72 h. Product precipitated on addition of diethyl ether (20 mL), filtered and washed with diethyl ether. Crude solid was further dissolved in methanol (10 mL) and product precipitated on addition of diethyl ether (100 mL), filtered and washed with diethyl ether to yield a light brown solid in 86% yield (743 mg, 1.19 mmol).

Mpt = >270 °C

Molecular formula $C_{26}H_{26}Br_2N_2O_6$

Molecular weight 622.30 $gmol^{-1}$

^{1}H NMR (400 MHz, $(CD_3)_2SO$) δ ppm 11.31 (s, 2H, *OH*), 9.45 (d, *J*= 5.2 Hz, 2H, *H2, H2'*), 8.56 (d, *J*= 9.6 Hz, 2H, *H8, H8'*), 8.40 (d, *J*= 8.4 Hz, 2H, *H4, H4'*), 8.14 (d, *J*= 9.6 Hz, 2H, *H7, H7'*), 8.06 (dd, *J*= 8.4 Hz, 5.2 Hz, 2H, *H3, H3'*), 6.28 (s, 4H, *H11, H11'*), 4.30 (q, *J*= 6.8 Hz, 4H, *H13, H13'*), 1.31 (t, *J*= 6.8 Hz, 6H, *H14, H14'*)

^{13}C NMR (100 MHz, $(CD_3)_2SO$) δ ppm 166.26 (CO, *C12, C12'*), 156.29 (C, *C6, C6'*), 147.38 (CH, *C2, C2'*), 144.42 (CH, *C4, C4'*), 133.71 (C, *C10, C10'*), 130.71 (C, *C9, C9'*), 127.57 (CH, *C7, C7'*), 122.44 (CH, *C3, C3'*), 121.29 (CH, *C8, C8'*), 114.26 (C, *C5, C5'*), 62.46 (CH_2, *C13, C13'*), 57.72 (CH_2, *C11, C11'*), 13.99 (CH_3, *C14, C14'*)

IR (neat) (cm^{-1}) 2967, 2907, 1752 (COOEt), 1610, 1593, 1537, 1463, 1426, 1371, 1323, 1298, 1204, 1091, 1057, 1017

HRMS (EI, 70 eV, *m/z*) Found $[M-H]^+$ 461.1699, $C_{26}H_{25}N_2O_6^+$ requires 461.1713

(+/–)-1,1'-Dimethyl-6,6'-dihydroxy-5,5'-biquinoline (136)

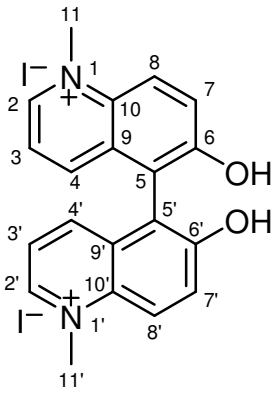

To a stirred solution of (+/–)-6,6'-dihydroxy-5,5'-biquinoline (**130**) (100 mg, 0.35 mmol) in NMP (0.50 mL) was added methyl iodide (0.22 mL, 0.49 g, 3.47 mmol). Reaction mixture was heated at 90 °C for 2 h and then allowed cool to room temperature. Product precipitated on addition of diethyl ether (10 mL), filtered and washed with diethyl ether. Crude solid was further dissolved in methanol (5 mL) and product precipitated on addition of diethyl ether (50 mL), filtered and washed with diethyl ether to yield a yellow solid in 79% yield (158 mg, 0.28 mmol).

Mpt = >270 °C

Molecular formula $C_{20}H_{18}I_2N_2O_2$

Molecular weight 572.18 $gmol^{-1}$

^{1}H NMR (400 MHz, $(CD_3)_2SO$) δ ppm 11.19 (s, 2H, *OH*), 9.31 (d, *J*= 5.6 Hz, 2H, *H2, H2'*), 8.62 (d, *J*= 9.6 Hz, 2H, *H8, H8'*), 8.21 (d, *J*= 8.8 Hz, 2H, *H4, H4'*) 8.03 (d, *J*= 9.6 Hz, 2H, *H7, H7'*), 7.92 (dd, *J*= 8.8 Hz, 5.6 Hz, 2H, *H3, H3'*), 4.69 (s, 6H, *H11, H11'*)

^{13}C NMR (100 MHz, $(CD_3)_2SO$) δ ppm 156.34 (C, *C6, C6'*), 146.40 (CH, *C2, C2'*), 142.51 (CH, *C4, C4'*), 133.72 (C, *C10, C10'*), 130.58 (C, *C9, C9'*), 126.93 (CH, *C7, C7'*), 122.32 (CH, *C3, C3'*), 121.49 (CH, *C8, C8'*), 114.36 (C, *C5, C5'*), 45.76 (CH_3, *C11, C11'*)

IR (neat) (cm^{-1}) 3063, 2994, 1611, 1533, 1372, 1321, 1294, 1241, 1183, 1144, 1037

HRMS (EI, 70 eV, *m/z*) Found $[M-H]^+$ 317.1281, $C_{20}H_{17}N_2O_2^+$ requires 317.1290

6,6'-Dihydroxy-5,5'-biquinoline-3,3'-dicarboxylic acid dimethyl ester (137a)

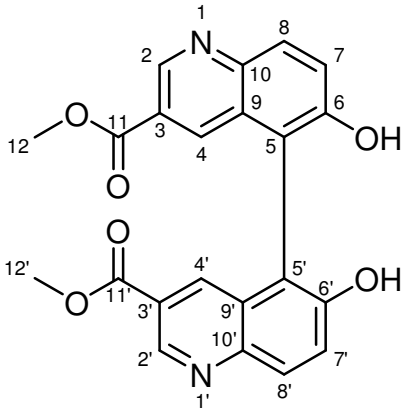

To a stirred mixture of copper (II) chloride dihydrate (0.403 g, 2.36 mmol) in methanol (30 mL) under a nitrogen atmosphere was added a solution of benzylamine (0.860 mL, 0.844 g, 7.87 mmol) in methanol (5 mL) and the solution was stirred for 10 minutes. A solution of 6-hydroxy-quinoline-3-carboxylic acid methyl ester (**142**) (0.200 g, 0.98 mmol) in methanol (15 mL) was added and the reaction mixture was refluxed for 24 h. The reaction mixture was filtered and the green precipitate was washed with methanol (3 x 10 mL) and allowed to dry. Green precipitate was dissolved in deionised water (6 mL), concentrated hydrochloric acid (12 mL, 32%, 10.17 M), followed by the addition of concentrated ammonia (30 mL) at 0 °C and product precipitated on the addition of deionised water (100 mL). Mixture was filtered to yield the title compound as a brown solid in 21% yield (42 mg, 0.10 mmol).

Mpt = >270 °C

Molecular formula $C_{22}H_{16}N_2O_6$

Molecular weight 404.37 $gmol^{-1}$

^{1}H NMR (400 MHz, $(CD_3)_2SO$) δ ppm 10.22 (br, 2H, *OH*), 9.13 (s, 2H, *H2, H2'*), 8.16 (d, *J*= 8.6 Hz, 2H, *H8, H8'*), 7.98 (s, 2H, *H4, H4'*), 7.77 (d, *J*= 8.6 Hz, 2H, *H7, H7'*), 3.77 (s, 6H, *H12, H12'*)

^{13}C NMR (100 MHz, $(CD_3)_2SO$) δ ppm 165.28 (C), 154.24 (C), 145.85 (CH), 144.87 (C), 134.25 (CH), 130.57 (CH), 127.43 (C), 124.49 (CH), 122.63 (C), 114.55 (C), 52.35 (CH_3)

IR (neat) (cm^{-1}) 3057, 2954, 1721 (COOMe), 1599, 1500, 1439, 1418, 1371, 1344, 1291, 1240, 1195, 1112, 1099

HRMS (EI, 70 eV, *m/z*) Found $[M+H]^+$ 405.1086, $C_{22}H_{17}N_2O_6^+$ requires 405.1087

6-Hydroxy-quinoline-3-carboxylic acid ethyl ester (140)

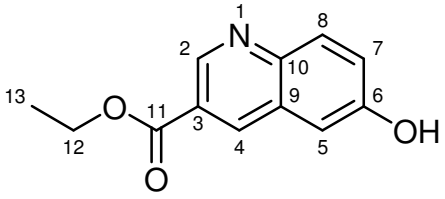

To a stirred solution of 5-hydroxy-2-nitrobenzaldehyde (**138**) (334 mg, 2.00 mmol) in ethanol (10 mL) was added tin (II) chloride dihydrate (1.81 g, 8.00 mmol) and 3,3-diethoxypropionic acid ethyl ester (**139**) (0.97 mL, 950 mg, 5.00 mmol) under argon atmosphere. Reaction mixture was refluxed at 90 °C for 4 h and allowed to cool overnight. Volatiles were removed *in vacuo*, residue was dissolved in ethyl acetate (20 mL) and quenched with saturated aqueous $NaHCO_3$ (20 mL). The resulting emulsion was filtered through a pad of celite and washed with ethyl acetate. Aqueous layer was separated and washed with ethyl acetate (3 x 15 mL). The combined organic layers were washed with brine, dried over anhydrous magnesium sulfate, filtered and volatiles were removed *via* rotary evaporation to yield a crude residue. Crude product was purified by column chromatography (SiO_2, hexane/ethyl acetate 10:1) to yield the title compound as a yellow solid in 44% yield (190 mg, 0.88 mmol).

Mpt = 208-210 °C, **Lit Mpt** = 189 ºC[13]

Molecular formula $C_{12}H_{11}NO_3$

Molecular weight 217.22 $gmol^{-1}$

^{1}H NMR (400 MHz, $(CD_3)_2SO$) δ ppm 10.31 (s, 1H, *OH*), 9.07 (d, *J*= 1.4 Hz, 1H, *H2*) , 8.75 (d, *J*= 1.4 Hz, 1H, *H4*) , 7.95 (d, *J*= 9.0 Hz, 1H, *H8*), 7.46 (dd, *J*= 9.0 Hz, 2.6 Hz, 1H, *H7*), 7.35 (d, *J*= 2.6 Hz, 1H, *H5*), 4.38 (q, *J*= 7.0 Hz, 2H, *H12*), 1.36 (t, *J*= 7.0 Hz, 3H, *H13*)

^{13}C NMR (100 MHz, $(CD_3)_2SO$) δ ppm 164.95 (CO, *C11*), 156.25 (C, *C6*), 145.92 (CH, *C2*), 144.46 (C, *C10*), 136.45 (CH, *C4*), 130.28 (CH, *C8*), 127.96 (C, *C9*), 124.55 (CH, *C7*), 122.69 (C, *C3*), 109.59 (CH, *C5*), 61.05 (CH_2, *C12*) 14.11 (CH_3, *C13*)

IR (neat) (cm^{-1}) 2958, 2909, 2685, 2548, 1724 (COOEt), 1621, 1603, 1476, 1411, 1321, 1239, 1220, 1136, 1098, 1016

^{1}H and ^{13}C NMR data in agreement with the literature.[13]

6-Hydroxy-quinoline-3-carboxylic acid methyl ester (142)

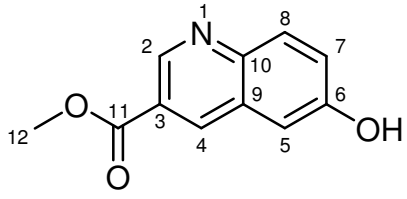

To a stirred solution of 5-hydroxy-2-nitrobenzaldehyde (**138**) (1.59 g, 9.50 mmol) in methanol (50 mL) was added tin (II) chloride dihydrate (8.58 g, 38.01 mmol) and 3,3-dimethoxypropionic acid methyl ester (**141**) (3.36 mL, 3.52 g, 23.75 mmol) under argon atmosphere. Reaction mixture was refluxed at 90 °C for 4 h and allowed to cool overnight. Volatiles were removed *in vacuo*, residue was dissolved in ethyl acetate (200 mL) and quenched with saturated aqueous $NaHCO_3$ (150 mL). The resulting emulsion was filtered through a pad of celite and washed with ethyl acetate. Aqueous layer was separated and washed with ethyl acetate (3 x 75 mL). The combined organic layers were washed with brine (100 mL), dried over anhydrous magnesium sulfate, filtered and volatiles were removed *via* rotary evaporation to yield a crude residue. Crude product was purified by column chromatography (SiO_2, hexane/ethyl acetate 10:1) to yield the title compound as a yellow solid in 46% yield (0.892 g, 4.39 mmol).

Mpt = 210-212 °C

Molecular formula $C_{11}H_9NO_3$

Molecular weight 203.19 $gmol^{-1}$

^{1}H NMR (400 MHz, $(CD_3)_2SO$) δ ppm 10.32 (s, 1H, *OH*), 9.06 (d, *J*= 2.0 Hz, 1H, *H2*) , 8.76 (d, *J*= 2.0 Hz, 1H, *H4*) , 7.95 (d, *J*= 9.2 Hz, 1H, *H8*), 7.46 (dd, *J*= 9.2 Hz, 2.6 Hz, 1H, *H7*), 7.35 (d, *J*= 2.6 Hz, 1H, *H5*), 3.92 (s, 3H, *H12*)

^{13}C NMR (100 MHz, $(CD_3)_2SO$) δ ppm 165.44 (CO, *C11*), 156.26 (C, *C6*), 145.88 (CH, *C2*), 144.45 (C, *C10*), 136.55 (CH, *C4*), 130.27 (CH, *C8*), 127.95 (C, *C9*), 124.60 (CH, *C7*), 122.46 (C, *C3*), 109.61 (CH, *C5*), 52.30 (CH_3, *C12*)

IR (neat) (cm^{-1}) 3009, 2952, 2663, 2580, 1719 (COOMe), 1633, 1587, 1577, 1500, 1445, 1368, 1358, 1320, 1273, 1264, 1159, 1141, 1109

HRMS (EI, 70 eV, *m/z*) Found $[M+H]^+$ 204.0657, $C_{11}H_{10}NO_3^+$ requires 204.0661

7.8 Catalyst screen for asymmetric Morita-Baylis-Hillman reactions

(+/–)-2-(1-Hydroxy-3-phenylpropyl)cyclohex-2-enone (151d)

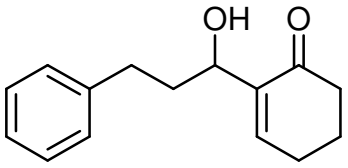

(+/–)-Bi-2-naphthol (**45**) (57 mg, 10 mol%) was dissolved in anhydrous THF (1 mL) under argon atmosphere. At 0 ^oC, 2-cyclohexen-1-one (**149b**) (0.389 mL, 385 mg, 4 mmol) was added, followed by 1 M triethylphosphine in THF (4 mL, 472 mg, 4 mmol) and hydrocinnamaldehyde (**150a**) (0.263 mL, 268 mg, 2 mmol). After 1 h, reaction mixture was allowed to stir at room temperature for 48 h. Volatiles were removed *via* rotary evaporation to yield crude product as an oil. Crude product was purified by column chromatography (SiO_2, hexane/ethyl acetate 10:0.3) to yield the title compound as a yellow oil in 59% yield (273 mg, 1.19 mmol).

Molecular formula $C_{15}H_{18}O_2$

Molecular weight 230.302 $gmol^{-1}$

^{1}H NMR (400 MHz, $CDCl_3$) δ ppm 7.31-7.18 (m, 5H), 6.88 (t, *J*= 4.4 Hz, 1H), 4.36-4.33 (m, 1H), 3.08 (s, 1H), 2.87-2.64 (m, 2H), 2.45-2.37 (m, 4H), 2.06-1.92 (m, 4H)

^{13}C NMR (100 MHz, $CDCl_3$) δ ppm 200.87 (C), 146.23 (CH), 141.88 (C), 140.62 (C), 128.51 (2CH), 128.39 (2CH), 125.82 (CH), 71.13 (CH), 38.69 (CH_2), 37.65 (CH_2), 32.26 (CH_2), 25.70 (CH_2), 22.54 (CH_2)

^{1}H and ^{13}C NMR data in agreement with the literature.[14]

General procedure for the synthesis of 2-(1-hydroxy-3-phenylpropyl)cyclohex-2-enone (151d) with chiral substituted BINOLs

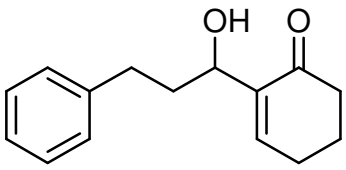

Chiral substituted BINOL (Chapter 5, table 5.6) catalyst (2 mol%) was dissolved in anhydrous THF under argon atmosphere. At 0 ^oC, 2-cyclohexen-1-one (**149b**) (1 mmol) was added, followed by 1 M triethylphosphine in THF (0.5 mmol) and hydrocinnamaldehyde (**150a**) (1 mmol). After 3 h, reaction mixture was allowed to stir at room temperature for 45 h. Volatiles were removed *via* rotary evaporation to yield crude product as an oil. Crude product was purified by column chromatography (SiO_2, hexane/ethyl acetate 10:0.3) to yield the title compound as a yellow oil (Results are presented in Chapter 5).

Molecular formula $C_{15}H_{18}O_2$

Molecular weight 230.302 $gmol^{-1}$

7.9 Conditions used to determine ee of 151d

Column	Lux 2
Mobile phase	Hexane/isopropanol 9:1
Flow rate	1 mL/min
Detection wavelength	254 nm
Injection volume	10 μL

7.10 Retention times for racemic and optically active 151d

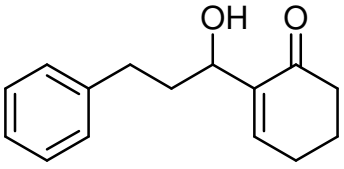

(+/–)-**151d**

Peak	Retention time
1	14.399 min
2	18.116 min

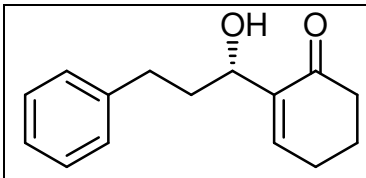

(–)-**151d**

Peak	Retention time
1	15.861 min
2 (major)	19.073 min

HPLC chromatograms for racemic (+/−)-2-(1-hydroxy-3-phenylpropyl)cyclohex-2-enone (**151d**) (Figure 7.1) and for chiral 2-(1-hydroxy-3-phenylpropyl)cyclohex-2-enone (**151d**) (Figure 7.2) are representative examples of chromatograms obtained during this study.

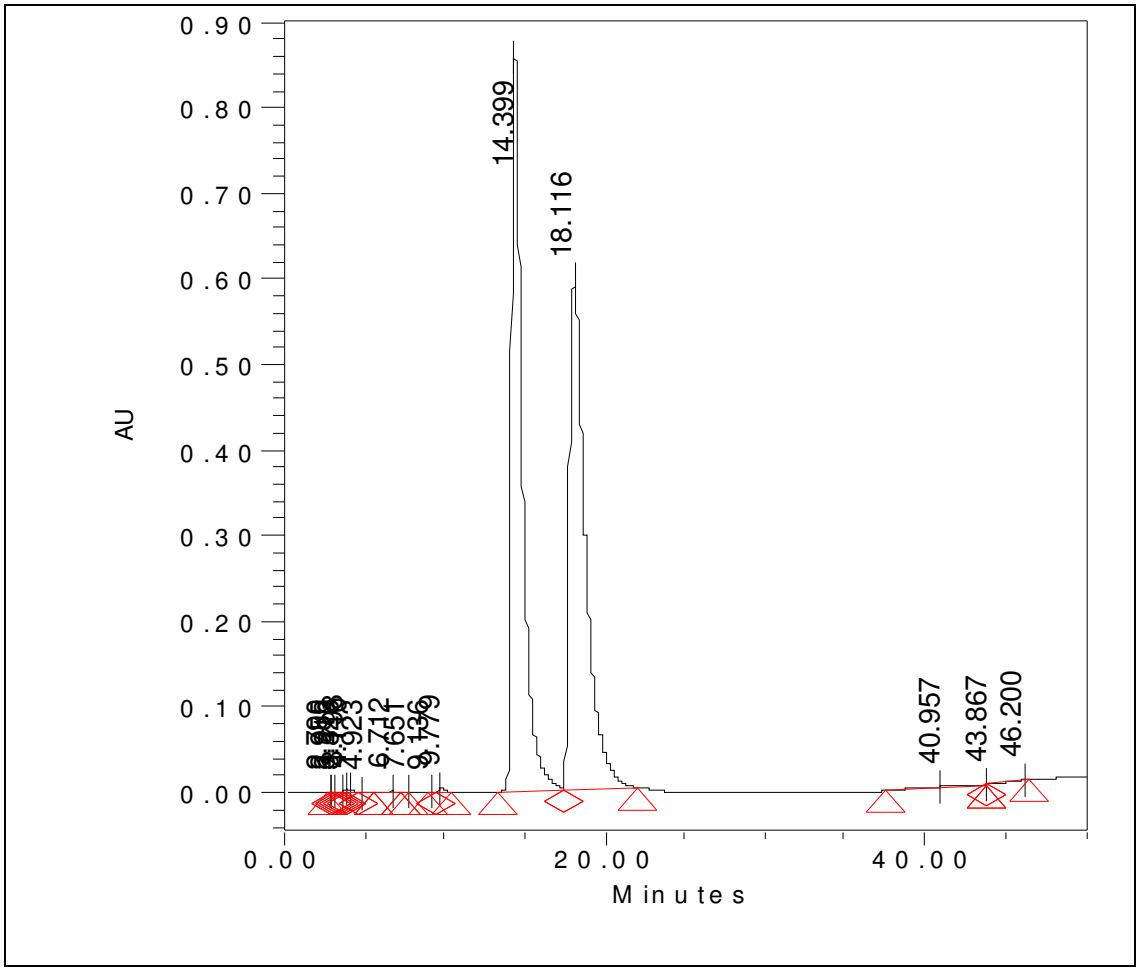

	Peak	Retention time	% Area	Area	%ee
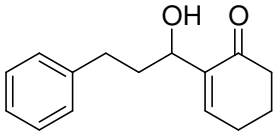 (+/–)-151d	1	14.399 min	49.19	41573962	0.8
	2	18.116 min	49.98	42240493	

Fig 7.1 HPLC chromatogram for racemic **151d** (Catalyst (+/−)-**45**, Lux 2 column, 9:1 hexane:i-PrOH, 1.0 mL/min, 254 nm).

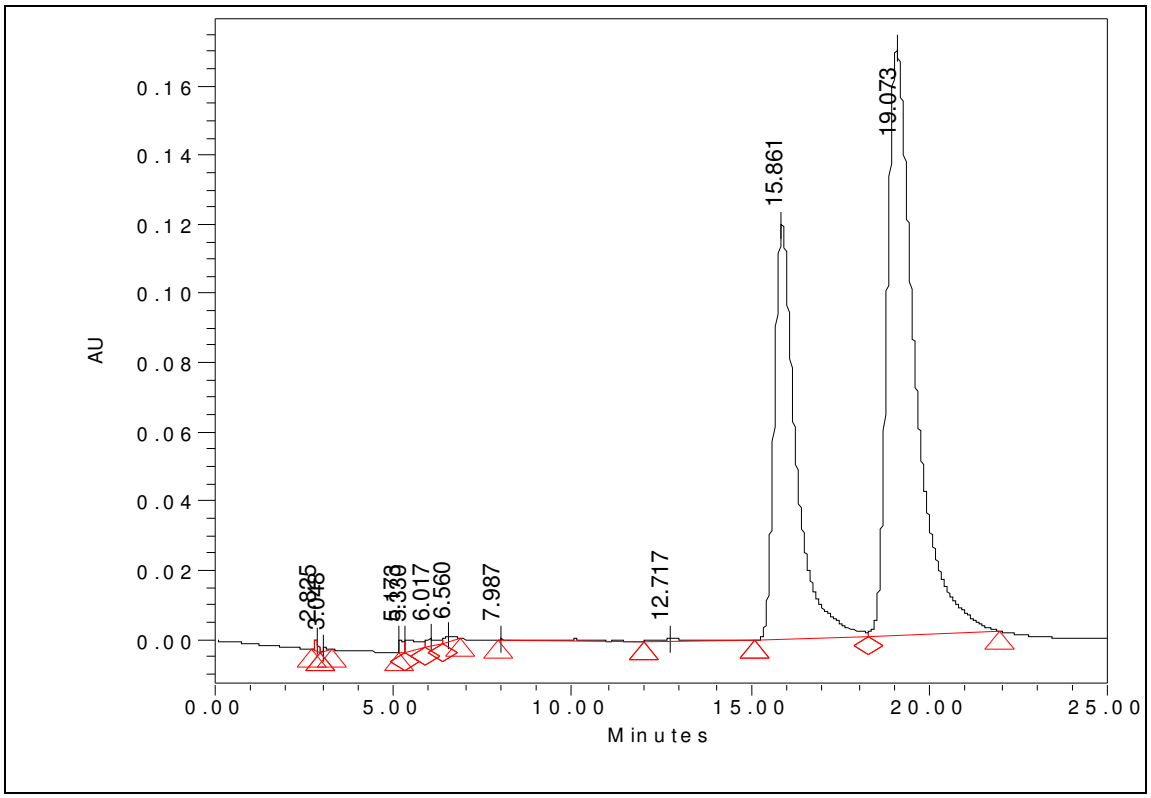

	Peak	Retention time	% Area	Area	%ee
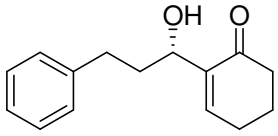 (–)-151d	1	15.861 min	34.78	5149562	29
	2	19.073 min	62.90	9313108	

Fig 7.2 HPLC chromatogram for chiral **151d** (Catalyst (+)-(*R*)-**114b**, Lux 2 column, 9:1 hexane:i-PrOH, 1.0 mL/min, 254 nm).

7.11 References

(1) D. Amsterdam, *Antibiotics in Laboratory Medicine,* 4th ed. V. Lorian, Williams & Wilkins, Baltimore, MD, 1996.

(2) Methods for Dilution Antimicrobial Susceptibility Tests for Bacteria that Grow Aerobically. Approved Standard – Seventh Edition. Document M07-A7. Clinical Laboratory Standard Institute, Wayne, PA, **2006.**

(3) Reference Method for Broth Dilution Antifungal Susceptibility Testing of Yeasts. Approved standard. Document M27-A3. Clinical Laboratory Standard Institute, Wayne, PA, **2008**.

(4) Reference Method for Broth Dilution Antifungal Susceptibility Testing of Filamentous Fungi. Approved standard. Document M38-A2. Clinical Laboratory Standard Institute, Wayne, PA, **2008**.

(5) B. Panzenböck, P. Bartunek, M. Y. Mapara and M. Zenke, *Blood,* 1998, **92**, 3658-3668

(6) CytoTox-ONE homogeneous membrane integrity assay (G7892, Promega)

(7) Caspase-Glo 3/7 assay (G8091, Promega)

(8) CellTiter-Blue cell viability assay (G8082, Promega)

(9) ISO 14593: Water quality, Evaluation of ultimate aerobic biodegradability of organic compounds in aqueous medium. Method by analysis of inorganic carbon in sealed vessels (CO_2 headspace test), 1999.

(10) S. Kobayashi, K. Kusakabe, S. Komiyama and H. Ishitani, *J. Org. Chem.,* 1999, **64**, 4220-4221.

(11) T. R. Wu, L. Shen and J. M. Chong, *Org. Lett.,* 2004, **6**, 2701-2704.

(12) Y. Chen, L. Yang, Y. Li, Z. Zhou, K. Lam, A. S. C. Chan and H. Kwong, *Chirality,* 2000, **12**, 510-513.

(13) H. Venkatesan, F. M. Hocutt, T. K. Jones and M. H. Rabinowitz, *J. Org. Chem.*, 2010, **75**, 3488-3491.

(14) N. T. McDougal and S. E. Schaus, *J. Am. Chem. Soc.,* 2003, **125**, 12094-12095.

Appendix

Antimicrobial and biodegradation data for known organocatalysts

Proline derived catalysts							
Organism	Time (h)	**89/91**	**92**	**94**	**41a**	**8**	**97**
S.aureus	24 h	>2000	>2000	>2000	>2000	>2000	>2000
	48 h	>2000	>2000	>2000	>2000	>2000	>2000
MRSA	24 h	>2000	>2000	>2000	>2000	>2000	>2000
	48 h	>2000	>2000	>2000	>2000	>2000	>2000
S.epidermidis	24 h	>2000	>2000	>2000	>2000	>2000	>2000
	48 h	>2000	>2000	>2000	>2000	>2000	>2000
Enterococcus sp.	24 h	>2000	>2000	>2000	>2000	>2000	>2000
	48 h	>2000	>2000	>2000	>2000	>2000	>2000
E.coli	24 h	>2000	>2000	>2000	>2000	>2000	>2000
	48 h	>2000	>2000	>2000	>2000	>2000	>2000
K.pneumoniae	24 h	>2000	>2000	>2000	>2000	>2000	>2000
	48 h	>2000	>2000	>2000	>2000	>2000	>2000
K.pneumoniae **ESBL** positive	24 h	>2000	>2000	>2000	>2000	>2000	>2000
	48 h	>2000	>2000	>2000	>2000	>2000	>2000
P.aeruginosa	24 h	>2000	>2000	>2000	>2000	>2000	>2000
	48 h	>2000	>2000	>2000	>2000	>2000	>2000

Results obtained by collaborator

Table 1: IC_{95} (μM) values for proline derivatives (**8**, **41a**, **89**, **91**, **92**, **94** and **97**) with antibacterial activity >2000 μM

Proline derived catalysts							
Organism	Time (h)	**89/91**	**92**	**94**	**41a**	**8**	**97**
C.albicans (ATCC44859)	24h	>2000	>2000	>2000	>2000	>250	>2000
	48h	>2000	>2000	>2000	>2000	>250	>2000
C.albicans (ATCC90028)	24h	>2000	>2000	**2000**	>2000	>250	>2000
	48h	>2000	>2000	>2000	>2000	>250	>2000
C.parapsilosis (ATCC22019)	24h	>2000	>2000	>2000	>2000	>250	>2000
	48h	>2000	>2000	>2000	>2000	>250	>2000
C.krusei (ATCC6258)	24h	>2000	>2000	>2000	**2000**	>250	>2000
	48h	>2000	>2000	>2000	>2000	>250	>2000
C.krusei (E28)	24h	>2000	>2000	>2000	>2000	>250	>2000
	48h	>2000	>2000	>2000	>2000	>250	>2000
C.tropicalis (156)	24h	>2000	>2000	**2000**	**2000**	>250	>2000
	48h	>2000	>2000	>2000	>2000	>250	>2000
C.glabrata (20/I)	24h	>2000	>2000	>2000	>2000	>250	>2000
	48h	>2000	>2000	>2000	>2000	>250	>2000
C.lusitaniae (2446/I)	24h	>2000	>2000	>2000	>2000	>250	>2000
	48h	>2000	>2000	>2000	>2000	>250	>2000
Trichosporon asahii (1188)	24h	>2000	>2000	>2000	>2000	>250	>2000
	48h	>2000	>2000	>2000	>2000	>250	>2000
Aspergillus fumigatus (231)	24h	>2000	>2000	>2000	>2000	>250	>2000
	48h	>2000	>2000	>2000	>2000	>250	>2000
Absidia corymbifera (272)	24h	>2000	>2000	>2000	>2000	>250	>2000
	48h	>2000	>2000	>2000	>2000	>250	>2000
Trichophyton mentagrophytes (445)	72h	>2000	>2000	**2000**	>2000	>250	>2000
	120h	>2000	>2000	>2000	>2000	>250	>2000

Table 2: Antifungal IC_{80}/IC_{50} (μM) values for proline derivatives (**8**, **41a**, **89**, **91**, **92**, **94** and **97**)

Organism	Time (h)	**106**	**15**	**107**
C. albicans (ATCC44859)	24	>500	>1000	>125
	48	>500	>1000	>125
C. albicans (ATCC90028)	24	>500	>1000	>125
	48	>500	>1000	>125
C. parapsilosis (ATCC22019)	24	>500	**1000**	>125
	48	>500	**1000**	>125
C. krusei (ATCC6258)	24	>500	>1000	>125
	48	>500	>1000	>125
C. krusei (E28)	24	>500	>1000	>125
	48	>500	>1000	>125
C. tropicalis (156)	24	>500	**1000**	>125
	48	>500	**1000**	>125
C. glabrata (20/I)	24	>500	>1000	>125
	48	>500	>1000	>125
C. lusitaniae (2446/I)	24	>500	**1000**	>125
	48	>500	**1000**	>125
T. asahii (1188)	24	>500	>1000	>125
	48	>500	>1000	>125
A. fumigatus (231)	24	>500	>1000	>125
	48	>500	>1000	>125
A. corymbifera (272)	24	>500	>1000	>125
	48	>500	>1000	>125
T. mentagrophytes (445)	72	>500	**1000**	>125
	120	>500	**1000**	>125

Table 3: Antifungal IC_{80}/IC_{50} (μM) values for Jacobsen thioureas (**15, 106** and **107**)

Organism	Time (h)	**108**	**38a**	**81a**
S. aureus	24	>2000	>2000	>500
	48	>2000	>2000	>500
MRSA	24	>2000	>2000	>500
	48	>2000	>2000	>500
S. epidermidis	24	>2000	>2000	>500
	48	>2000	>2000	>500
Enterococcus sp.	24	>2000	>2000	>500
	48	>2000	>2000	>500
E. coli	24	>2000	>2000	>500
	48	>2000	>2000	>500
K. pneumoniae	24	>2000	>2000	>500
	48	>2000	>2000	>500
K. pneumoniae - ***ESBL***	24	>2000	>2000	>500
	48	>2000	>2000	>500
P. aeruginosa	24	>2000	>2000	>500
	48	>2000	>2000	>500

Table 4: MIC/IC_{95} (μM) values for cinchona alkaloid derivatives (**38a**, **81a** and **108**)

Organism	Time (h)	**108**	**38a**	**81a**
C. albicans (ATCC44859)	24	>2000	>2000	**500**
	48	>2000	>2000	**500**
C. albicans (ATCC90028)	24	>2000	>2000	**500**
	48	>2000	>2000	**500**
C. parapsilosis (ATCC22019)	24	>2000	>2000	**125**
	48	>2000	>2000	**125**
C. krusei (ATCC6258)	24	>2000	>2000	**500**
	48	>2000	>2000	**500**
C. krusei (E28)	24	>2000	>2000	**500**
	48	>2000	>2000	**500**
C. tropicalis (156)	24	>2000	>2000	**500**
	48	>2000	>2000	**500**
C. glabrata (20/I)	24	>2000	>2000	**500**
	48	>2000	>2000	**500**
C. lusitaniae (2446/I)	24	>2000	>2000	**125**
	48	>2000	>2000	**125**
T. asahii (1188)	24	>2000	>2000	>500
	48	>2000	>2000	>500
A. fumigatus (231)	24	>2000	>2000	>500
	48	>2000	>2000	>500
A. corymbifera (272)	24	>2000	>2000	>500
	48	>2000	>2000	>500
T. mentagrophytes (445)	72	>2000	>2000	>500
	120	>2000	>2000	>500

Table 5: Antifungal IC_{80}/IC_{50} (μM) values for cinchona alkaloid derivatives (**38a, 81a** and **108**)

Organism	Time (h)	**109**	**19**	**110**
S. aureus	24	>2000	>2000	>2000
	48	>2000	>2000	>2000
MRSA	24	**2000**	>2000	>2000
	48	**2000**	>2000	>2000
S. epidermidis	24	>2000	>2000	**2000**
	48	>2000	>2000	**2000**
Enterococcus sp.	24	>2000	>2000	>2000
	48	>2000	>2000	>2000
E. coli	24	>2000	>2000	>2000
	48	>2000	>2000	>2000
K. pneumoniae	24	>2000	>2000	>2000
	48	>2000	>2000	>2000
K. pneumoniae – ***ESBL***	24	>2000	>2000	>2000
	48	>2000	>2000	>2000
P. aeruginosa	24	>2000	>2000	>2000
	48	>2000	>2000	>2000

Table 6: MIC/IC_{95} (μM) values for MacMillan imidazolidinones (**19**, **109** and **110**)

Organism	Time (h)	**109**	**19**	**110**
C. albicans (ATCC44859)	24	>2000	>2000	>2000
	48	>2000	>2000	>2000
C. albicans (ATCC90028)	24	>2000	>2000	>2000
	48	>2000	>2000	>2000
C. parapsilosis (ATCC22019)	24	>2000	>2000	>2000
	48	>2000	>2000	>2000
C. krusei (ATCC6258)	24	>2000	>2000	>2000
	48	>2000	>2000	>2000
C. krusei (E28)	24	>2000	>2000	>2000
	48	>2000	>2000	>2000
C. tropicalis (156)	24	>2000	>2000	>2000
	48	>2000	>2000	>2000
C. glabrata (20/I)	24	>2000	>2000	>2000
	48	>2000	>2000	>2000
C. lusitaniae (2446/I)	24	>2000	>2000	>2000
	48	>2000	>2000	>2000
T. asahii (1188)	24	>2000	>2000	**2000**
	48	>2000	>2000	>2000
A. fumigatus (231)	24	>2000	>2000	>2000
	48	>2000	>2000	>2000
A. corymbifera (272)	24	>2000	>2000	>2000
	48	>2000	>2000	>2000
T. mentagrophytes (445)	72	>2000	>2000	**2000**
	120	>2000	>2000	**2000**

Table 7: Antifungal IC_{80}/IC_{50} (μM) values for MacMillan imidazolidinones (**19**, **109** and **110**)

Compound	% Biodegradation			
	6 d	14 d	21 d	28 d
SDS	78	86	85	90
26b	0	2	1	1
41a	5	1	4	1
45a	0	0	4	3
45b	0	0	5	3
48a	0	2	2	2
48b	0	4	6	4
50a	0	0	4	2
50b	0	0	0	1
92	5	1	0	0
97	2	0	0	0
100	0	0	4	3
101	1	2	5	0
102	0	2	6	5
105a	0	4	2	1
105b	0	0	2	3

Table 8: Biodegradation results for organocatalysts (**26b**, **41a**, **45a**, **45b**, **48a**, **48b**, **50a**, **50b**, **92**, **97**, **100**, **101**, **102**, **105a** and **105b**)

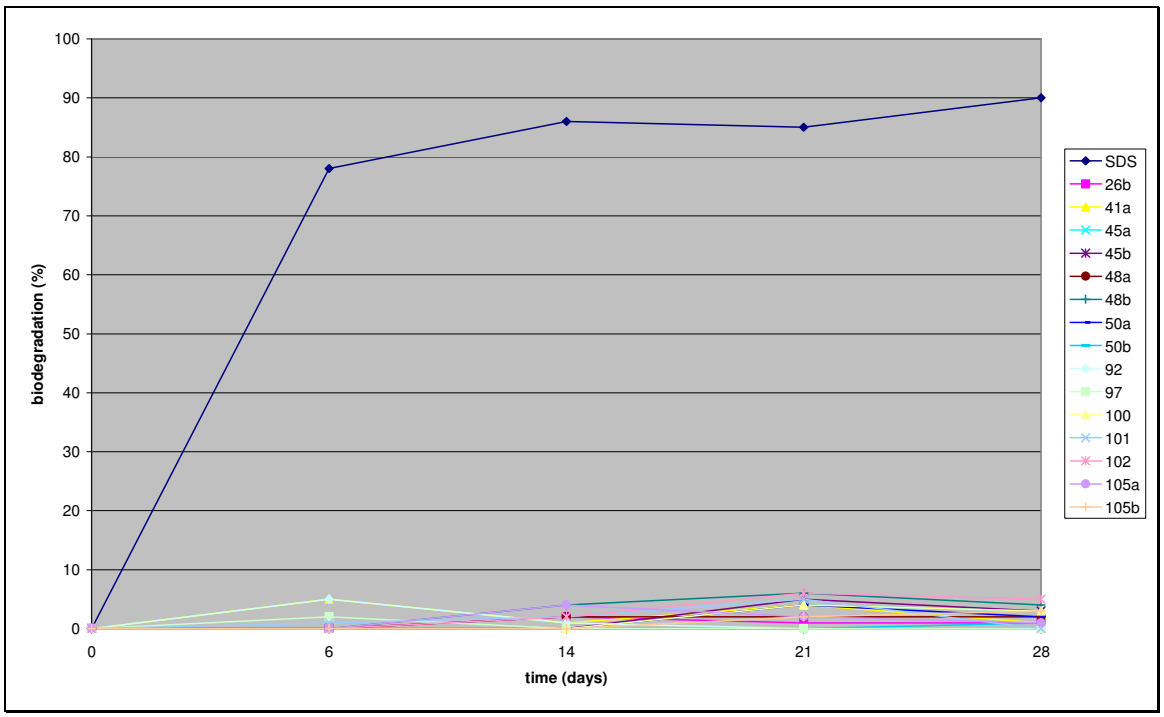

Fig 1 Biodegradation curves for organocatalysts (**26b**, **41a**, **45a**, **45b**, **48a**, **48b**, **50a**, **50b**, **92**, **97**, **100**, **101**, **102**, **105a** and **105b**)

Compound	Concentration (mgC/L)	Molar concentration of test sample	Inhibition (%)
26b + SDS	20 + 20	83 μM	0
41a + SDS	20 + 20	98 μM	0
45a + SDS	20 + 20	83 μM	2
45b + SDS	20 + 20	83 μM	0
48a + SDS	20 + 20	83 μM	4
48b + SDS	20 + 20	83 μM	0
50a + SDS	20 + 20	83 μM	18
50b + SDS	20 + 20	83 μM	4
92 + SDS	20 + 20	333 μM	0
97 + SDS	20 + 20	79 μM	0
100 + SDS	20 + 20	54 μM	0
101 + SDS	20 + 20	79 μM	0
102 + SDS	20 + 20	76 μM	9
105a + SDS	20 + 20	83 μM	0
105b + SDS	20 + 20	83 μM	6

Table 9: Inhibition of SDS biodegradation by organocatalysts (**26b**, **41a**, **45a**, **45b**, **48a**, **48b**, **50a**, **50b**, **92**, **97**, **100**, **101**, **102**, **105a** and **105b**)

NMR studies of polysubstituted BINOLs

All NMR experiments were carried out in deuterated solvents such as $CDCl_3$, d_6-DMSO, d_6-acetone and d_4-methanol depending on chemical solubility and signal resolution. Solvent effects will be discussed for relevant spectra.

The molecular structures of polysubstituted BINOLs contain a C_2 symmetric axis, which results in the two substituted naphthol units being chemically and magnetically equivalent when the substituents are the same for each unit (Figure 2).

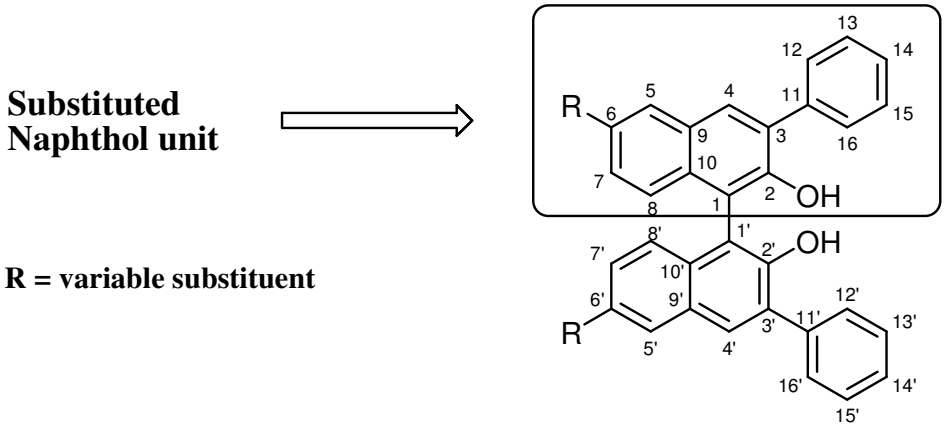

Fig 2 General structure of polysubstituted BINOL with numbering

Each substituted naphthol unit is composed of benzene and a phenol fused together, with the carbon atom at C1 position linking to another substituted naphthol unit, at C3 a phenyl ring is positioned and at C6 various substituents are placed such as bromo, methoxy, *n*-butyl and a carboxylic acid. Substituents at C6 contribute different electronic effects to the naphthol ring which results in different chemical shifts for some protons in the naphthol unit.

Within each substituted naphthol unit the proton and carbon atoms at 12 and 16 are chemically equivalent to each other. Also atoms at 13 and 15 are chemically equivalent to

each other. All other proton and carbon atoms within the substituted naphthol unit are not chemically and magnetically equivalent to each other.

^{1}H NMR studies of polysubstituted BINOLs

In this section the NMR spectra of the racemic BINOL target molecules is discussed. Identical spectra were recorded for the single enantiomers.

^{1}H NMR study of (+/–)-6,6'-dibromo-3,3'-diphenyl-2,2'-dihydroxy-1,1'-binaphthyl (123)

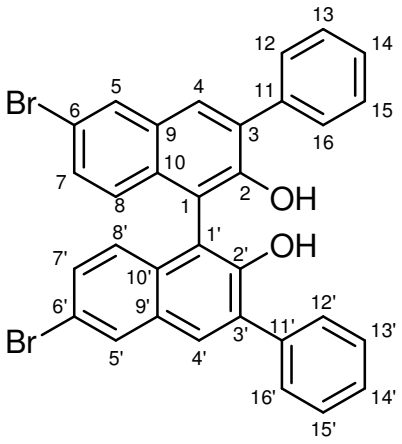

(123)

For the ^{1}H NMR spectrum of (+/–)-6,6'-dibromo-3,3'-diphenyl-2,2'-dihydroxy-1,1'-binaphthyl (**123**), six spin coupled aromatic proton signals, one non-spin coupled aromatic proton and a non-spin coupled hydroxyl signal are present (Figure 3).

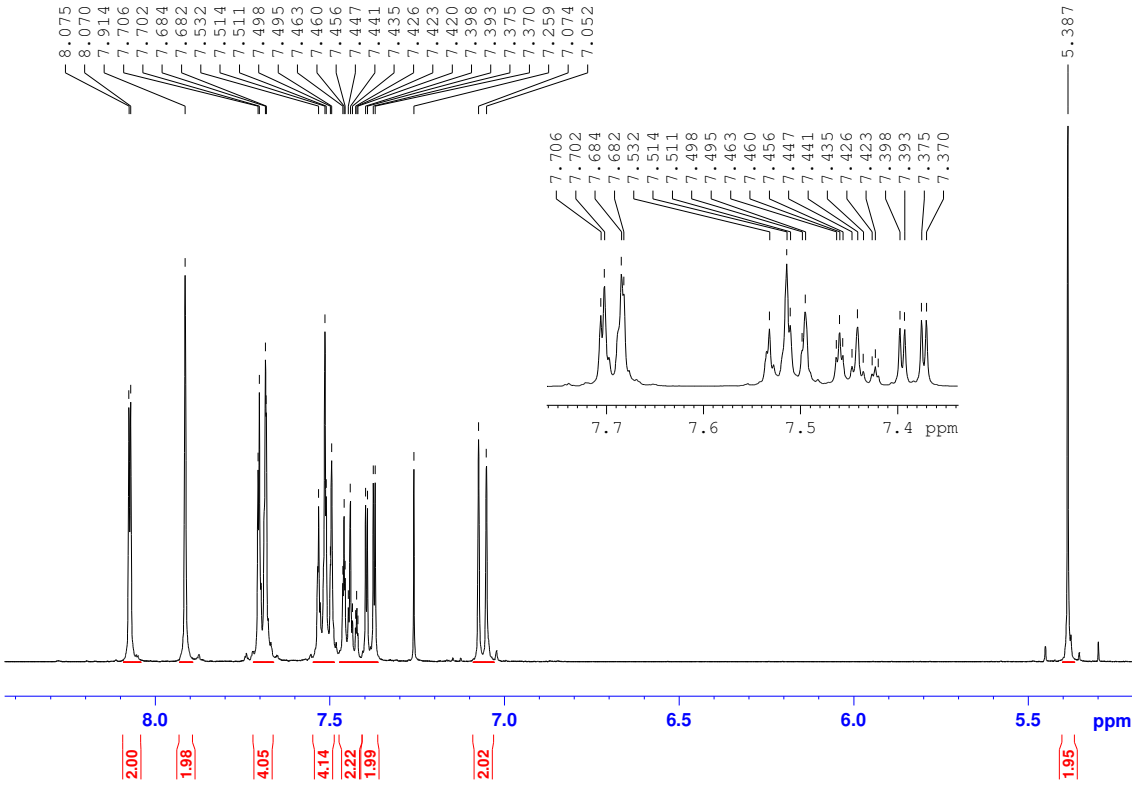

Fig 3 ^{1}H NMR spectrum for (+/–)-6,6'-dibromo-3,3'-diphenyl-2,2'-dihydroxy-1,1'-binaphthyl (**123**)

A doublet at 8.07 ppm and a singlet at 7.91 ppm are distinctly observed. The doublet with a coupling constant of 2.0 Hz correlates with *H5 H5'* and the singlet correlates with *H4 H4'*. Between 7.69-7.44 ppm the protons of the phenyl ring at position 3 reside. These protons give rise to a complicated splitting pattern. The downfield signal at 7.69 ppm is correlating with *H12 H12' H16 H16'* showing a doublet of doublets. This proton is split as it is coupling with protons that are *ortho* and *meta* to its position. Protons for *H13 H13' H15 H15'* appear as a doublet of doublets at 7.51 ppm with a coupling constant of 7.6 Hz and 1.2 Hz. The more shielded *para* proton *H14 H14'* gives a triplet of triplets at 7.44 ppm. Remaining aromatic protons are a doublet of doublets at 7.38 ppm and a doublet at 7.06 ppm. The doublet of doublets is assigned to *H7 H7'* with coupling constants of 2.0 Hz and 9.0 Hz as it couples with *H5 H5'* (*meta* coupling) and *H8 H8'* (*ortho* coupling) protons. While the doublet which represents *H8 H8'* has a coupling constant of 9.0 Hz as it couples with *H7 H7'*. The hydroxyl signal appears at 5.39 ppm as a singlet.

^{1}H NMR study of (+/−)-6,6-dimethoxy-3,3'-diphenyl-2,2'-dihydroxy-1,1-binaphthyl (111)

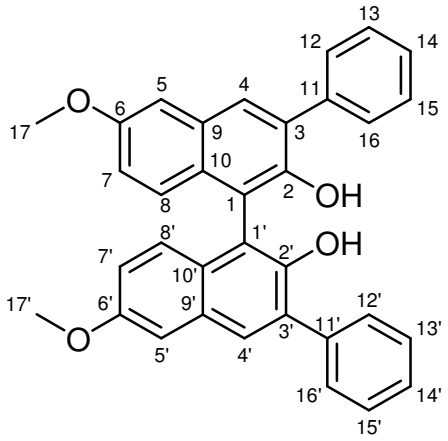

(111)

In the proton NMR spectrum of (+/−)-6,6-dimethoxy-3,3'-diphenyl-2,2'-dihydroxy-1,1-binaphthyl (**111**) (Figure 4) there is a marked difference in the chemical shift for protons at *H5 H5'* and *H7 H7'* when compared to the ^{1}H spectrum for (**123**). These protons are shifted more upfield (shielded) due to the electron donating methoxy group. *H7 H7'* is the most shielded aromatic proton, observed as a doublet of doublets at 7.04 ppm with coupling constants of 9.0 Hz and 2.8 Hz. The signal for *H5 H5'* appears as its usual doublet at 7.28 ppm with a coupling constant of 2.8 Hz. A slight downfield shift at 7.19 ppm is noted for *H8 H8'*. All other aromatic protons stay relatively the same compared to the ^{1}H NMR spectrum for (**123**). The methyl signal comes at 3.94 ppm as a singlet with an integration of 6 and the hydroxyl signal resides at 5.31 ppm as a singlet.

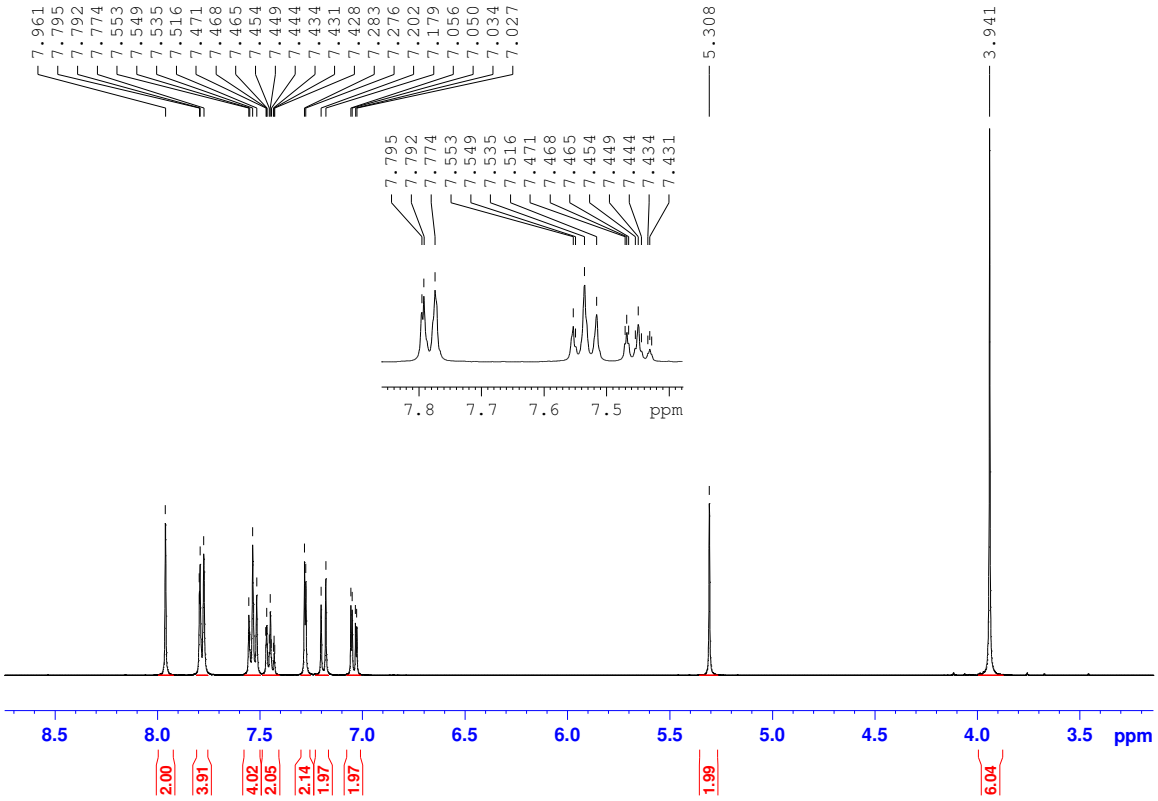

Fig 4 ^{1}H NMR spectrum of (+/−)-6,6-dimethoxy-3,3'-diphenyl-2,2'-dihydroxy-1,1-binaphthyl (**111**)

^{1}H NMR study of (+/−)-6,6'-dipentan-1-one-3,3'-diphenyl-2,2'-dihydroxy-1,1'-binaphthyl (118)

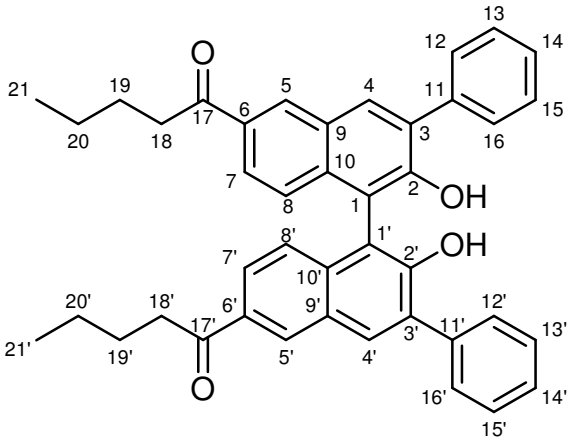

(118)

Compound **118** has an electron-withdrawing ketone substituent at the *6 6'* position and this results in a downfield shift for some protons, especially for protons that are *ortho* to its position on the aromatic ring. A doublet at 8.51 ppm with a coupling constant of 1.6 Hz is assigned to *H5 H5'*. Proton signal for *H7 H7'* appears at 7.82 ppm as a doublet of doublets. Both protons are *ortho* to the ketone substituent at position *6 6'* and there chemical shifts are more downfield when compared to there respective signals in the ^{1}H spectrum for compound **123**. The downfield shift for these protons is due to the deshielding effect contributed by the electron withdrawing ketone substituent. This is not surprising, as electron withdrawing substituents on aromatic compounds are *meta* directing while the *ortho* and *para* positions are deshielded.

The singlet at 8.12 ppm correlates with *H4 H4'*. Proton signals for the phenyl substituent reside between 7.73 ppm and 7.44 ppm. A downfield shift is noted for the hydroxyl signal at 5.84 ppm. Proton signals for the butyl chain appear in the aliphatic region of the ^{1}H NMR spectrum. A triplet at 3.01 ppm with a coupling constant of 7.4 Hz is the most downfield signal in the aliphatic region and corresponds with *H18 H18'*. At 1.72 ppm a triplet of triplets is observed for *H19 H19'*. The proton signal for *H20 H20'* comes at 1.41 ppm as a quartet of triplets. Remaining triplet at 0.95 ppm with a coupling constant of 7.4 Hz is the most upfield signal for this ^{1}H spectrum and belongs to the methyl protons *H21 H21'*.

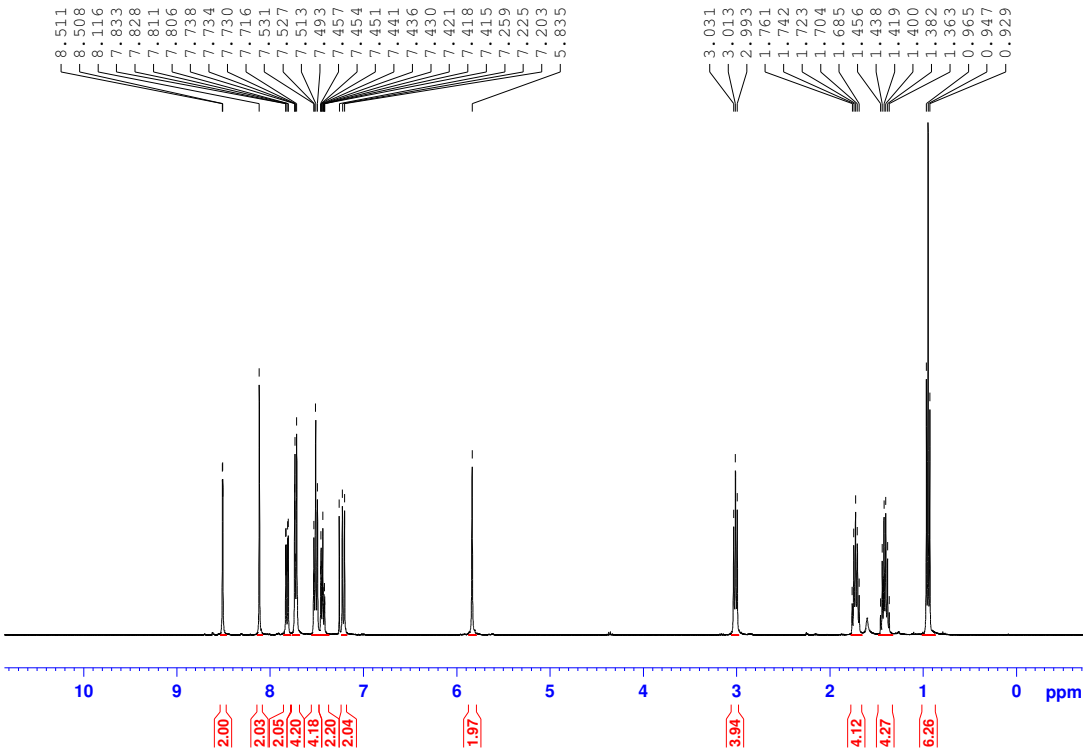

Fig 5 ^{1}H NMR spectrum of (+/–)-6,6-dipentan-1-one-3,3'-diphenyl-2,2'-dihydroxy-1,1-binaphthyl (**118**)

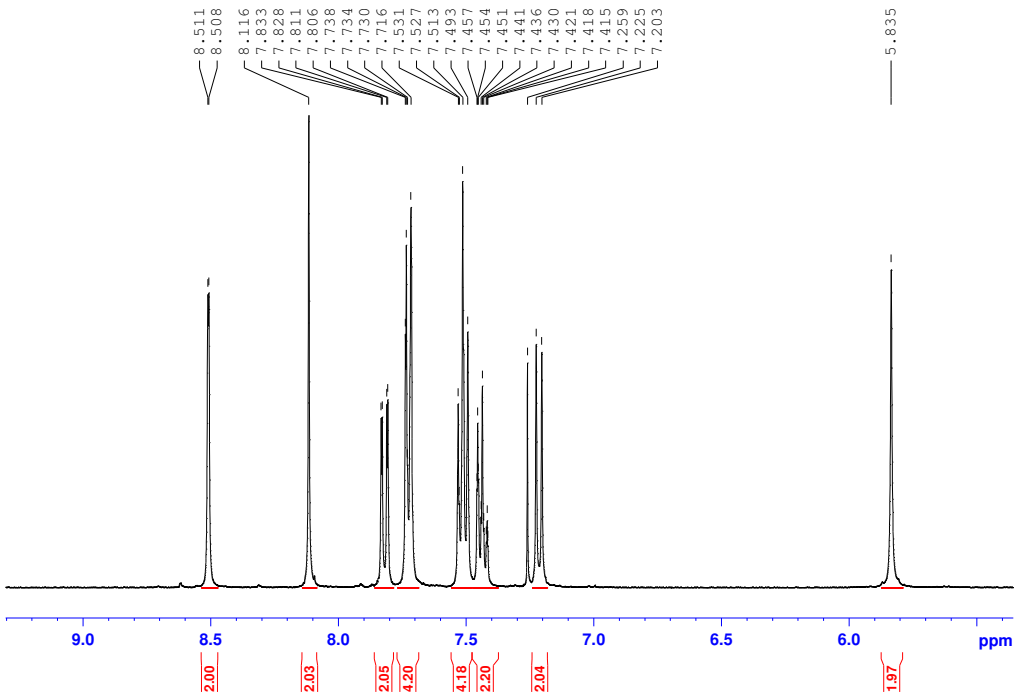

Fig 6 Enlarged proton aromatic spectrum of (+/–)-6,6-dipentan-1-one-3,3'-diphenyl-2,2'-dihydroxy-1,1-binaphthyl (**118**)

Electronic effects contributing to different proton chemical shift

From the proton NMR discussion of compounds **111**, **118** and **123** the effect of electron donating and withdrawing substituents on binaphthyl protons is notable (Table 10). Protons *H5 H5'* and *H7 H7'* are shifted more upfield when an electron donating substituent is present at the 6 6' position and are shifted downfield when an electron withdrawing substituent is present. For instance, methoxy has an electron donating effect on *H5 H5'* and *H7 H7'* while the pentan-1-one (alkylcarbonyl) substituent deshields these proton signals. As well, the differences for proton chemical shifts were noted for other substituents like ethoxy, *n*-butyl and pentynyl. (Table 10) when compared to the bromo substituent.

Compound	**R**	***H4, H4'***	***H5, H5'***	***H7, H7'***	***H8, H8'***	***OH***
111	OMe	7.96	7.28	7.04	7.19	5.31
112	OEt	7.90	7.23	7.00	7.14	5.23
114	*n*-Butyl	7.98	7.71	7.20*	7.20*	5.32
117	Pentynyl	7.95	7.99	7.32	7.13	5.40
118	Pentan-1-one	8.12	8.51	7.82	7.21	5.84
123	Br	7.91	8.07	7.38	7.06	5.39

*protons overlap

Table 10: Selected ^{1}H NMR spectral data for compounds (**111, 112, 114, 117, 118** and **123**)

^{13}C NMR study of polysubstituted BINOLs

From the general structure of a polysubstituted BINOL (Figure 2), seven tertiary and seven quaternary carbon signals would be expected to be seen in the ^{13}C NMR spectrum plus the additional carbon signals contributed by the variable substituent.

^{13}C NMR and DEPT 135 spectroscopic study of (+/–)-6,6-dimethoxy-3,3'-diphenyl-2,2'-dihydroxy-1,1-binaphthyl (111)

A total of fifteen carbon signals are observable in the ^{13}C spectrum of (+/–)-6,6-dimethoxy-3,3'-diphenyl-2,2'-dihydroxy-1,1-binaphthyl (**111**). In the upfield region at 55.44 ppm the methyl signal is clearly evident (Figure 7). All the remaining aromatic carbon signals reside between 156.59 ppm and 106.72 ppm. From the DEPT 135 it is possible to distinguish the tertiary and quaternary carbon signals. All seven quaternary carbon signals are not present in the DEPT 135 while the seven tertiary carbon signals and the methyl carbon signal are present (Figure 8).

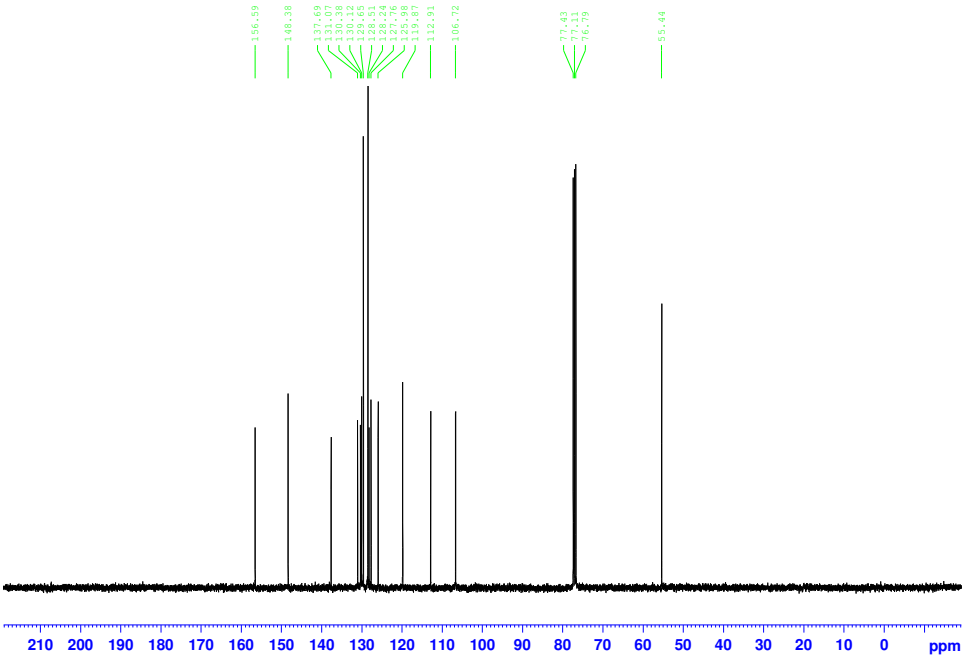

Fig 7 ^{13}C NMR spectrum of (+/–)-6,6-dimethoxy-3,3'-diphenyl-2,2'-dihydroxy-1,1-binaphthyl (**111**)

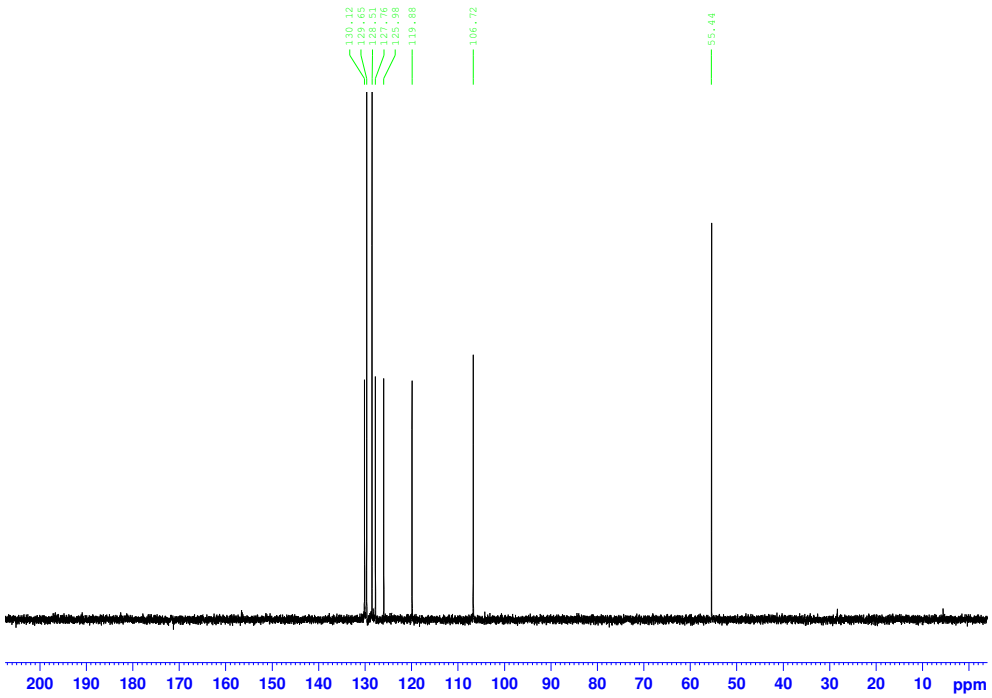

Fig 8 DEPT 135 spectrum of (+/–)-6,6-dimethoxy-3,3'-diphenyl-2,2'-dihydroxy-1,1-binaphthyl (**111**)

Electronic effects on carbon signals

A selection of carbon signals for the polysubstituted BINOLs are presented in Table 11. The effects of electron donating and withdrawing substituents is notable for carbon signals at *C5 C5'* and *C7 C7'*. The methoxy substituent shields *C5 C5'* and *C7 C7'* while the electron withdrawing bromo and pentan-1-one substituents deshield these positions as can be seen in Table 11.

Compound	R	*C4, C4'*	*C5, C5'*	*C7, C7'*	*C8, C8'*	*C2, C2'*
111	OMe	130.12	106.72	119.88	125.98	148.38
112	OEt	130.05	107.50	120.14	125.92	148.28
114	*n*-Butyl	130.90	126.93	128.99*	128.99*	149.52
				124.27*	124.27*	
117	Pentynyl	131.05	131.18	130.33	124.26	150.45
118	Pentan-1-one	132.97	130.24	125.64	124.60	152.20
123	Br	130.41*	130.41*	130.64	126.08	150.26
		130.37*	130.37*			

* indistinguishable carbons in hmqc

Table 11: Selection of ^{13}C NMR spectral data for compounds **111, 112, 114, 117, 118** and **123**

Solvent effects in ^{1}H and ^{13}C spectra for polysubstituted BINOLs

^{1}H NMR spectrum of (+/–)-6,6'-dicarboxyl-3,3'-diphenyl-2,2'-dihydroxy-1,1'-binaphthyl (115)

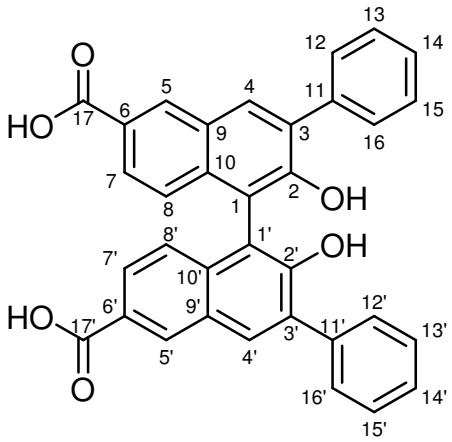

(115)

The proton NMR spectrum for (+/–)-6,6'-dicarboxyl-3,3'-diphenyl-2,2'-dihydroxy-1,1'-binaphthyl (**115**) was carried out in d_6-DMSO (Figure 9) and d_4-methanol (Figure 11). It was not possible to run the proton NMR spectrum in deuterated chloroform as the compound was insoluble for this solvent. In d_6-DMSO all expected proton signals are present, the carboxylic acid proton is observed as a broad singlet at 12.84 ppm. Carboxylic acid protons usually appear this downfield due to the anisotropic field and the nearby electronegative oxygen atom.[1] The hydroxyl on the naphthyl ring resides at 8.85 ppm. This signal is shifted more downfield in d_6-DMSO than previously seen for compounds **111**, **118** and **123** in deuterated chloroform. Deuterated DMSO is a hydrogen bonding solvent and hydroxyl signals appear more downfield for this solvent when compared to non-hydrogen bonding solvents like deuterated chloroform**.**[1] Due to the electron withdrawing nature of the carboxylic acid, protons *H5 H5'* and *H7 H7'* appear downfield at 8.65 ppm and 7.73 ppm respectively. The proton signal for *H7 H7'* is overlapping with the *ortho* phenyl protons *H12 H12' H16 H16'* and can not be seen directly. Remaining phenyl protons reside between 7.50 ppm and 7.40 ppm. A singlet at 8.18 ppm is observed for *H4 H4'* and a doublet at 6.98 ppm is correlating with *H8 H8'*.

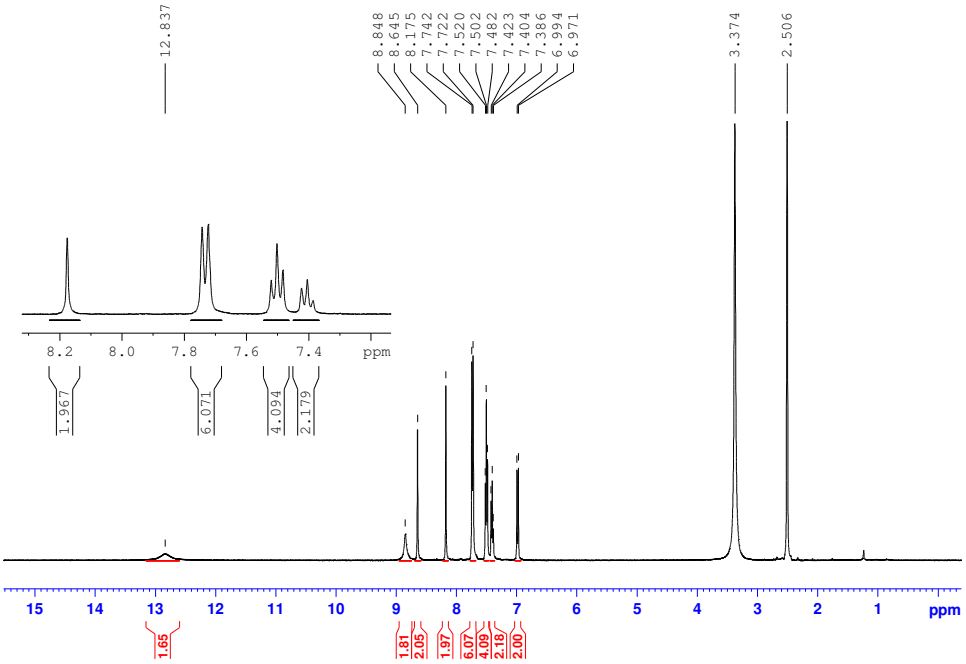

Fig 9 ^{1}H NMR spectrum of (+/–)-6,6'-dicarboxyl-3,3'-diphenyl-2,2'-dihydroxy-1,1'-binaphthyl (**115**) in d_6-DMSO

A D_2O shake was performed to verify the carboxylic acid and hydroxyl signals at 12.84 ppm and 8.85 ppm, respectively. After the D_2O shake, the hydroxyl and carboxylic acid signals are not observed in the proton spectrum as they have exchanged with the deuterium in D_2O (Figure 10).

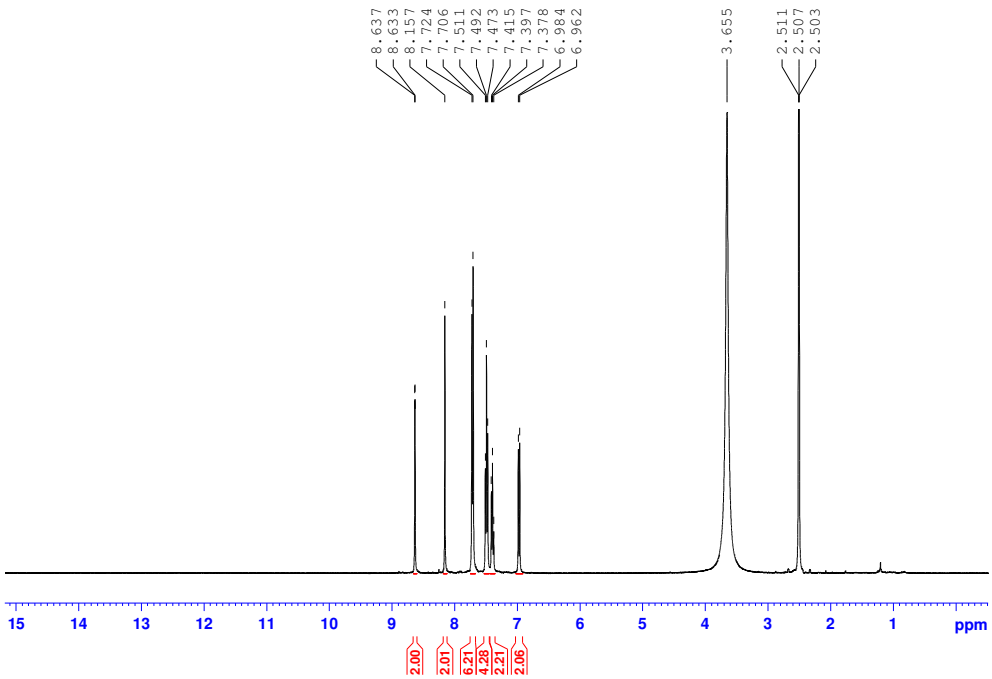

Fig 10 ^{1}H NMR spectrum of (+/–)-6,6'-dicarboxyl-3,3'-diphenyl-2,2'-dihydroxy-1,1'-binaphthyl (**115**) after D_2O shake in d_6-DMSO

For the ^{1}H NMR spectrum of **115** in deuterated methanol the aromatic proton signals are clearly resolved. The overlap between *H7 H7'* and *H12 H12' H16 H16'* is not observed as both signals come at separate chemical shifts. Proton signal for *H7 H7'* appears at 7.83 ppm as a doublet of doublets with coupling constants 1.6 Hz and 8.8 Hz. Between 7.78 and 7.40 ppm the phenyl proton signals reside. A doublet at 8.69 ppm is observed for *H5 H5'* and the singlet at 8.11 ppm represents *H4 H4'*. Both hydroxyl and carboxylic acid signals are not observed in the proton spectrum, probably as they have exchanged with deuterium from the deuterated methanol.

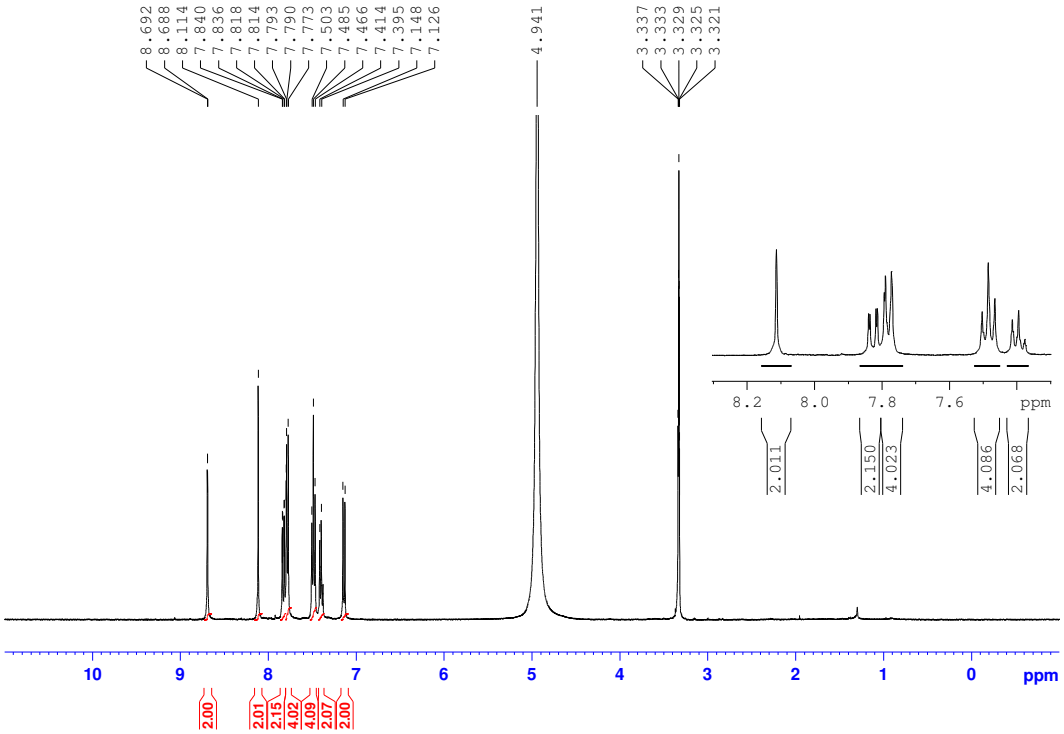

Fig 11 ^{1}H NMR spectrum of (+/–)-6,6'-dicarboxyl-3,3'-diphenyl-2,2'-dihydroxy-1,1'-binaphthyl (**115**) in d_4-methanol

^{13}C NMR spectra for (+/–)-6,6'-dibromo-3,3'-diphenyl-2,2'-*bis*(methoxymethoxy)-1,1'-binaphthyl (125)

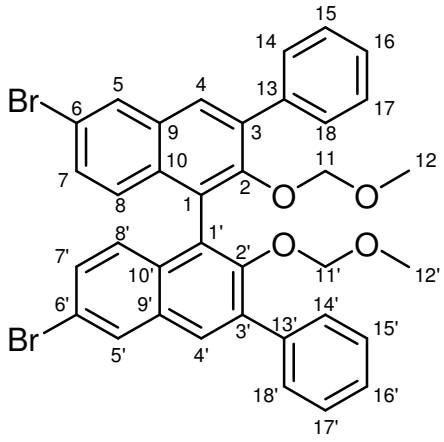

(125)

In the ^{13}C NMR spectrum for (+/–)-6,6'-dibromo-3,3'-diphenyl-2,2'-*bis*(methoxymethoxy)-1,1'-binaphthyl (**125**) a difference is noted for the number of carbon signals observable in $CDCl_3$ and d_6-acetone. A total of sixteen carbon signals should be seen for this compound. However, when the spectrum was carried out in $CDCl_3$ a total of fourteen carbons were noted (Figure 12). The missing 2 carbon signals are overlapping with other carbon signals. While in d_6-acetone the expected 16 carbon signals were present and clearly resolved (Figure 13).

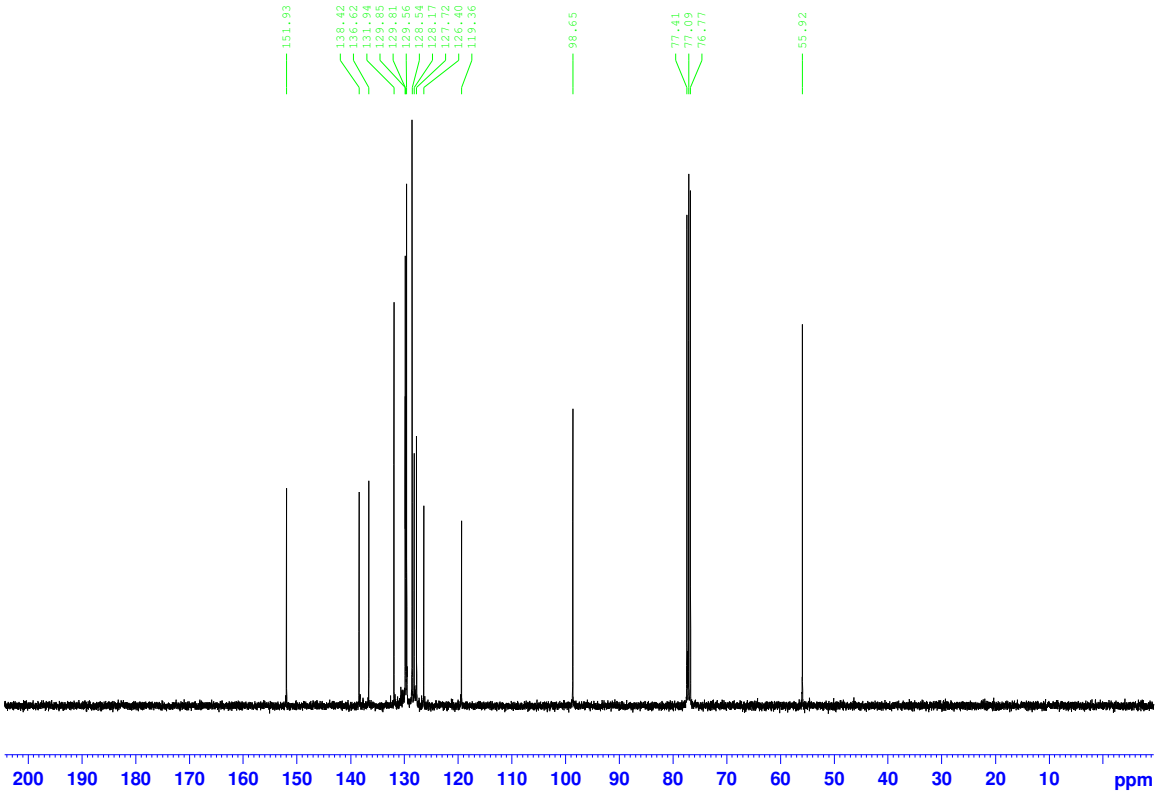

Fig 12 ^{13}C NMR spectrum of (+/–)-6,6'-dibromo-3,3'-diphenyl-2,2'-*bis*(methoxymethoxy)-1,1'-binaphthyl (**125**) in $CDCl_3$

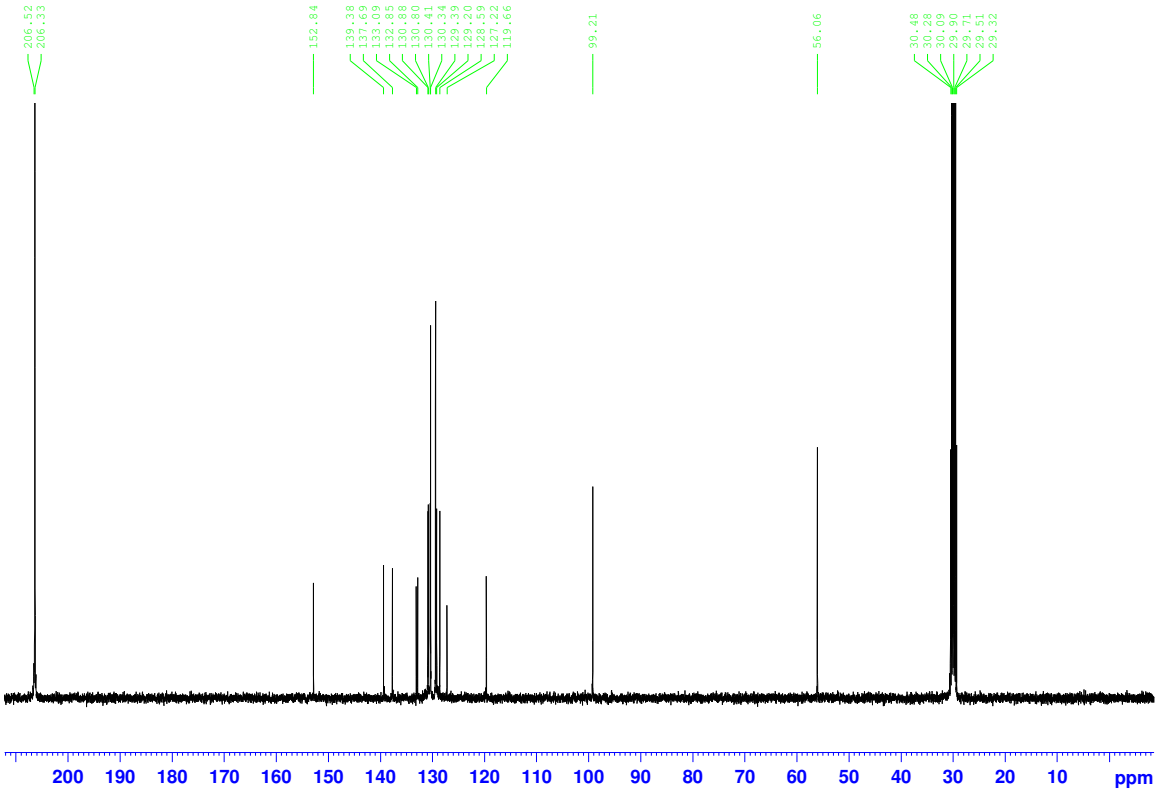

Fig 13 ^{13}C NMR spectrum of (+/−)-6,6'-dibromo-3,3'-diphenyl-2,2'-*bis*(methoxymethoxy)-1,1'-binaphthyl (**125**) in d_6-acetone

NMR studies of biquinoline derivatives

The molecular structures of biquinoline derivatives contain a C_2 symmetric axis, which results in the two quinoline units being chemically and magnetically equivalent when the substituents are the same for each unit.

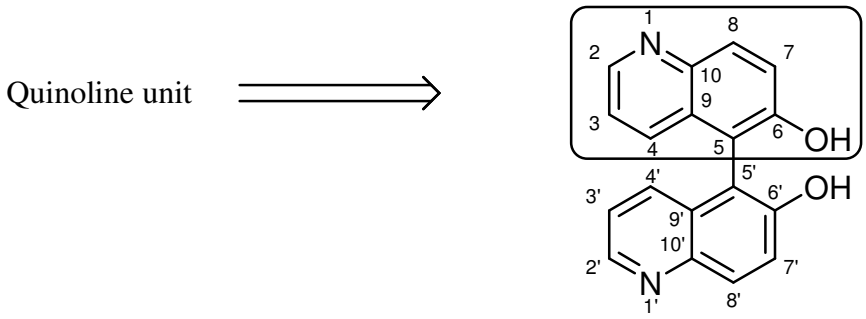

Fig 14 General structure of biquinoline with numbering

Each quinoline unit is composed of pyridine and a phenol fused together, with the carbon atom at C5 position linking to another quinoline unit. Modification of the nitrogen position is possible with various alkylating agents resulting in the generation of *N*-alkylated biquinoline salts.

Proton and carbon atoms within the quinoline unit are not chemically and magnetically equivalent to each other. In the ^{1}H NMR spectrum for biquinoline, 5 spin coupled proton signals and a non-spin coupled hydroxyl signal are expected plus additional signals contributed by the substituents.

^{1}H NMR study of quinoline and biquinoline derivatives

^{1}H NMR study for (+/–)-1,1'-ethoxycarbonylmethyl-6,6'-dihydroxy-5,5'-biquinoline (135)

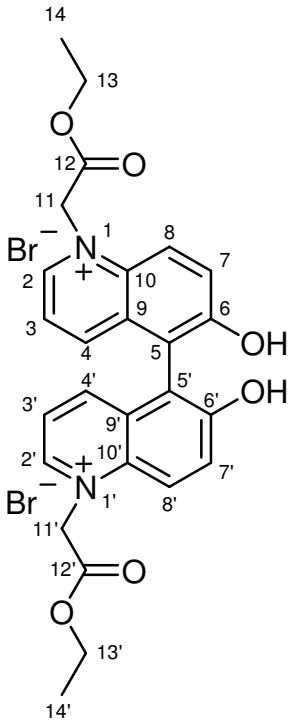

(135)

For the ^{1}H NMR spectrum of (+/–)-1,1'-ethoxycarbonylmethyl-6,6'-dihydroxy-5,5'-biquinoline (**135**) in d_6-DMSO , five spin coupled aromatic proton signals, two spin coupled aliphatic proton signals, one non-spin coupled aliphatic proton and a non-spin coupled hydroxyl signal are present (Figure 15). The singlet at 11.31 ppm is corresponding with the hydroxyl group and is the most downfield signal for this spectrum. A doublet of doublets at 8.06 ppm with coupling constants 8.4 Hz and 5.2 Hz can be seen for *H3 H3'*. This proton signal appears as a doublet of doublets as it is coupling with *H2 H2'* and *H4 H4'*. The doublet at 8.40 ppm with a coupling constant of 8.4 Hz correlates with *H4 H4'* and the doublet at 9.45 ppm with a coupling constant of 5.2 Hz belongs to *H2 H2'*. Remaining doublets at 8.56 ppm and 8.14 ppm with coupling constants of 9.6 Hz are corresponding to *H8 H8'* and *H7 H7'* respectively. Within the aliphatic region of the spectrum a downfield singlet at 6.28 ppm is noted for *H11 H11'*. A

quartet at 4.30 ppm with a coupling constant of 6.8 Hz is observed for *H13 H13'*. Proton signal for *H14 H14'* appears at 1.31 ppm as a triplet with a coupling constant of 6.8 Hz.

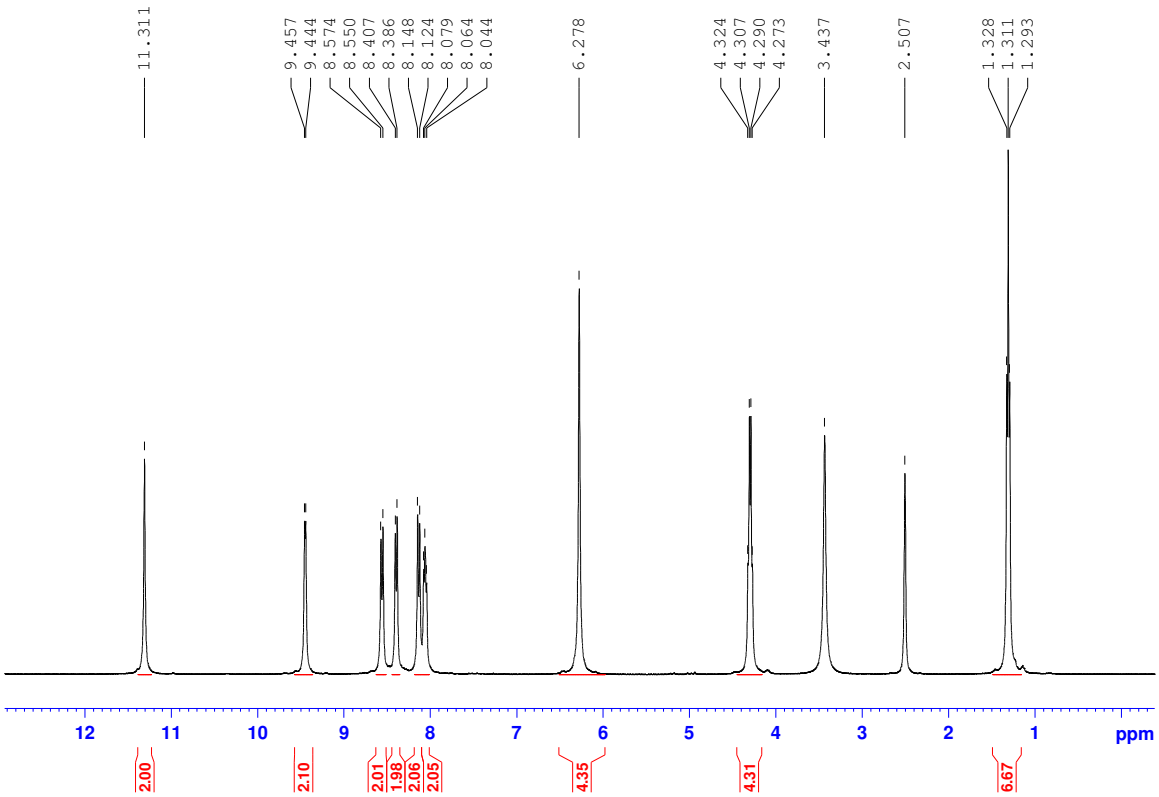

Fig 15 ^{1}H NMR spectrum of (+/−)-1,1'-ethoxycarbonylmethyl-6,6'-dihydroxy-5,5'-biquinoline (**135**)

Effect of *n*-alkyl substituents on aromatic proton signals for biquinoline compounds

Following the *n*-alkylation of the biquinoline scaffold a significant change in chemical shifts can be seen for the ^{1}H NMR spectrum of **134**, **135** and **136** when compared to the ^{1}H NMR spectrum of **130** (Table 12). All aromatic protons are shifted downfield as a result of the electron withdrawing quaternary nitrogen. The greatest downfield shift for proton signals is observable for the ethoxy compound (**135**) as can be seen in Table 12.

Compound	R	*H2, H2'*	*H3, H3'*	*H4, H4'*	*H7, H7'*	*H8, H8'*	*OH*
130	Unsubstituted	8.66	7.25	7.35	7.60	8.01	8.90
134	*n*-butyl	9.39	7.92	8.25	8.08	8.73	11.15
135	Ethoxycarbonyl methyl	9.45	8.06	8.40	8.14	8.56	11.31
136	methyl	9.31	7.92	8.21	8.03	8.62	11.19

Table 12: Selected proton signals for biquinoline compounds **130, 134, 135** and **136**

^{1}H NMR study of 6-hydroxy-quinoline-3-carboxylic acid methyl ester (142)

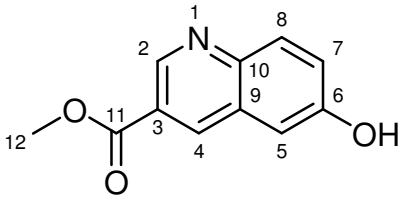

142

For **142**, the hydroxyl proton signal can be seen at 10.32 ppm as a broad singlet in the ^{1}H NMR spectrum in d_6-DMSO (Figure 16). Proton *H2* is observed as a doublet with a coupling constant of 2.0 Hz at a downfield shift of 9.06 ppm. The doublet for *H4* with a coupling constant of 2.0 Hz is evident at 8.76 ppm. A proton signal for *H7* at 7.46 ppm is coupling with *H8* and *H5*, resulting in a doublet of doublets with coupling constants 9.2 Hz and 2.6 Hz. The adjacent *H8* resides at 7.95 ppm as a doublet and the doublet at 7.35 ppm is noted for *H5*. Methyl signal can be seen at 3.92 ppm with an integration of 6 protons.

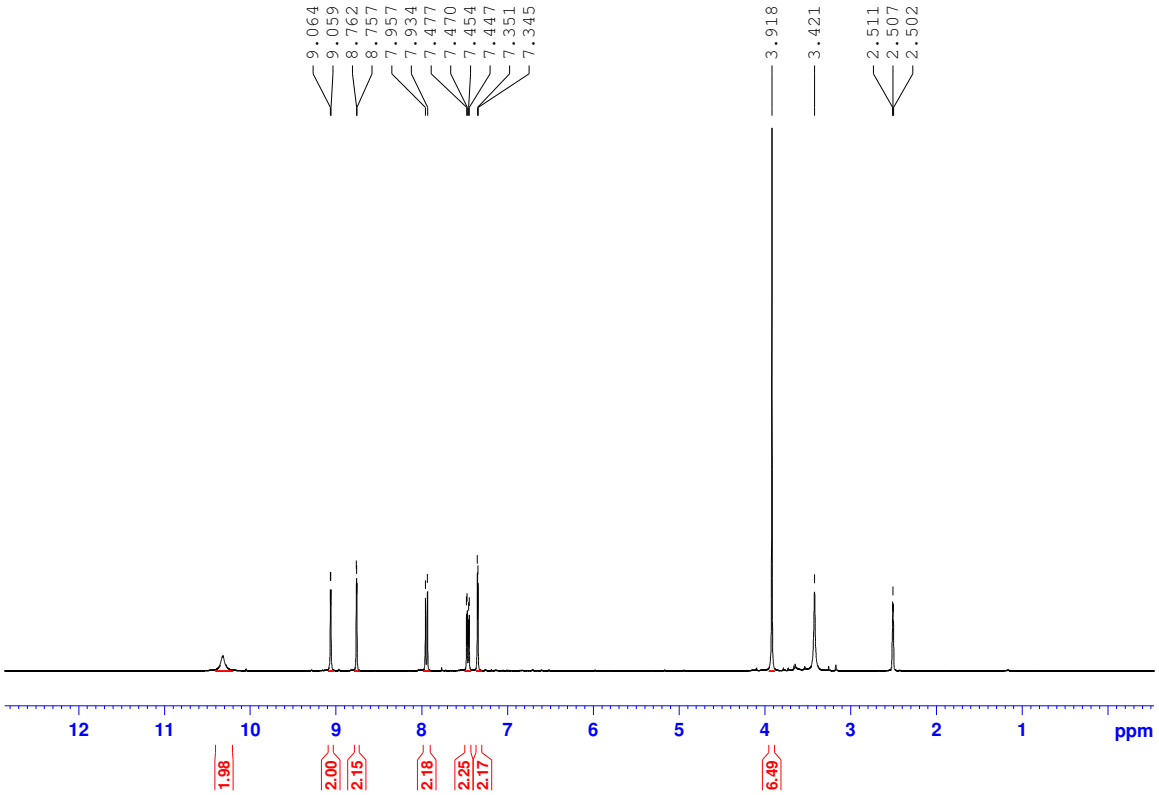

Fig 16 [1]H NMR spectrum of 6-hydroxy-quinoline-3-carboxylic acid methyl ester (**142**)

[1]H NMR study of 6,6'-dihydroxy-5,5'-biquinoline-3,3'-dicarboxylic acid dimethyl ester (137a)

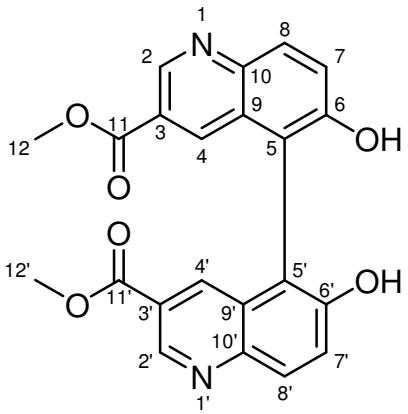

(137a)

In the ^{1}H NMR spectrum of 6,6'-dihydroxy-5,5'-biquinoline-3,3'-dicarboxylic acid dimethyl ester (**137a**) in d_6-DMSO, a broad downfield singlet at 10.22 ppm is evident for the hydroxyl group (Figure 17). Both *H8 H8'* and *H7 H7'* are coupling with each other at 8.16 ppm and 7.77 ppm, respectively, with a coupling constant of 8.6 Hz. A singlet at 9.13 ppm is corresponding with *H2 H2'* and the singlet at 7.98 is correlating with *H4 H4'*. Coupling is not evident between *H2 H2'* and *H4 H4'* possibly due to line broadening. In the upfield region of the spectrum the methyl signal can be seen at 3.77 ppm as a singlet.

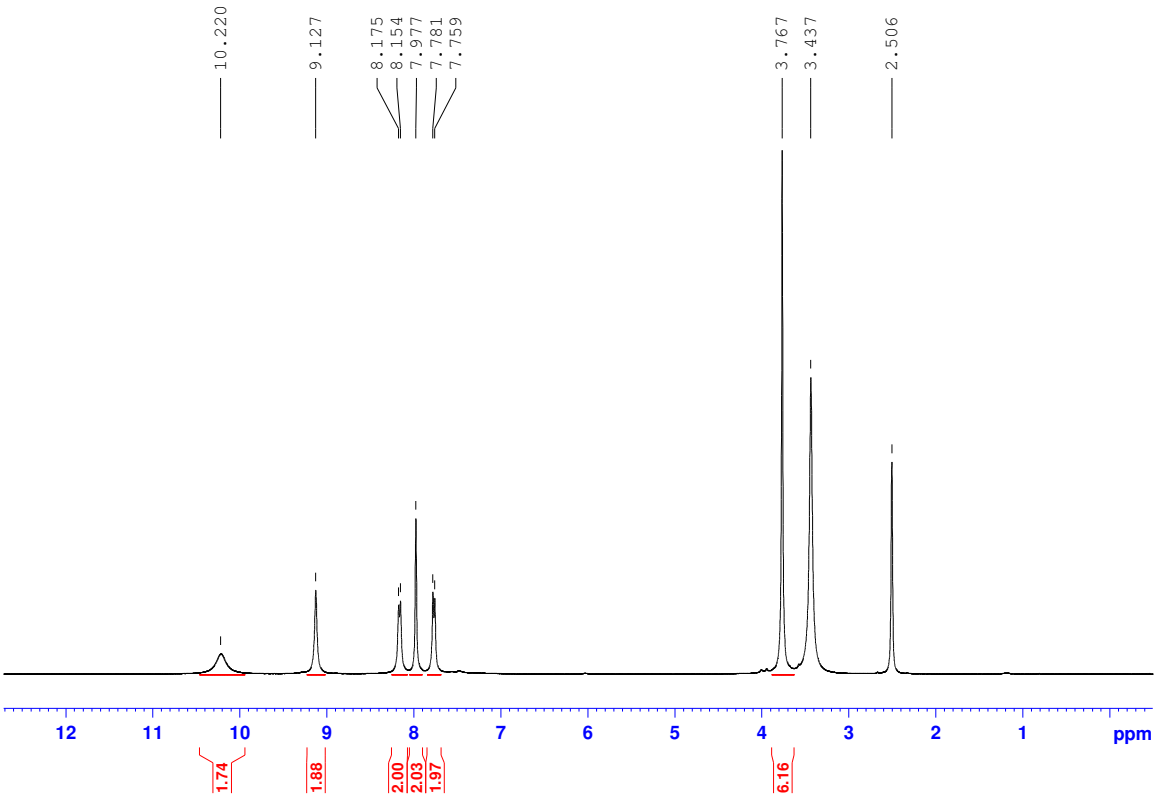

Fig 17 ^{1}H NMR spectrum of 6,6'-dihydroxy-5,5'-biquinoline-3,3'-dicarboxylic acid dimethyl ester (**137a**)

^{13}C and DEPT 135 studies of quinoline and biquinoline derivatives

^{13}C and DEPT 135 NMR study of 6-hydroxy-quinoline-3-carboxylic acid methyl ester (142)

In the ^{13}C spectrum of **142** in d_6-DMSO, a total of 11 carbon signals can be seen (Figure 18). A downfield chemical shift at 165.44 ppm is noted for the carbonyl group and in the DEPT 135 NMR spectrum (Figure 19) this peak is not observed. In the upfield region of the spectrum a signal for the methyl ester is evident at 52.30 ppm. All remaining carbon signals belong to the aromatic carbon atoms within the quinoline unit.

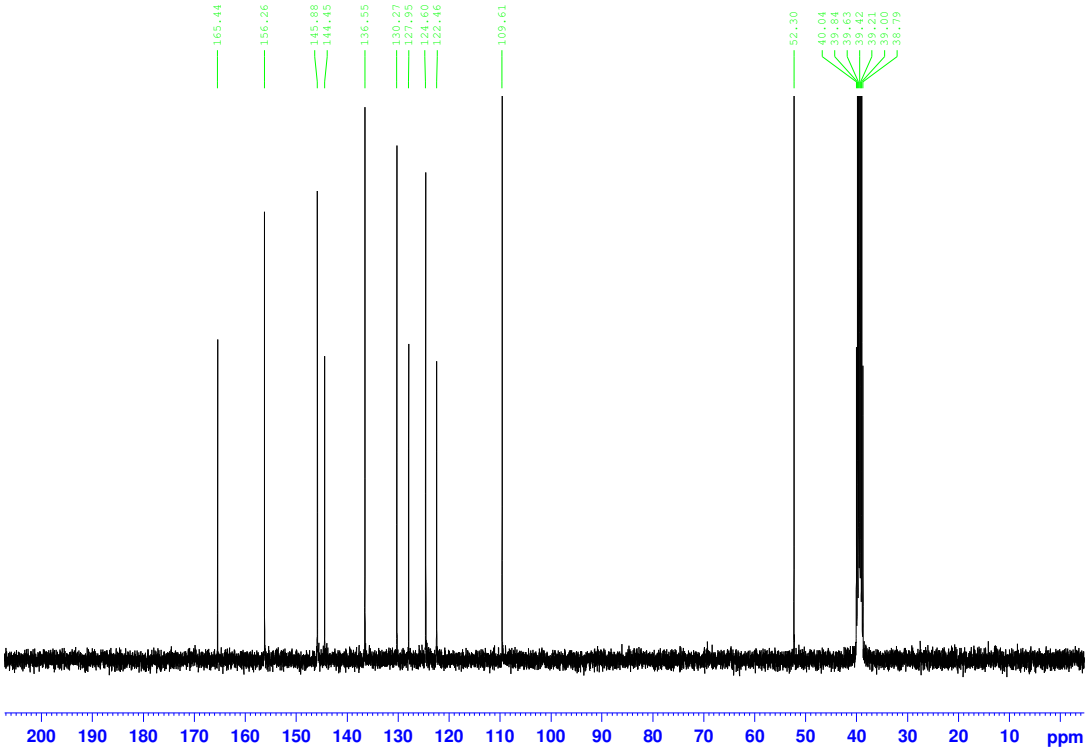

Fig 18 ^{13}C NMR spectrum of 6-hydroxy-quinoline-3-carboxylic acid methyl ester (**142**)

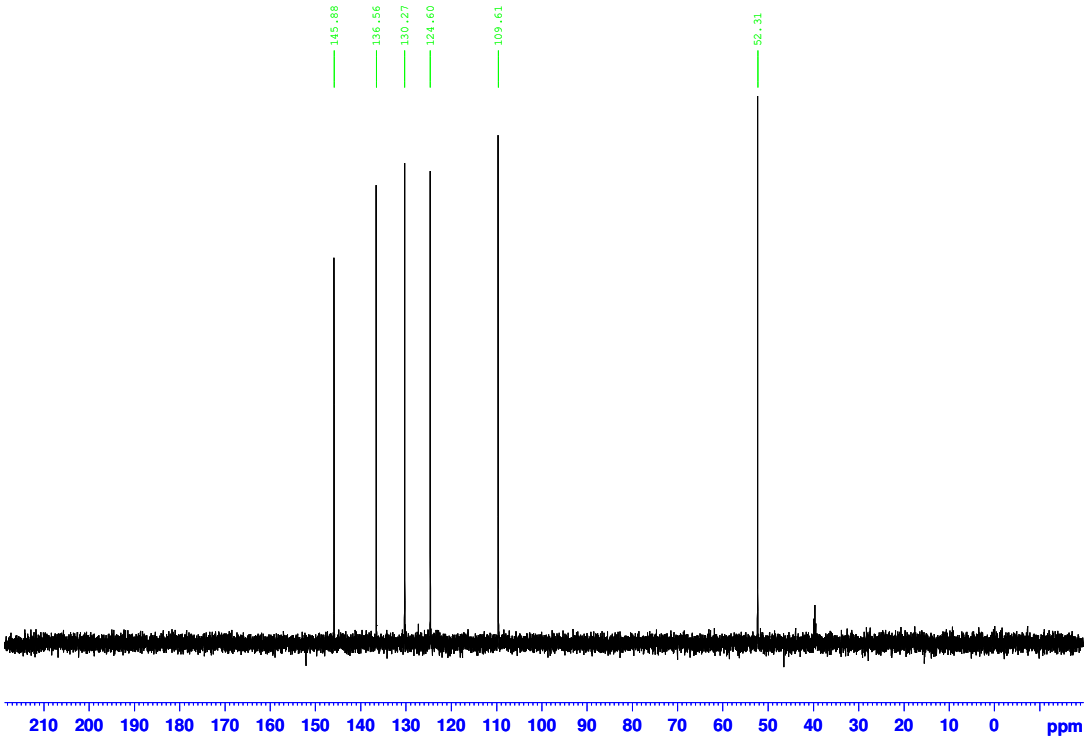

Fig 19 DEPT 135 spectrum of 6-hydroxy-quinoline-3-carboxylic acid methyl ester (**142**)

^{13}C and DEPT 135 NMR study of 6,6'-dihydroxy-5,5'-biquinoline-3,3'-dicarboxylic acid dimethyl ester (137a)

A total of 11 carbon signals can be seen in the ^{13}C NMR spectrum of 6,6'-dihydroxy-5,5-biquinoline-3,3'-dicarboxylic acid dimethyl ester (**137a**) in d_6-DMSO (Figure 20). The carbonyl signal is evident at 165.28 ppm and is not observed in the DEPT 135 (Figure 21). The upfield signal at 52.35 ppm is corresponding with the methyl ester group. All remaining aromatic carbon signals reside between 154.24 ppm and 114.55 ppm. In the DEPT 135 spectrum, four tertiary carbon signals and a methyl signal can be seen.

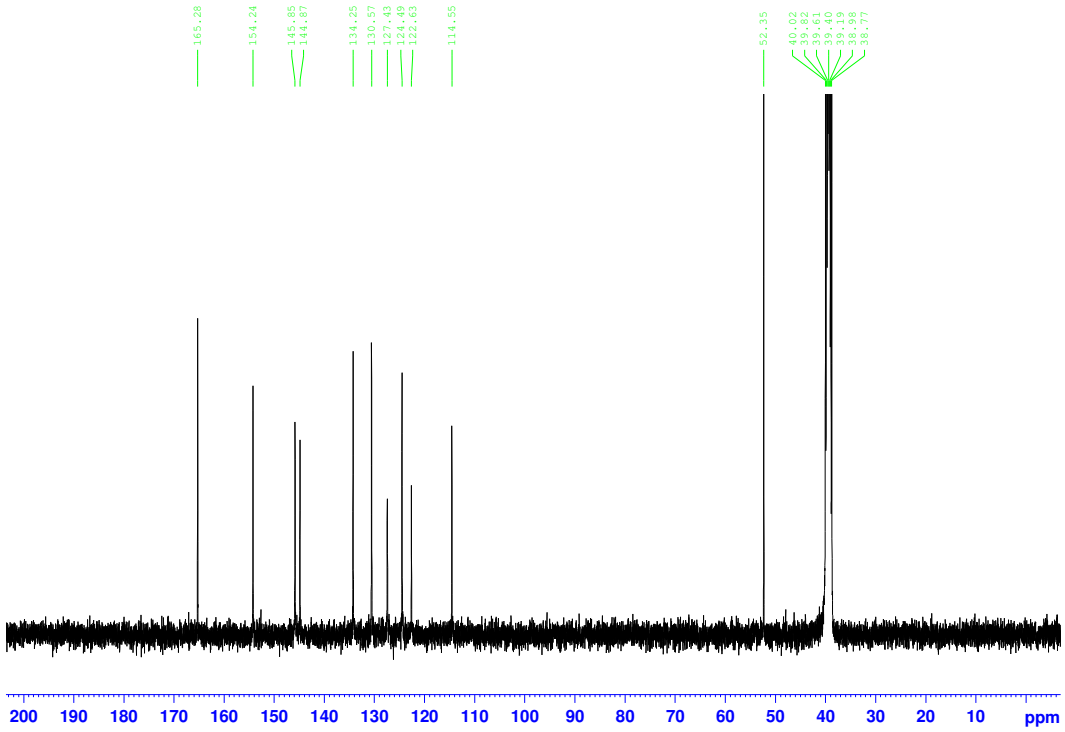

Fig 20 ^{13}C NMR spectrum of 6,6'-dihydroxy-5,5'-biquinoline-3,3'-dicarboxylic acid dimethyl ester (**137a**)

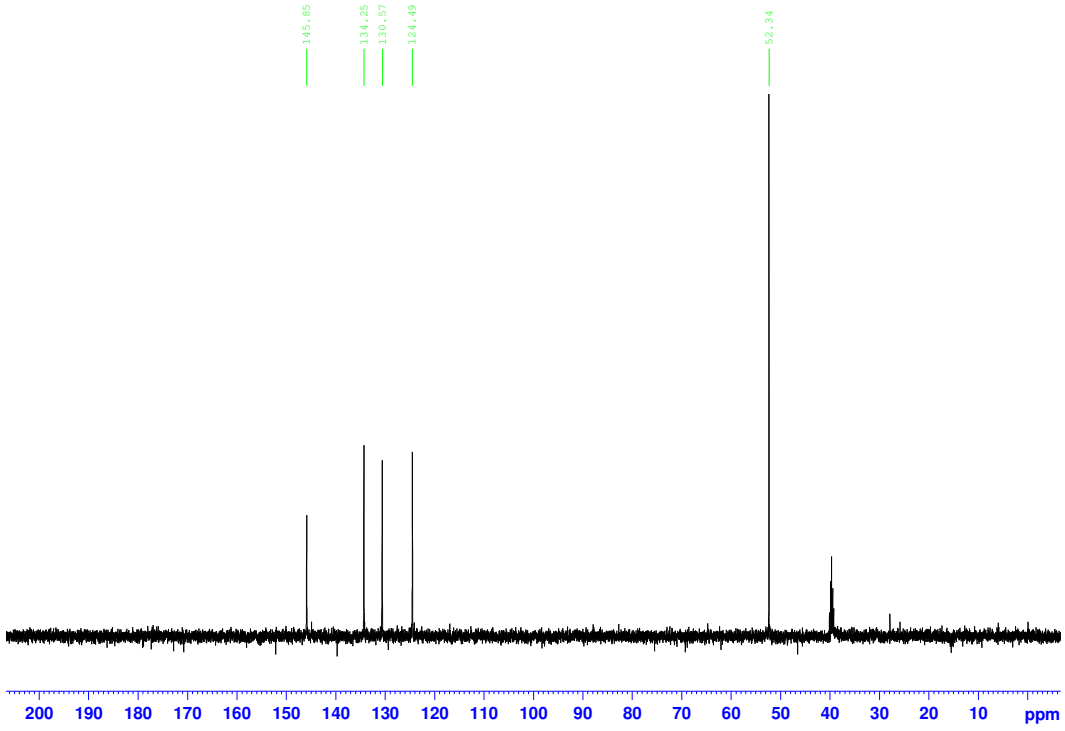

Fig 21 DEPT 135 NMR spectrum of 6,6'-dihydroxy-5,5'-biquinoline-3,3'-dicarboxylic acid dimethyl ester (**137a**)

Difference between 137a and 142 proton and carbon spectra

The difference between the proton and carbon spectra for **137a** and **142** further verifies proof of structure for **137a** (Table 13 and 14).

A total of 6 proton signals are present for **142** in ^{1}H NMR spectrum while for **137a** a total of 5 proton signals are present. The proton signal at *H5* is present in the proton spectrum of **142** while absent in the spectrum of **137a** which suggests that dimerisation has occurred in this position. As well *H7* appears as a doublet of doublets in the ^{1}H spectrum of **142** but is a doublet in the spectrum of **137a**, this suggest that the *meta* coupling for *H7* apparent in **142** is absent in **137a** as this compound has dimerised at C5.

Proton	142	137a
OH	10.32 (s)	10.22 (s)
H2	9.06 (d)	9.13 (s)
H4	8.76 (d)	7.98 (s)
H5	7.35 (d)	-
H7	7.46 (dd)	7.77 (d)
H8	7.95 (d)	8.16 (d)
H12	3.92 (s)	3.77 (s)

Table 13: Proton data for **137a** and **142**

Both **137a** and **142** have a total of 11 carbon signals present for each ^{13}C NMR spectrum. **142** includes 5 tertiary, 5 quaternary and a primary carbon signal for its spectrum while **137a** includes 4 tertiary, 6 quaternary and a primary carbon signal. The absence of a tertiary carbon signal and the extra quaternary carbon signal for the spectrum of **137a** compared to **142** further supports the dimerised molecule.

142	137a
165.44 (CO)	165.28 (CO)
156.26 (C)	154.24 (C)
145.88 (CH)	145.85 (CH)
144.45 (C)	144.87 (C)
136.55 (CH)	134.25 (CH)
130.27 (CH)	130.57 (CH)
127.95 (C)	127.43 (C)
124.60 (CH)	124.49 (CH)
122.46 (C)	122.63 (C)
109.61 (CH)	114.55 (C)
52.30 (CH_3)	52.35 (CH_3)

Table 14: ^{13}C data for **137a** and **142**

References

(1) R. M. Silverstein, G. C. Bassler and T. C. Morrill, *Spectrometric Identifications of Organic Compounds*, 6th ed.; John Wiley & Son: New York, 1998; pp 144-279